



HAL
open science

Study on the integration of controllability and diagnosability of reactive distillation columns as from the conceptual design step. Application to the production of ethyl acetate.

Mayra Figueiredo-Fernandez

► To cite this version:

Mayra Figueiredo-Fernandez. Study on the integration of controllability and diagnosability of reactive distillation columns as from the conceptual design step. Application to the production of ethyl acetate.. Chemical and Process Engineering. Institut National Polytechnique de Toulouse - INPT; Universidade de São Paulo (Brésil), 2013. English. NNT : 2013INPT0059 . tel-04557796

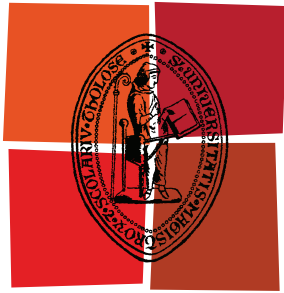
HAL Id: tel-04557796

<https://theses.hal.science/tel-04557796>

Submitted on 24 Apr 2024

HAL is a multi-disciplinary open access archive for the deposit and dissemination of scientific research documents, whether they are published or not. The documents may come from teaching and research institutions in France or abroad, or from public or private research centers.

L'archive ouverte pluridisciplinaire **HAL**, est destinée au dépôt et à la diffusion de documents scientifiques de niveau recherche, publiés ou non, émanant des établissements d'enseignement et de recherche français ou étrangers, des laboratoires publics ou privés.



Université
de Toulouse

THÈSE

En vue de l'obtention du
DOCTORAT DE L'UNIVERSITÉ DE TOULOUSE

Délivré par :
Institut National Polytechnique de Toulouse (INP Toulouse)

Discipline ou spécialité :
Génie des procédés et de l'environnement

Présentée et soutenue par :
Mayra Figueiredo-Fernandez
le : lundi 15 juillet 2013

Titre :
Study on the integration of controllability and diagnosability of reactive distillation columns as from the conceptual design step. Application to the production of ethyl acetate

Ecole doctorale :
Mécanique, Energétique, Génie civil et Procédés (MEGeP)

Unité de recherche :
Laboratoire de Génie Chimique - LGC

Directeur(s) de Thèse :
Xuan Mi Meyer, INP-ENSIACET-LGC
Galo Antonia Carrillo Le Roux, Univ. Sao Paulo - LSCP

Rapporteurs :
Jens Uwe-Repke, TU Bergakademie Freiberg
Marco Giuliatti, UFSCAR

Membre(s) du jury :
Xavier Joulia, INPT
Jean-Michel Reneaume, ENSGTI
Richard Macret, Rhodia

FICHA CATALOGRÁFICA

Fernandez, Mayra Figueiredo

Study on the integration of controllability and diagnosability of reactive distillation columns as from the conceptual design step: application to the production of ethyl acetate / M.F.

Fernandez. -- São Paulo, 2013.

338 p.

Tese (Doutorado) - Escola Politécnica da Universidade de São Paulo. Departamento de Engenharia Química.

1.Destilação reativa 2.Simulação 3.Catálise 4.Projeto de processos 5.Controlabilidade 6.Diagnosticabilidade 7.Acetato de etila I.Universidade de São Paulo. Escola Politécnica. Departamento de Engenharia Química II.t.

Study on the integration of controllability and diagnosability of reactive distillation columns as from the conceptual design step. Application to the production of ethyl acetate.

ABSTRACT

Reactive distillation involves complexities on process dynamics, control and supervision. This work proposes a methodology integrating controllability and diagnosability as from conceptual design. The choice of the most appropriate feasible configuration is conducted through an indices-based method, regarding steady-state and dynamic simulations, for the ethyl acetate production. Experimental campaigns were performed to acquire reliable models. The methodology highlights the process sensitivities and shows that three degrees of freedom of the double-feed column can be manipulated to ensure the industrial specifications; the controlled variables are selected at similar specific locations for all column configurations. Concerning diagnosis, the use of composition sensors seems to be the most appropriate solution, but the same performances can be reached with more temperature sensors judiciously placed.

Key words: reactive distillation, process design, dynamic modeling, heterogeneous catalyst, controllability, diagnosability, ethyl acetate

Etude de l'intégration de la contrôlabilité et de la diagnosticabilité des colonnes de distillation réactive dès la phase de conception. Application à la production d'acétate d'éthyle.

RESUME

La distillation réactive est un exemple emblématique de l'intensification de procédés. Cependant, le couplage réaction/séparation génère des complexités importantes en termes de dynamique, de contrôle et de supervision qui constituent une barrière pour leur mise en œuvre industrielle. Ces aspects doivent être considérés dès la phase de conception sous peine de concevoir une colonne difficilement contrôlable. Une méthodologie existante est étendue afin d'y intégrer les aspects de contrôlabilité et de diagnosticabilité. L'étape de conception étudie les courbes de résidu et extractives réactives, identifie les paramètres opérationnels et propose des configurations de colonne respectant les spécifications. La meilleure configuration est choisie sur des critères de contrôlabilité par l'analyse de différents indicateurs quantitatifs et qualitatifs identifiés à l'aide de simulations en régime permanent et dynamique. La méthodologie est appliquée à la production industrielle d'acétate d'éthyle. Deux campagnes expérimentales ont permis de fiabiliser le modèle de simulation de la colonne. La méthodologie permet d'identifier les sensibilités et montre que il est possible d'agir sur les trois degrés de liberté de la colonne double alimentation pour atteindre les spécifications industrielles ; les variables contrôlées sont sélectionnées dans des sections spécifiques, similaires pour différentes configurations de colonne. Concernant le diagnostic, l'utilisation de capteurs de composition semble la plus pertinente mais la complexité de leur utilisation industrielle (cout) peut être contournée par la sélection d'un nombre plus important de capteurs de température judicieusement positionnés. Les résultats de contrôlabilité et de diagnosticabilité sont en cohérence et bien intégrés dans la conception des colonnes réactives.

Mots clés: distillation réactive, conception de procédés, simulation dynamique, catalyse hétérogène, contrôlabilité, diagnosticabilité, acétate d'éthyle

Estudo da Integração da controlabilidade e da diagnosticabilidade de colunas de destilação reativa desde a etapa de projeto. Aplicação à produção de acetato de etila.

RESUMO

A destilação reativa é um exemplo emblemático de intensificação de processos. Entretanto, a aplicação simultânea de reação e separação gera complexidades importantes com relação à dinâmica, ao controle e à supervisão criando uma barreira para a implementação industrial desses processos. Esses aspectos devem ser considerados desde a etapa de projeto para evitar a proposta de uma coluna dificilmente controlável. Os trabalhos da tese estendem uma metodologia existente, a fim de integrar os aspectos de controlabilidade e de diagnosticabilidade. A etapa de concepção estuda as curvas de resíduo e as curvas extrativas reativas, identifica parâmetros operacionais e propõe configurações de coluna respeitando as especificações. A melhor configuração é escolhida com base em critérios de controlabilidade pela análise de diferentes indicadores quantitativos e qualitativos identificados com base em simulações dos regimes estacionário e dinâmico. A metodologia é aplicada à produção industrial de acetato de etila. Duas campanhas experimentais adaptaram e validaram o modelo de simulação da coluna. A metodologia permite identificar as sensibilidades e mostra que os três graus de liberdade da coluna com dupla alimentação podem ser manipulados para atender as especificações industriais; as variáveis controladas são selecionadas em seções específicas, similares em diferentes configurações de coluna. Para o diagnóstico, o uso de sensores de composição se mostra mais pertinente, mas a complexidade de sua aplicação industrial (custo) pode ser evitada pela seleção de uma maior quantidade de sensores de temperatura, criteriosamente posicionados. Os resultados de controlabilidade e de diagnosticabilidade são coerentes e foram integrados com sucesso na etapa de projeto das colunas reativas.

Palavras chaves: destilação reativa, projeto de processos, simulação dinâmica, catálise heterogênea, controlabilidade, diagnosticabilidade, acetato de etila

To all the times I crossed the sea... It was worth!

*“Ó mar salgado, quanto do teu sal
São lágrimas de Portugal!
Por te cruzarmos, quantas mães choraram
Quantos filhos em vão rezaram!
Quantas noivas ficaram por casar
Para que fosses nosso, ó mar!”*

*Valeu a pena? Tudo vale a pena
Se a alma não é pequena.
Quem quere passar além do Bojador
Tem que passar além da dor.
Deus ao mar o perigo e o abismo deu
Mas nele é que espelhou o céu.”*

*“Oh salt-laden sea, how much of your salt
Is tears of Portugal!
To cross you, how many mothers wept
How many sons in vain prayed!
How many brides-to-be brides remained
So you were ours, oh Sea!*

*Was it worth? Everything is worth
If the soul is not small.
Whoever wants to go beyond (cape) Bojador
Has to go beyond pain.
To the sea gave God peryl and the abyss
But in it He also mirrored heaven.”*

Mar Português, Fernando Pessoa

My PhD thesis was developed under the supervision of different laboratories, different academic and industrial partners, different countries and cultures. I would like to thank everyone who, somehow, gave me this opportunity and contributed to this great adventure!

To my academic supervisors in Toulouse, Xuan Meyer and Marie-Véronique Le Lann, merci pour votre orientation, complicité et confiance pendant ces dernières années. Votre rigueur et vos conseils, mais aussi votre sensibilité autour de mes séjours en France, ont été essentiels pour le bon déroulement du travail. Je vous exprime toute mon admiration et amitié. Nos visio-conférences vont me manquer ...

To my academic supervisor in São Paulo, Galo Le Roux, obrigada pela vontade em realizar esse projeto, que começou com o intercâmbio entre as Escolas em 2006, sempre ajudando com toda não-tão-simples burocracia e guiando meu trabalho.

To my industrial supervisor in Lyon, Mathias Brehelin, merci pour le savoir transmis, les discussions toujours intéressantes, d'un point de vue professionnel mais aussi personnel, l'ambition et la confiance depuis mes tout premiers pas chez Rhodia en 2008 (maintenant membre du Groupe Solvay).

To the president of the jury Mr Xavier Joulia, qui m'a récupéré à l'aéroport quand je suis arrivée pour débiter mes études en France, il y a déjà 7 ans ... Nous ne pouvions pas imaginer le succès de cette histoire. Merci de l'avoir rendu possible et d'avoir accepté de présider ce moment de conclusion.

To the reviewers of the thesis, Mr Jens Uwe-Repke and Mr Marco Giulietti, thank you for the interest on the work and the attention provided on reading and discussing it.

To Nguyen Huynh, Michel Meyer and Jean-Michel Reneaume, merci pour avoir suivi mes travaux avec grand intérêt et pour avoir accepté de participer au jury de thèse.

To Mr Didier Tanguy and Mr Richard Macret, merci pour votre confiance en mes travaux et pour votre accompagnement dans mes perspectives d'intégration au groupe Solvay au Brésil.

To my family, queridos papai, mamãe e Mariana, obrigada por tudo que me proporcionaram e que me trouxe até aqui. Obrigada por alimentarem esse sonho, compreenderem as saudades, sempre com muito apoio e carinho. Obrigada pelos olhos cheios de orgulho ao assistirem à defesa dessa tese!

To him, who crossed the sea even more times than I did, Ricardo, obrigada por estar sempre pertinho, entendendo e incentivando, mesmo quando longe... Tudo foi muito mais gostoso por termos aproveitado juntos!

To all friends and colleagues who shared some enriching and unforgettable moments in some laboratory during these last years, I thank you and I really hope to keep in touch.



Toulouse, July 2013

Table of Contents

LIST OF FIGURES	XVII
LIST OF TABLES	XXI
INTRODUCTION	XXIII

I. STATE OF THE ART 1

1. REACTIVE DISTILLATION	7
1.1 PROCESS INTENSIFICATION	8
1.2 REACTIVE DISTILLATION	9
1.2.1 Technology issues	12
1.2.2 Design of reactive columns	15
1.2.3 Simulation models	18
1.2.4 Dynamics and control strategies	20
1.3 SIMULTANEOUS DESIGN AND CONTROL OF CHEMICAL PROCESSES	25
1.4 DIAGNOSIS OF COMPLEX PROCESSES	28
1.4.1 Process diagnosis using fuzzy logic	29
1.5 THE STUDY PROPOSED	31
2. THE ETHYL ACETATE SYSTEM	33
2.1 A TECHNICAL PROFILE	34
2.2 SOLVAY CONTEXT	38

II. MATERIALS AND METHODS 39

3. EXPERIMENTAL DEVICES	45
3.1 DEFINITION OF RELIABLE PARAMETERS FOR THE SYSTEM MODEL	46
3.1.1 Pilot characteristics	46
3.1.2 Data acquisition	49
3.2 SENSITIVITY APPROACH IN A REAL REACTIVE COLUMN	51
3.2.1 Pilot characteristics	51
3.2.2 Data acquisition	53
4. DESIGN METHODOLOGY FOR REACTIVE DISTILLATION COLUMNS	55
4.1 SEQUENTIAL APPROACH	56
4.1.1 Feasibility analysis	57
4.1.2 Synthesis step	58
4.1.3 Conceptual design step	59
5. TOOLS AND METHODS TO HANDLE CONTROLLABILITY AND DIAGNOSABILITY ASPECTS	61
5.1 SIMULATION AND CONTROLLABILITY ANALYSIS	62
5.2 PROCESS DIAGNOSIS	62
5.2.1 The fuzzy classification technique LAMDA	62
5.2.2 Sensors selection	66
5.2.3 P3S [®] software	66

III. SYSTEM STEADY STATE AND DYNAMIC MODELING	69
6. MODELING THE SYSTEM WITH EXPERIMENTAL VALIDATION	75
6.1 EXPERIMENTAL DYNAMIC WORKS IN THE LITERATURE	76
6.2 EXPERIMENTAL PROCEDURE.....	77
6.3 EXPERIMENTAL RESULTS	79
6.3.1 Steady state analysis	79
6.3.2 Study of the transient regimes	82
6.4 STEADY STATE MODEL	88
6.4.1 Understanding the adjustable coefficient for reaction efficiency	90
6.4.2 Understanding the adjustable coefficient for heat losses	92
6.5 DYNAMIC MODEL.....	93
6.5.1 Verification of the temperature sensors reliability.....	99
6.5.2 Understanding the adjustable initial values for liquid holdup.....	100
6.6 CONCLUSIONS	102
IV. CONTROLLABILITY METHODOLOGY.....	105
7. THE INDICES-BASED CONTROLLABILITY ANALYSIS.....	111
7.1 SELECTING CONTROLLED VARIABLES	112
7.2 STEADY STATE SIMULATIONS	113
7.2.1 The Sensitivity matrix.....	114
7.2.2 Singular Value Decomposition	115
7.2.3 Condition number	117
7.2.4 Intersivity index.....	119
7.2.5 Loops pairing.....	119
7.3 DYNAMIC SIMULATIONS	122
7.3.1 PID tuning.....	122
7.3.2 Quantitative errors measurement	123
7.4 CONTROLLABILITY CRITERIA	124
8. CONTROLLABILITY STUDY OF A COLUMN CONFIGURATION	125
8.1 APPLICATION EXAMPLE.....	126
8.2 TEMPERATURE INFERENCEIAL CONTROL.....	127
8.3 COMPOSITION CONTROL	135
8.3.1 Simultaneous control of temperature and composition	138
8.3.2 Controlling the product specifications directly	140
8.3.3 Impact of the composition analyzers sensitivity	142
8.4 CONCLUSIONS	146
V. CONTROLLABILITY ANALYSIS AS FROM THE DESIGN STEP	149
9. DESIGN METHODOLOGY FOR THE ETHYL ACETATE REACTIVE SYSTEM	155
9.1 THE DESIGN METHODOLOGY	156
9.2 THERMODYNAMIC STUDY.....	156
9.2.1 Phase equilibrium	156
9.2.2 Kinetics data.....	159

9.3	FEASIBILITY ANALYSIS	160
9.3.1	Reactive residue curves	160
9.3.2	Extractive residue curves	162
9.3.3	Feasible steady states	164
9.4	SYNTHESIS STEP	166
9.5	CONCEPTUAL DESIGN STEP	168
10.	CONTROLLABILITY ANALYSIS OF THE ETHYL ACETATE REACTIVE SYSTEM	171
10.1	INTRODUCTION	172
10.2	CHOICE OF THE COLUMN CONFIGURATION IN FUNCTION OF CONTROLLABILITY	172
10.3	INDUSTRIAL SPECIFICATIONS	178
10.4	COMPARISON OF DIFFERENT COLUMN CONFIGURATIONS	185
10.4.1	Adding separation stages above upper feed stream	186
10.4.2	Adding reactive stages below the lower feed stream	190
10.4.3	Adding reactive stages between feed stages	195
10.5	CONCLUSIONS	199
11.	EXPERIMENTAL UNDERSTANDING OF THE CONTROLLABILITY APPROACH	203
11.1	UNDERSTANDING THE PROCESS DEGREES OF FREEDOM	204
11.2	APPLICATION OF THE CONTROLLABILITY CALCULATIONS	208
VI. DIAGNOSABILITY METHODOLOGY		213
12.	THE DIAGNOSABILITY ANALYSIS	219
12.1	THE SYSTEM BEHAVIORAL MODEL	220
12.1.1	Faults scenarios	220
12.1.2	Diagnosis based on classification methods	222
12.2	SENSORS SELECTION	225
12.3	CONCLUSIONS	229
VII. EPILOGUE		231
CONCLUSIONS AND PERSPECTIVES		237
NOMENCLATURE		243
REFERENCES		247
APPENDICES		259
I.	THERMODYNAMIC STUDY OF THE BINARIES	260
II.	MATHEMATICAL MODELING OF PROCESSES AND ADVANCED CONTROLLERS DESIGN	264
III.	CLASSIFICATION ALGORITHMS	288
IV.	PROGRAMMING CODES MATLAB®	296
V.	DYNAMIC SIMULATIONS	298

List of Figures

Figure 1.1. Classification of multifunctional reactors in relation to the phases present.....	9
Figure 1.2. From the conventional process to the reactive distillation process	9
Figure 1.3. Counter-current vapor-liquid contact in multistage tray (a) and in packed columns (b) (Krishna, 2003).....	13
Figure 1.4. Structured catalyst internals: catalyst bales (a) and structured sandwich packing (b) (Krishna 2003)	14
Figure 1.5. Complexity of the reactive distillation models, based on assumptions of phase or chemical equilibrium.....	19
Figure 2.1. Optimal configuration of the complete EtOAc system (Tang et al. 2003).....	36
Figure 3.1. Simplified scheme of pilot 2011	46
Figure 3.2. Liquid distributor schematic.....	47
Figure 3.3. Reboiler scheme of pilot 2011	48
Figure 3.4. Feed line scheme.....	48
Figure 3.5. Pilot 2011 configuration.....	49
Figure 3.6. Digital control system interface 2011	50
Figure 3.7. Simplified scheme of column 2013.....	52
Figure 3.8. Reboiler scheme of pilot 2013.....	52
Figure 3.9. Schmickler and Fritz bubble cap trays.....	52
Figure 3.10. Pilot 2013 configuration.....	53
Figure 3.11. Digital control system interface pilot 2013	54
Figure 4.1. Constitutive approaches of the design methodology (Théry-Hétreux et al. 2012).....	56
Figure 5.1 : LAMDA algorithm with marginal & global adequacies.....	64
Figure 5.2 Scheme of P3S® diagnosis procedure.....	68
Figure 6.1. Column scheme	78
Figure 6.2. Temperature measures at each distributor, for all tests.....	80
Figure 6.3. Compositions at D5 (a), D4 (b), D3 (c) and D2 (d)	81
Figure 6.4. Temperatures before and after a 10% increase of the external reflux feed flow rate	82
Figure 6.5. Mass compositions at the distillate (a) and at the bottom (b) before and after a 10% increase of the external reflux feed flow rate	83
Figure 6.6. Temperature in liquid distributors before and after a 10% decrease of the external reflux feed flow rate	84
Figure 6.7. Mass compositions at the distillate (a) and at the bottom (b) before and after a 10% decrease of the external reflux feed flow rate	84
Figure 6.8. Temperature in liquid distributors before and after a 10% increase of the acetic acid feed flow rate	85
Figure 6.9. Mass compositions at the distillate (a) and at the bottom (b) before and after a 10% increase of the acetic acid feed flow rate	85
Figure 6.10. Temperature in liquid distributors before and after a 10% increase of the ethanol feed flow rate	86
Figure 6.11. Compositions at the distillate (a) and at the bottom (b) before and after a 10% increase of the ethanol feed flow rate	86
Figure 6.12. Temperature in liquid distributors before and after a reduction of heat duty	87
Figure 6.13. Mass compositions at the distillate (a) and at the bottom (b) before and after a reduction of heat duty	87
Figure 6.14. Mass fractions at the distillate (a) and at the bottom (b).....	89
Figure 6.15. Steady state composition and temperature profiles.....	90

Figure 6.16. Comparison of composition profiles for test n°2 (stoichiometric feed) and n°6 (ethanol excess)	92
Figure 6.17. Influence of heat loss on composition and temperature profiles, test n°1.....	92
Figure 6.18. Experimental versus simulated temperature (a) and distillate mass composition (b) evolution in test n°3	94
Figure 6.19. Experimental versus simulated temperature (a) and distillate mass composition (b) evolution in test n°4	95
Figure 6.20. Experimental versus simulated temperature (a) and distillate mass composition (b) evolution in test n°5	96
Figure 6.21. Experimental versus simulated temperature (a) and distillate mass composition (b) evolution in test n°6	97
Figure 6.22. Experimental versus simulated temperature (a) and distillate mass composition (b) evolution in test n°7	97
Figure 6.23. Comparison of measured and samplings bubble temperatures for test n°3 (a) and test n°4 (b).....	100
Figure 6.24. Experimental and simulated temperature evolution in test n°5, where “Simul” represents the adapted values for the hydrodynamics and “BadSimul” considers the default values.....	102
Figure 8.1. Reactive distillation column scheme for the sensitivity analysis	126
Figure 8.2. Sensitivity matrix considering only temperature sensors.....	128
Figure 8.3. Singular vectors matrix considering only temperature sensors	129
Figure 8.4. Dual-ended inferential control variables after an increase of water in the ethanol feed flow	131
Figure 8.5. Dual-ended inferential control product specifications after an increase of water in the ethanol feed flow.....	131
Figure 8.6. Triple-ended inferential control variables after an increase of water in the ethanol feed flow.....	134
Figure 8.7. Triple-ended inferential control product specifications after an increase of water at the ethanol feed flow ...	134
Figure 8.8. Sensitivity matrix considering each component compositions sensors.....	135
Figure 8.9. Singular vectors matrix considering all column sensors.....	136
Figure 8.10. Composition control variables after an increase of water in the ethanol feed flow	137
Figure 8.11. Composition control product specifications after an increase of water in the ethanol feed flow.....	138
Figure 8.12 Temperature and composition control variables after an increase of water in the ethanol feed flow.....	139
Figure 8.13. Temperature and composition control product specifications after an increase of water in the ethanol feed flow	140
Figure 8.14. Specification control variables after an increase of water in the ethanol feed flow.....	141
Figure 8.15. Sensitivity matrix considering each component compositions sensors with 3 types of analyzers	143
Figure 8.16. Singular vectors matrix considering all column sensors with 3 types of analyzers	143
Figure 8.17. Three-analyzer composition control variables after an increase of water in the ethanol feed flow.....	145
Figure 8.18. Three-analyzer composition control product specifications after an increase of water in the ethanol feed flow	146
Figure 9.1. General principle of the design methodology	156
Figure 9.2. Iso-temperature lines for the ternary mixture EtOH-EtOAc-H ₂ O.....	157
Figure 9.3. Liquid-liquid envelopes for the ternary mixtures (Tang et al. 2005a)	157
Figure 9.4. rRCM of the system HOAc + EtOH \Leftrightarrow EtOAc + H ₂ O	161
Figure 9.5. Locus of the rRCM unstable point for different values of pressure	162
Figure 9.6. rExCM of the system HOAc + EtOH \Leftrightarrow EtOAc + H ₂ O.....	163
Figure 9.7. Locus of the rExCM unstable point for different values of Fu/V.....	163
Figure 9.8. Feasibility analysis of the double-feed configuration.....	165
Figure 9.9. Composition profiles obtained from Synthesis step, column with 16 stages	167
Figure 9.10. Composition profiles obtained from Synthesis step, column with 21 stages	167
Figure 9.11. (a) composition and (b) EtOAc generation profiles from Conceptual Design step, column with 16 stages	168
Figure 9.12. (a) composition and (b) EtOAc generation profiles from Conceptual Design step, column with 21 stages	169

Figure 9.13. (a)molar and (b)transformed composition profiles from Conceptual Design step, column with 16 stages ...	168
Figure 9.14. (a)molar and (b)transformed composition profiles from Conceptual Design step, column with 21 stages ...	169
Figure 10.1. Column Design16 scheme	173
Figure 10.2. Sensitivity matrices of column Design16.....	174
Figure 10.3. Singular vectors matrix considering only temperature sensors, column Design16.....	174
Figure 10.4. Singular vectors matrix considering all sensors, column Design16.....	175
Figure 10.5. Column Design21 scheme	175
Figure 10.6. Sensitivity matrices of column Design21.....	176
Figure 10.7. Singular vectors matrix considering only temperature sensors, column Design21.....	177
Figure 10.8. Singular vectors matrix considering all sensors, column Design21.....	177
Figure 10.9. Column Design28 scheme	180
Figure 10.10. Mass compositions and transformed composition column Design28 profile.....	180
Figure 10.11. Steady state regime details for column Design28.....	181
Figure 10.12. Inferential control variables after a decrease of acid feed flow rate, column Design28.....	182
Figure 10.13. Inferential control specifications after a decrease of acid feed flow rate, column Design28.....	182
Figure 10.14. Composition control variables after a decrease of acid feed flow rate, column Design28	182
Figure 10.15. Composition control specifications after a decrease of acid feed flow rate, column Design28	183
Figure 10.16. Inferential control variables after an increase of acid feed flow rate, column Design28.....	183
Figure 10.17. Inferential control specifications after an increase of acid feed flow rate, column Design28.....	184
Figure 10.18. Composition control variables after an increase of acid feed flow rate, column Design28	184
Figure 10.19. Composition control specifications after an increase of acid feed flow rate, column Design28	184
Figure 10.20. Column Design30a scheme	186
Figure 10.21. Sensitivity matrices of column Design30a.....	186
Figure 10.22. Singular vectors matrix considering only temperature sensors, column Design30a.....	187
Figure 10.23. Inferential control variables after an increase of acid feed flow rate, column Design30a.....	188
Figure 10.24. Inferential control specifications after an increase of acid feed flow rate, column Design30a	188
Figure 10.25. Singular vectors matrix considering all sensors, column Design30a.....	189
Figure 10.26. Composition control variables after an increase of acid feed flow rate, column Design30a	190
Figure 10.27. Composition control specifications after an increase of acid feed flow rate, column Design30a	190
Figure 10.28. Column Design30b scheme	190
Figure 10.29. Sensitivity matrices of column Design30b.....	191
Figure 10.30. Singular vectors matrix considering only temperature sensors, column Design30b.....	192
Figure 10.31. Inferential control variables after an increase of acid feed flow rate, column Design30b.....	192
Figure 10.32. Inferential control specifications after an increase of acid feed flow rate, column Design30b	193
Figure 10.33. Singular vectors matrix considering all sensors, column Design30b.....	193
Figure 10.34. Composition control variables after an increase of acid feed flow rate, column Design30b	194
Figure 10.35. Composition control specifications after an increase of acid feed flow rate, column Design30b	194
Figure 10.36. Column Design30c scheme.....	195
Figure 10.37. Sensitivity matrices of column Design30c.....	195
Figure 10.38. Singular vectors matrix considering only temperature sensors, column Design30c	196
Figure 10.39. Inferential control variables after an increase of acid feed flow rate, column Design30c	196
Figure 10.40. Inferential control specifications after an increase of acid feed flow rate, column Design30c.....	197

Figure 10.41. Singular vectors matrix considering all sensors, column Design30c	197
Figure 10.42. Composition control variables after an increase of acid feed flow rate, column Design30c.....	198
Figure 10.43. Composition control specifications after an increase of acid feed flow rate, column Design30c	198
Figure 10.44. Temperature and Composition control variables after an increase of acid feed flow rate, column Design30c.....	199
Figure 10.45. Temperature and Composition control specifications after an increase of acid feed flow rate, column Design30c.....	199
Figure 11.1. Configuration and instrumentation of a typical industrial distillation column	205
Figure 11.2. Configuration and instrumentation of the pilot distillation column.....	206
Figure 11.3. Experimental unstable behaviors of (a) streams flow rates and (b) column temperatures	207
Figure 11.4. Sensitivity matrices of the pilot column	209
Figure 11.5. Singular vectors matrix considering the temperature sensors of the pilot column.....	210
Figure 11.6. Experimental stable behaviors of (a) streams flow rates and (b) column temperatures	212
Figure 12.1. Simulated fault scenario	221
Figure 12.2. Descriptors population represented by all the system measurements	222
Figure 12.3. 14 classes resulting from self-learning classification of all the process sensors	223
Figure 12.4. Descriptors population represented by system temperatures and manipulated variables measurements	224
Figure 12.5. 10 classes resulting from self-learning classification without composition sensors	224
Figure 12.6. 14 classes resulting from supervised-learning classification without composition sensors.....	225
Figure 12.7. Descriptors population represented by the selected sensors	228
Figure 12.7. 14 classes resulting from supervised-learning classification with the sensors selected.....	228
Figure C.1. Sequence of tools and methods used for the design methodology.....	240
Figure AI.1. Binary xy and boiling temperature diagrams of the system ethanol – acetic acid	260
Figure AI.2. Binary xy and boiling temperature diagrams of the system water – acetic acid.....	261
Figure AI.3. Binary xy and boiling temperature diagrams of the system ethyl acetate – acetic acid	261
Figure AI.4. Binary xy and boiling temperature diagrams of the system ethyl acetate – water.....	262
Figure AI.5. Binary xy and boiling temperature diagrams of the system ethyl acetate – ethanol.....	262
Figure AI.6. Binary xy and boiling temperature diagrams of the system ethanol – water.....	263
Figure AII.1: Closed-loop system used to apply the IMC methodology	277
Figure AIII.1 Scheme of LAMDA calculations	288
Figure AIII.2 Scheme of LAMDA classification algorithm	293
Figure AIII.3 Scheme of sensors selection by the membership margin criterion	295
Figure AV.1. Inferential control variables after an increase of water in ethanol feed, column Design30a.....	298
Figure AV.2. Inferential control specifications after an increase of water in ethanol feed, column Design30a.....	298
Figure AV.3. Inferential control variables after a decrease of acid feed flow rate, column Design30a	299
Figure AV.4. Inferential control specifications after decrease of acid feed flow rate, column Design30a	299
Figure AV.5. Composition control variables after an increase of water in ethanol feed, column Design30a	299
Figure AV.6. Composition control specifications after increase of water in ethanol feed, column Design30a	300
Figure AV.7. Composition control variables after a decrease of acid feed flow rate, column Design30a	300
Figure AV.8. Composition control specifications after a decrease of acid feed flow rate, column Design30a.....	300
Figure AV.9. Inferential control variables after an increase of water in ethanol feed, column Design30b.....	301
Figure AV.10. Inferential control specifications after an increase of water in ethanol feed, column Design30b.....	301

Figure AV.11. Inferential control variables after a decrease of acid feed flow rate, column Design30b	302
Figure AV.12. Inferential control specifications after a decrease of acid feed flow rate, column Design30b	302
Figure AV.13. Composition control variables after an increase of water in ethanol feed, column Design30b	302
Figure AV.14. Composition control specifications after an increase of water in ethanol feed, column Design30b	303
Figure AV.15. Composition control variables after a decrease of acid feed flow rate, column Design30b.....	303
Figure AV.16. Composition control specifications after a decrease of acid feed flow rate, column Design30b.....	303
Figure AV.17. Inferential control variables after an increase of water in ethanol feed, column Design30c.....	304
Figure AV.18. Inferential control specifications after an increase of water in ethanol feed, column Design30c.....	304
Figure AV.19. Inferential control variables after a decrease of acid feed flow rate, column Design30c.....	305
Figure AV.20. Inferential control specifications after a decrease of acid feed flow rate, column Design30c	305
Figure AV.21. Composition control variables after an increase of water in ethanol feed, column Design30c.....	305
Figure AV.22. Composition control specifications after an increase of water in ethanol feed, column Design30c.....	306
Figure AV.23. Composition control variables after a decrease of acid feed flow rate, column Design30c	306
Figure AV.24. Composition control specifications after a decrease of acid feed flow rate, column Design30c.....	306
Figure AV.25. Temperature and composition control variables after an increase of water in ethanol feed, column Design30c.....	307
Figure AV.26. Temperature and composition control specifications an increase of water in ethanol feed, column Design30c.....	307
Figure AV.27. Temperature and composition control variables after a decrease of acid feed flow rate, column Design30c.....	308
Figure AV.28. Temperature and composition control specifications after a decrease of acid feed flow rate, column Design30c.....	308

List of Tables

Table 6.1. Operational parameters of tests	79
Table 6.2. Product stream compositions.....	79
Table 6.3. Reactant conversion rates.....	80
Table 6.4. Parameters defined in the Aspen Plus® steady state model	88
Table 6.5. Adjustable coefficient for reaction efficiency	89
Table 6.6. Initial stage liquid fraction for each packing present at the column	101
Table 7.1. Recapitulation of the controllability criteria.....	124
Table 9.1. Binary parameters for the NRTL model.....	157
Table 9.2. Azeotropic data	157
Table 9.3. Kinetic data	160
Table 9.4. Attainable product compositions provided in the Feasibility Analysis step.....	166
Table 10.1. Controllability criteria for the column configuration analysis	200
Table 10.2. Controllability criteria for the column configuration analysis	200
Table 12.1. Rank of the most relevant sensors among all the column measurements.....	226
Table 12.2. Rank of the most relevant sensors among the temperature and manipulated variable measurements	226

Introduction

In chemical and petrochemical industries not only economic issues, such as energy consumption or product purity, are to be considered, but also environmental and sustainable issues are important so as to avoid products out of their specifications or accidents in the plant. These industries have invested time and money in research activities and innovation, being highly receptive to new technologies. The development of modern equipment based on smaller devices, new scientific principles and production methods is known as process intensification.

In this context of process intensification, the reactive distillation is established as a promising technology. In this process, reaction and distillation phenomena are implemented simultaneously in one column, increasing reaction conversion, reducing capital and investment costs and consuming lower resources. This technique is especially adapted to equilibrium-limited reactions such as esterification reactions. In fact, a key issue in the production of esters is the low reaction conversion and, as a result, heavy capital investments and high energy consumption are unavoidable. Reactive distillation becomes thus a very attractive way to reduce these costs.

Although reactive distillation processes show significant advantages, the combination of reaction and separation leads to complex phenomena inside the column. The number of measurements and operational degrees of freedom are also reduced, causing high coupling between the variables. Moreover, these couplings result on high non-linearity in the system. The closed-loop dynamics and, consequently, the control of such processes become a challenge for its successful industrial application.

The typical design of a distillation column stands on the sequential proposition of the column configuration, based on ideal economic and environmental criteria, and the further control strategy, so as to respond well to the possible disturbances the system may encounter. However, the literature concerning control of reactive systems highlights that the methods developed for distillation columns are not directly transposable to reactive distillation columns: when the dynamic aspects of the reactive column are not considered at the early design steps, the result may be a unity very difficult to control.

The objective of this study is to provide an entire methodology for the design of reactive distillation processes that considers controllability and diagnosability aspects as from the early conceptual phase. Some heuristic key rules and column characteristics which provide better operable systems are identified. The methodology relies on a sequential and progressive introduction of process complexity and the use of different in-house tools and a commercial process simulator.

The PhD work was developed under supervision of different academic and industrial laboratories, taking advantage of each knowledge expertise.

- The Laboratoire de Génie Chimique (LGC, France) develops a methodology and the required tools for the pre design of reactive distillation columns, which mixes different techniques proposed in the literature. It is based on the process static analysis and has been applied on several academic and industrial applications.
- The Laboratoire d'Analyse et d'Architecture des Systèmes (LAAS, France) is a reference on process control and diagnosis. Fuzzy classification techniques and tools for process diagnosis and supervision have been developed in this research center.
- The activities developed at the Laboratório de Simulação e Controle de Processos (LSCP), or Centro de Estudos de Sistemas Químicos (CESQ, Escola Politécnica da Universidade de São Paulo, Brazil), are directed towards the modeling, optimization and control of chemical processes of industrial significance.
- The Solvay Research and Innovation Center (France) experts are recognized for their skills in materials, polymerization synthesis and processes, catalysis, physico-chemistry, process safety and chemical engineering, environment, analytical techniques, knowledge management and industrial property. Pilot-scale reactive columns are available for the experimental approaches.

The PhD manuscript is presented through seven Parts:

Part I presents the state of the art, beginning by an introduction on the process intensification approach, followed by the features of the reactive distillation process, with its interests, challenges, technologies and the recent advances on process design, modeling, control and diagnosis. The ethyl acetate system with its respective works on design and control are also discussed.

The materials and methods, concerning the experimental devices, the computational tools and the techniques used at each step of the design methodology are detailed in Part II.

The objective of Part III is the definition of a reliable simulation model, based on experimental data obtained from a real pilot-scale reactive column for the heterogeneously catalyzed production of ethyl acetate. The assessment of column configuration, operating and hydrodynamic parameters allows the definition of steady-state and dynamic models which represents well the process tendencies and

behaviors. The responses to different disturbances are analyzed and a detailed discussion of the hydrodynamics and the heterogeneous catalyst complexities is conducted.

Part IV deals with the indices-based method to analyze process controllability, based on the simulation model. Different qualitative and quantitative criteria are identified from the literature and adapted to the reactive distillation column specific case. The control structure selection starts with the sensitivity analysis of the different outputs with respect to the inputs available for control. Three degrees of freedom of the double-feed column are manipulated and control loops are identified to show high sensitivity, good balances and small interferences. The methodology is applied to the production of ethyl acetate, highlighting the specific sensitivities. The control configuration proposed is subjected to validation via dynamic simulations with respect to the key regulatory tasks.

In Part V, the entire design methodology is applied to the ethyl acetate system, with consideration of the real product specifications and system perturbations. The thermodynamic feasibility analysis studies the reactive residue curves and the reactive extractive curves. Synthesis step identifies reliable operating parameters and proposes feasible column configurations. Steady state simulations reflect the process sensitivities and the controllability criteria are calculated in function of different feasible column configurations. The system dynamic simulation is then studied, by considering the properly chosen control loops. Heuristics key-rules are identified with the objective of designing better controllable columns. A second experimental study is conducted so as to exemplify the controllability calculations.

Part VI presents the approach for the diagnosability analysis of the proposed reactive column based on iterative classification methods. With data obtained from the ethyl acetate process simulation, the sensor placement procedure allows the selection of key measurement locations to rapidly detect abnormal operating conditions. The importance of each sensor is understood as from the design step.

Finally, the main contributions are synthesized in the conclusion and some work perspectives are suggested. General nomenclature, references and appendices are given at the end of the manuscript.

FIRST PART

I. STATE OF THE ART

1.	Reactive distillation	7
2.	Ethyl acetate system	33

This part outlines the scientific context in which the work is performed. The concepts regarding the process intensification approach are presented and the reactive distillation system is discussed in depth in chapter 1. The process advantages, challenges and technology are mentioned, followed by the recent advances regarding its design, modeling, control and diagnosis. Chapter 2 deals with the interests and studies developed for the production of ethyl acetate by reactive distillation, which is our industrial case study.

C'est dans le cadre du développement durable et de la compétitivité de l'industrie chimique que s'inscrit l'intensification des procédés. Stakiewicz et Moulijn (2000) ont défini l'intensification des procédés comme étant le développement de nouveaux équipements ou de nouvelles techniques qui, comparées aux techniques couramment utilisées, permettront de diminuer de façon conséquente le rapport taille des équipements/ capacité de production, la consommation d'énergie et la formation de produits indésirables de façon à aboutir à une technologie plus sûre et moins coûteuse.

Les méthodes liées à l'intensification de procédés regroupent les séparations hybrides, les réacteurs multifonctionnels, l'utilisation de sources d'énergie non conventionnelles et diverses autres méthodes de mesure et de contrôle. Parmi les réacteurs multifonctionnels qui regroupent la réaction avec un transfert de matière, on peut identifier un tout particulièrement attractif : la distillation réactive.

Le procédé de distillation réactive est la mise en œuvre simultanée des opérations de réaction et de distillation multi étagée dans un même appareil. Les avantages de la distillation réactive concernent l'augmentation de la conversion due au déplacement de l'équilibre chimique, la meilleure sélectivité réactionnelle, une séparation facilitée car les réactions chimiques peuvent éliminer certains azéotropes ordinaires présents dans le mélange non réactif, l'intégration énergétique et l'économie d'échelle quand les recyclages ne sont plus nécessaires, etc. Cependant, la mise en œuvre d'un procédé de distillation réactive, combinant réaction et séparation, n'est pas toujours économiquement et/ou techniquement avantageuse et il faut s'assurer que le système présent satisfait un certain nombre de critères, tels que la cohérence entre les températures opératoires, les vitesses de réaction, les écarts de volatilité entre les réactifs et les produits, la durée de vie du catalyseur, etc.

Pour accéder à la faisabilité et à la conception des procédés de distillation réactive, chercheurs académiques et industriels proposent des outils basés sur des études thermodynamiques, cinétiques et hydrodynamiques et développent des méthodologies et logiciels pour la conception, la simulation, l'optimisation et le contrôle de ces procédés.

Cependant, les importants couplages entre les phénomènes de réaction et séparation, et les fortes intégrations des bilans massiques et énergétiques sont des défis pour la conception des colonnes réactives. Selon Huss et al. (1999) et Théry-Hétreux et al. (2005a), toutes les méthodes de conception incluent les trois étapes suivantes: l'analyse de faisabilité, la synthèse du procédé et la conception proprement dite. Les techniques développées peuvent être classifiées dans 3 catégories (Almeida-Rivera

et al. 2004b, Li et al. 2012) : (i) les méthodes graphiques, (ii) les méthodes d'évolution heuristiques, et (iii) les méthodes d'optimisation.

Due à la complexité des procédés intensifiés, résultante des fortes intégrations entre des phénomènes simultanés, lorsque la conception du procédé est menée avec des analyses statiques, en regardant uniquement les aspects économiques et environnementaux, la colonne proposée peut être très difficilement contrôlable. La contrôlabilité d'un procédé peut être définie comme la facilité avec laquelle l'unité peut être maintenue dans un état stationnaire spécifique. Pour améliorer les caractéristiques menant à une bonne contrôlabilité, deux méthodes principales existent : les méthodes basées sur l'optimisation et les méthodes séquentielles avec des indices qui permettent d'anticiper le comportement.

En plus de la contrôlabilité du procédé, la diagnosticabilité doit aussi être considérée. La diagnosticabilité peut être définie comme l'habilité à détecter des conditions opératoires normales et anormales, afin d'éviter des pertes de performance, de prévenir des arrêts de l'unité et de d'assurer un fonctionnement avec des conditions opératoires propres en toute sécurité.

L'objectif de la thèse est donc d'intégrer différentes techniques et proposer une méthodologie complète pour la conception de procédés de distillation réactive en considérant des aspects de contrôlabilité et de diagnosticabilité dès les premières étapes de sa conception.

Cette méthodologie repose tout d'abord sur la méthodologie développée au LGC (Laboratoire de Génie Chimique, Toulouse, France) pour la conception d'une colonne thermodynamiquement viable. L'analyse de faisabilité et la synthèse du procédé sont menées par des méthodes graphiques. Puis, grâce à l'un logiciel de simulation de la colonne, on regarde les aspects stationnaires et dynamiques. La sensibilité du procédé aux différentes perturbations pouvant l'affecter est étudiée et une méthode d'analyse de contrôlabilité par le calcul des indices est réalisée pour différentes configurations faisables, en identifiant les caractéristiques de la colonne les plus appropriées en termes de contrôlabilité. Les données de simulation dynamique sont la base pour les calculs de la diagnosticabilité, qui suit la méthodologie développée au LAAS (Laboratoire d'Analyse et d'Architecture des Systèmes, Toulouse, France) sur la base de techniques de classification en logique floue.

La méthodologie est appliquée à la production d'acétate d'éthyle par esterification de l'acide acétique et de l'éthanol. Des règles heuristiques sont identifiées pour améliorer la contrôlabilité et la diagnosticabilité dès la phase de conception du procédé.

No contexto do desenvolvimento sustentável e da competitividade da indústria química, surge a intensificação de processos. Stakiewicz e Moulijn (2000) definiram intensificação de processos como sendo o desenvolvimento de novos equipamentos e de novas técnicas que, comparadas às técnicas convencionalmente utilizadas, permitirão diminuir significativamente a relação entre o tamanho dos equipamentos e a capacidade de produção, o consumo de energia e a formação de produtos indesejáveis de maneira a obter tecnologias mais seguras e menos custosas.

Os métodos relacionados à intensificação de processos agrupam as separações híbridas, os reatores multifuncionais, o uso de fontes de energia não convencionais e outros métodos diversos de medição e de controle. Entre os reatores multifuncionais, nos quais a reação ocorre simultaneamente com outra operação, pode-se identificar um caso particularmente atrativo: a destilação reativa.

O processo de destilação reativa consiste na implementação simultânea de operações de reação e de destilação em um mesmo aparelho. As vantagens da destilação reativa são o aumento da conversão graças ao deslocamento do equilíbrio químico, uma melhor seletividade reacional, a separação é facilitada quando as reações químicas eliminam alguns azeótropos presentes na solução não reativa, a integração energética, a economia de escala dado que reciclagens não são mais necessárias, etc. Entretanto, a implementação do processo de destilação reativa, combinando reação e separação, nem sempre é economicamente e/ou tecnicamente vantajosa; deve-se assegurar que o sistema considerado satisfaça a uma certa quantidade de critérios, tais como a coerência entre as temperaturas de operação, as velocidades de reação, as diferenças de volatilidade entre os reagentes e os produtos, o tempo de vida do catalisador, etc.

Para garantir viabilidade e confiança no projeto de processos de destilação reativa, pesquisadores acadêmicos e industriais propõem ferramentas baseadas em estudos termodinâmicos, cinéticos e hidrodinâmicos e desenvolvem metodologias e softwares para a modelagem, simulação, otimização e controle desses processos.

Entretanto, a coexistência dos fenômenos de separação e de reação e a forte interação entre os balanços de massa e energia constituem desafios importantes para o projeto de colunas reativas. De acordo com Huss et al. (1999) e Théry-Hétreux et al. (2005a), todos os métodos de projeto incluem as três etapas seguintes: a análise de viabilidade, a síntese do processo e a concepção. As técnicas já

desenvolvidas podem ser classificadas em três categorias (Almeida-Rivera et al. 2004b, Li et al. 2012): (i) os métodos gráficos, (ii) os métodos heurísticos evolutivos, e (iii) os métodos de otimização.

Dada a complexidade dos processos intensificados, resultante das fortes interações entre os diferentes fenômenos, quando o projeto do processo é realizado com base em análises estacionárias, considerando apenas aspectos econômicos e ambientais, a coluna proposta pode ser de difícil controle. A controlabilidade de um processo, portanto, pode ser definida como a facilidade com a qual a unidade é mantida em um regime estacionário específico. Para melhorar as características que conduzem à boa controlabilidade, dois métodos principais existem: os métodos baseados em otimização e os métodos sequenciais com índices que permitem antecipar o comportamento.

Além da controlabilidade do processo, a diagnosticabilidade também deve ser considerada. A diagnosticabilidade pode ser definida como a habilidade em detectar as condições de operação normais e anormais, com o objetivo de evitar perdas de desempenho, de prevenir paradas da unidade e de assegurar um funcionamento em condições de operação totalmente seguras.

O objetivo da tese é o de identificar e integrar diferentes técnicas e propor uma metodologia completa para o projeto de colunas de destilação reativas considerando aspectos de controlabilidade e de diagnosticabilidade desde as primeiras etapas de sua concepção.

Essa metodologia se baseia inicialmente na metodologia desenvolvida no LGC (Laboratoire de Génie Chimique, Toulouse, France) para o projeto de uma coluna termodinamicamente viável. A análise de viabilidade e a síntese do processo são realizadas por métodos gráficos. Em seguida, graças a um software de simulação da coluna, aspectos estacionários e dinâmicos são observados. A sensibilidade do processo em relação a diferentes perturbações potenciais é estudada e um método de análise de controlabilidade pelo cálculo de índices é implementado para diferentes configurações viáveis, identificando assim as características mais apropriadas da coluna em relação à controlabilidade. Os dados adquiridos com a simulação dinâmica servem de base para os cálculos de diagnosticabilidade, que seguem a metodologia desenvolvida no LAAS (Laboratoire d'Analyse et d'Architecture des Systèmes, Toulouse, France) com base em técnicas de classificação com lógica difusa.

A metodologia é aplicada à produção de acetato de etila por esterificação de ácido acético e etanol. Regras heurísticas são identificadas para melhorar a controlabilidade e a diagnosticabilidade desde a etapa de projeto do processo.

CHAPTER

1

Reactive Distillation

1.1 PROCESS INTENSIFICATION

Sustainable development is defined as a pattern of resource use that aims to meet human needs while preserving the environment so that these needs can be met not only in the present, but in the indefinite future. Sustainable development seeks a balance between economic improvement and environmental protection.

In chemical engineering, sustainable development is mainly applied by improving security, employing resources effectively and minimizing investment and production costs. A successful way of achieving these goals lies in process intensification. Process intensification, which promotes technological innovation, is an alternative to the industry growing strategy via trade (merger, splitter, takeovers,...). It consists in a new approach to process design that considers the interactions among different unit operations from the outset, rather than optimizing them separately. These advances are clearly encouraged by the competitiveness among chemical industries.

Process intensification can be present at all steps of the production chain: stock, reaction, separation, product isolation and analysis, drying, packing, etc. Generally, it is achieved through the definition of new specific equipment or new methods. The former approach is the development of new devices so as to attain the intensification objectives; the latter is based on a different exploration of the existing equipment.

The methods conceived in the frame of process intensification can be classified into three categories: hybrid operations (such as distillation with membranes, Gomez et al. 2009), multifunctional reactors (such as reactors with chromatography, reactors with membranes or reactive distillation, They et al. 2002) and the use of non-conventional energy sources (such as solar energy, ultrasound). Among multifunctional reactors, the reactive separation principle has been frequently applied in academic and industrial studies: in the same device in which the chemical reaction occurs, at least one separation operation is added. This operation may be based on mass transfer, momentum, phase splitting, etc. A classification of the multifunctional reactors in function of the number and the nature of the phases present was given by Agar (1999) and is designed in Figure 1.1.

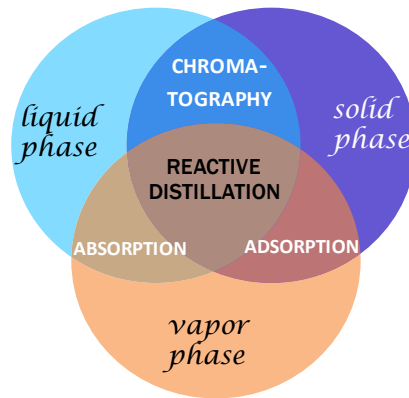


Figure 1.1. Classification of multifunctional reactors in relation to the phases present

1.2 REACTIVE DISTILLATION

In recent years, increasing attention has been directed towards reactive distillation (RD) processes as a successful multifunctional reactor example. Reactive distillation means the simultaneous implementation of reaction and distillation in a counter-current operated column, where chemical equilibrium can be superimposed on vapor liquid equilibrium.

This technique is especially useful for equilibrium-limited reactions; conversion can be increased far beyond what is expected from thermodynamic equilibrium due to the continuous removal of reaction products from the reactive zone by distillation. This integration helps to reduce capital and investment costs and may be important for sustainable development due to a lower consumption of resources.

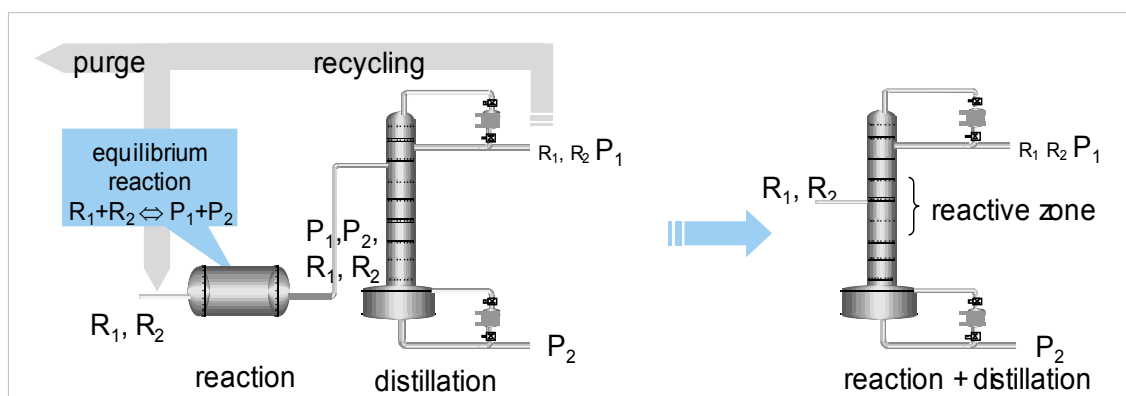


Figure 1.2. From the conventional process to the reactive distillation process

Sharma and Mahajani (2003) give a detailed review of the candidate reactions which have been investigated for reactive distillation and the respective authors. The large number of reactions account for etherifications, esterifications, synthesis of acetates, transesterifications, hydrolysis, acetalizations,

hydrations, dehydrations, alkylations, dealkylations, isomerizations, chlorinations, hydrogenations, dehydrogenations, carbonylations, laminations, alcoholysis, etc.

The main advantages of the reactive distillation process were organized by Harmsen (2007) according to the Triple *P* (*Profit, Planet, People*). Existing reactive distillation process applications have been showing important savings in capital and energy costs from 15% to 80% in comparison to conventional applications, in which a reactor is followed by several distillation columns (Rock 2002, Siirola 1996, Harmsen 2003, 2004). The most emblematic and successful industrial example of reactive distillation is the Eastman-Kodak process developed for the production of methyl acetate, in which both investment and operating costs have been divided by five compared to the former process (Agreda et al 1990).

The main business drivers are the economical advantages (*Profit*) listed as:

- Higher conversion due to the continuous displacement of the chemical equilibrium as a result of products being removed from the column by distillation,
- Lower feedstock costs due to better selectivity; some secondary reactions can be neglected and thus less byproducts to be separated,
- Higher production quality; products are heated only once, reducing thermal degradation risks in comparison to sequential heating in reactors and separation columns,
- Scale economy; the costs with pumps, valves, tubing and other instrumentation are reduced when recycling is not needed,
- Energy requirement reduction due to heat integration; now only one device is heated and the heat provided by exothermal reactions can be used in separation phenomena,
- Longer catalyst life duration; the column temperatures are limited to the bubble temperature of the solution,
- Easier separation; chemical reaction can eliminate some physical azeotropes present at the non-reactive solution and distillation limits can be overcome owing to the reaction.

As environmental advantages (*Planet*), the following are highlighted:

- Lower gas emissions due to the reduction of equipment and connections,
- Reduction of carbon dioxide emissions because less energy is required.

The social acceptance (*People*) is also of crucial interest:

- Improvements in safety, health and society impact by the need of lower reactive content,
- Higher reliability of the system, due to lower space occupation, less rotating equipment and less equipment in general, requiring less maintenance,
- The heat of the reaction is removed by evaporation; hence a higher reaction rate results at a higher evaporation rate with few changes in reaction temperature. Runaway behavior of a reactive distillation is therefore generally less severe than that of a conventional reactor.

However, the application of a reactive distillation process, combining the phenomena of separation and reaction, is not always economically and/or technically advantageous. This combination is possible only if the conditions for both operations can be combined. These system characteristics must satisfy:

- The favorable temperatures for reaction should be compatible with the temperatures that are favorable for separation,
- The difference in volatility between components should be such that the reactants can remain in the column while the products can be easily removed as the separation products,
- The reaction rate should be reasonably large so as to limit the necessary liquid holdup and column geometry,
- Reactive distillation is adapted to equilibrium-limited or competitive reactions,
- Rather for liquid-phase reactions because there is very little holdup in the vapor phase,
- In the case of heterogeneous catalysis, the catalyst life cycle should be coherent with the reaction and the economic viability of the process.

Reactive distillation is a complex system in which the combination of separation and reaction zones leads to complex interactions between vapor-liquid equilibrium, mass transfer rates, diffusion and chemical kinetics. Harmsen (2007) stated what he identified as the main barriers for commercial application of the process:

- Great challenge for process synthesis and design, due to the different phenomena simultaneously present. Methods and software facilitating the design become increasingly more sophisticated and a large number of commercial applications show that the design problems have been solved for equilibrium-limited reactions. For irreversible reactions, no method and little information for conceptual design are available in the open literature,

- The phenomena interactions result in important nonlinearities in the process dynamics and few degrees of freedom in comparison to the conventional process, which makes its control and diagnosis difficult. Only dynamic simulations would provide feasible and reliable control designs, adding important difficulty. In the process intensification context, a feasible configuration for operation may not be an easy controllable column,
- Need of expensive pilot plant development for validation. This step is of strong importance to acquire reliable information on mass transfer, pressure drop, hydrodynamics, etc. However, currently pilot plants of modest sizes give limited representation of the real process and scale-up knowledge is willing to reduce risks and costs. Hence validated scale-up knowledge is needed,
- Difficulty in starting-up and in operating. So as to obtain successful start-up and shut-down phases, an entire dynamic behavior analysis would be necessary.

1.2.1 *Technology issues*

In addition to the focus given to the conceptual design and modeling of the RD process, special attention is also paid to equipment design and catalysis. Within the scope of conventional distillation, there is a large variety of possible equipment and internals. For RD systems, more detailed information is needed to understand hydrodynamics and mass transfer under the specific vapor-liquid conditions. Here the concepts underlying the selection of the most appropriate catalyst and hardware are discussed.

Homogeneous catalysis

The easiest way to turn a conventional distillation column into a reactive column is to feed a liquid catalyst at the top of the device. The technique is known as homogeneous catalysis and has been used since 1920 for the production of methyl acetate by the Eastman Kodak process. Some important characteristics can be listed:

- Schoenmaker and Bessling (2003) claimed that homogeneous catalysis allows the reaction velocity to be influenced by changing the catalyst concentration; thus, the reaction can be adapted over a wide rate range to the needs of the distillation equipment,
- The liquid catalyst can be introduced mixed with any other process feed stream,

- The use of homogeneous catalysis increases the size and the operation costs of the column because greater holdups are necessary to reach the reaction chemical equilibrium,
- Homogeneous catalysis is commonly given by the use of strong acids, which can cause important corrosion if the column materials are not well adapted,
- Additional costs for an extra separation step are necessary for catalyst recycling,
- Due to common high volatilities of the acid catalysts, the column configurations are restricted to the ones with reactive zone at all stages located below the liquid catalyst feed. Stages solely dedicated to separation are only enabled above the catalyst feed.

To reach an important liquid holdup at each column stage necessary to perform the reaction, the most appropriate technology is the tray column. The use of packing columns is possible only when the reaction rate is relatively fast which allows small liquid holdups. Possible hardware are presented in Figure 1.3.

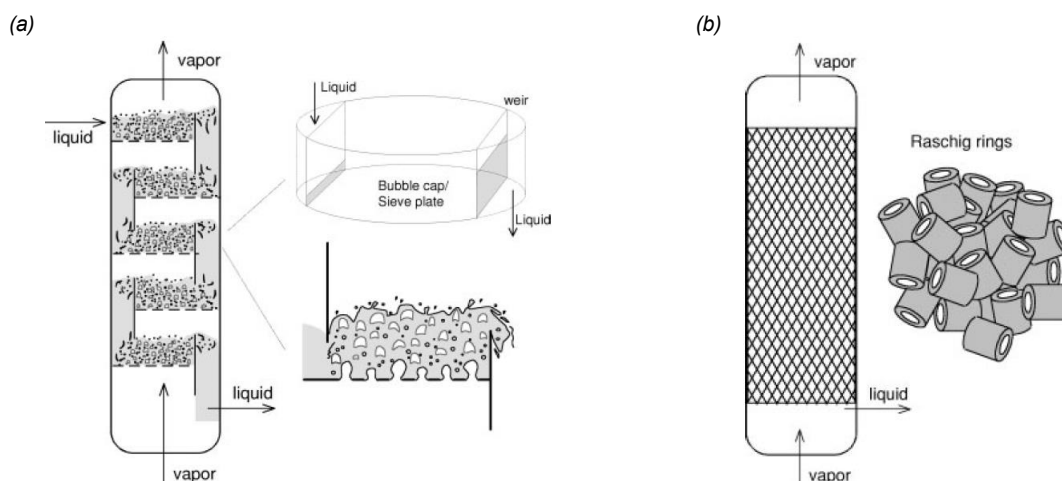


Figure 1.3. Counter-current vapor-liquid contact in multistage tray (a) and in packed columns (b) (Krishna, 2003)

Heterogeneous catalysis

So as to deal with the drawbacks discussed above, academic and industrial researchers have been developing new technologies to consider heterogeneous catalysis inside the distillation columns. Catalysis is provided by solid particles of a diameter from 0.5 to 3mm. However, these solid catalyst particles cannot be randomly used as distillation packing because they would form a mass too compact for the upward flow of the vapor and the downward flow of the liquid. Heterogeneous catalysis requires a structure to fix the catalytic particles in the reaction zone, known as a structured packing. The major task

of the catalyst structure is to ensure an adequate contact between catalyst surface and liquid phase. The main characteristics of heterogeneous catalysis are listed below:

- Possibility of determining the catalyst concentration in each column sections and, as a consequence, the placement of precise locations for the reaction occurrence,
- The possibility of enhancing the reaction velocity by higher temperature or pressure is limited, because the catalyst generally consists of ion-exchange particles, whose temperature range is limited (Schoenmaker and Bessling 2003),
- The outlet products do not need any further purification regarding catalyst concentration,
- Typically, catalysts must be regenerated or replaced from time to time, which requires shut-down of the column operation so as to change the entire internal structure. Hence, the catalyst particles lifecycle should be in coherence with the process evolution schedule, so as to avoid production breaks only for catalyst substitution,
- Easiness of maintenance and safety; the solid particles remain inside the packing pockets.

To better grasp the technology, some heterogeneous catalyst structures are given in Figure 1.4.

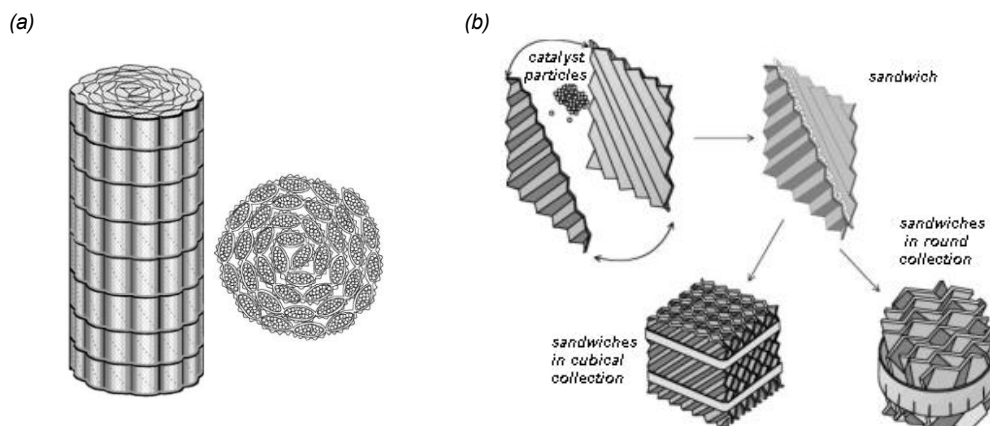


Figure 1.4. Structured catalyst internals: catalyst bales (a) and structured sandwich packing (b) (Krishna 2003)

In the first configuration, used by Chemical Research & Licensing, the catalyst particles can be enclosed in cloth wrapped in the form of bales. Pockets are sewn into a folder cloth and then solid catalyst particles are loaded into the pockets. The pockets are then sewn shut and the resulting belt is rolled with alternating layers of steel mesh to form a cylinder of 'catalyst bales'. The steel mesh has voids to allow vapor traffic and vapor-liquid contact (Krishna 2003, Johnson and Dallas 1994, Subawalla et al. 1997).

The second structure has been successfully licensed by Sulzer (Katapak-S) and Kock-Glitsch (Katamax), where the catalyst particles are layered between two corrugated sheets of metal wire gauze forming a sandwich structure. Individual sandwiches are assembled together to create open cross-flow channels. Structured packing is available from laboratory to industrial scale and the ratio of catalyst volume fraction to separation efficiency can be varied over a wide range, so the design of a reactive distillation column can be further optimized to better fit each reaction system (Götze and Bailer, 1999). Detailed information concerning hydrodynamics, mass transfer, liquid holdup, pressure drop and residence time is given by Behrens et al (2006, 2008) and Götze and Bailer (2001).

1.2.2 Design of reactive columns

To better understand the process behavior, industrial and academic researchers have been developing their own methods to assess the feasibility and the design of the reactive distillation process in particular cases. These developments require the ability of proposing appropriate tools based on reliable thermodynamic, kinetic and hydrodynamic models, but also of suggesting methodologies and software for efficient conceptual design, simulation, optimization and robust control of these processes.

Process design is defined as the determination of dimension and operating parameters that allow the system to run cost effectively at all desired production rates and product splits, so as to achieve product purities and so as not to violate other process, equipment and machinery constraints.

The meaningful advantages of reactive distillation processes over conventional design are consequences of the innovative process topology with much enhanced degree of internal mass and energy integration. As a consequence, the conceptual design of these columns becomes a great challenge for process engineering. The combination between the reaction operation and the separation phenomenon should follow stringent requirements of process intensification and can considerably influence the process thermodynamic efficiency. There are many different methods available in the literature for screening, analysis and design of RD columns. According to Huss et al. (1999) and Théry-Hétreux et al. (2005a), all these methods should include the three steps as follows:

1. Feasibility analysis, which consists in verifying that, for given feed conditions, the expected objectives (purity of distillate or of residue product, recovery ratio, conversion ratio) are attainable, from a thermodynamic point of view. If necessary, the feed conditions can be varied in order to attain these objectives. If the feasibility is not achieved, the process objectives are to be revised.

2. Synthesis of the process, which is based on a more rigorous analysis to confirm (or infirm) the results obtained at the feasibility step. These results are exploited to determine the configurations and some operating parameters of the column: number of plates, relative positions of reactive zones and pure separation ones, feed locations, minimum reflux ratio, etc.

3. Conceptual design itself, devoted to the calculations of equipment size, reflux ratio, heat duties, or even the necessary amount of catalyst or liquid holdup. At this moment, the configurations and the parameters defined are coherent to meet the process specifications and can be optimized.

So far, many techniques have been developed for feasibility analysis, synthesis and conceptual design of reactive distillation columns and they can be generally classified into three categories (Almeida-Rivera et al. 2004b, Li et al. 2012): (i) Graphical methods; (ii) Heuristic evolutionary methods; and (iii) Optimization-based methods.

The graphical methods received considerable attention over the past 20 years. Some approaches originally designed for conventional distillation columns, such as the Mac Cabe - Thiele and the Ponchon-Savarit methods, were modified and successfully applied to reactive processes (Lee et al. 2000, 2001).

Wahnschafft and Westerberg (1993) suggested a graphical method based on the analysis of pinch point curves. Pinch points are the fixed points of a relevant column section and are categorized as stable nodes (column profiles approach the point, higher boiling point), unstable points (the profiles leave the point, lower boiling point), and saddle points (profiles pass by the pinch point). The point locations are dependent on feed ratio, feed and product compositions, operating pressure and energy demand (Bausa et al. 1998, Lee et al. 2003). Later, Avami (2013) proposed a design technique that discusses how the location of pinch points in the middle section determines the feasible range of energy demand for double-feed columns, by the use of Feed-Angle methods (Kraemer et al. 2011, Avami et al. 2012).

The most representative graphical methods are based on the reactive Residue Curve Maps (*rRCM*) (Ung and Doherty 1995, They 2002, Brehelin 2006). A reactive residue curve is defined by the locus of the liquid compositions remaining from a simple batch reactive distillation process and is obtained through the simulation of the process for various initial liquid compositions. Several applications can be cited: Huang et al. (2005) investigated the *rRCMs* of the propyl acetate synthesis reaction; Almeida-Rivera et al. (2004a) analyzed the homogeneous reactive distillation synthesis of methyl tert-butyl ether using *rRCMs*; They et al. (2005b) presented an entire design methodology for the production

of methyl-tert-butyl-ether and methyl acetate based on the analysis of their *rRCMs*; recently, Zheng et al. (2013) calculated and studied the *rRCM* of the ethyl acetate synthesis reaction.

To assess the feasibility analysis of double-feed reactive columns, Théry-Hétreux et al. (2012) recently introduced the concept of reactive Extractive Curve Maps (*rExCM*), which approximates the liquid compositions in the reactive middle section of the same column and enables to formulate a necessary condition for the feasibility of double-feed units quite similar to single feed RD columns.

Other methods are also addressed in the literature: Bifurcation Analysis (Wang et al. 2008b), Static Analysis (Giessler et al. 1999) and Attainable Regions Method (Glasser et al. 1987).

The feasibility analysis techniques presented can be combined with the Boundary-Value method for the process synthesis step, which performs tray-by-tray calculations as a function of energy demand (Barbosa et Doherty 1987a, 1987b). The main idea is that a feasible double-feed RD column contains a continuous path from distillate to bottom such that the rectifying and the stripping profiles intersect the middle-section profile and determine the minimum energy demand.

Graphical methods are extremely helpful in understanding the fundamental insights of RD processes, but its application becomes more complex in the case of multiple-reaction systems due to the increased dimensionality (Lee and Westerberg, 2001). After the use of graphical methods, further refinement with simulation-based computational tools would be the decisive basis for the process design.

Heuristic evolutionary methods, on the other hand, are based on available heuristics or an economic objective function to guide process synthesis and design (Subawalla et Fair 1999, Kaymak et Luyben 2003). The methods feature great simplicity in principle and relatively small intensity in computer requirement, but frequently fail to find the optimum combination between the reaction and the separation phenomena. Li et al. (2012) developed a generalized heuristic procedure considering the relocation of feed stages, the redistribution of catalyst and the determination of the system pressure. For the derivation of a thermodynamically efficient process design, Huang et al. (2010) divide RD column into three broad categories, involving reactions from highly exothermic to highly endothermic, and derived a stepwise design procedure by simultaneously combining the effect of mass and internal energy integration.

Finally, conceptual design by optimization is based on either mixed-integer nonlinear programming (MINLP) or mixed-integer dynamic optimization (MIDO) formulations. Gomez et al. (2003, 2006) successfully proposed a MINLP formulation for optimal design of a catalytic distillation column based on

generic algorithm with a non-equilibrium model. Several other authors, such as Stichlmair and Frey (2001), Jackson and Grossmann (2001), Georgiadis et al. (2002) and Kookos (2011) also applied optimization approaches to the design of RD columns. Detailed process models are provided and the optimization criterion is commonly the total annual cost or the energy demand. However, Li et al. (2012) stated that the optimization methods are likely to solve complicated problems, but they suffer from the need of detailed problem formulations and extreme difficulties in searching for the global optimum especially in the case of highly non-linear or non-convex systems.

1.2.3 Simulation models

A process simulation model is the representation of the process behavior with purely mathematical expressions. Reactive distillation models have to consider both the chemical and the physical phenomena. Two types of model are discussed in the literature: equilibrium stage models (EQ), which assume that outlet streams of each stage are at the phase equilibrium, and non-equilibrium models (NEQ), which explicitly take into account the rate-based equations for heat and mass transfer. The chemical reaction can be modeled by considering chemical equilibrium or reaction kinetics; the chemical equilibrium model is actually the stationary solution of the kinetic model, for which all derivatives with respect to time become zero.

The equations system that models equilibrium stages assumption are known as MESH equations, MESH being an acronym referring to different types of equations; M is for the material balance equations, E equations relate the phase equilibrium, S are the summation of fractions equations and H accounts for the appropriate phase enthalpies and energy balances. Only a limited amount of data is needed to develop RD models when the assumption of phase and chemical equilibrium is used.

Non-equilibrium models take into account finite mass and energy transfers; they are more rigorous from a transfer point of view. These models are recommended in advanced stages of RD process development, when technological choices are to be made, but its implementation is much more complex because the amount of information needed to develop reliable models greatly exceeds that needed for equilibrium models.

Figure 1.5 shows the different model complexities; the abscissa axis account for reaction model complexity and the ordinate axis accounts for physical model complexity.

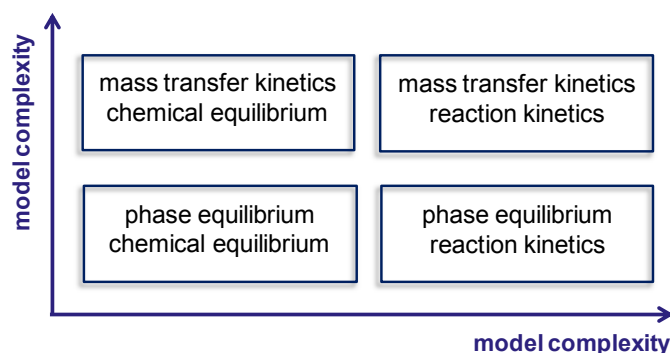


Figure 1.5. Complexity of the reactive distillation models, based on assumptions of phase or chemical equilibrium

Applications of the EQ and the NEQ models to reactive distillation were deeply reviewed by Taylor and Krishna (2000). Though EQ models are commonly used as an approximation for RD simulations; some authors compared the approaches and found important conclusions: Lee and Dudukovic (1998) described an NEQ model for homogeneous RD in tray columns and they found close agreement between the prediction of EQ and NEQ models only when the tray efficiency could correctly be predicted for the EQ model. Sundmacher et al. (1999) compared the EQ stage with Murphree efficiency and NEQ model simulations of the MTBE and TAME processes to experimental data. They found that a rigorous NEQ model was necessary to describe the TAME process, but both the NEQ and the EQ stage model could adequately represent the MTBE process. The work by Baur et al. (2000) compared the EQ and NEQ models for the hydration of ethylene oxide to ethylene glycol, highlighting the importance of using the NEQ model to observe the phenomena of multiple steady states.

Thus, there can be a significant difference between EQ and NEQ models for some real systems and more representative results could be obtained by an approach based on non-equilibrium models (Higler et al. 1998, Rouzineau et al. 2005, Druart et al. 2004). However, the use of detailed correlation data are necessary to describe transfer phenomena (thermal exchange coefficients, interfacial surface, thickness of the transfer film, diffusion coefficients, etc.) and the acquisition of reliable information is not always an easy task, especially in the case of complex solutions. A small deviation of the parameters value would result on wrong results, losing the advantage of NEQ models precision the system modeling. Hence, finding reliable model parameters is often the bottleneck in model development (Hasse, 2003). There is a lack of suitable experimental works with the explicit purpose of model validation. It is unlikely that any company would build a new reactive distillation without any pilot plant test or reliable references. Reliable scale-up techniques are also of major importance for real applications.

Moreover, RD processes have been observed to show distinct nonlinear behavior such as multiple steady states, self-sustained oscillations and nonlinear wave propagation, which is influenced by the properties of the reactive system and the operation conditions (Kumar and Kaistha 2008a, 2008b, Kienle and Marquardt 2003). A vital aim of process design and synthesis is therefore to reduce the complexity of the system in order to enable simple solutions to be recognized quickly.

1.2.4 *Dynamics and control strategies*

In view of the increasing emphasis placed on safe, efficient and profitable plant operations, the guarantee of good economic performance of the complex RD process relies on a suitable and reliable process control.

The first step to carry out effective control systems design is the understanding and the interpretation of the process dynamic behavior itself, with no assistance or interference of the controllers. The essence of dynamic analysis is the investigation of the process time-dependent behavior, which is very useful to analyze the response to disturbances and the sensitivity of different measurement points, to define consequent sensor placements and to decide which control action to implement, for example. Because there is no information flowing back the system, this configuration is classified as open loop. Several authors developed rigorous reactive distillation dynamic models (Rahul et al. 2009, Peng et al. 2003, Mahdipoor et al. 2007) and some of them used information from experimental work (Mihal et al. 2010, Xu et al. 2005). The experimental validation is shown to be very important so as to identify reliable parameters concerning hydrodynamics and technology of reactive columns.

When the response of all dynamic processes is modified by the influence of controllers, the new configuration is classified as a closed loop. The objective of a closed-loop process is to modify the system response by manipulating some variables in order to attain process specifications (in terms of production, purity...). The extent to which this response can be modified is determined by the knowledge of the intrinsic process characteristics, the nature of inherent limitations and the versatility of the hardware elements available for implementing the controller. The dynamic behavior thus needs to be carefully understood and several variables are available to be controlled or manipulated. Singh et al. (2005a) defined the control structure as the number of control loops and the specific input-output pairing in these loops. Sharma and Singh (2010) conducted a detailed review of RD control, by introducing the main concepts and presenting many applications.

Process Variables

A typical processing unit is characterized by its variables, usually corresponding to quantities as temperature, flow rate, pressure, level, composition, etc. In order to design a control system, these variables are commonly classified under one of the following conditions:

- Controlled variables (also known as output variables) provide information about the internal state of the process, and need to be maintained between specific range values,
- Manipulated variables (also known as input variables) are able to stimulate the process and to promote changes in its internal conditions. The nature of the input change will quantitatively and qualitatively determine the consequent process output response,
- State variables are essential to completely describe the internal state of the process,
- Measured variables are those whose values are available by direct on-line measurements. At the same time some input or output variables can be available for measurement, some cannot. The latter ones may be called unmeasured variables,
- Disturbance variables are those over which the operator has no control. They represent any external independent influence or perturbation on the system, and can be measurable or immeasurable.

In the reactive distillation process, the possible candidates for manipulated variables are the distillate flow rate, reflux ratio or reflux rate at the top of the column, the heating rate, bottoms flow rate, or reboiler ratio at the bottom of the column, the composition of reactants in the feed stream or the feed flow rate. Possible candidates for measured variables are column pressure, reboiler level, condenser level, product or column compositions and column temperatures.

Similarly to non reactive distillation, a hierarchy of different control tasks exists in reactive distillation. The lowest regulatory level concerns the control of column pressure and liquid levels in the reboiler and in the condenser. At the highest level, product purities are controlled. When the reaction has two different products, the specifications of both product streams need to be controlled.

The control of column pressure and liquid levels, sometimes known as the inventory control schemes, can be achieved with standard methods, as in the non-reactive distillation case. However, composition control of RD columns may introduce additional complexities. The online measurement of concentration is usually slow and expensive; it would be often required to send a solution sample to the

plant analytical laboratory. Possible current solutions are the use of online spectroscopy, faster and reliable, or the inferential control schemes, where the product compositions are inferred from temperature measurements. For the separation of multi-component mixtures, algebraic correlations, based on process models and plant data, can be developed to relate the mole fraction of the heavy component to several different tray temperatures. The parameters in these correlations may be updated, if necessary, as actual composition measurements become available. Temperature inferential control is widely used in reactive distillation columns (Kumar and Kaistha 2008, Lee et al. 2007, Luyben and Yu 2008).

Feedback, Feedforward and Nonlinear Controllers

The design of control process systems in closed-loop configurations may follow different strategies. The function of a control system is to ensure that the closed-loop system is first stable and has desirable dynamic and steady-state response characteristics and the most commonly used strategies are the feedback, the feedforward, or a combination of feedback and feedforward controllers. Another advanced strategy successfully used for more complex systems is the model predictive controller.

In feedback control, the process variable to be controlled is measured and the measurement is used to adjust another process variable which can be manipulated. In feedforward control, the disturbance variable is measured and used to manipulate another process variable; the controlled variable is not measured. Thus, in principle, feedforward control is able to provide perfect control in the sense that the controlled variable would be maintained at the set point, if the model representing the interaction of the disturbance on the output variable is perfectly known.

By its inherent nature, feedback control is not capable of perfect control since the controlled variable must deviate from the set point before a corrective action is taken. However, an extremely important advantage of feedback control is that corrective action is taken regardless of the source of disturbance. The ability to handle unmeasured disturbances of unknown origin is a major reason why feedback controllers have been so widely used in industrial practice.

Model Predictive Control (MPC) is the most widely used of all advanced control methodologies for real multivariable systems in chemical industries practice. The process model is used to predict future outputs over a predefined time period, and future input changes are determined in order to optimize an objective criterion expressed as a function of future errors between predicted output values and the desired setpoints and future control inputs.

For chemical processes with severe nonlinear behavior, strong factors motivate further researches for nonlinear control. These researches face the difficulty that nonlinear models are much more difficult to build and their inversion – required for the implementation of the MPC controller – is not trivial. However, due to the fact that the objective of control system is, by definition, to keep the steady state operating conditions of process outputs, the systems would be in the vicinity of steady state conditions and therefore linearized models can be adequate to linear controller implementation. The mathematical design of these controllers is discussed in Appendix II.

In recent years, the number of publications and articles concerning the dynamics and control of reactive distillation has been increasing. The great majority follows major steps in designing and installing a control system: the first step is the formulation of control objectives; then, dynamic mathematical models of the process are developed and they allow the analysis and characterization of the process dynamic behavior; the next step is to devise a control structure to meet the control objectives while satisfying process constraints, by selecting the appropriate variables and designing the most suitable controller.

Several authors investigated the RD process control for quaternary systems and addressed the issues concerning the control structure selection and the implication of column characteristics. Al-Arfaj and Luyben (2000) verified that increasing liquid holdup, and thus the catalyst presence, improves the process dynamic controllability and that single-end temperature control can keep both products at specified purity values, even for large disturbances, if reactive-zone holdup is sufficiently large. Sneesby (1999), however, showed the better performance of the two-point control scheme when compared to the one-point scheme. Actually, the vast majority of the literature uses two-point inferential control schemes (Gruner 2003, Huang et al. 2004, Kaymak and Luyben 2005, Lai et al. 2007, Kumar and Kaistha 2008, 2009). Recently, Demirel and Kaymak (2013) show that a three-point inferential control improves the control performance for different systems. Fewer authors consider the online composition control instead of temperature measures (Volker et al. 2007, Cheng and Yu 2005, Kawathekar and Riggs 2007).

Tray selection has been commonly carried out by a sensitivity analysis of the steady state regime (Kumar and Kaistha 2009, Babu et al 2009, Kawathekar and Riggs 2007). Useful tools to select controlled and manipulated variables are the Singular Value Decomposition or the Relative Gain Array (Cheng and Yu 2005, Kaymak and Luyben 2005, Lee et al. 2007, Kookos 2011). The effects of feed tray locations were addressed by Cheng and Yu (2005).

Proportional only (P) controllers are used for inventory control and Proportional-Integral (PI) controllers are the most frequently used to control production performance. They are arranged in single input – single output feedback strategies (Al-Arfaj and Luyben 2000, Wang et al. 2008). Controller tuning methods have been improved and new methods have been presented: Relay Feedback test (Lin et al., 2006), Internal Model Control (Garcia and Morari, 1982), Tyreus-Luyben rules, Ziegler-Nichols settings (Lin et al. 2006, Kumar and Kaistha 2009, Wang et al. 2008, Lee et al. 2007). Moreover, fewer publications concern the application of advanced controllers such as Model Predictive Controllers, Optimal or Nonlinear controllers (Kawathekar and Riggs 2007, Miranda et al. 2008, Babu et al 2009, Gruner et al. 2003). These techniques are detailed in Appendix II.

Control system requirements

Some important concepts regarding process control were defined by Seider et al. (1999), Seborg et al. (1989) and Luyben and Yu (2008). They enable the qualification of the process control strategies:

- Controllability: the ease with which a continuous plant can be held at a specific steady state,
- Resiliency: the degree to which a processing system can meet its design objectives despite external disturbances and uncertainties in its design parameters,
- Switchability: the ability to move a process from one stationary point to another,
- Robustness: occurs when the control system is insensitive to changes in process conditions and errors in the assumed process model,
- Stability: when a finite input change is implemented in a physical system, the resulting transient response ultimately settles to a new steady state, instead of growing infinitely,
- Rangeability: the region of disturbances for which the control system is able to provide stable effective control and maintains reasonable product specifications,
- Operability: the ability of the process to return to the steady state in spite of unknown but bounded disturbances,
- Observability: a measure for how well internal states of a system can be inferred by knowledge of its external outputs.

1.3 SIMULTANEOUS DESIGN AND CONTROL OF CHEMICAL PROCESSES

Historically, the process development approach has been conducted by a two-step method: first, the process engineer completes the design based only on static analysis, with quantification of economic and environmental criteria and the plant is built, and second, the control engineer implements the control structure aiming at meeting all the performance objectives. Therefore, the control system design only starts once the main features of the process have been already established.

However, there is no guarantee that a process flowsheet that has been developed to optimize some steady-state economic objective will provide good plant-wide dynamic performance. Most modern chemical plants are complex networks of multiple interconnected, nonlinear process units, often with multiple recycle and by-pass streams and energy integration. These performance difficulties introduced by the specific process and integrated equipment designs had to be overcome by overly complicated control strategies (Luyben, 2004). Moreover, the fluctuating economy, characterized by varying customer demands, leads to changes in the process specifications and the process design must be able to adapt to these changes.

So, when the conceptual design of a reactive distillation process is optimally obtained based on static analysis, regarding only economics and environmental criteria, the result may be a unit very difficult to control. A coherent design is not complete and intelligent management decisions about what process to build should not be made until dynamic performance is evaluated.

It is thus appropriate to consider the system dynamic operability as from the conceptual design step. A reliable, accurate and straightforward methodology for the examination of the operability characteristics of a process that permits ranking competitive designs would be of great use (Georgakis et al., 2004). The engineering time spent at these early stages can reap huge economic benefits later on in the project in terms of rapid, trouble-free start-ups, reduced product-quality variability, less-frequent emergency shutdowns, reduced environmental contamination and safer operation (Luyben, 2004).

Important engineering trade-offs need to be faced during RD processes conception. For example, economically optimal designs provide columns with diameters, number of trays and holdups as small as possible. However, from the standpoint of dynamics and control, the ability of the column to ride through disturbances is usually improved by having more volume capacity. Lin et al. (2011) observed that the reactive section distribution is also an effective decision variable for the balance of design and control. In

addition, the use of adequate sensors is important for the system operation, such as thermocouples, solution samplings and flow measurements, especially regarding their response time. The inclusion of these measurements in the original equipment design and the choice of their right places in the column, when it is still inexpensive and easy, is of considerable importance. Having to make field modification in an operating column can be very expensive and may need a long time to be accomplished (Luyben, 1992).

According to Yuan et al. (2011), controllability is viewed as an inherent characteristic of chemical processes and one of the most important aspects of process operability, because it can be used to assess the attainable operation of a given process and improve its dynamic performance. The process controllability depends on many different aspects, such as plant design and specific process dynamics, sensitivity to uncertainty, measurement location and time response, actuator constraints, and disturbance characteristics. Fisher et al. (1988a, 1988b, 1988c) were the pioneers to assess process controllability at the early design steps. For improving the controllability characteristics of a process, there are two main design methods: the optimization-based method and the controllability indices-based anticipating sequential method.

In optimization-based frameworks the problem is formulated as a mathematical superstructure capable of attaining a given steady state economic objective and concurrently respecting dynamic operability, model uncertainty and the synthesis of optimal controllers (Yuan et al., 2011). Sakizlis et al. (2004) developed techniques for simultaneous process and control design methodology based on mixed integer dynamic optimization algorithms. Different approaches with conventional PI or advanced model-based predictive controllers were discussed for a typical distillation column. Miranda et al. (2008) solved an overall optimization problem, by comparing the simultaneous design and control approach to the conventionally used sequential approach. The Nonlinear Programming (NLP) and the Pontryagin's minimum principle were applied to a reactive column. Recent optimization-based works were presented by Chawankul et al. (2005), Patel et al. (2008), Babu et al. (2009) and Sharifzadeh (2013). The optimization-based approaches show strong benefits for the utilization of simultaneous design and control, with the ability to consider multiple specifications. The complex RD process models results, however, on strong complexity to the optimization equations and constraints, which makes the solution of superstructures difficult and time consuming. Moreover the solutions are very dependent of a dynamic model and may be unrealistic in practice as a consequence of an error modeling.

On the other hand, the basic idea of the controllability indices-based anticipating methods is that controllability analysis is integrated into the process design and the control system design is conducted only later, enabling the screening of alternative designs for controllability. The development of controllability metrics is based on the concepts of functional and structural controllability and switchability (e.g. RHP zeros, time delays, RGA and condition number). The prime benefits of this analysis are its relatively simple implementation in complex processes and the straight forward way of calculating every metric (Sakizlis et al. 2004). The effect of RHP zeros on the controllability of chemical processes was studied by Holt and Morari (1985); the severity of control deterioration increases with increasing proximity of the zeros to the imaginary axis. Morari (1983) proposed the corresponding minimum singular values and input magnitudes to judge the attainable process performance; plants with higher minimum singular values should be favored because they can handle larger disturbances. Skogestad and Morari (1987) used the Relative Gain Array as a framework to measure the attainability of perfect control or the limits to the physical realization of the perfect controller. Also the Singular Value Decomposition analysis of the process transfer function can be used to characterize the effects of manipulated variable constraints and model uncertainties. Vaca (2009) compared different steady-state designs using the Condition Number provided by Singular Value Decomposition. The mixing of these quantitative criteria was also investigated (Wolff et al. 1992, Moore 1992).

Subsequently, so as to determine the steady-state indices and the closed-loop performance, the controllers are introduced and the respective dynamic behavior can be assessed and ranked based on the Integral Squared Error and the frequency domain specifications such as bandwidth, magnitude ratio, phase angle, and peak log modulus regarding different perturbations (Yuan et al., 2011). Thus, controllability assessment deals with whether the plant is controllable, but also with the way of how to provide efficient control structures and controllers design. Simulation-based frameworks make use of exhaustive closed-loop dynamic simulations for controllability tests aiming at realistic ranking of alternative designs. This approach requires extensive time for performing several runs.

Both optimization and indices-based methods commonly perform linear analysis around a steady-state operating condition that will be the most desirable. Morari (1992) showed that controllability evaluation based on a linearized model around a specified steady state gives correct information even for strongly nonlinear systems, but is not satisfactory for highly nonlinear operating regions, such as start-up, shutdown, and batch or semi-batch-processes.

By accepting that all processes are inherently dynamic and that dynamic operation is inevitable, some studies explicitly consider dynamic models at the optimization design step and are not restricted to a small operating region around steady-states. Although uncertainty or disturbances seem to be solved in the design steps, uncertainty in the models will arise in practice. Due to the high cost of obtaining a detailed dynamic model and the significant computational effort required, the applications are currently restricted to small-scale problems (Mohideen et al. 1997, Terrazas-Moreno et al. 2008, Sandoval et al. 2009). The analyses of controllability indices can be extended to nonlinear models, by adapting the criteria calculations. As an example, the Nonlinear Block Relative Gain was given by Nikolau (1989).

Finally, Yuan et al. (2011), Kumar and Kaistha (2009b) and Vega and Pinto (2008) performed bifurcation and stability analysis to provide guidance for making processes more controllable by eliminating or avoiding undesirable behaviors.

1.4 DIAGNOSIS OF COMPLEX PROCESSES

In addition to the control aspects of the reactive distillation process, the subject of diagnosis is also of interest. The objective of process diagnosis is to rapidly detect its abnormal operating conditions so as to avoid reduction on its performance, to prevent for plant breaking down and to promote proper operation with more security to the surroundings. When a fault condition happens, it may be necessary to immediately stop the plant or to switch the variable set points or even the entire control structure of the process, which results in high maintenance costs. Then, the ability to detect the tendency that causes the fault condition is strongly attractive. Isaza (2007) highlighted, however, the difficulty of predicting operating conditions of a complex process, due to its high dynamic nonlinearities.

Orantes (2006) divided the diagnosis methods into two categories: quantitative or qualitative. The quantitative diagnosis is based on the modeling of systems or signals, and can be applied as a mono-signal, when the variables measurements are independent from each other, or as a multi-signal approach, when mathematical relations link the variables. Mono-signal methods can be the analytical redundancy, the spectral analysis or statistical approaches. Multi-signal methods use the concepts of parity space, observers or parametric estimations (Olivier-Maget 2007, Olivier-Maget et al. 2009). Faults are detected when there are discrepant values between the real measurements and the variables defined in the model. The qualitative diagnosis, on the other hand, concerns mainly models issues from artificial intelligence, artificial neural networks, fuzzy inference systems or pattern recognition. These methods

most often need a learning step based on historical data, which can be stored by process automation systems (Fisher 1936, Lim et al. 2000).

For complex processes, the computational diagnosis based on mathematical models assumes a deep knowledge of the process, which is an important challenge considering the strong dynamics nonlinearities in reactive distillation systems. Moreover, there can be unknown parameters and a high number of variables possibly dependent on each other or with inaccurate measurements. Thus, the behavior is more commonly obtained by the analysis of historical data from normal and abnormal operating conditions.

Akbaryan and Bishnoi (2001) remarked that the maintenance of complex systems must be considered based on the information given by all variables and the classic supervision based on a unique variable lead to difficulties in predicting and anticipating abnormal operating conditions.

Among the qualitative diagnosis methods, classification techniques perform the procedures of learning and recognition with the process historical data to obtain information of the operating conditions. The learning phase classifies the information, corresponding to normal and abnormal functioning situations and the recognition of new data can be done online, by identifying the class that best represents the new values of the variables.

1.4.1 Process diagnosis using fuzzy logic

The plant monitoring systems treat a large number of variables and a considerable amount of uncertain information. For the human operators, it is difficult to analyze a large number of measurements at the same time, but they are able to deal with unexpected conditions and to take decisions. The human-machine compromise enables the creation of adapted strategies to avoid dysfunctional situations and reduces workload and errors conducted by human operators.

The identification of process conditions based in methods of fuzzy classification is a compromise between automation and human operator's intervention. The main advantage of fuzzy logic is its ability to handle and to manipulate inaccurate and noisy data. Fuzzy logic can be seen as an appropriate tool widely used in system control and diagnosis due to its simplicity and effectiveness, rather than classical techniques that show unsatisfactory results when the systems are highly nonlinear and dimensional.

The results of process diagnosis based on fuzzy logic results are the adequacy degrees of the measurements to different operating conditions at the same time. Decisions can be taken to prevent dysfunctional situations, because it is possible to know when the system is at a normal operating condition and some parameter is tending towards a dysfunctional situation. So there is a possibility of anticipating and preventing of faults by reducing the tendency of the respective parameter to this faulty direction. The higher knowledge of the real situation supports decisions of the human operator and enhances his/her perception of the process sensitivities (Isaza 2007, Isaza et al., 2009).

Based on fuzzy logic, there are three main conceivable techniques for system diagnosis:

- Coalescence methods: based on the analysis of the distances between the values. One can cite the C-Means technique, and its extensions Fuzzy C-Means and GK-Means,
- Neural Networks: based on non-linear statistical data modeling tools. This technique has been successfully used to process diagnosis (Lurette 2003, Bezdek 1981, 2005),
- LAMDA (Learning Algorithm for Multivariable Data): is a compromise between the two methods cited above. It can simultaneously handle quantitative and qualitative data (Isaza, 2007, Isaza et al., 2008, Isaza et al., 2009) and has been recently extended to interval data.

The classification technique can also be the basis for a sensor placement methodology. Orantes et al. (2006, 2007) proposed three different criteria for the selection of the most relevant sensors for diagnosis of dysfunction situations: probabilistic entropy, non-probabilistic entropy and variance.

Finally, the process diagnosability can be defined as the ability to detect normal and abnormal operating conditions. A study on diagnosability as from the design step of reactive distillation processes would be of great relevance to ensure a good operability of the conceived columns, to detect fault tendencies and to preview the installation of the most relevant sensors. Reactive distillation diagnosability analysis at the design step has not been proposed yet.

1.5 THE STUDY PROPOSED

Finally, the study proposed in this PhD thesis can be contextualized.

The methodology for the pre design of reactive distillation columns developed at the LGC (Laboratoire de Génie Chimique, Toulouse, France) is based on the process static analysis. So, due to the important effects of the nonlinearities present on the system, an important concern on complementing the work by integrating controllability and diagnosability aspects exists.

The methodology for the diagnosis of systems and sensors selection developed at the LAAS (Laboratoire d'Analyse et d'Architecture des Systèmes, Toulouse, France) is based on fuzzy classification methods and can address complex systems.

The objective is then to integrate different techniques and to provide an entire methodology for the conceptual design of reactive distillation columns, by considering controllability and diagnosability aspects as from the early steps.

First, the pre-design methodology performs the process feasibility analysis and synthesis through graphical methods. Based on the feasible reactive column configurations proposed, software for simulation on both steady and transient states provide more information about the system. The model considers physical equilibrium and reaction kinetics, and both open-loop and closed-loop simulations are performed, with PI feedback controllers. The process sensitivity is calculated and a controllability indices-based anticipating sequential method is conducted to analyze different feasible configurations and to identify the most appropriate column characteristics, as a function of the controllability criteria. The simulation data is then analyzed by the diagnosis procedure and the diagnosability aspects are discussed. Finally, controllability and diagnosability key rules are identified to sustain the design of reactive distillation columns.

It should be known that an entire dynamic behavior analysis of a chemical process would consider start-up and shut-down phases in addition to operation conditions, but they are not included in this study. Detailed information can be found in the works of Reepmeyer et al. (2003, 2004).

The methodology is to be applied for the production of ethyl acetate by the esterification of ethanol and acetic acid, in a Solvay industrial context.

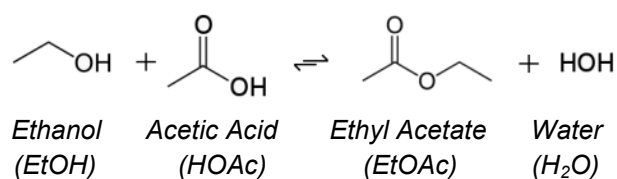
The ethyl acetate system

2.1 A TECHNICAL PROFILE

Ethyl acetate (EtOAc) is an ester; an organic compound with the chemical formula $\text{CH}_3\text{COOCH}_2\text{CH}_3$. At room temperature, it is a colorless liquid with a fruity odor. The boiling point at atmospheric pressure is 77.1°C and its molecular weight is 88.1g/mol . It is slightly soluble in water and soluble in most organic solvents, such as alcohol, acetone, ether and chloroform.

Ethyl acetate is used primarily as a solvent and diluent, being favored because of its low cost and low toxicity. Some applications concern glues, nail polish removers, decaffeinating tea and coffee, manufacture of printing inks, surface coatings and thinners, nail varnish removers and perfumes. The consumption of ethyl acetate in the paint and ink segment was estimated to constitute about 25% of the total demand. In perfumes, it evaporates quickly, leaving only the scent of the perfume on the skin. Ethyl acetate is also used as artificial fruit essences and aroma enhancers, artificial flavors for confectionery, ice cream and cakes. An additional application is in the manufacture of flexible packaging and polyester films. In 2004, estimated 1.3M tons were produced worldwide (Dutia 2004).

EtOAc is obtained by the esterification reaction of ethanol and acetic acid using catalysts such as sulfuric acid, para-toluene-sulphonic acid or ion exchange resins. Recent studies on the reaction catalysis were performed by Gurav and Bokade (2010), Antunes et al. (2011), Tang (2012) and Phung et al. (2013). Physical properties of the quaternary mixture were presented by Calvar et al. (2005) and Kustov et al. (2012). The thermodynamics and kinetics data will be presented in chapter 9. The reaction can be presented as:



Industrial grade ethyl acetate is available with minimum purity of 85.0%wt. The most common commercial procedures to produce EtOAc are presented in a simple esterification reactor of ethanol with acetic acid on both batch and continuous modes. However, one of the key issues in the production of EtOAc is the equilibrium limitation from the reversible reaction of acid and alcohol; in a batch reactor, the ethyl acetate has been reported to achieve the maximum purity of 52.0% (Konakom et al. 2010, 2011). Several separation steps are thus needed for further purification, resulting in important capital and operating costs.

Intensified production processes

So as to break the equilibrium limitation and achieve a high conversion, the reactive distillation became an interesting alternative to produce ethyl acetate. Actually, the application of reactive distillation for systems involving an esterification or transesterification reaction has been considered since 1921 (Keyes, 1932). Detailed information for sequential design and control of the acetic acid esterification with five different alcohols, ranging from C1 to C5, was given by Luyben and Yu (2008).

The literature concerning the production of EtOAc by intensified processes significantly evolved during the last decade. Chinese National Petroleum developed a one step ethanol process in which ethanol is partially oxidized to acetic acid and then esterified with excess ethanol to give ethyl acetate (Dutia, 2004). The coupling of reaction and pervaporation membranes was studied by Lv et al. (2012) and Hasanoglu and Dincer (2011). The former authors increased the ethanol conversion by selectively removing the water from the reboiler of a reactive distillation and recycling the acetic acid into the feed. The latter authors used perm-selective to ethyl acetate membranes and the reactant conversions were increased by the continuous removal of ethyl acetate from the reaction medium.

The reactive distillation design proposed by Tang et al. (2003) is a common reference in the literature and was considered in several following studies (Tang et al. 2005b, Lee et al. 2007, Lai et al. 2008, Tsai et al. 2008). It includes a RD and a stripping column, with the streams and the devices specified as shown in Figure 2.1. The vapor from the RD column is withdrawn to an overhead decanter where it is condensed and split into two phases: an organic phase and an aqueous phase. While the aqueous phase is drawn out of the process as waste, part of the organic phase is refluxed back to the RD column and the rest is fed into the stripping column for further purification. An additional water flow is needed to have separate liquid phases in the decanter. The bottom product of the RD column is rich in acetic acid and thus recycled along with the fresh acid feed. The top product of the stripper is recycled back to the decanter. The final stripper bottom stream consists of EtOAc with a purity over 99.5%wt. Homogeneous catalyst is considered, with concentration assumed to be 0.4%vol.

Commonly, the alcohol feed is composed by the industrial grade alcohol (Tang et al. 2003, Lee et al. 2007, Lai et al. 2008) and an excess of acetic acid is necessary to achieve nearly complete conversion of ethanol (Tang et al. 2003, Kloker et al. 2004, Lee et al. 2007). It should be mentioned, however, that an excess of acetic acid is not desired in commercial applications due to greater costs of feed stock and

effluents treatment and that the use of excess reactant in the RD process increase capital and energy costs when compared to neat operation (Luyben and Yu, 2008).

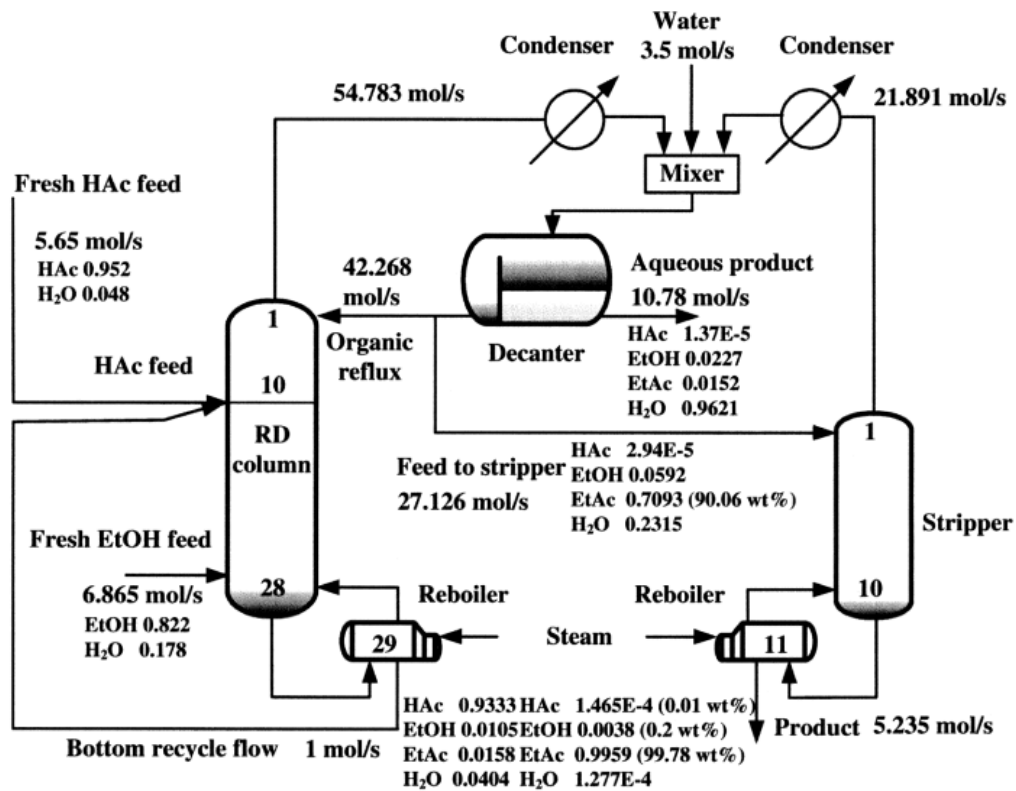


Figure 2.1. Optimal configuration of the complete EtOAc system (Tang et al. 2003)

Detailed experiments on RD steady-state operation were also conducted. Kenig et al. (2001) detailed the ethyl acetate synthesis by homogeneous catalysis: the process feasibility was examined using the reactive residue curves, the process was simulated with an in-house tool based on a rate-based model and a set of experiments was performed in a glass reactive tray column with 80 bubble cap trays. Kloker et al. (2004) carried out steady-state experiments in a laboratory-scale column (50mm diameter and 3m packing height) and in a semi-industrial scale (162mm diameter and 12m packing height), with four different internals for heterogeneous catalyst. The scale-up from laboratory to industrial size columns was enabled by a model simulation in Aspen Custom Modeler[®]. Finally, the complex two-column configuration proposed by Tang et al. (2003) was experimentally conducted by Lai et al. (2008) so as to study the initial charges in the column holdups and a start-up procedure for continuous production. Six experimental runs with different initial charges and operating conditions showed that initial holdup composition plays a critical role for a successful start-up.

Moreover, based on the prosperous application of the reactive distillation, increasing attention has been given to improve the process performance for the ethyl acetate production: Tsai et al. (2008) added external reactors to a single-tray reactive distillation column, which increased both the process conversion and the total annual cost. Smejkal et al. (2009) coupled a fixed-bed reactor and a reactive distillation column utilizing strong ion-exchange resin as catalyst, and verified the simulation results by experimental studies. Konakom et al. (2010, 2011) proposed a dynamic optimization strategy to produce ethyl acetate of 90% by using an 8-hours batch RD column. Hu et al. (2011) increased the reactive distillation efficiency by using a mass separation entrainer: n-butyl acetate is selected to withdraw the accumulated water from the RD column rectifying section. Moreover, ethyl acetate can also be produced by reactive distillation from transesterification of butyl acetate (Wang et al. 2010) or methyl acetate (Bonet 2006).

All works proved that the production of ethyl acetate by reactive distillation can significantly increase conversion as compared to conventional reactors.

Dynamics and control

Many papers address the RD process design and an increasing number have been considering the dynamics and control aspects of the EtOAc esterification. One of the pioneer works was presented by Burkett and Rossiter (2000), who studied the control strategy in a single industrial RD column where the reaction occurred at the column base. Then, Vora and Daoutidis (2001) showed superior performance of the nonlinear controller over both linear and the conventional PI controller, also to control a single RD column. However, both works resulted in outlet streams not pure enough for industrial usage with the single column; the product stream needs further purification and waste stream needs to be treated.

As a continuation of their previous work, Tang et al. (2005b) considered the plant-wide design (Tang et al. 2003) and conducted a sensitivity analysis to identify the suitable sensors locations in the columns for temperature control, with respect to disturbances on the feed flowrates and compositions. Four alternative plant-wide control strategies were proposed, each closed-loop scheme was tested and the authors found that control of the product qualities by modulating two tray temperatures in the RD column and one tray temperature in the stripper is most appropriate. Two product purities – the content of EtOH and HOAc in the distillate – could be kept within acceptable specifications.

Then, based on the control structures studied by Tang et al. (2005b), Lee et al. (2007) analyzed four important control issues for the EtOAc production: (i) economic, (ii) steady-state deviation of key

product purities, (iii) degree of oscillation and settling time, and (iv) feasible region of disturbances for effective control. New control schemes were developed to improve the process operability, and a combination of open-loop and closed-loop sensitivity analysis methods was proposed to select locations for temperature control. It was concluded that, in function of the purity of the acid feed, one or two temperature control loops were to be introduced in the RD column; in both cases, one additional loop controls a temperature in the stripper column.

Later, Venkateswarlu and Reddy (2008) developed nonlinear model predictive control (NMPC) strategies in the perspective of the RD column, by using stochastic optimization algorithms. The controller performance was evaluated by applying it to the single input-single output control of an ethyl acetate esterification with double-feed configuration. The results demonstrated better performance of the stochastic optimization based NMPCs over a conventional proportional-integral (PI) controller, a linear model predictive controller (LMPC), and a NMPC based on sequential quadratic programming.

It is important to point out that no experiments under dynamic conditions were found for the ethyl acetate system.

2.2 SOLVAY CONTEXT

Rhodia is a member of the Solvay Group and is a world leader in the development and production of specialty chemicals. Its industrial facility in Paulínia, Brazil, is one of the major producers of ethyl acetate in the world.

The current production process consists in one reactor and a series of separation devices for further purification of the ester. A company strategic project was then initiated to improve the ethyl acetate production by installing a reactive distillation in the process. The objective is to replace the existing reactor and the first distillation column of the separation trend by a reactive column, so as to increase the esterification conversion.

Due to the fact that the other present devices are to be maintained, stringent specifications are to be met in both distillate and bottom products of the reactive column: there is a maximum limit for the contents of both ethanol and acetic acid in the distillate and the acid content in the bottom. Some studies concerning the design parameters of the column, such as technology and catalysis have been developed, but the operability and controllability aspects have not yet been addressed.

SECOND PART

II. MATERIALS AND METHODS

3.	Experimental devices	45
4.	Design methodology for reactive distillation columns	55
5.	Tools and methods to handle controllability and diagnosability aspects	61

The proposed controllability analysis and the related experimental validations request the use of different materials and methods. The approach lies on a progressive introduction of the process complexity and, as a consequence, different calculation methods and tools are sequentially applied for each methodology step. Chapter 3 details the experimental pilot devices used for the model validations. Chapter 4 presents the existent methods for the conceptual design of reactive distillation columns, from which an adaptation to the ethyl acetate case is derived. Chapter 5 discusses the use of simulation software, classification programs and other computational calculations for the controllability and diagnosability approaches.

Les analyses de contrôlabilité et de diagnosticabilité, ainsi que les études expérimentales, utilisent différents matériels et méthodes. La méthodologie de conception proposée est basée sur l'introduction progressive de la complexité du procédé, avec application séquentielle de différents outils et méthodes.

Le Chapitre 3 présente les équipements utilisés lors des expérimentations. D'abord, avec l'objectif d'obtenir les paramètres nécessaires pour définir un modèle fiable du procédé, des manipulations expérimentales sont réalisées dans une colonne réactive à échelle pilote, dans le Research & Innovation Center of Solvay à Lyon, France. Le pilote est appelé *pilot2011* et les résultats sont étudiés dans le Chapitre 6. La distillation réactive produit l'acétate d'éthyle par esterification avec catalyse hétérogène de l'éthanol et l'acide acétique. Le diamètre de la colonne est de 75mm et son hauteur est de 7m. Le pilote est conçu avec 7 sections modulaires de 1m, avec un distributeur de liquide placé au-dessus de chaque section, numérotés vers le haut (D1-D7). Les 5 sections centrales sont garnies avec le garnissage structuré KATAPAK Sp-Labo, où la catalyse hétérogène est obtenue par des résines échangeuses d'ions acides. La deuxième approche expérimentale est aussi réalisée dans le Research & Innovation Center of Solvay, avec l'objectif d'étudier la méthodologie pour l'analyse de contrôlabilité et la compréhension des sensibilités et de l'opérabilité du pilote. Le nouveau pilote est appelé *pilot2013* et les résultats sont discutés dans le Chapitre 11. Ce nouveau pilote est composé de 6 sections modulaires, avec des plateaux à cloche, pour la mise en œuvre de la réaction en catalyse homogène.

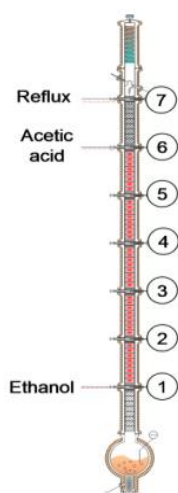


Figure 3.1. Schéma simplifié de la colonne *pilot2011*

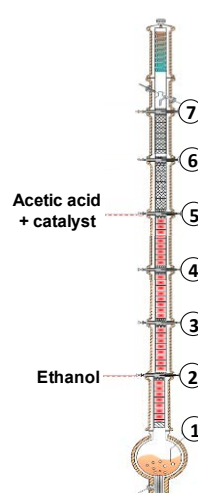


Figure 3.7. Schéma simplifié de la colonne *pilot2013*

Le Chapitre 4 présente la méthodologie développée au LGC (Laboratoire de Génie Chimique, Toulouse, France) pour la conception de colonnes de distillation réactive, laquelle sera adaptée pour la production d'acétate d'éthyle dans le Chapitre 9. La méthodologie combine différentes approches proposées dans la littérature, basées sur l'analyse statique du procédé. Une combinaison d'algorithmes est utilisée pour les étapes d'analyse de faisabilité et de synthèse. C'est un outil créé en Fortran, interfacé avec MatLab[®] pour les propriétés graphiques et avec Simulis[®] pour les données thermodynamiques. La configuration de colonne résultante de cette analyse est ensuite simulée dans Aspen Plus[®].

L'analyse de faisabilité (Théry, 2002) étudie les courbes de résidu réactives et les courbes extractives réactives du système pour évaluer les performances atteignables en termes de taux de conversion, taux de récupération et pureté. L'étape de synthèse émet des considérations de débits molaires constants, reflux fini et réalise les bilans de matière en négligeant les effets thermiques. La synthèse propose des paramètres de configuration de colonne : taux de reflux minimal, et, pour un taux choisi, le nombre d'étages théoriques, le nombre et la localisation des étages réactifs et le placement des alimentations. L'étape de conception introduit le bilan enthalpique et considère les aspects thermiques. Les paramètres opératoires nécessaires pour atteindre les spécifications de la réaction et de la séparation sont définis par simulation dans Aspen Plus[®].

Le Chapitre 5 présente les outils et méthodes utilisées pour les analyses de contrôlabilité et de diagnosticabilité du système. La simulation du procédé en régime permanent est conduite sous Aspen Plus[®] et le régime obtenu est une initialisation pour la simulation dynamique dans Aspen Plus Dynamics[®]. Quelques indices de contrôlabilité qui nécessitent des calculs matriciels complexes sont calculés dans Matlab[®] ou dans Microsoft Excel, qui permet aussi le tracé de graphiques pour évaluer la sensibilité de la colonne et les performances de la structure de commande.

L'analyse de diagnosticabilité est réalisée à l'aide du logiciel P3S[®], développé au sein du LAAS (Laboratoire d'Analyse et d'Architecture des Systèmes, Toulouse, France). La méthode de classification LAMDA basée sur la logique floue permet la détection de différentes classes qui représentent les régimes de fonctionnement normal et anormal du procédé. La technique MEMBAS permet l'identification des capteurs les plus discriminants pour cette classification et diagnostic qui en résulte.

As análises de controlabilidade e de diagnosticabilidade, assim como os estudos experimentais, usam diferentes materiais e métodos. A metodologia de projeto proposta é baseada na introdução progressiva de complexidade no processo, com a aplicação sequencial de diferentes ferramentas e métodos.

O Capítulo 3 apresenta os equipamentos utilizados nos estudos experimentais. Primeiro, com o objetivo de adquirir os parâmetros necessários para definir um modelo confiável do processo, experimentos são conduzidos em uma coluna reativa em escala piloto, no *Research & Innovation Center of Solvay* em Lyon, França. O piloto é chamado *pilot2011* e os resultados são discutidos no Capítulo 6. A destilação reativa produz acetato de etila pela esterificação com catálise heterogênea de ácido acético e etanol. O diâmetro da coluna é 75mm e sua altura é 7m. O piloto é constituído de 7 seções modulares de 1m, com um distribuidor de líquido colocado acima de cada seção, numerados do fundo ao topo (D1-D7). As 5 seções centrais são preenchidas com o recheio estruturado KATAPAK Sp-Labo, onde a catálise heterogênea é obtida por resinas trocadoras de íons. A segunda abordagem experimental foi também conduzida no *Research & Innovation Center of Solvay*, com objetivo de estudar a metodologia para análise de controlabilidade e o entendimento da sensibilidade e da operabilidade do piloto. O novo piloto é chamado *pilot2013* e os resultados são discutidos no Capítulo 11. Esse novo piloto é composto de 6 seções modulares, com pratos *bubble-cap*, para a implementação da reação em catálise homogênea.

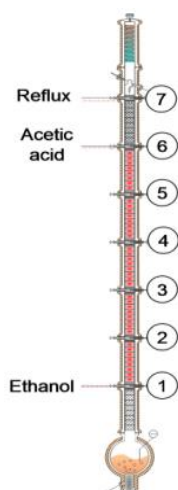


Figura 3.1. Esquema simplificado da coluna pilot2011

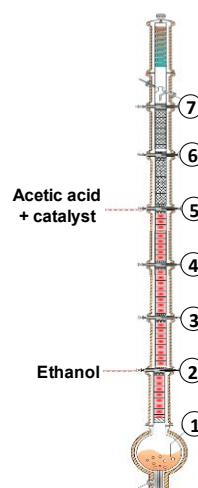


Figura 3.7. Esquema simplificado da coluna pilot2013

O Capítulo 4 apresenta a metodologia existente, desenvolvida no LGC (Laboratoire de Génie Chimique, Toulouse, France) para o projeto de colunas de destilação reativa, a qual foi adaptada para a produção de acetato de etila no Capítulo 9. A metodologia combina diferentes abordagens propostas na literatura, baseadas em análises estáticas do processo. Uma combinação de algoritmos é utilizada para as etapas de análise de viabilidade e de síntese. Trata-se de uma ferramenta criada em Fortran, que se comunica com o MatLab[®] para funcionalidades gráficas e com o Simulis[®] para aspectos termodinâmicos. A configuração de coluna resultante dessas etapas é em seguida simulada em Aspen Plus[®].

A análise de viabilidade (Théry, 2002) estuda as curvas de resíduo reativas e as curvas extrativas reativas do sistema para avaliar as performances atingíveis em termos de taxa de conversão, taxa de recuperação e purezas. Na etapa de síntese assumem-se considerações de fluxos molares constantes, refluxo finito e realizam-se os balanços de massa ignorando os efeitos térmicos. A síntese propõe os parâmetros de configuração da coluna: taxa mínima de refluxo e, para uma taxa escolhida, a quantidade de estágios teóricos, a quantidade e a localização dos estágios reativos e a localização das alimentações. A etapa de concepção introduz o balanço de energia e considera os aspectos térmicos. Os parâmetros de operação necessários para atingir as especificações da reação e da separação são definidos por simulação em Aspen Plus[®].

O Capítulo 5 apresenta as ferramentas e métodos usados para as análises de controlabilidade e de diagnosticabilidade do sistema. A simulação do processo em regime permanente é realizada em Aspen Plus[®] e o regime obtido é uma inicialização para a simulação dinâmica em Aspen Plus Dynamics[®]. Alguns índices de controlabilidade que necessitam cálculos matriciais complexos são conduzidos no Matlab[®] ou no Microsoft Excel, que permite também o desenho de gráficos para avaliar a sensibilidade da coluna e o desempenho da estrutura de controle.

O estudo de diagnosticabilidade é realizado com o software P3S[®], desenvolvido no LAAS (Laboratoire d'Analyse et d'Architecture des Systèmes, Toulouse, France). O método de classificação LAMDA, baseado em lógica difusa, permite a detecção de classes diferentes que representam regimes de funcionamento normais e anormais do processo. A técnica MEMBAS permite a identificação dos sensores mais discriminantes para essa classificação e o diagnóstico resultante.

Experimental devices

3.1 DEFINITION OF RELIABLE PARAMETERS FOR THE SYSTEM MODEL

Aiming at acquiring all the necessary parameters for the definitions of reliable model of the process, experimental manipulations were conducted in a lab-scale reactive column pilot in the Research & Innovation Center of Solvay at Lyon, France. The technology used here will be denoted as “pilot 2011” and the results obtained will be further discussed in Chapter 6.

3.1.1 Pilot characteristics

The reactive distillation for the heterogeneous catalyzed esterification of ethanol and acetic acid to ethyl acetate and water is studied. Experiments were carried out in a lab-scale pilot which consists of a glass column with an inner diameter of 75mm and a height of 7m. It is divided into 7 modular sections of 1m, with a liquid distributor at the top of each modular section, numbered bottom-up (D1 – D7).

The column operates with three different feed flows: the acetic acid feed is injected at distributor D6, the ethanol feed is injected at distributor D1 and a third feed flow, which is called Reflux, is assimilated to an external reflux and is introduced into the column at distributor D7. This external reflux is representative of the organic phase coming from a decanter in which different streams of the process are mixed. The distillation pilot column is schematized in Figure 3.1, with its respective distributors.

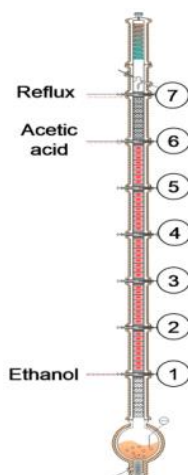


Figure 3.1. Simplified scheme of pilot 2011

The liquid distributors allow an uniform distribution of the liquid feed in the packing, avoiding any liquid flow through the wall. The distributors reduce the wall effects that would decrease the mass transfer and promotes better contact between liquid and packing, enhancing both phenomena of phase separation and reaction on catalyst pores. A representative scheme is given in Figure 3.2.

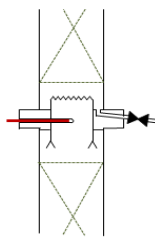


Figure 3.2. Liquid distributor schematic

The column is operated at atmospheric pressure and is thermally insulated, using insulated jackets.

The packing structure has the following characteristics:

- The modular section at the top of the column is filled with Sulzer DX structured packing (number of theoretical stages ~8)
- The 5 central modular sections are filled with KATAPAK SP-Laboractive structured packing and with an acidic ion-exchange resin as the heterogeneous catalyst. The structured packing enlarges the internal surface and promotes turbulences so that the mass transfer between the liquid and the vapor phase, and the interaction of the liquid phase and the reactive catalyst pores are increased (number of theoretical stages ~11)
- The modular section at the bottom of the column is filled with the structured packing Sulzer CY (number of theoretical stages ~8)

A classical glass condenser is vertically positioned above the column. In the chosen configuration, the vapour stream is fully condensed at the top of the column and withdrawn as the distillate flow. After passing through the condenser, the distillate goes to a heat exchanger to be cooled to ambient temperature (between 15°C and 30°C) by glycolic water at 5°C so as to avoid the evaporation of the ethyl acetate during sample withdrawal. The distillate goes further to a 5-litre decanter where it splits into two different phases. The interface level is regulated manually because the production of the aqueous phase is relatively small.

The column reboiler is equipped with a guided coaxial waves transmitter to measure the liquid level and with a flow control valve enabling the liquid level regulation in the reboiler by acting on the outlet residue flow rate. The temperature measurement of the contained liquid is performed by a thermocouple surrounded by a thermowell filled with oil so as to ensure the thermal transfer between the liquid and the sensor. A second thermocouple is installed for safety purposes.

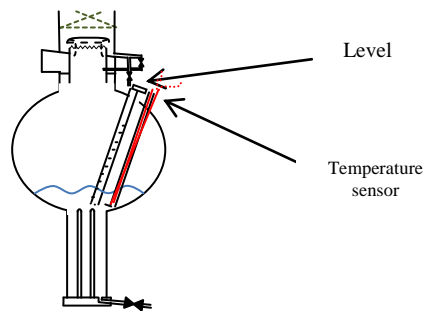


Figure 3.3. Reboiler scheme of pilot 2011

The heat duty of the column is regulated by controlling the temperature of the circulating oil inside the reboiler heat element. In order to maintain a constant heat during pilot experiments (so as to ensure constant distillate flow rate), the difference between the oil temperature and the liquid temperature was maintained constant.

Each feed line consists of a tank placed on a scale, under inert atmosphere (ensured by a nitrogen line connection) and siphoned using a vacuum flask. A volumetric pump takes the liquid from this flask and pumps it into a tubing line made of:

- a pressure safety valve set at 5 bars
- a dashpot that attenuates the pulsations from the pump
- a Coriolis mass flow meter
- a check valve set at 2 bars, in order to maintain a determined pressure into the line and to ensure a constant flow in the pump. If necessary, this element can be bypassed.

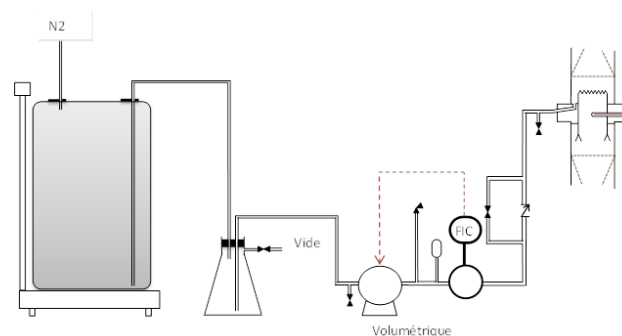


Figure 3.4. Feed line scheme

The acetic acid feed line is electrically heated up to 30°C, so as to avoid its solidification (its melting point is about 16.6°C). The flow meter measurements are numerically filtered before entering the flow controllers, which act on the frequency of the pump-variators. Thus, regular and constant flows are obtained over time.

A more detailed scheme of the entire reactive distillation pilot is given in Figure 3.5.

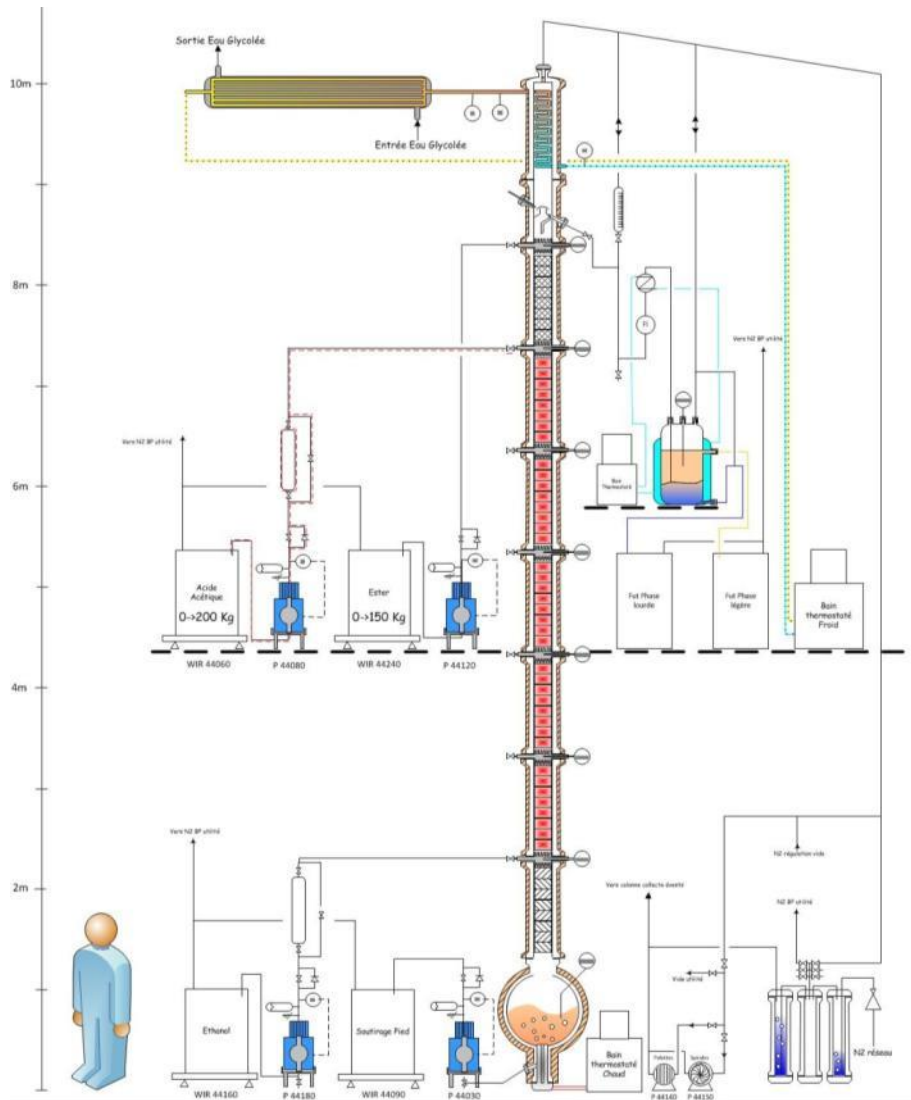


Figure 3.5. Pilot 2011 configuration

It is worth mentioning that the pilot plant configuration and operating conditions were not designed to provide the best productivity or product purity but to acquire data on column characteristics and system behavior, following its dynamic tendencies and responses to perturbations.

3.1.2 Data acquisition

The plant's instrumentation provides seven temperature measurements in the vapor phase of each liquid distributor, and two temperature measurements in the liquid phase of the reboiler and distillate line. In addition, temperature measurements of the cooling liquid entering and exiting the condenser and the oil that heats the reboiler are provided. All the measures are obtained by thermocouples. The five flow

rates – three feed flows, the produced distillate and residue – and the pressure drop on the column are also registered. Measurements of both the flow rate and the temperature of the cooling fluid are placed in the input and in the output of the condenser. All the process variables, such as flow rates, temperatures, reboiler liquid level and system pressure are collected and monitored by a standard digital process control system. The user interface is shown in Figure 3.6.

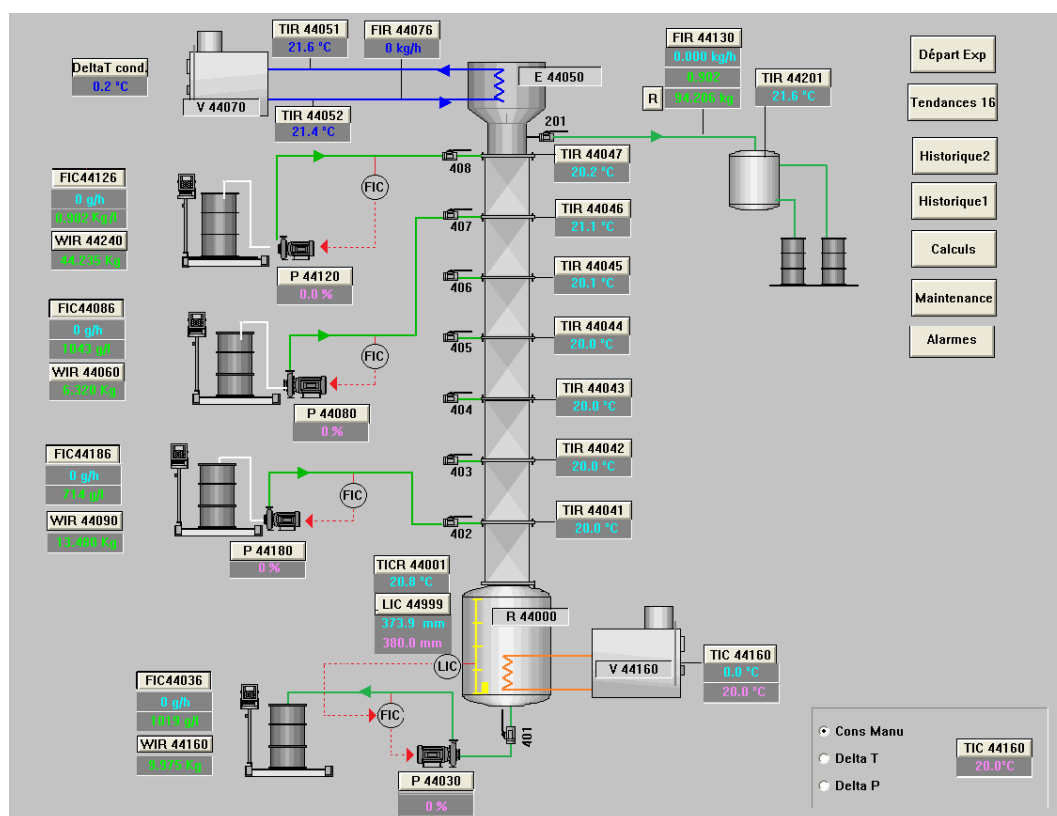


Figure 3.6. Digital control system interface 2011

During experimental runs, liquid phase samples were withdrawn from four liquid distributors D2, D3, D4 and D5 (because the other three distributors D1, D6 and D7 received the feed flows and their valves were not available) as well as from the distillate. At the bottom of the column, the reboiler geometry and the requested high liquid level result in an important residence time. In order to withdraw a representative sample of the composition at the bottom line, a derivation of the down-coming liquid was introduced just above the reboiler.

The esterification reaction studied includes four components: ethanol, acetic acid, ethyl acetate and water. The analytical methodology must thus quantify the composition of all the components of the quaternary system; three different methods were consequently applied: gas chromatography, Karl Fischer method and acid-base titration.

Then, the data reconciliation procedure was conducted by a computational tool. The set of data consists of 5 flow-rate and 20 mass compositions measurements. Random errors are assumed to follow a normal distribution and the reconciliation procedure minimizes the weighted least squares of the errors between the reconciled and the measured variables. The weight is the inverse of the measurements covariance matrix, which is a classic approach called Gauss-Markov estimator (Walter and Pronzato, 2010). By balances, reaction equations and physical constraints considerations, the calculations resulted in values of flow rates and compositions that respect the column mass balance with high accuracy (error $< 10^{-6}$).

3.2 SENSITIVITY APPROACH IN A REAL REACTIVE COLUMN

A second experimental campaign was also conducted at the Research & Innovation Center of Solvay at Lyon, France. Once the methodology to study the controllability of reactive distillation columns has been developed, the purpose of the new experiments was the comprehension of the column sensitivities and operability. Aiming at differentiating both experimental campaigns, the new devices are presented as “pilot 2013”. The study conclusions are discussed in Chapter 11.

3.2.1 Pilot characteristics

The reactive distillation pilot column consists of a glass column with an inner diameter of 50mm and a height of 6m. It is divided into 6 modular sections of 1m, with a liquid distributor at the top of each modular section.

The esterification reaction occurs with the sulfuric acid as a homogenous catalyst, with a mass proportion of 3% in relation to the acetic acid feed flow rate. The two feed flows are the ethanol flow, which is injected one modular section above the reboiler, and the acetic acid which is introduced together with the catalyst one modular section from the top of the column. Due to the low volatility of the sulfuric acid, this catalyst is present in all the sections below its feed location. As a consequence, the reaction may occur in all these sections. A zone solely dedicated to separation is only possible above the catalyst feed location, which is represented by the top modular section of the present pilot.

The scheme of the liquid distributors and the feed lines are similar to the ones of pilot 2011, presented in Figures 3.2 and 3.4, respectively. The new distillation column is schematized in Figure 3.7.

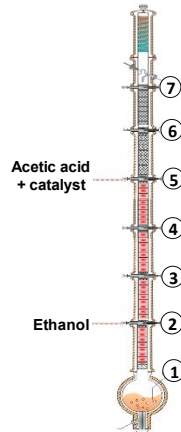


Figure 3.7. Simplified scheme of column 2013

The heat of the column is regulated by controlling the temperature of the circulating oil inside the reboiler heat element. The column is surrounded by a vacuum silver jacket, so external perturbations were neglected. Figure 3.8 represents the reboiler, with its thermocouples and the absence of level regulation.

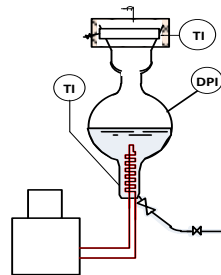


Figure 3.8. Reboiler scheme of pilot 2013

Each modular section is filled with 10 bubble cap trays provided by QVF (Schmickler and Fritz).

Bubble caps are recommended for reactive columns in order to increase the liquid holdup and enable the chemical reaction. The expected trays efficiency is 65%, providing 35 theoretical stages in the column. Schemes of the trays and of the entire pilot are given below.

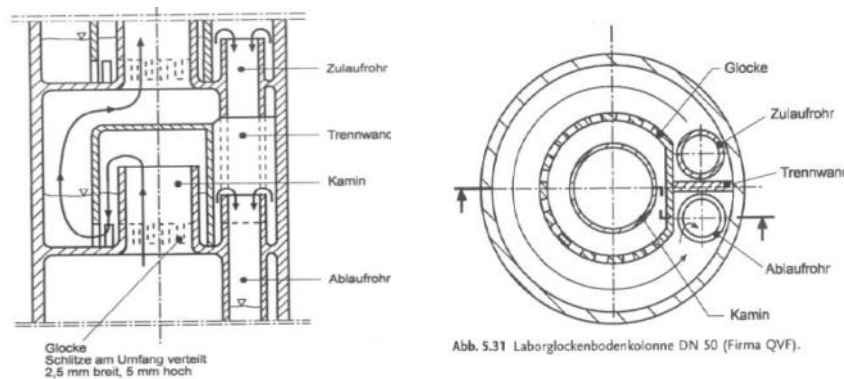


Figure 3.9. Schmickler and Fritz bubble cap trays

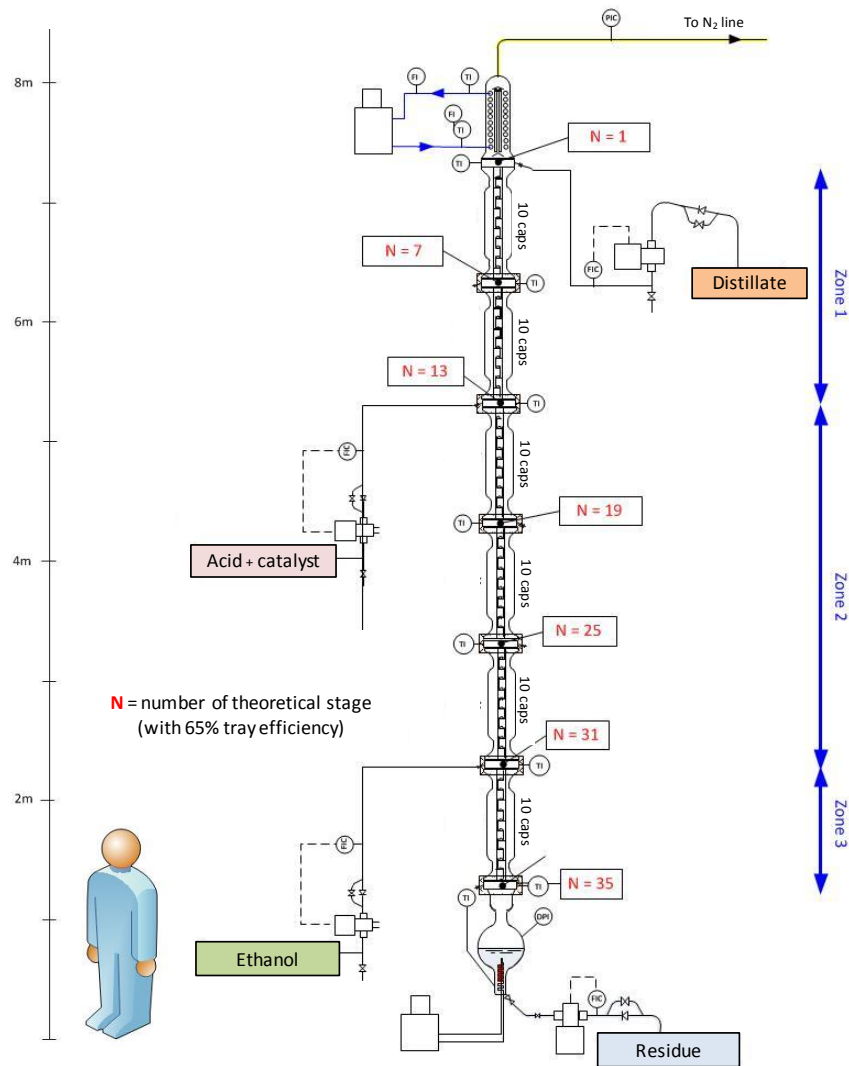


Figure 3.10. Pilot 2013 configuration

3.2.2 Data acquisition

The plant instrumentation provides six temperature measurements in the vapor phase of each liquid distributor, and two temperature measurements in the liquid phase of the reboiler and distillate line. In addition, temperature measurements of the cooling liquid entering and exiting the condenser and the oil that heats the reboiler are provided. All the measures are obtained by Pt-100. The streams flow rates are given by Coriolis flow meters and the pressure drop is registered. An energy balance of the condenser, based on the flow rate and the input and output temperature of the cooling fluid, provides the amount of vapor produced. Once the distillate flow rate is known, the reflux ratio can be calculated.

The process variables are monitored by a standard digital process control system; the user interface is depicted in Figure 3.11.

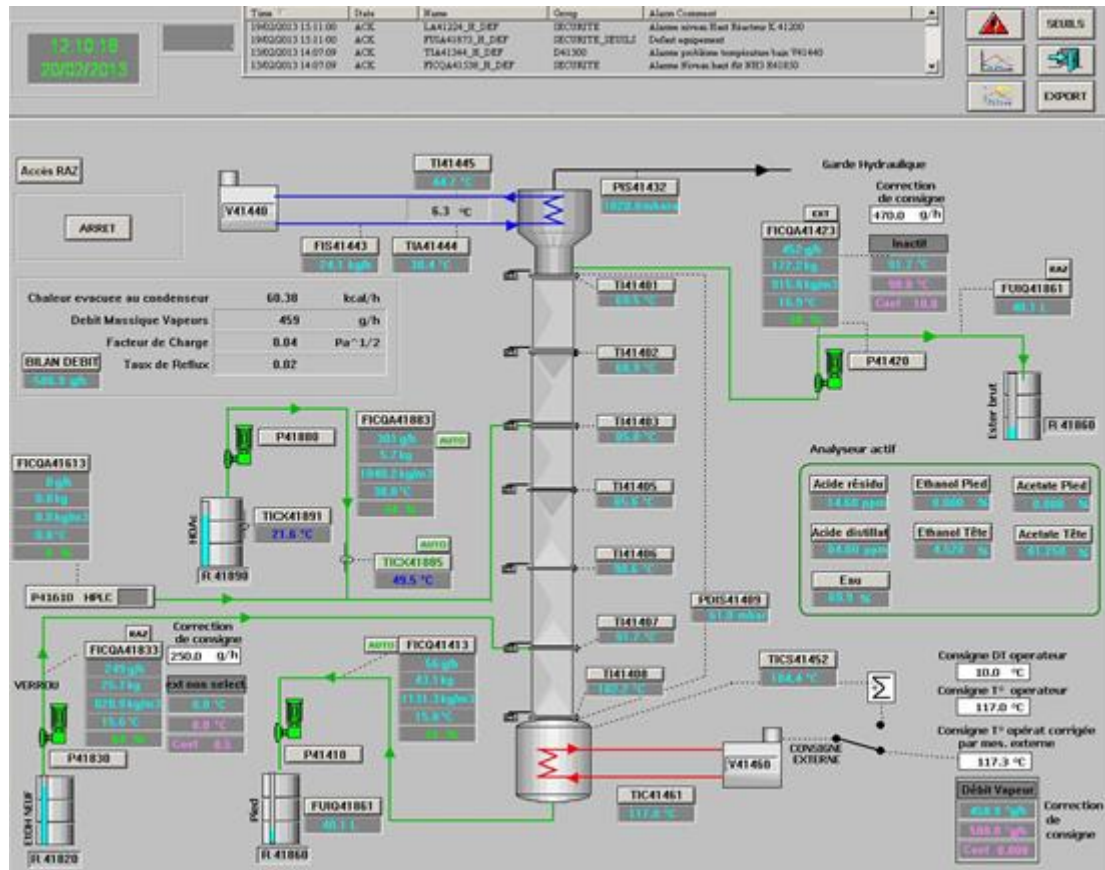


Figure 3.11. Digital control system interface pilot 2013

Online composition analyzers were used in the distillate and on the residue lines. A liquid sample was used for the distillate, whereas the residue was sampled in gas phase at the reboiler stage. The chromatography analysis method provides the composition of ester, alcohol and acid each 13 minutes. It was also possible to take periodic samplings of these lines in order to validate the measures with additional offline chromatography analysis and to obtain the water composition by the Karl Fischer method.

An important advantage of this pilot configuration is the addition of three possible regulations so as to improve the operability of the column and the validation of the controllability approach. The independent manipulated variables are the heat duty, the ethanol feed flow rate and the distillate flow rate. Several controlled variables were available for each regulation; the user should select one of the temperatures in the distributors or the product components composition.

Design methodology for reactive distillation columns

4.1 SEQUENTIAL APPROACH

The design of reactive column requires the use of tools based on reliable thermodynamics and reaction models.

The LGC (Laboratoire de Génie Chimique, Toulouse, France) develops a methodology for the design of reactive distillation systems, which combines different approaches proposed in the literature and is based on static analysis. Through a sequential approach, the PSI (Procédés et Systèmes Industriels) department of this Laboratory developed a tool dedicated to the feasibility analysis and the pre-design of reactive distillation columns (They et al. 2002, 2005, 2012). Different types of software were developed and successively applied. The approach is schematized in Figure 4.1 (They et al. 2012).

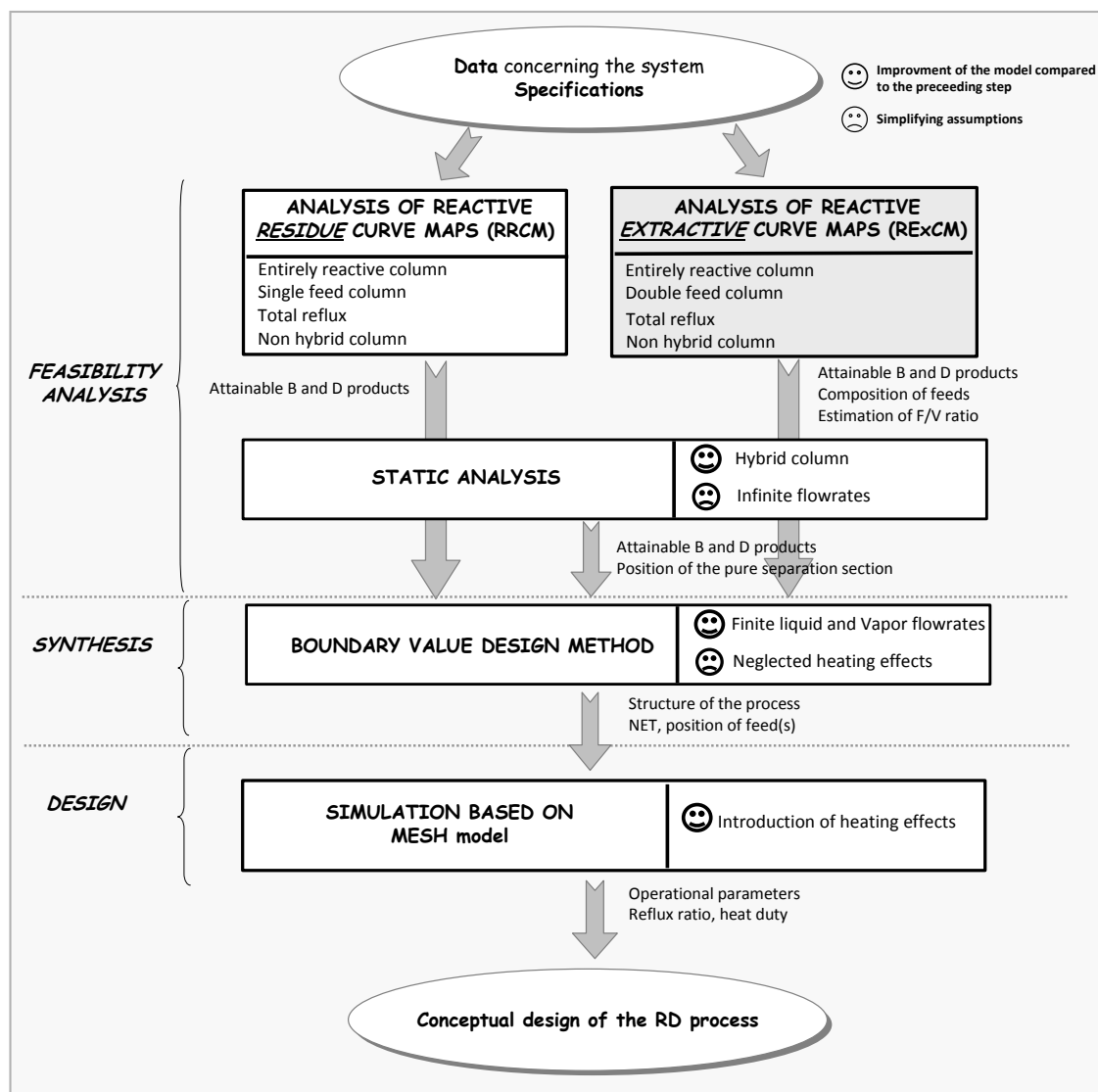


Figure 4.1. Constitutive approaches of the design methodology (Théry-Hétreux et al. 2012)

First, a combination of algorithms is used for feasibility and synthesis calculations. This has been developed in an in-house tool implemented in Fortran, interfaced with MatLab[®] for its graphical facilities and connected to the thermodynamic properties server Simulis[®]. Then, the column configuration is defined in Aspen Plus[®] and process simulation at steady state provides more operational parameters at the conceptual design step.

The main interest is that the tools lie in a sequential and progressive introduction of process complexity; from a minimal set of information concerning the physicochemical properties of the system (pure components physical properties, phase and reaction equilibria), successive refinements are considered. The techniques applied in the feasibility analysis, the synthesis and the conceptual design lead to the project of the unit and the specification of its operating conditions.

Currently, the procedure can be considered for reactive column systems with one or two feeds, for any number of equilibrium reactions and liquid phase splitting, as far as the system respects the constraint that the number of component minus the number of reaction minus 1, i.e. the variance of the system, is equal to 2. This constraint is related to the fact that part of the methodology currently lies on a 2D-graphical analysis. This methodology has already been successfully applied to different industrial case and reactive systems (Théry 2002, Brehelin 2006, Bonet 2006, Steger 2006, Bellassaoui 2006).

4.1.1 Feasibility analysis

The feasibility analysis step proposed by Théry (2002) is based on two successive approaches. First, reactive residue curves maps (rRCM) enlighten the nature of the singular points of the system and the possible reactive or non-reactive distillation boundaries. Then, for hybrid columns (consisting of reactive and non-reactive sections), steady state analysis selects the most adapted feed composition to achieve the given objectives and evaluates the attainable performances regarding conversion rate, recovery ratio and purity.

A reactive residue curve is defined by the locus of the liquid composition, in equilibrium with the vapor composition, remaining from a simple batch reactive distillation process (referenced as the Rayleigh distillation for non-reactive system). The calculation of each curve consists of the integration of the mass balance differential equations, respecting the restrictions of both chemical and phase equilibria. A reactive residue curve map is obtained by the simulation of the reactive distillation process for various initial liquid compositions.

The residue curve maps allow graphic analysis leading to feasibility conclusions about the process. Some examples are developed and discussed in detail by Théry (2002) and Brehelin (2006).

An interesting characteristic of the analysis of reactive residue curves is that it allows the exploitation of reliable results obtained from simple distillation analysis. Ung and Doherty (1995) exploited the methodology for non-reactive systems to systems with one instantaneous equilibrium reaction; the authors introduced a set of transformed composition variables of which values remain constant during the reaction and that sum to unity. These transformed variables are a mathematic artifice that is independent of the reaction extent and reduces the dimensionality of the problem by one. As a consequence, the dimension of the space of residue curve maps is also reduced and the graphical analysis is facilitated. For quaternary reactive systems, the mole-fraction space that was tetrahedral becomes planar in transformed composition variable coordinates. The analysis of rRCM suggests the possible need of plates for pure separation or more feed locations.

Although feasibility conditions can be specified, residue curves are conceived for the analysis of entirely reactive columns and one representative feed flow. To assess the feasibility analysis of double feed columns, the concept of reactive extractive curves is adopted (Théry et al., 2012). Reactive extractive curves may represent the liquid composition profile in the stages present between the two feed plates. The extractive reactive curve is also obtained by the integration of mass balance differential equations. These concepts will be deeper discussed with the application in chapter 9.

The feasibility methodology based on an infinite reflux/infinite number of stage assumption (∞/∞ analysis) determines if the expected objectives for the system are physically attainable by a reactive distillation column, whether a double feed is needed but it does not give any information on the size of the process. The methodology moves then forward to the synthesis step.

4.1.2 *Synthesis step*

The synthesis step lies on Mac Abe-Thiele type assumptions: finite reflux, constant molar overflow, and all thermal effect are neglected. It provides the column configuration parameters: minimum reflux ratio, and, for a given reflux ratio and a number of feed, the number of theoretical plates, the number and location of reactive plates, the location of feed plates.

The methodology applied by Théry et al. (2005) considers the Boundary Value Design Method introduced for reactive systems by Barbosa and Doherty (1987). The specifications required for the synthesis are inherited from the previous feasibility analysis.

By solving the mass balance equations coupled with physical equilibrium equations between the top of the column and a rectifying stage and between the bottom and a stripping stage, the composition profiles are obtained in the rectifying, middle and stripping sections of the reactive column. The profiles calculated necessarily depend on the reflux ratio. When the rectifying, middle and stripping profiles intersect, a feasible steady state is then identified. As these profiles are calculated stage by stage, the number of stages required in each section of the column can also be estimated.

The tool developed can currently treat different configurations including one or two pure separation zones and one or two feed plates.

4.1.3 *Conceptual design step*

The synthesis step relies only on calculations of mass balance and both physical and chemical equilibrium equations; thermal phenomena are ignored. To refine the results, the conceptual design phase introduces enthalpy balances and phenomena such as heat of reaction, thermal loss, heat of mixture, etc, are then considered.

Simulation software is used to evaluate and to adjust the necessary operation parameters to reach the reaction and separation specifications. This has been done with Aspen Plus[®] for the simulation of processes in steady-state. Théry- Hétreux et al. (2012) mentioned that, given the pressure, the column configuration and the feed characteristics, the degree of freedom of the MESH model is equal to 2: to saturate this degree of freedom, the purity and the partial flow rate of the desired component (at the top or at the bottom of the column) are set. Then, the simulation provides feasible reactive distillation column operating parameters to achieve the initial specifications, such as the required reflux ratio and heat duties. This configuration is a reliable initialization condition for further optimization of the process and can be refined with more rigorous models, which can consider non-equilibrium equations, kinetically controlled reactions, etc. Gomez (2003) conducted an optimization study in this context.

The reactive distillation study will begin then by a pre-design procedure based on the techniques proposed by the LGC. The existing tools will be adapted for the ethyl acetate system and new methods considering the dynamic aspects will be developed to evolve the methodology.

Tools and methods to handle controllability
and diagnosability aspects

5.1 SIMULATION AND CONTROLLABILITY ANALYSIS

The process simulation and the controllability study methodology are mainly based on computational methods. Different commercial tools are used:

- For the process simulation, different softwares commercialized by AspenTech society are used. Aspen Plus[®] integrates process modeling analysis and design tools, allowing the analysis of the system behavior. Aspen Plus Dynamics[®] extends Aspen Plus[®] steady-state models into dynamic process models, enabling design and verification of process control schemes, safety studies, failure analysis, etc.
- Matlab[®] is a programming environment for algorithm development, data analysis, visualization and numeric computation. It is used for the controllability criteria calculations.
- Spreadsheets on Microsoft Excel enable matrices calculations for the column sensitivity analysis and graphics drawing to evaluate the control structures performances.

5.2 PROCESS DIAGNOSIS

The diagnosability step is carried out using P3S[®] (Process Sensor Selection and Situation Assessment), an in-house software developed by the LAAS (Laboratoire d'Analyse et d'Architecture des Systèmes) in the frame of the European project CHEM (Kempowsky, 2004). This tool integrates the LAMDA classification algorithm and the MEMBAS technique for sensor location, detailed hereafter.

5.2.1 *The fuzzy classification technique LAMDA*

Within the fuzzy techniques presented in Chapter 1, section 1.4, for system diagnosis, the technique LAMDA, for Learning Algorithm for Multivariable Data Analysis, is developed by the group DISCO, at the LAAS in Toulouse (France) and dedicated to the process diagnosis based on the analysis of multidimensional data after a learning procedure. This technique has been successfully applied for the diagnosis of systems in different domains: psychology (Galindo and Aguilar-Martin, 2002), biotechnology (Waissman, 2000), industrial chemical processes (Kempowsky, 2004) (Orantes et al, 2006, 2007) and breast cancer prognosis (Hedjazi et al., 2010a).

LAMDA is a fuzzy methodology of clustering and classification, based on finding the global membership degree of a pattern to an existing class, considering all the contributions of each of its features (here represented by sensors). A 'class' can be defined as a set of individuals that present similarity in their behavior. In the case of process diagnosis, those classes will represent the different faulty or normal operating conditions.

The design of the classifier is performed during the learning step based on historical recorded data and one *individual* of this data base corresponds to the set of sensors information at each time. This technique is well adapted to complex, nonlinear or interdependent dynamic systems, because there is no need of a precise phenomenological mathematical model of the process. However, this method being based on the measured sensor values, it is important to have reliable techniques of automatic measurements.

Each measured element, also called individual, is represented by its parameters or sensors measurements, also called descriptors. All individuals have a fixed number of descriptors. Different fuzzy logic functions are available for fuzzification of parameters including quantitative, qualitative or interval parameters and the aggregation of the information is performed through a logic connective. The choice of the fuzzification functions and the connective is made during the learning step design.

The adequacy rules used to classify the individuals were proposed by Aguilar-Martin and Balssa (1980). The technique is based on determining the global membership degree of an individual to an existing class, considering all the contributions of each of its parameters. This contribution is the marginal adequacy degree (*MAD*) and their combination using fuzzy logic connectives as aggregation operators generates the values of Global Adequacy Degree (*GAD*) of an individual to a class (Aguilar and López de Mántaras 1982). Different functions can be used to compute the *MAD* according to the type of data processed; details can be found in Appendix III. The *GAD* of an individual for each class is function of the *MADs* that represent the contribution of each descriptor of the individual. Their aggregation is obtained by using fuzzy connectives (Figure 5.1).

It is important to highlight that the performance of each procedure depends on the right selection of its algorithm's parameters. LAMDA classification methodology was studied by Orantes (2006), Isaza (2007, 2009) and Hedjazi et al. (2010a), providing the information and calculations presented in Appendix III.

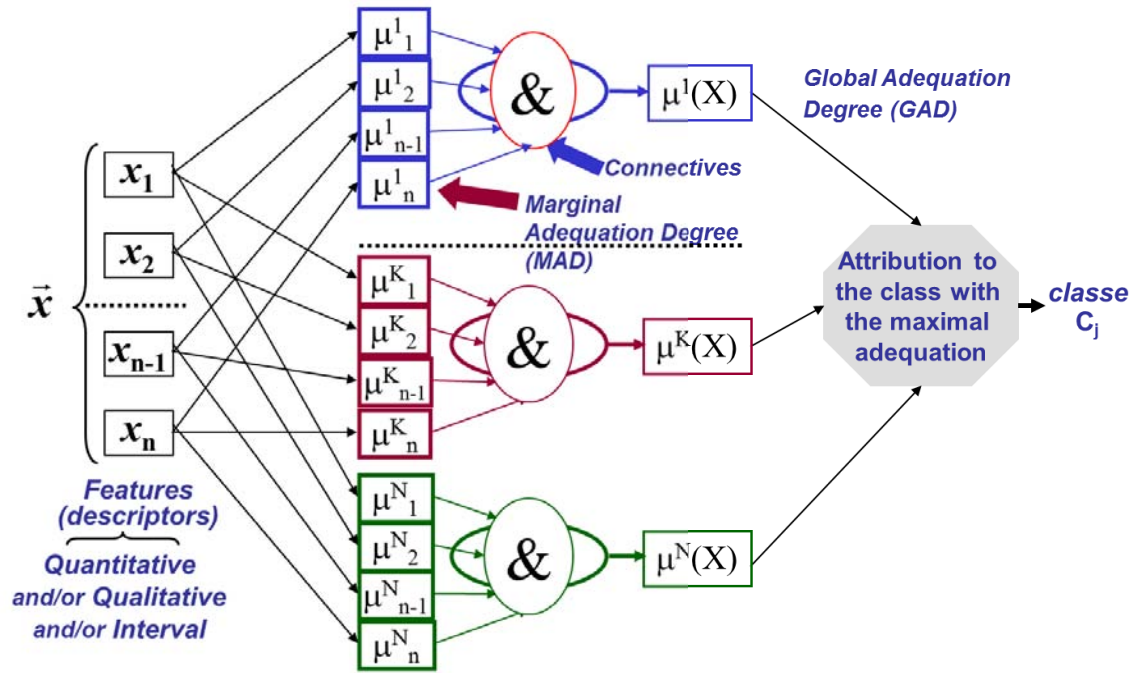


Figure 5.1 : LAMDA algorithm with marginal & global adequacies.

Fuzzy logic connectives are fuzzy versions of the binary logic operators, particularly, intersection (*t-norm*) and union (*t-conorm*). The aggregation function (Piera and Aguilar, 1991) is a linear interpolation between *t-norm* (γ) and *t-conorm* (β) where the parameter is called *exigency* (see Appendix III for details on calculations).

An element is assigned to the class with the maximum GAD (see Figure 5.1). To avoid the assignment of a not very representative element to a class, i.e. an element with a small membership, a minimum global adequacy threshold is employed, called the *Non-Informative Class (NIC)*. The *NIC* is always defined in order that all the descriptors in the data space have the same adequacy degree to this class. The concept of the *NIC* is important for LAMDA calculations, and it is used for the process of creation of a new class. The existence of the *NIC* acts like a limitation or a threshold for the allocation decision: none of the individuals will be assigned to another class if its GAD is not superior to the *NIC* one.

Learning and recognition phases

Chapter 1, section 1.4, mentioned that classification methods are based on the learning and the recognition phases. Moreover, the learning phase can be generally categorized into methods based on supervised learning or methods based on self-learning.

Supervised learning techniques request a prior knowledge of the classes and their parameters. In the LQMDQ method, *MAD* functions are calculated from the running or historical data, the individuals are assigned to the classes which are imposed by the expert. The parameters of each class will be a combination of the characteristics of the elements included in the class. During the recognition task, each time that an individual is assigned to the *NIC* class, i. e., its adequacy degree to the *NIC* has the highest value compared with the existing classes, the individual is considered non-recognized. Other non-fuzzy supervised techniques most commonly applied are the Principal Component Analysis (Fisher, 1936), the K-Nearest Neighbours (Fix and Hodges, 1951), the Neural Networks (Lurette, 2003), the Classification and Regression Trees (Lim et al., 2000).

In case of self-learning techniques, the classes are created as an individual of the data base is processed; this technique is also called Clustering (Bezdek et al., 2005). In this case, each time that an individual is assigned to the *NIC* class, a new class is created with this individual and the parameters of the *NIC*. If this individual is assigned to an existing class, the parameters of this class are actualized with the values from the individual. The classification method proposes then a first scenario to the expert, who valid these results considering acceptable physical interpretations.

The self-learning technique does not need prior information to initialize the classification if the *NIC* is considered when the first individual is processed. A new class is created each time if its *GAD* is superior to the *GAD* of the existing classes. Although, it is also possible to initialize the procedure with the classification done by an expert or by a previous phase of supervised learning, and only actualize these classes during new data acquisition; in this case, the *NIC* is affected only when there is no other possible classes to assign the new individual.

Supervised and self-learning approaches can be complementary. The entire procedure may begin by a self-learning without initialization, followed by a series of classifications with initialization based on the classes already defined, whose parameters may evolve, in order to obtain a satisfied partition.

This group of classes allows then a final recognition phase: the historical data is analyzed and an actual individual can be assigned to an existing class. The classes already established can be identified and interpreted as the representation of possible operating conditions of the system. The procedure of learning and recognition is also resumed in Appendix III.

5.2.2 Sensors selection

A reliable diagnosis of process is achieved when the information analyzed is the most relevant. This information is provided by the sensors placed on the process. A solution is to place a great number of sensors, but it would result on both a prohibitive cost and a high amount of non-pertinent information, complicating the analysis.

The LAMDA methodology, as explained above, considers all descriptors of the system. This approach can be refined considering a sensor location method. The challenge is to answer the following questions: Where are the best locations to place the sensors? What is the optimal number of sensors? Which is the type of sensors that will give the most reliable information to supervise the process?

Hedjazi et al. (2010b) developed a sensor selection method based on a membership margin maximization that estimates the contribution of each descriptor (sensor) in the membership space, which is characterized by a fuzzy weight. The proposed method is known as MEMBAS and its main interest relies on the ability to handle mixed-type data (quantitative, qualitative and interval) as well as a high quantity of descriptors. It enables the handling of large dimensional data and improves the performance of the classifier. The technique will be used in Chapter 12 to address the diagnosability of the reactive distillation system. The MEMBAS method is described in Appendix III.

5.2.3 P3S[®] software

P3S[®] was developed under LabWindows to assess the qualitative situation of a given industrial process by treating the data offline and online.

The offline procedure characterizes the process, by generating its '*behavioral model*' from the results of a learning classification technique of a data set. The behavioral model corresponds to the assignment of significant functional states to the classes generated from a given data set; a constant dialogue with the human expert is then required.

The offline procedure consists of two main steps in P3S[®]: the class generation, with the application of a supervised learning or a self-learning method, and the assignment of the resulting classes, or groups of classes, into meaningful functional states. The interaction with the expert is necessary to tune up the classifier parameters and to reasonably map the classes into physical states.

During self-learning phase, P3S[®] also allows the user to define the maximal percentage of desired variation and the maximal number of interactions, influencing the time to achieve system stability.

Online procedure can be used during plant operation. The objective would be to analyze real-time data and to identify the current functional state of the process, based on the behavioral model determined on the offline procedure. The online recognition allows the continuous detection, location and identification of a dysfunction or a fault.

The procedure

The instruction manual of P3S[®] is detailed in Kempowsky (2011). A brief explanation is given here.

The data analyzed in P3S[®] are obtained from the loading of a context and a population. They can be historical measurements of an experimental run or values given by process simulation.

The offline procedure begins by loading a new context; this file normally contains the number of descriptors and their type (numeric or symbolic). Then, a population is loaded; this file contains the individuals that will be used for training. It must have the same number and type of descriptors as in the context. In the case of self-learning method, there are no pre-defined classes because there is no preliminary knowledge of how the individuals are assigned. In the case of supervised learning, there may have an additional field corresponding to the pre-defined classes.

After successfully loading a context and population, it is possible to run the algorithm. To apply the calculations for learning and classification procedures, some parameters need to be chosen for quantitative descriptors analysis: membership margin function, logic operators and exigency level. Membership margin functions and logical operators, or fuzzy connectives, are chosen from heuristic considerations. The logic operators are selected from two different families (*T-norm* and *T-conorm*) in order to aggregate all the *MADs* of an individual to a class. They are a “fuzzy” representation of logical intersection and union operators respectively '*AND*' and '*OR*'.

The user may use mixed connectives of the same family by choosing an exigency level between 0 and 1 which allows weighting between the '*AND*' and '*OR*' operators. By changing the exigency level value, different partitions based on the same data set may be obtained.

Once the classification has been made, P3S[®] graphically displays the resulting class assigned to each individual. It is also possible to view the complete information for each class.

When a suitable classification is obtained, the user must assign the different classes into representative functional states. First, the user creates a list of possible significant states and then, the table of classes and states must be related and filled up.

Finally, online procedure can be applied on P3S[®], by continuously recognizing the functional state of the process from real-time data of sensors and actuators or other information from process variables.

The latest version of the software considers also the methodology for sensors placement, with the classification margin as the criterion for selection. The user may rank the descriptors and the result appears in a table or in a bar-plot form. To restart the classification, the user can select a number of active descriptors or chose a minimum threshold.

Because the diagnosis by P3S[®] uses only the collected data and does not need a representative mathematical model of the process, there are high interests on its application for complex systems analysis and the nonlinearities of reactive distillation processes are considered.

The procedure applied for the process diagnosis into P3S[®] is organized as shown in Figure 5.2:

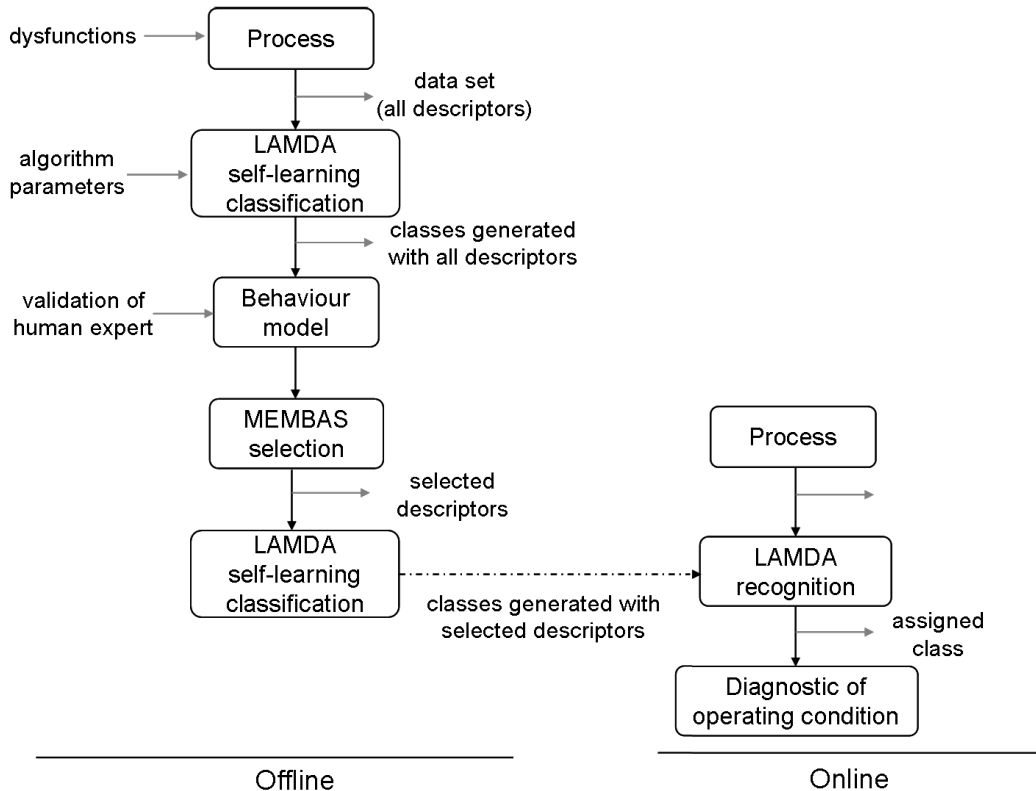


Figure 5.2 Scheme of P3S[®] diagnosis procedure

III. SYSTEM STEADY STATE AND DYNAMIC MODELING

6.	Modeling the system with experimental validation	75
----	--	-------	----

To better understand the reactive distillation process, steady-state and dynamic models are defined based on several experimental data obtained at a pilot plant for the production of ethyl acetate from esterification of acetic acid and ethanol. For the steady-state approach, experiments are performed with both excess of alcohol and stoichiometric feed and the equilibrium model parameters are detailed. Predicted and measured results show good agreement and they reveal an important catalyst activity dependency on the operating conditions. In the transient experiments, the operational parameters such as feed flow rates, reflux ratio and heat duty are perturbed and the consequent open loop dynamic responses are identified. The experimental validation is essential to provide realistic hydrodynamic parameters, to understand the sensitive parameters such as the heat losses and to adapt values for the heterogeneous catalyst holdup in function of the system. A reliable dynamic model represents the process tendencies and responses well. The complexities observed with the use of the heterogeneous catalyst explain why the great majority of industrial columns are under homogeneous catalysis configuration.

Pour avoir une bonne compréhension du comportement complexe du procédé de distillation réactive et être capable de proposer une conception fiable de la structure de la colonne, des analyses détaillées en régime permanent et en régime dynamique sont nécessaires.

Le Chapitre 6 débute par une recherche bibliographique, en présentant les études expérimentales réalisées en fonctionnement dynamique et souligne l'importance de l'approche expérimentale pour valider le modèle de la production d'acétate d'éthyle par distillation réactive. L'objectif est la définition d'un modèle représentatif du système en état stationnaire et en état dynamique, basé sur plusieurs données expérimentales obtenues dans une colonne réelle à l'échelle pilote. La production d'acétate d'éthyle par estérification de l'acide acétique avec de l'éthanol en catalyse hétérogène est étudiée.

La colonne pilote est celle présentée au Chapitre 3. Elle est constituée de 7 sections modulaires, dont les 5 sections centrales sont équipées avec le garnissage structuré KATAPAK SP, remplis avec des résines acides, le catalyseur hétérogène, et les deux autres sections sont équipées d'une structure non catalytique. Les paramètres opératoires tels que les températures, débits, perte de charge et niveaux de liquide sont collectés et suivis dans un outil de contrôle-commande. Des échantillons liquides sont prélevés à chaque distributeur de liquide et dans les courants de sortie de la colonne.

Pour l'analyse du régime permanent, des essais sont réalisés en excès d'éthanol et en alimentation stœchiométrique. Le régime dynamique est étudié à la suite de plusieurs perturbations sur le système : augmentation et diminution du débit d'alimentation d'acide, augmentation et diminution du taux de reflux et baisse de la chauffe apportée au bouilleur.

Le logiciel Aspen Plus[®] est utilisé pour développer le modèle de simulation en régime permanent. Les paramètres intrinsèques tels que la thermodynamique (modèle NRTL pour l'équilibre entre phases et Hayden O'Connell pour la dimérisation de l'acide acétique en phase vapeur) et la cinétique réactionnelle du système sont tirés d'anciennes études menées chez Solvay. Les paramètres opérationnels tels que les débits, pression et chauffe sont observés à chaque essai, et les pertes thermiques sont calculées en fonction des matériaux et des températures du pilote. La colonne est représentée avec 27 étages théoriques plus le bouilleur. Les résultats obtenus par simulation et ceux observés sont en cohérence pour tous les essais. La Figure 6.15 ci-dessous montre les résultats de simulation (représentés par des traits continus) et les valeurs expérimentales (points). Le modèle d'équilibre est donc bien représentatif du système en fonctionnement continu.

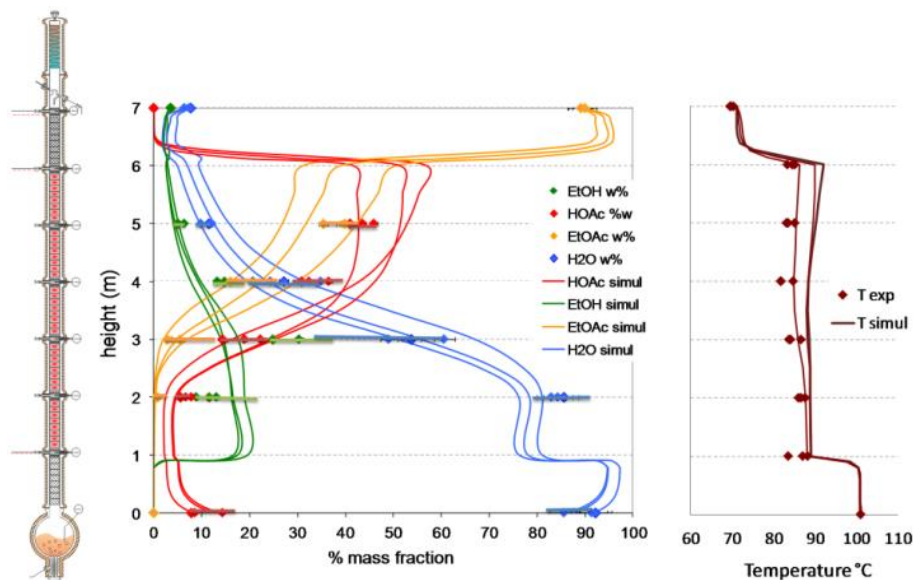


Figure 6.15. Profils de composition et température en régime permanent

Une observation importante est la comparaison des essais avec alimentation stœchiométrique et ceux en excès d'éthanol : les différentes ratios d'alimentation influencent les compositions le long de la colonne et, par conséquent, l'activité de la résine catalytique. Pour une bonne représentativité du modèle, un coefficient est adapté pour l'efficacité de la réaction à chaque configuration d'alimentation.

Le suivi des essais en dynamique a permis d'appréhender les paramètres sensibles et les influences externes. Avec l'acquisition détaillée des paramètres hydrodynamiques et technologiques, le modèle est exporté dans Aspen Plus Dynamics[®]. Les tendances et le comportement dynamique du système sont bien représentés. Une discussion approfondie concerne les complexités de la catalyse hétérogène et des rétentions liquides au sein de la structure catalytique, ce qui devient un défi pour l'application industrielle de la distillation réactive. En fait, les compositions des composés aqueux résultent d'une mauvaise distribution du liquide, entravant la bonne maîtrise de la réaction en catalyse hétérogène. Dans un contexte industriel, en présence de plusieurs impuretés significatives, un changement fréquent du catalyseur est demandé et, en conséquence, entraîne un démontage de l'installation. Ces constatations ont conduit à considérer la catalyse homogène pour les études qui ont suivi.

L'application de cette approche expérimentale pour la production d'acétate d'éthyle avec catalyse hétérogène en comportement dynamique est une contribution importante à l'état de l'art de la distillation réactive et ces travaux ont été acceptés comme publication dans la revue *Chemical Engineering Research & Design*.

Para obter melhor compreensão do comportamento complexo do processo de destilação reativa e propor um projeto confiável da estrutura de coluna, análises detalhadas em estado estacionário e em regime dinâmico são necessárias.

O Capítulo 6 começa com uma breve pesquisa bibliográfica, apresentando os estudos experimentais conduzidos em colunas com funcionamento dinâmico e enfatiza a importância da abordagem experimental para validar o modelo da produção de acetato de etila por destilação reativa. O objetivo é a definição de um modelo representativo do sistema em estado estacionário e dinâmico, baseado em diversos dados experimentais obtidos em uma coluna real em escala piloto. A produção de acetato de etila por esterificação de ácido acético com etanol em catalise heterogênea é estudada.

A coluna piloto é apresentada no Capítulo 3. Ela é constituída de 7 seções modulares, das quais as 5 seções centrais são equipadas com recheio estruturado KATAPAK SP, preenchido com resinas ácidas, o catalisador heterogêneo, e as duas outras seções são equipadas de estruturas não catalíticas. Os parâmetros de operação tais como temperaturas, vazões, perda de carga e níveis de líquido são coletados e observados através de um software de controle. Amostras da fase líquida são coletadas em cada distribuidor e nas correntes de saída da coluna.

Para análise do estado estacionário, experimentos são realizados com excesso de etanol e com alimentação estequiométrica. O regime dinâmico foi estudado após diferentes perturbações no sistema: aumento e diminuição da vazão de alimentação do ácido, aumento e diminuição da taxa de refluxo e diminuição do calor fornecido ao refeedor.

O software Aspen Plus[®] foi usado para desenvolver o modelo de simulação em estado estacionário. Os parâmetros intrínsecos tais como termodinâmica (modelo NRTL para o equilíbrio entre fases e Hayden O'Connell para a dimerização do ácido acético em fase vapor) e cinética reacional do sistema são obtidos de estudos anteriores conduzidos na Solvay. Os parâmetros de operação tais como vazões, pressão e aquecimento são observados em cada experimento, e as perdas térmicas são calculadas em função dos materiais e das temperaturas do piloto. A coluna é representada com 27 estágios teóricos mais o refeedor. Os resultados obtidos por simulação e os observados experimentalmente são coerentes em todos os experimentos. A Figura 6.15 abaixo mostra os resultados de simulação (representados por traços contínuos) e os valores experimentais (pontos). Em conclusão, o modelo de equilíbrio é representativo do sistema em funcionamento contínuo.

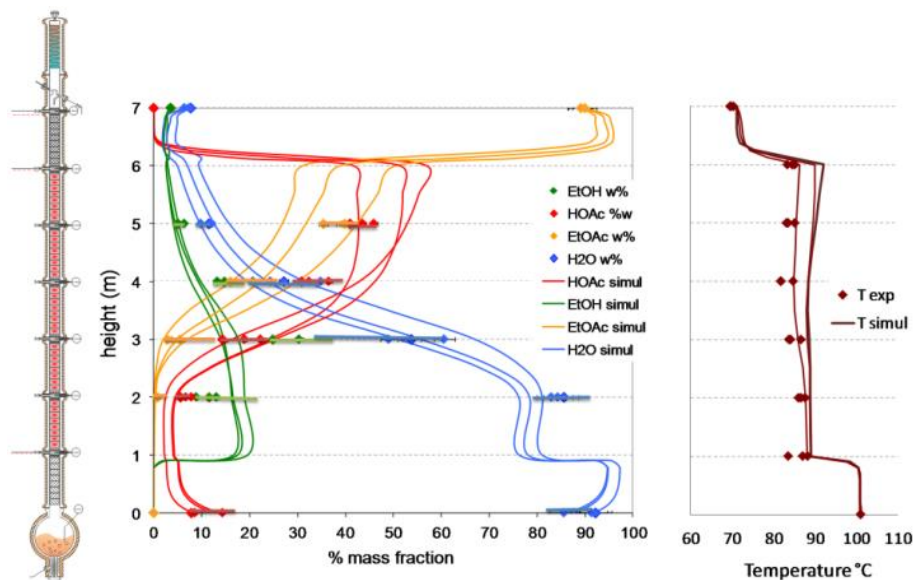


Figura 6.15. Perfis de composição e de temperatura em estado estacionário

Uma observação importante é a comparação entre os experimentos com excesso de etanol e aqueles com alimentação estequiométrica: as diferentes alimentações influenciam as composições ao longo da coluna e, conseqüentemente, a atividade da resina catalítica. Para uma boa representatividade do modelo, um coeficiente foi inserido e adaptado na eficiência da reação para cada configuração de alimentação.

O acompanhamento dos experimentos dinâmicos permitiu o conhecimento dos parâmetros sensíveis e das influências externas. Com a aquisição detalhada dos parâmetros hidrodinâmicos e tecnológicos, o modelo é exportado para o Aspen Plus Dynamics[®]. As tendências e o comportamento dinâmico do sistema são bem representados. Uma discussão aprofundada trata das complexidades da catalise heterogênea e das retenções de líquido na estrutura catalítica, o que se configura como um desafio para a aplicação industrial da destilação reativa. De fato, a presença dos componentes aquosos resulta em uma má distribuição do líquido, impedindo uma boa compreensão da reação em catalise heterogênea. Em um contexto industrial, com a presença de diversas impurezas, a substituição frequente do catalisador seria necessária, o que demandaria a desmontagem da instalação. Essas constatações levaram à adoção da catálise homogênea para os estudos subsequentes.

A aplicação dessa abordagem experimental para a produção de acetato de etila com catálise heterogênea em comportamento dinâmico é uma contribuição importante ao estado da arte da destilação reativa e esse trabalho foi aceito como publicação na revista *Chemical Engineering Research & Design*.

Modeling the system with experimental validation

6.1 EXPERIMENTAL DYNAMIC WORKS IN THE LITERATURE

The reactive distillation process is a complex system in which the combination of separation and reaction operations leads to complex interactions between phase equilibrium, mass transfer rates, diffusion and chemical kinetics. As a consequence, the analysis of transient regime operation is made necessary to better understand the process behavior and the present nonlinearities.

The dynamic behavior of reactive separation systems has attracted great attention in recent academic and industrial studies. Although great effort has been applied to model and to simulate the dynamic behavior of the process, very little experimental work has been carried out in transient conditions. Some authors developed rigorous dynamic models, but only experimental data from steady state operations were considered for model validation. Kenig et al. (1999) developed a rigorous rate-based dynamic model for reactive absorption processes that was validated by the comparison of the sour gases reactive absorption in air purification packed columns simulation against pilot-plant steady-state experiments. Mihal et al. (2009) studied a hybrid reactive separation system consisting of a heterogeneously catalyzed reactive distillation column and a pervaporation membrane located in the distillate stream. The steady state behavior model was validated by comparison with the experiment data from the work done by Kotora et al. (2008) and the system dynamic behavior during step changes was investigated by simulation. Other authors reported dynamic experimental data on batch-operated columns for the production of methyl acetate: Schneider et al. (1999) included the explicit calculation of heat and mass transfer rates in a rigorous dynamic rate-based approach and the experiments on a batch distillation column showed good agreement with simulation results. Noeres et al. (2004) considered a rigorous rate-based dynamic model for designing a batch heterogeneously catalyzed reactive distillation and good agreement was verified for compositions and temperatures through the column after forced perturbations on reflux ratio. Singh et al. (2005) studied esterification reaction of acetic acid with n-butanol in a packed distillation column with the commercial catalytic packing KATAPAK-S and non-catalytic wire gauze. A dynamic equilibrium stage model was developed to analyze the influence of various operating parameters and several trials were carried out; reasonably good agreement between the experimental and simulation results was said to be verified, but results were only shown for one representative attempt. Xu et al. (2005) developed a detailed three-phase non-equilibrium dynamic model for simulating batch and continuous catalytic distillation processes. The simulation results were in good agreement with the experimental data obtained from the production of diacetone alcohol using Amberlite IRA-900 as a

catalyst. Experiments were performed with the column under total reflux and the transient behavior was studied after a decrease of the reboiler duty. Finally, Volker et al. (2007) conducted closed-loop experiments to validate a control system proposition. The authors designed a multivariable controller for a medium-scale reactive distillation column and semi-batch experiments in closed-loop configuration were conducted so as to demonstrate control performance for the production of methyl acetate by esterification. Sequential perturbations on reflux ratio and on acid feed were introduced to a batch operation reactive column.

To our knowledge, there is a lack of experimental studies concerning the ethyl acetate reactive distillation system in continuous dynamic conditions in the literature. A detailed experimental analysis would be of great importance in order to provide a good representative simulation model for the heterogeneously catalyzed system. The parameters concerning column geometry (reboiler design, column diameter), technology (catalyst, packing characteristics) and hydrodynamics (liquid retentions, flooding considerations) require realistic values that can only be well identified based on an experimental validation. The objective of this chapter is thus the definition of both steady-state and dynamic models and the generation of the required experimental data on a continuous heterogeneously catalyzed reactive pilot column. Several experimental trials were conducted to investigate the transient process behavior and to collect continuous and dynamic data for a sufficient model validation. Discussions were developed concerning the complexities of the reactive distillation process, the possible steady state multiplicities and the sensitivities due to heat losses, specific operating conditions and the heterogeneous catalysis. The importance of considering all these peculiarities in the interpretation of a dynamic model is highlighted and hence the developed model combining information from the steady state and from the dynamic regime is accepted for the representation of the ethyl acetate system.

6.2 EXPERIMENTAL PROCEDURE

The materials and methods adopted for the experimental campaign were presented in Chapter 3. The reactive distillation pilot is schematized again in Figure 6.1, with its respective seven modular sections and liquid distributors.

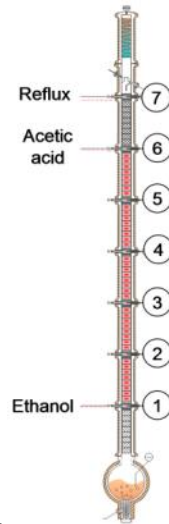


Figure 6.1. Column scheme

Before starting the experimental tests with the esterification components, some experiments were carried out with water in order to calibrate the pumps, to estimate heat losses, to verify heat equipments, to determine start-up and shut-down procedures.

All the tests were performed as follows: the day before the experiment, the column was heated up under total reflux conditions without any feeds and remained at these conditions for in least 12 hours. At the beginning of the test, the next morning, the three feed streams: acid, alcohol and external reflux were switched on and the system was observed until steady state conditions were reached. Stable operational conditions were normally reached after approximately 7 hours of experiment. Due to the fact that only temperatures were measured online, the identification of steady state conditions was assumed to happen when temperatures were stable at the column distributors. The knowledge of the compositions was only possible after the experimental runs, because offline laboratory analyses were adopted, which required more time for preparation and calculations.

Through twelve experiments, different perturbations were performed and a substantial number of data were collected, such as flow rate measures, temperature and composition profiles. The tests were chosen to work under alcohol excess feed configuration in order to consume all the acid and to meet the stringent acid specification for acetates. For the purposes of comparison, an additional test at steady state with stoichiometric feed configuration was conducted. Table 6.1 shows the operating feed conditions and the perturbation conducted at each test.

Table 6.1. Operational parameters of tests

test	Steady-state configuration	Dynamic perturbation
1	ethanol excess	-
2	stoichiometric feed	-
3	ethanol excess	+10% reflux mass flow
4	ethanol excess	-10% reflux mass flow
5	ethanol excess	+10% acid mass flow
6	ethanol excess	+10% ethanol mass flow
7	ethanol excess	heat perturbation

In tests n°3, 4, 5, 6 and 7, after steady-state conditions were obtained, a perturbation of one parameter was caused in the column, with the attempt to keep all the other parameters constant. These perturbations strongly disturbed the system – temperatures changed rapidly – and its behavior was monitored for the next approximately 4 or 5 hours. As a consequence of the laboratory opening times constraints, there was not always sufficient time to wait for the system to reach the new operating point.

6.3 EXPERIMENTAL RESULTS

6.3.1 Steady state analysis

Except for test n°2 (different feed ratio), the target steady state, with ethanol excess feed configuration, was the same for all the tests. The feed ratio and the results of the product stream compositions are shown in Table 6.2.

Table 6.2. Product stream compositions

test	Feed ratio	Distillate			Bottom			
	(molar)	(%mass)			(%mass)			
	EtOH/HAc	EtAc	EtOH	H ₂ O	HAc	H ₂ O	EtOH	EtAc
1	1.13	89.2	3.7	7.1	11.9	88.1	0.0	0.0
2	1.04	91.5	2.6	5.9	21.2	78.9	0.0	0.0
3	1.12	88.7	3.7	7.6	17.4	82.6	0.0	0.0
4	1.12	88.8	3.5	7.7	11.2	88.8	0.0	0.0
5	1.13	89.9	3.6	6.5	8.6	91.4	0.0	0.0
6	1.12	89.1	3.5	7.4	14.4	85.6	0.0	0.0
7	1.13	88.8	3.5	7.7	7.8	92.2	0.0	0.0

While distillate compositions were nearly the same for all tests, the compositions at the bottom were less reproducible. Conversion rates were calculated:

$$X_{HOAc} = \frac{N_{HOAc}^{feed} - N_{HOAc}^{bottom}}{N_{HOAc}^{feed}} \quad X_{EtOH} = \frac{N_{EtOH}^{feed} - N_{EtOH}^{bottom}}{N_{EtOH}^{feed}}$$

Table 6.3. Reactant conversion rates

test	X HOAc	X EtOH
1	97.2%	86.2%
2	93.6%	90.0%
3	96.1%	86.1%
4	97.7%	86.1%
5	97.8%	86.5%
6	96.7%	86.7%
7	98.4%	86.9%

For an approximately 12% ethanol molar excess feed (tests n°1, 3, 4, 5, 6 and 7), the conversion rates were almost the same with a mean value of 96.9% for acetic acid and 86.9% for ethanol.

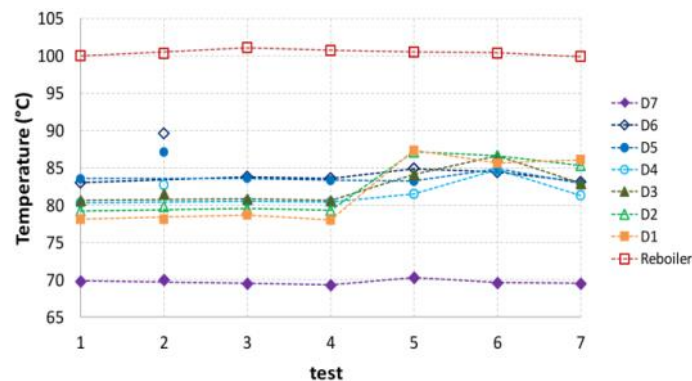


Figure 6.2. Temperature measures at each distributor, for all tests

As shown in Figure 6.2, temperatures from the column lower sections had a marked increase after test n°4. The steady states obtained at the beginning of the experimental campaign (test n°1, 3, 4) were different from the later ones (tests n°5, 6, 7), although they remain similar among them.

In Figure 6.3, it can be observed that the compositions in D4 and D5 kept almost constant through all tests, while compositions in D2 and D3 strongly changed in the last tests of the campaign; this fact confirms the observation of the increment in the column lower sections temperatures. Actually, with the increase in water content and the decrease in ethanol content, higher values of temperature are

expected. The obtaining of two different steady states through the experiments is thus accepted and this is further understood with the simulation results. It is worth noting that, despite the presence of different profiles inside the column, the compositions of product streams remain similar. This can be the consequence of the separation-only sections above and below the reactive section.

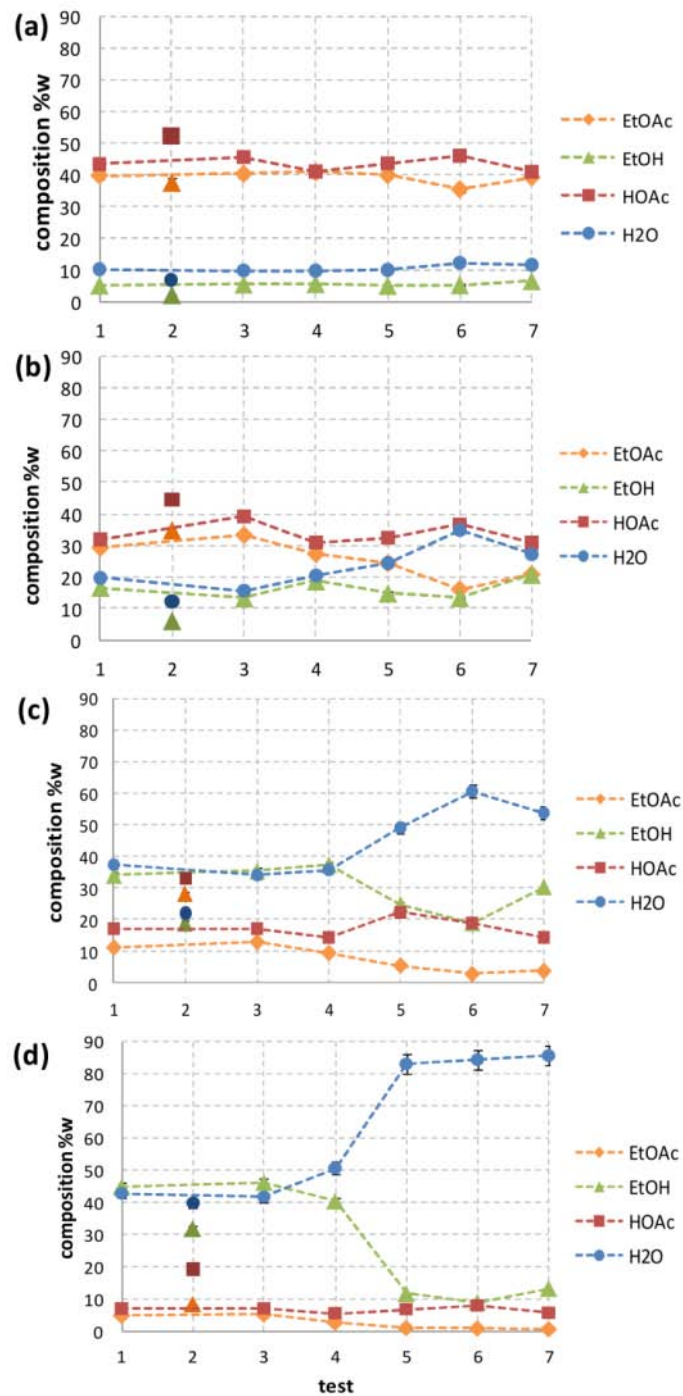


Figure 6.3. Compositions at D5 (a), D4 (b), D3 (c) and D2 (d)

6.3.2 Study of the transient regimes

The experimental campaign resulted in five tests with representative transient data. The perturbations occurred under open-loop conditions, by changing only one variable. The moment of perturbation is represented in the graphs by a vertical straight line.

The perturbation of reflux rate and feed flow rates were imposed as step changes and they correspond to the experimental perturbation because the action was conducted at the values given to the pumps, which respond almost instantaneously. The perturbation on the heat duty was conducted by dropping the set point of the heat duty controller – i.e. a step change of -3°C of the temperature difference between oil and reboiler liquid.

Test n°3: +10% of external reflux flow rate

Before the perturbation, the temperature in the reboiler was approximately 100°C and all the other temperatures throughout the column were between 70 and 85°C . The temperatures evolution along test n°3 is represented in Figure 6.4. The temperature changes occur first at the stages in which the reactants feed streams are injected: liquid distributors D1 and D6. Their responses are faster and have a higher gain than the other ones. Then, the temperatures at D4 and D5 also decreased, and new steady state conditions seem to be obtained 2h after the perturbation.

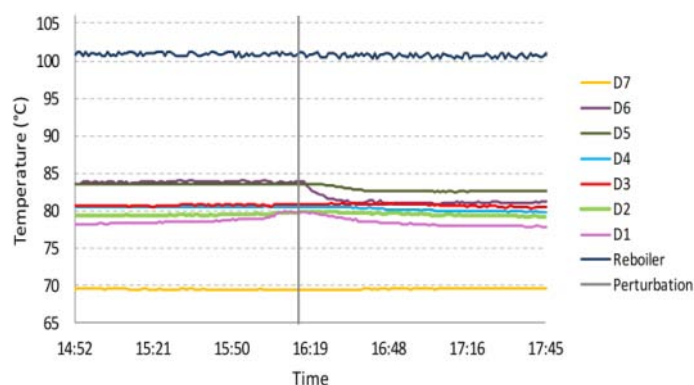


Figure 6.4. Temperatures before and after a 10% increase of the external reflux feed flow rate

Regarding compositions in Figure 6.5 before the perturbation, the composition at the distillate was observed to be more stable than the composition at the bottom of the column. The contents of water and ethanol at the bottom were not constant even when the constant temperatures allow the assumption that the steady state conditions were reached. This fact highlights the disadvantage of not having online composition measures during the operation these intensified systems. The increment of the reflux ratio, at

constant heat conditions, resulted in an increase in distillate flow rate and in distillate ester content and a decrease in the water content. At the bottom, both water and acid contents decreased resulting in a higher ethanol fraction.

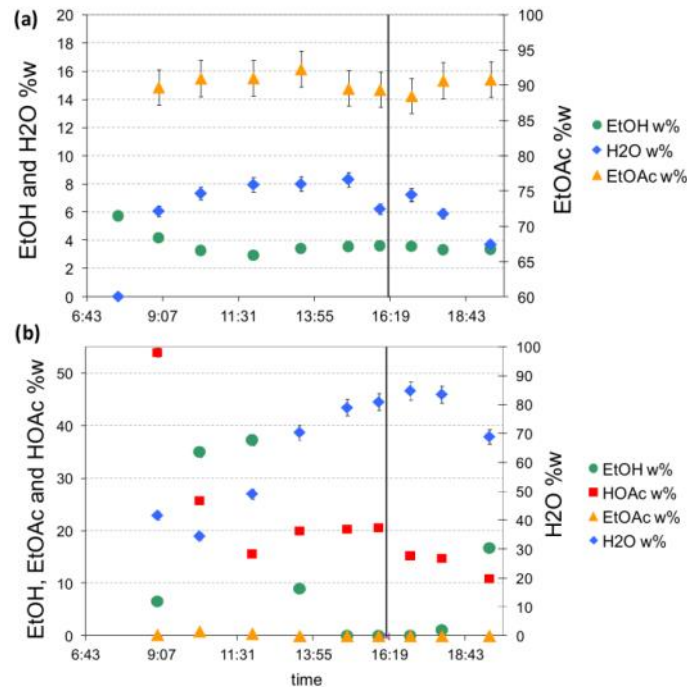


Figure 6.5. Mass compositions at the distillate (a) and at the bottom (b) before and after a 10% increase of the external reflux feed flow rate

Test n°4: -10% of external reflux flow rate

After approximately 2h of assumed steady state conditions, the external reflux mass flow rate was reduced by 10%. An unexpected behavior was verified in the temperature at D1 before the reflux perturbation: a positive step of approximately 2°C suddenly occurred. This temperature seems to be highly sensitive to the operation conditions and this fact can be verified also after perturbation, because the temperatures from D1 and D6 were the first ones to react. Both of them are measured where the reactant feeds are located, and this behavior was also verified for test n°3. The other temperatures also rose over time, and marked gradients were observed at D2 and D3

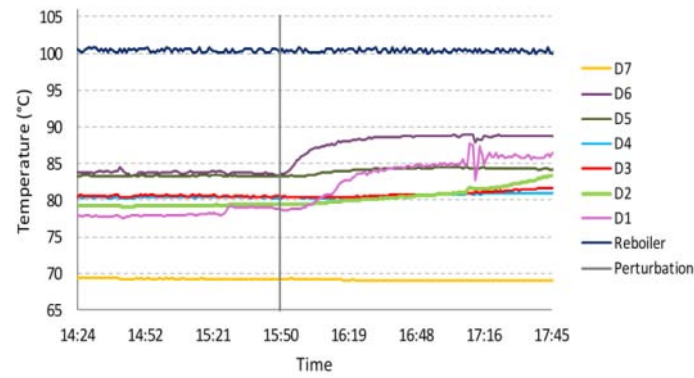


Figure 6.6. Temperature in liquid distributors before and after a 10% decrease of the external reflux feed flow rate

Regarding composition, as expected, the behavior was in the opposite direction of the one observed for test n°3: there was a decrease in distillate flow rate and in distillate ester content, being replaced by water and ethanol. At the column bottom, the water content increased, replacing the acid.

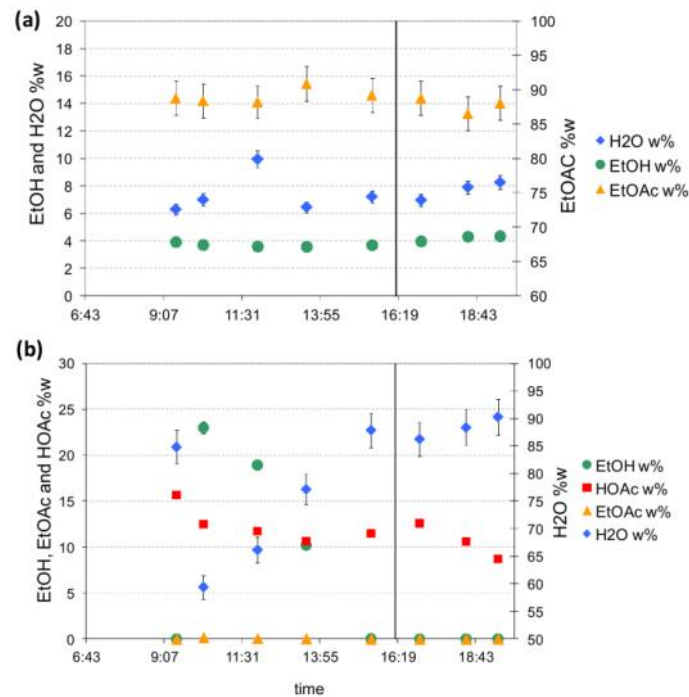


Figure 6.7. Mass compositions at the distillate (a) and at the bottom (b) before and after a 10% decrease of the external reflux feed flow rate

Test n°5: +10% of acetic acid feed flow rate

During test n°5, the acetic acid feed flow rate was increased by 10% and consequently almost all the temperatures rose, but they showed different responses. Temperatures at D4 and D5 remain with constant positive gradient until the end of the experiment. At distributor D6, a step of approximately 2°C was verified and the temperature continued to increase after it. The temperature at D3 decreased right

after the perturbation but its behavior changed later and it started to rise. The temperatures from both distributors D1 and D2 showed oscillations but remain with mean values closer to the ones observed at nominal regime. Actually, the top sections of the column were more affected by the perturbation on acid feed than the bottom sections, due to the proximity to acid feed location. The experiment was stopped before a new steady state was reached.

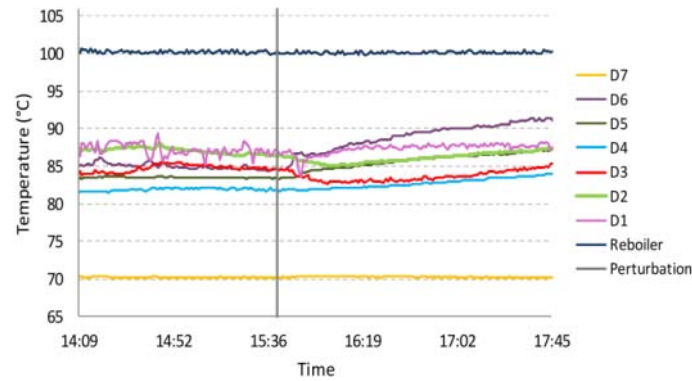


Figure 6.8. Temperature in liquid distributors before and after a 10% increase of the acetic acid feed flow rate

The compositions analysis shows that the water content in the distillate rose and it became less pure in ester. The bottom composition behavior testifies that the system was not exactly in steady state conditions before the perturbation of acid feed.

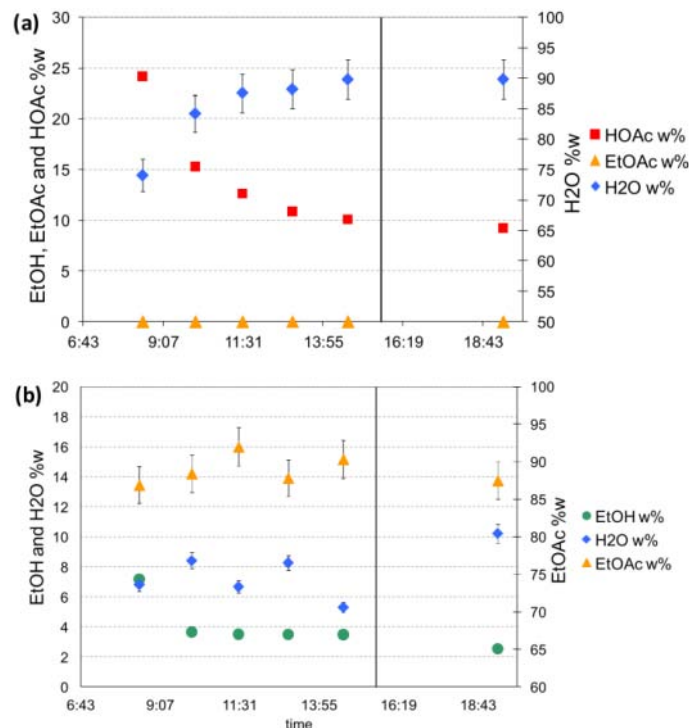


Figure 6.9. Mass compositions at the distillate (a) and at the bottom (b) before and after a 10% increase of the acetic acid feed flow rate

Test n°6: +10% of ethanol feed flow rate

After the perturbation by decreasing the ethanol feed flow rate, the temperatures decreased through the column due to the stronger presence of a light component. Their responses were less strong than in the case of the increase in acid flow rate. The temperatures at D1, D2, D3 and D4 changed faster than the temperatures at D5 and D6. Temperature at D1 drifted at approximately 1h30 after the perturbation.

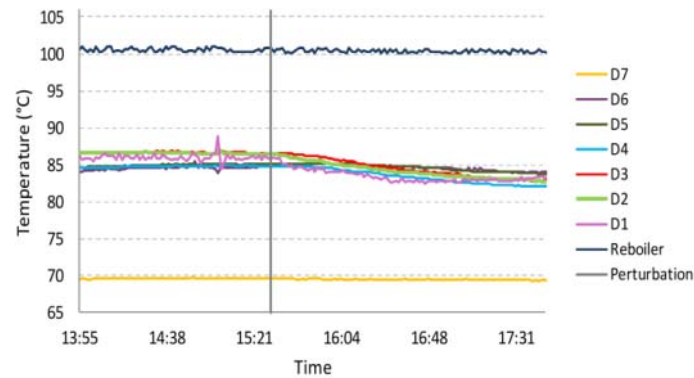


Figure 6.10. Temperature in liquid distributors before and after a 10% increase of the ethanol feed flow rate

As a result of the perturbation, a stronger influence was verified in the bottom composition; the increment of ethanol resulted in a higher conversion, dropping the amount of acetic acid.

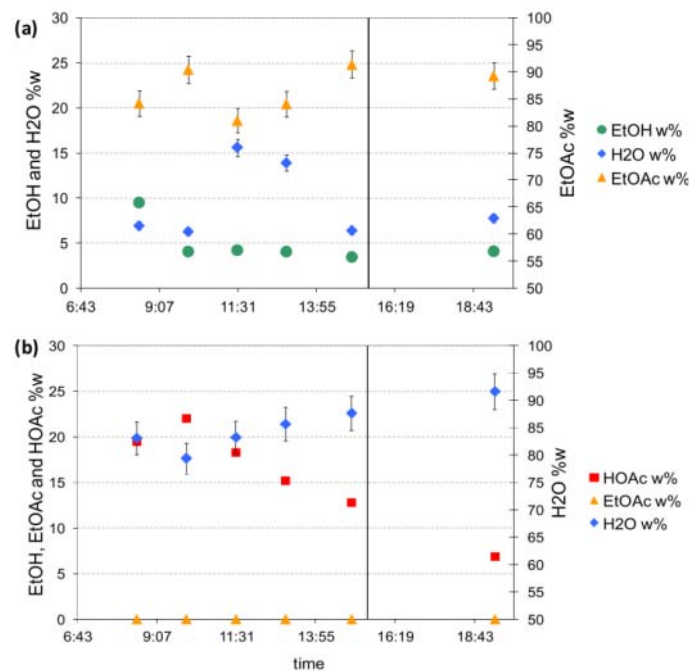


Figure 6.11. Compositions at the distillate (a) and at the bottom (b) before and after a 10% increase of the ethanol feed flow rate

Test n°7: reduction of heat duty

After the decrease of 3°C in the temperature difference between heat oil and reboiler liquid, the temperatures at the bottom sections, D1 to D3, were observed to drop with similar velocity among them, but the measures in the top sections remained constant. Actually, with less heat to the column, less vapor is produced and the amount of the inner liquid increases.

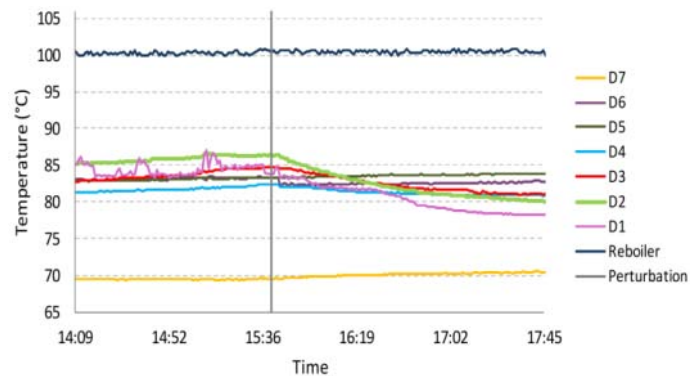


Figure 6.12. Temperature in liquid distributors before and after a reduction of heat duty

The first consequence in production was a sharp decrease in distillate flow rate, followed by a decline in heavy component content through the column. Both contents of ester on distillate and ethanol at the bottom thus increased.

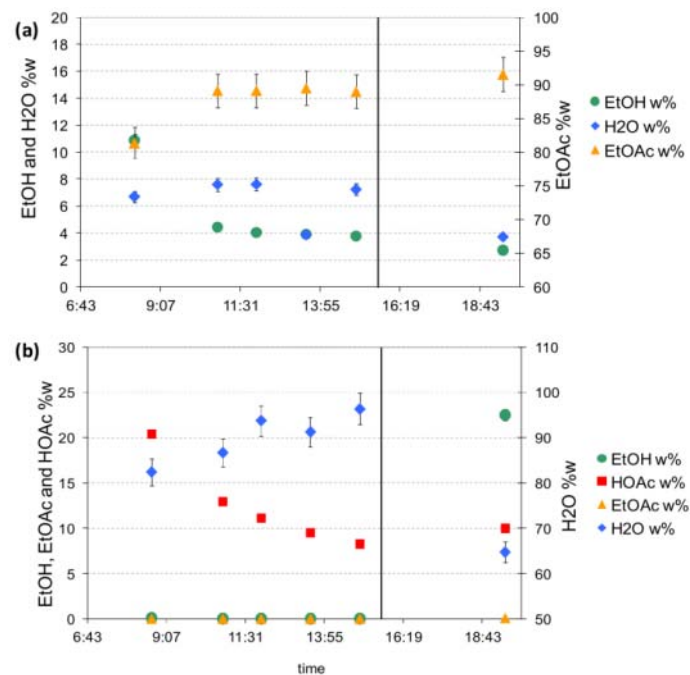


Figure 6.13. Mass compositions at the distillate (a) and at the bottom (b) before and after a reduction of heat duty

6.4 STEADY STATE MODEL

To represent the continuous reactive distillation system, a model was developed with the Aspen Plus[®] software. An equilibrium stage model was considered and it should be adapted for the process simulation and behavior prediction. It is worth mentioning that non-equilibrium models normally provide more details and more precise information to the simulation than the equilibrium models in the case of conventional packed distillation columns. However, the availability of reliable mass transfer correlations for the catalytic packing would be a prerequisite for the use of a non-equilibrium stage model. Even though Behrens (2006) proposes such correlation for KATAPAK[®]-SP, it cannot be considered reliable, since HETP-values resulting from this correlation are always independent of the type of packing, the test system, as well as the gas load and the liquid misdistribution effects. Consequently, the use of such correlations would not improve the accuracy of the simulation results, but even lowers their quality since the variation in separation performance is not considered for their definition.

Table 6.4. Parameters defined in the Aspen Plus[®] steady state model

Intrinsic parameters	Operating parameters	Adjustable parameters
- thermodynamics	- flow rates	- reaction efficiency
- kinetics	- heat duty	- heat loss
- pilot geometry	- pressure	
- technology		

Table 6.4 presents the different parameters to be determined for the equilibrium model. The intrinsic parameters were chosen from previous studies on thermodynamics and kinetics and from pilot analysis. The NRTL activity coefficient model was considered for the phase equilibrium and the Hayden–O’Connell equation of state was used to account for the acetic acid dimerisation in the vapor phase. To account for the equilibrium chemical reaction, two different kinetically controlled reactions were defined: one to represent the direct reaction and another to represent the inverse one. The operating parameters such as flow rates, pressure and heat duty were adapted from the conditions of each test. Concerning the adjustable parameters, it was necessary to adapt values of the global reaction efficiency to better fit the simulated conversion to experimental results. Different feed ratios were verified to influence the compositions through the column and, as a consequence, the catalyst resin activity. To deal with this fact, an adjustable coefficient C was considered; this fact is further clarified in Table 6.5.

Table 6.5. Adjustable coefficient for reaction efficiency

Ethanol excess	Stoichiometric feed (test n°3)
C = 0.5	C = 1

The heat loss was initially calculated from temperatures and materials present into the column and the resulting value is 200W, in which approximately 25% is the loss at the reboiler and the rest is linearly distributed throughout the column. However, it was also observed that the environmental conditions of each day strongly affect the pilot operation conditions and the adjustment of this parameter should be considered in the model.

Figure 6.14 compares the simulated mass composition of the distillate and of the bottom with the experimental results. They show good agreement between them.

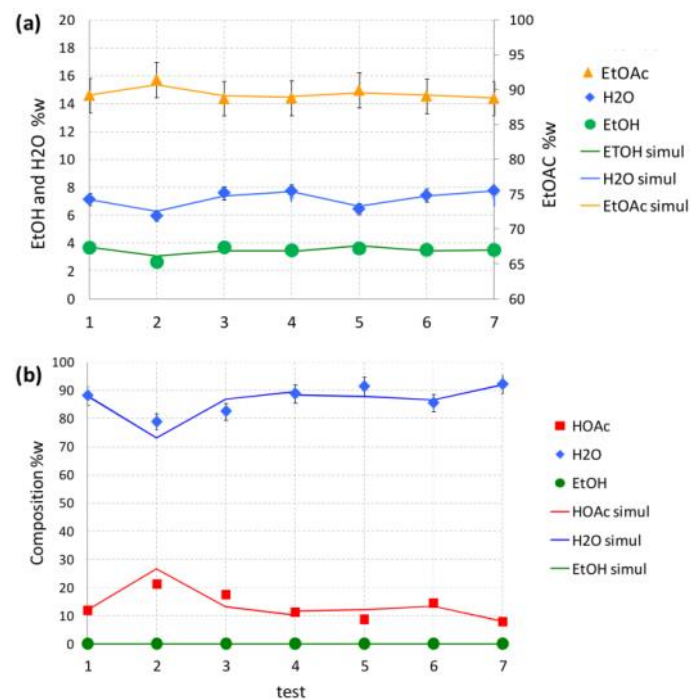


Figure 6.14. Mass fractions at the distillate (a) and at the bottom (b)

Figure 6.15 is a superposition of simulations and experimental results of tests n°1, 3 and 4. The simulated profiles are drawn by continue lines (–) and their experimental values are represented with diamond-shapes (◆). The straight horizontal continuous lines represent the range of measured compositions and it can be verified that simulation curves show agreement with the straight continue lines, concluding the reliability of the model.

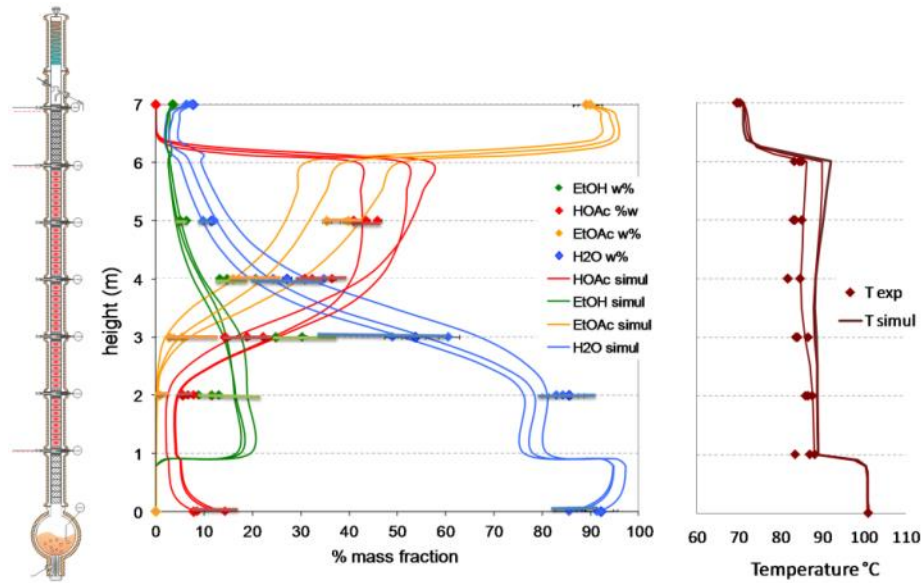
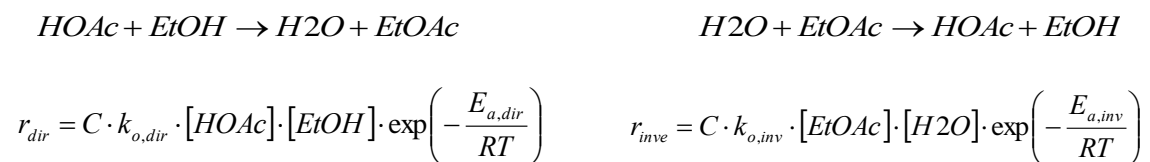


Figure 6.15. Steady state composition and temperature profiles

For the same steady state outputs, the composition profiles varied inside the reactive zone (height between 1m and 6m), but their values were almost similar inside the separation-only zones. In contrast with the reactive section that has a flat temperature profile, the separative sections show marked temperature gradients. A temperature measurement inside the separative section would be highly sensitive to a system dysfunction or a change in the steady state conditions. It is thus possible to infer the regulation of hybrid reactive columns by measures placed in the separative sections. This fact is verified in the literature by different authors (Lai et al., 2007, Kumar and Kaistha, 2009).

6.4.1 Understanding the adjustable coefficient for reaction efficiency

As mentioned before, to adapt the global reaction efficiency in Aspen Plus[®], an adjustable coefficient was considered in the reaction kinetics equations to account for the heterogeneous catalyst activity sensitivities. The kinetic law became:



Some assumptions can be drawn to justify this coefficient:

- Water inhibits the activity of the ions exchanger resin, when simultaneously present with the organic compounds that should react (Brehelin 2006, Darge and Thyron 1993, Grob and Hasse 2006). When aqueous components are present, disadvantageous transfer characteristics occur for the organic components on the catalytic packing due to different transfer rates between water and organic molecules to the pores of the catalyst; when the feed is at stoichiometric proportion, the composition of water through the column is observed to be significantly lower than when the feed is at ethanol excess (Figure 16).
- The model supposes that the liquid reaction occurs at continuous stirred tank conditions. However, the supposed liquid flow conditions are not verified in our tests, where the Peclet number is approximately 30.
- Liquid flow through the catalyst bags can be influenced by some phenomena that depend on the solution composition: the existence of preferential paths caused by the non-homogeneous swelling of the resin or the variable wettability of the catalyst structure in function of water solution content.

The need for this adjustable coefficient in the catalyst activity has already been discussed in the literature (Harbou et al., 2011, Beckmann et al., 2002). The authors believe that the specific characteristics of the catalytic packing and the disadvantageous flow characteristics, in addition to the different physical properties of the solutions, such as the relative volatilities, explain the different behavior of the process. Their considerations are coherent with the assumptions taken in this work.

The variation in compositions profiles, regarding results from one test with stoichiometric feed (test n°2) and another one with ethanol excess feed (test n°6) – representative of tests n°1, 3, 4, 5 and 7 – is compared in Figure 6.16. It can be observed that the composition in distillate is nearly the same, but the increased amount of acetic acid under stoichiometric feed conditions exits the column by changing the bottom composition.

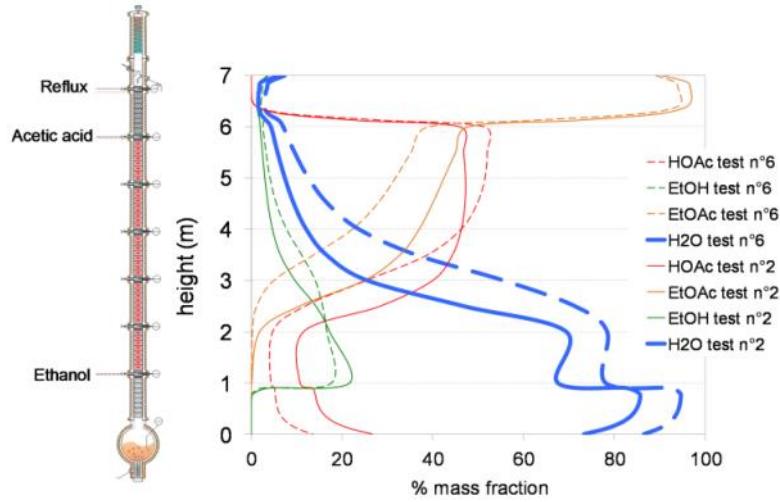


Figure 6.16. Comparison of composition profiles for test n°2 (stoichiometric feed) and n°6 (ethanol excess)

6.4.2 Understanding the adjustable coefficient for heat losses

Despite the fact that the target steady-state was the same for the twelve tests, two different steady-state conditions were obtained. Different weather conditions and thus different heat losses happened during the tests and it can be concluded that the heat loss has an important influence on the pilot operating conditions. In order to improve the system behavior representation, the initial heat loss calculated for the column was changed so as to decrease the distillate flow rate and to better fit the composition profiles. More representative values were found when the heat loss was increased by 11% in tests n°1, 3 and 4. When simulating the process with this new value, the distillate flow rate is reduced by 1.2%, which is almost invisible in historical data, but sufficient to improve the predicted profiles at the column bottom sections. Thus, the difference among the steady states obtained throughout the campaign could be the closer attention granted to the pilot manipulation as from test n°4.

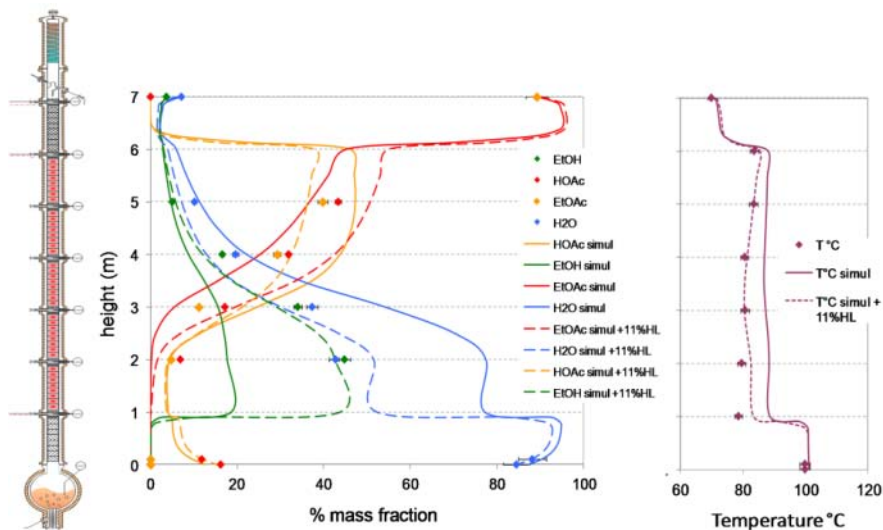


Figure 6.17. Influence of heat loss on composition and temperature profiles, test n°1

The phenomenon of steady-state multiplicities, commonly studied in reactive distillation columns, could also influence the attainment of different steady states through the experimental campaign. A deeper analysis of these possibilities is developed in the section dealing with the dynamic simulation of the process.

6.5 DYNAMIC MODEL

Once the column configuration and the operating parameters were validated, the system behavior in transient regime was analyzed developing a dynamic model. Here, the need of the experimental campaign is highlighted for the acquisition of realistic values for column geometry, technology and hydrodynamics. These parameters are very important to initialize the dynamic simulation and a small deviation can induce errors in the sensitivities, the instabilities and the responses of the process.

The values for reboiler design, diameter of the column and height of theoretical stages were directly considered from pilot observation. The liquid holdup in the reboiler was assumed constant during the experimental tests and the dynamic simulation, due to the presence of a level regulation. Specific liquid volume fractions were initialized for stages with structured reactive packing and flooding calculations were permitted. All the required informations were fed into the Aspen Plus[®] model and the steady state obtained was automatically exported as the initialization for the dynamic simulation in Aspen Plus Dynamics[®]. The values concerning column technology, geometry, heat loss, pressure, system thermodynamics and reaction kinetics remain constant during dynamic calculations.

The dynamic model operates under open-loop control conditions, i.e., the regulations are set in mode manual and directly deliver the fixed manipulated variables and no information from the outputs is considered. For the purpose of better representing the experiments, the heat duty and the reflux ratio are the specifications for the simulation degrees of freedom and the products flow rates and throughputs are the system responses.

First, the dynamic model represents the steady state evolution over time. The result is a stable steady state that remains in the values obtained with the Aspen Plus[®] simulation. Due to the difference that some simulated steady state showed as compared to the experimental results, a temperature bias was considered in each measure so as to compare the dynamic responses gains and delays in the next discussions. In order to represent all the transient responses, each perturbation was introduced into the

model. Aspen Plus Dynamics[®] provides the values of a wide range of process variables through the transient regimes; the evolution of the temperature values and the compositions in the distillate and in the bottom product can be thus analyzed. For clarity purposes and due to the fact that the most important temperature responses are verified inside the column, the graphs are presented with the temperatures from distributors D2 to D7, for the period of approximately 2h before until 2h after the perturbation; product output temperatures do not have exert strong influences.

Test n°3: +10% of external reflux flow rate

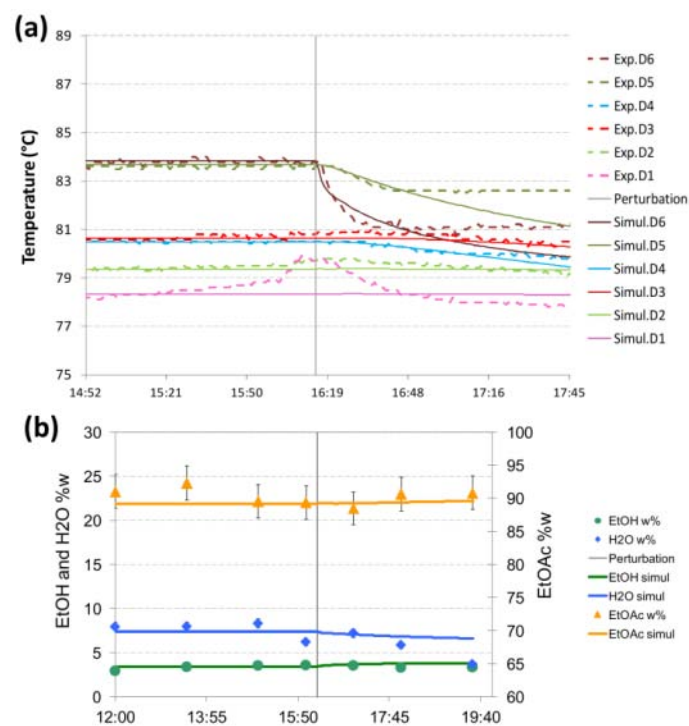


Figure 6.18. Experimental versus simulated temperature (a) and distillate mass composition (b) evolution in test n°3

As can be seen in Figure 6.18a, model predictions and experimental results are in good agreement for temperature. Nonetheless, the final values for the new steady state do not exactly match the experimental data for D5 and D6, the distributors closer to the top of the column. The unexpected behavior verified in D1, which increased before the perturbation and decreased later, was not predicted by the model. In Figure 6.18b, the simulated behavior is in good agreement with the measured ethyl acetate and ethanol contents, but the experimental values for water content decrease faster than the model.

Test n°4: -10% of external reflux flow rate

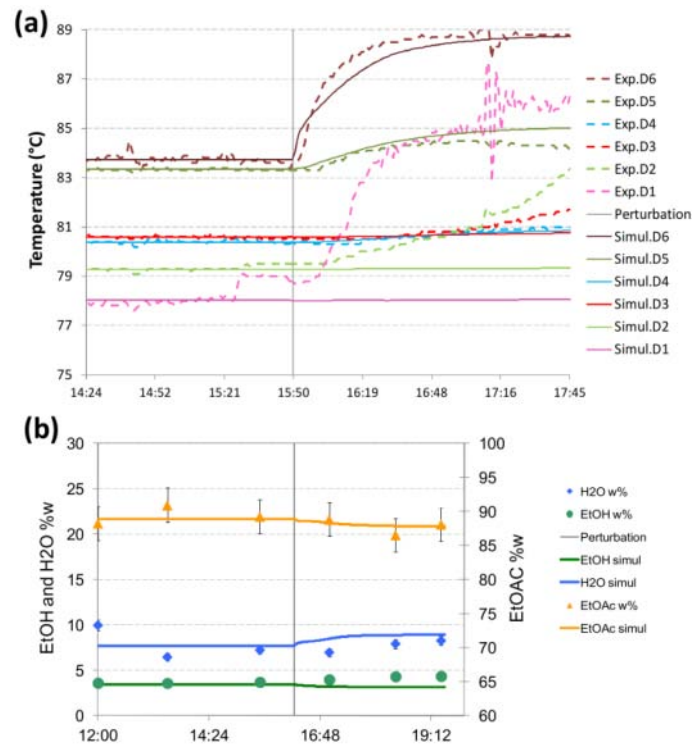


Figure 6.19. Experimental versus simulated temperature (a) and distillate mass composition (b) evolution in test n°4

The responses from the model and from the experimental data agree in directions, gain magnitudes and time constants for D3 to D6. Figure 6.19a allows observing that the temperatures at D1 and D2 drifted and the cause of this phenomenon is not considered in the model. It can be concluded that this behavior is not a direct consequence of the perturbation. The distillate composition evolution is well represented by the model in Figure 6.19b.

Test n°5: +10% of acid feed flow rate

In the case of test n°5, the model predictions showed similar response directions to the experiments, but their behavior were not the same: the experimental data had more instability after the perturbation and although the temperatures at D1, D2 and D3 returned to their previous values, the obtainment of a new steady state cannot be ensured in next 2 hours. Similarly to the unexpected behavior observed during test n°4, some temperatures (D5 and D6) drifted and the cause of this phenomenon is not considered in the model. When comparing the predicted and the measured values for distillate

composition, their magnitudes after perturbation are not the same. In coherence with the temperatures evolution, the pilot was observed to exert stronger influences than the ones predicted by the model.

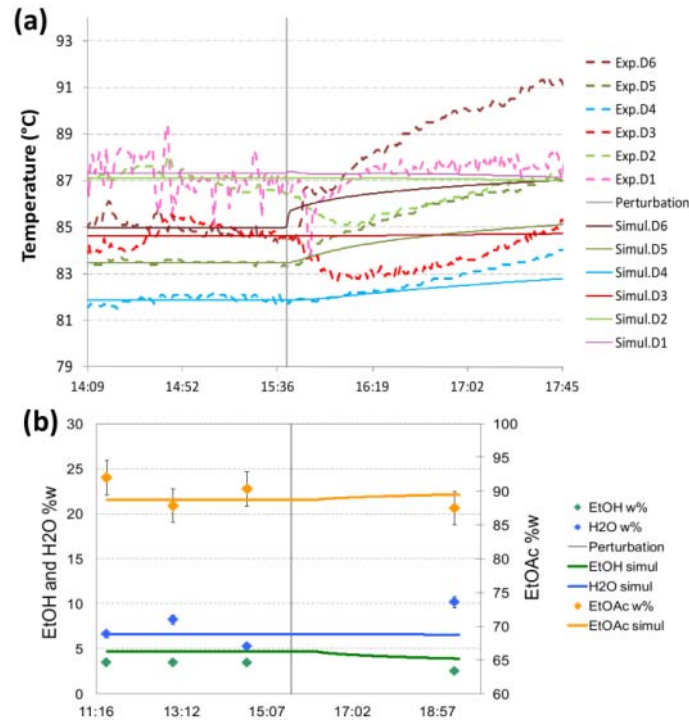


Figure 6.20. Experimental versus simulated temperature (a) and distillate mass composition (b) evolution in test n°5

Test n°6: +10% of ethanol feed flow rate

As can be seen in Figure 6.21, after the increase of the ethanol amount in the column, both measured and simulated temperature values followed the same tendencies, at approximately the same velocity. Yet, a new steady state was not reached in either the cases and the values at the end of the test were not the same between the model and the experiment. The final distillate composition has similar measured and predicted values. There were no important consequences due to this perturbation.

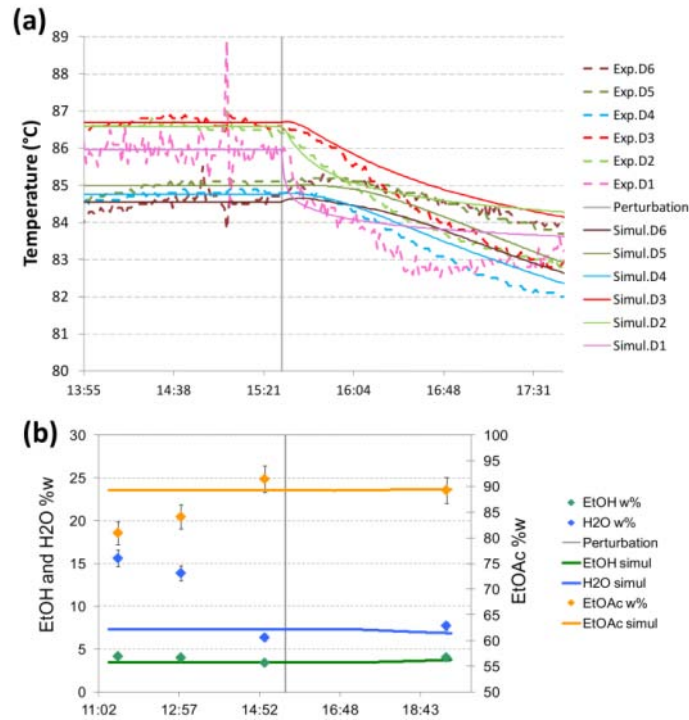


Figure 6.21. Experimental versus simulated temperature (a) and distillate mass composition (b) evolution in test n°6

Test n°7: reduction of heat duty

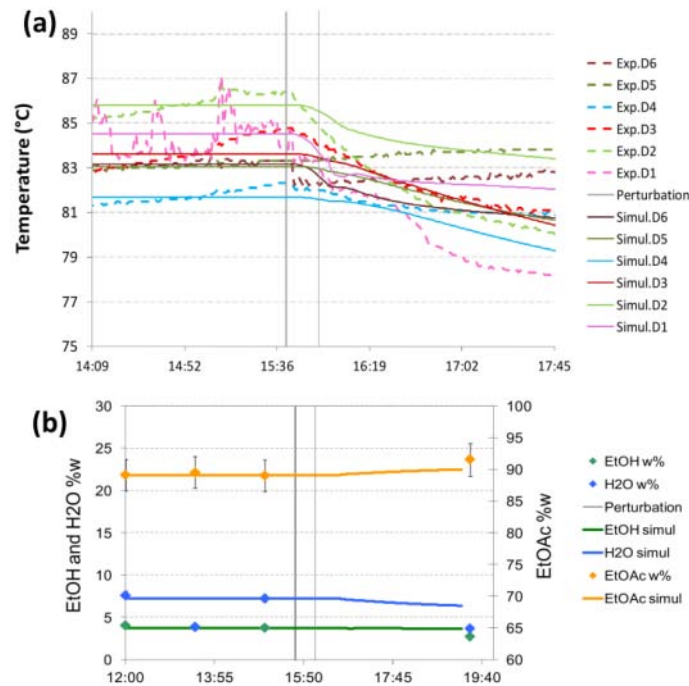


Figure 6.22. Experimental versus simulated temperature (a) and distillate mass composition (b) evolution in test n°7

The perturbation on heat duty during test n°7 was carried out by dropping by 3°C the difference between heat oil temperature and reboiler liquid. The real response of the heat device could be analyzed by the dynamic evolution of the oil temperature and for the purposes of representation on the model, a 20-minute ramp that decreased the heat duty by 5% was assumed. The beginning and the end of this ramp are represented by two different vertical lines in the graphs. The composition analysis exhibits that steady state conditions were not really verified in the experimental results and thus, stabilities of these temperatures after the perturbation could be expected. Again, the model responds slower than the measured data after the perturbation. An interesting observation is that the temperature at D1 shows an oscillation, which is followed by the model. Later, both results stabilize, but at different values.

The responses of the distillate composition have the same direction in the model and in the experiment. In coherence with the temperature responses, the model responds slower than the measured data to the perturbation.

Finally, after the analysis of each test and the model representation, it can be assumed that the column temperatures are strongly sensitive to external conditions and that the observed drifts on temperatures are the consequence of an operation condition that is not repeatable for all tests and it was not identified during pilot manipulations. External conditions were observed to have strong influence on the system due to the pilot geometry and this hypothesis may be accepted because the pilot dimensions provide large superficial contact with the environment. For example, it is possible that, during some tests (approximately 14h from morning to evening), the evolution of the ambient temperature inside the laboratory resulted in different heat loss values, but the model considers it constant. This geometric issue is expected not to occur in industrial-scale devices.

The analysis of the column transient regime shows greater discrepancy of the predicted and measured temperatures at D1 and D6; the fact that the feeds are positioned at these stages may induce additional perturbations. Moreover, several studies have shown that, as a consequence of the nonlinear interactions, complex open-loop behaviors such as steady state multiplicities, trajectories with complex attracting sets and dynamic bifurcations can occur quite frequently in reactive distillation, depending on the characteristics of the reaction system and on the operation conditions (Rosales-Quintero and Vargas-Villamil, 2009, Ramzan et al., 2010, Chen et al., 2002). The authors detect the difficult operating regions through the use of commercially available process simulators. Gehrke and Marquardt (1997) and Reder

et al. (1999) deeply analyzed the multiplicity phenomenon: they employed continuation algorithms in a simulation software and found an infinite number of steady state solutions in the column with an infinite number of trays at infinite reflux ratio. The authors performed some experimental tests, in which sustained oscillations could be found and three multiple steady states were attained in the real column for roughly the same bottoms flow rate. These evidences show the complex behavior of reactive distillation columns and the difficulty to achieve reliable stable conditions. It is, however, understood that an extended number of steady states will most likely not occur in a real column, and indeed this phenomenon was never observed during our experiments. The existence of different steady-states was due to different input values, such as the heat loss, as presented in section 6.4.2.

More precisely, Kumar and Kaistha (2008) and Lee et al. (2006) found through simulation that at fixed reflux rate, output multiplicity, with multiple output values for the same reboiler duty, causes the column to drift to an undesirable steady-state under open loop operation. Both works agree that it can be avoided for a fixed reflux ratio policy. Due to the fact that our pilot is under fixed reflux rate configuration, the results may be of importance for further studies aiming at an experimental confirmation of the steady state multiplicities.

6.5.1 *Verification of the temperature sensors reliability*

During the experimental campaign, some drifts in temperatures were observed – mainly during tests n°4 and 5 – and this phenomenon could not be precisely explained. Any specific action or any change in operational conditions was identified as the reason for this behavior.

Samplings of the solution inside the column were withdrawn during the experiment and compositions were measured by analytical methods. Their theoretical bubble temperature were calculated and compared to the experimentally measured temperatures to verify the reliability of the temperature measures.

It is worth noting that each liquid distributor has two accesses; one is the entry for the thermocouple – present in all distributors – and the other one allows either the placement of a valve to withdraw liquid samples or the introduction of a feed stream. Thus, it was not possible to obtain samplings from D1 and D6, because they receive feed streams. This fact is an inconvenient because some unexpected behaviors were observed exactly at these locations and they cannot be verified. We accept the results from the comparison at other distributors.

It can be concluded from Figure 6.23 that the experimental measures are coherent with the samplings in the majority of cases. This fact validates the reliability of the temperature sensors and thus the existence of unexplainable perturbations in the column, which were not predicted by the model.

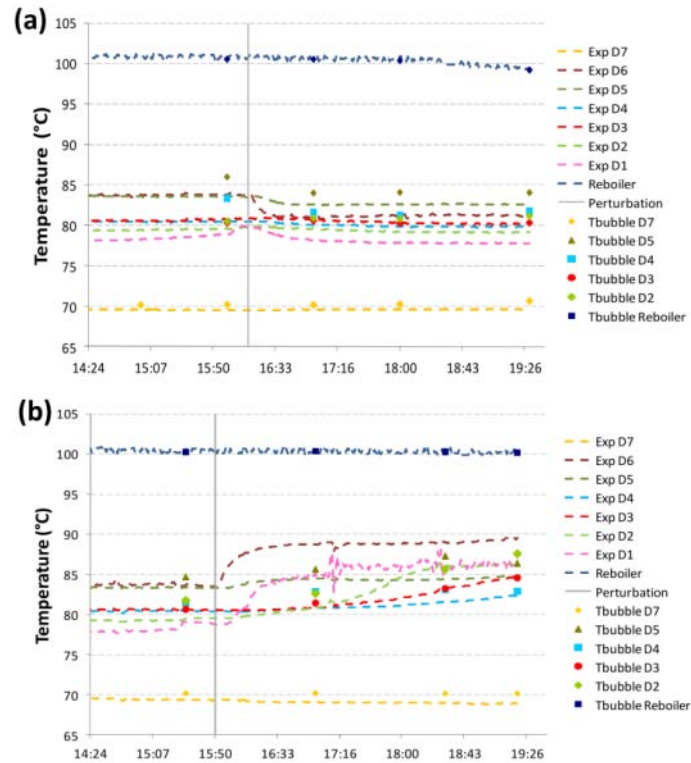


Figure 6.23. Comparison of measured and samplings bubble temperatures for test n°3 (a) and test n°4 (b)

6.5.2 Understanding the adjustable initial values for liquid holdup

In order to obtain a reliable dynamic model of the process, it is known that its geometric, technological and hydraulic parameters need to be detailed. When these parameters concern external measures, such as column height and diameter or reboiler and condenser dimensions, for example, the values can be obtained from pilot observation. However, when the parameters concern internal measures such as flow hydraulics due to packing characteristics, the evaluation becomes more difficult. It may be possible to accept the manufacturer specifications for some packing types, but in the case of structured reactive packing, the simple acceptance of the manufacturer specifications would not be very reliable.

Concerning the structured packing provided by Sulzer Chemtech® and used in our separative sections, extensive data obtained from experimental studies can be found in the literature. Dima et al. (2006) and Olujic et al. (2007) investigate the hydrodynamics of a counter-current gas-liquid flow laboratory-scale column structured with SulzerBX and MellapakPlus, respectively. The dynamic holdup

was calculated in function of the liquid load and values from 0.02 to 0.10 were found for the initial liquid holdup at each stage. The process simulator Aspen Plus[®] proposes a default fraction value of 0.05. The values are in agreement.

KATAPAK-SP Labo was used in the reactive section, which is a structured catalyst support for use in gas–liquid reaction systems in which catalyst pellets such as ion-exchange resins can be embedded. By combining catalyst containing wire gauze layers (catalytic layers) with layers of wire gauze packing (separation layers), it can achieve separation efficiencies equivalent to up to 4 theoretical stages per meter and catalyst volume fractions up to 50% (Gotze and Bailer, 2001). The performance of the KATAPAK-SP depends, however, on many parameters; the most important are dynamic liquid hold-up, pressure drop, residence time behavior, liquid physical properties and catalytic load point. Behrens et al. (2008) experimentally determined the static and dynamic liquid holdup characteristics of the catalyst-filled pockets as encountered in KATAPAK-SP. The authors explained that the value for dynamic liquid holdup was between those for the static liquid holdup and for the catalytic load point. A methanol-water mixture was used and static liquid holdup fractions higher than 0.3 were verified. Kramer et al. (1998) also stated that under gas-liquid trickling flow conditions, the static holdup at a packed bed of spherical particles may represent up to 25% or 33% of the total liquid holdup. It can be thus concluded that the initial liquid fraction in the reactive section is much higher than the holdups in the separative sections. It was then necessary to define different values to model the initial liquid fraction at each section of the column. The values that better represent the system behavior are given in Table 6.6.

Table 6.6. Initial stage liquid fraction for each packing present at the column

SulzerDX	KatapakSP-Labo	SulzerCY
0.02	0.45	0.05

All the required specifications for the structured catalytic packing highlight the need of a special attention when modeling a heterogeneous catalyzed column, where the presence of solid particles strongly influences the system. The value adopted for the reactive section (the most different from the default value proposed by Aspen Plus[®]) is deeply related to the specific operational conditions of the process and this is far from the idea of proposing a generic approach. The difficulties observed with the heterogeneous catalyzed columns explain why the great majority of industrial columns are under homogeneous catalysis configuration.

For the purpose of comparison, Figure 6.24 shows the experimental and different predicted values for the temperature evolution in the column during test n°5, for example. The continuous lines represent the model with the adapted and coherent values for the hydrodynamic parameters and the dotted lines account for the simulation with the default values. It can be verified that the right definition of the hydraulic parameters is of great importance to the model reliability.

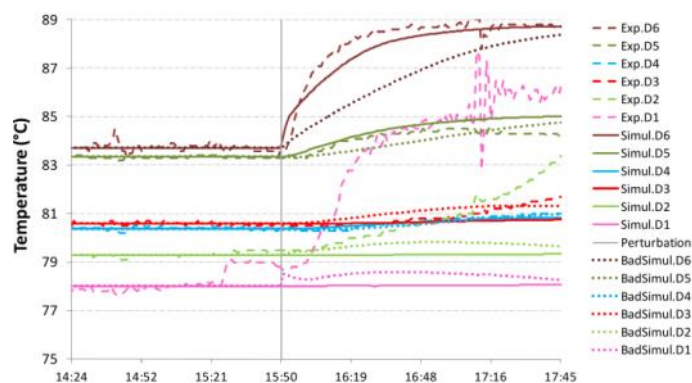


Figure 6.24. Experimental and simulated temperature evolution in test n°5, where “Simul” represents the adapted values for the hydrodynamics and “BadSimul” considers the default values

6.6 CONCLUSIONS

An experimental campaign was conducted for the production of ethyl acetate from esterification of acetic acid and ethanol in a reactive pilot column. Several tests were performed to determine the steady state conditions for a feed configuration with excess ethanol. A thorough analysis on steady state characteristics was performed and each test was simulated using the Aspen Plus[®] software. Good agreement was obtained between experimental and simulation results. One additional test was conducted under stoichiometric feed configuration and it was verified that the feed composition strongly influences the catalyst activity so that the reliability of the model requires an adaptation of the reaction kinetics for each operating condition. Important sensitivities of the pilot to heat duty and heat losses were also observed. In order to study the system dynamics, five experimental tests were performed and they provided representative results. Perturbations were carried out in alcohol and acid feed streams, reflux rate and heat duty and sufficient data was available for defining realistic geometry, technology and hydrodynamics of the pilot. The model was developed in Aspen Plus Dynamics[®] considering all the parameters and conditions present at the pilot and a specific discussion on the best representation of the heterogeneously catalyst and the related holdup was developed. The system hydraulics is also shown to

be strongly dependent on the present solution and its operating conditions. The values for liquid holdup must be adapted from those provided by the manufacturers or the simulation software in order to be representative. An important effort was necessary to develop a unique model that qualitatively and quantitatively represents the system tendencies and responses. The dynamic model obtained is a reliable representation of the proposed reactive distillation process and it can be used to predict other possible perturbations that an industrial site may face such as an impurity of water on the feed streams, for example. It is concluded that the reliability of a complex system model lies on the deep knowledge of its operating conditions and sensitive parameters. The requirement of experimental manipulations to obtain coherent model considerations is highlighted.

This study has been accepted as a publication to the international review *Chemical Engineering Research and Design*, 2013. The important interests, in comparison to previous works, is that the operating conditions were analyzed for a continuous process under different perturbations on feed flow rates, reflux flow rate and heat duty and the same derived model is in agreement with all the conditions. The application of this dynamic approach to the heterogeneously catalyzed ethyl acetate esterification is a significant new contribution to the present research concerning reactive distillation.

After all, the observations concerning the complexities of using heterogeneous catalyst in the reactive distillation column may hamper an industrial application. As presented, the composition of the solution with aqueous components and the liquid bad distribution inhibits a reliable mastery of the reaction. In a real industrial context, where the mixtures may have significant impurities, a frequent catalyst substitution or replacement would be necessary and, as a consequence, a dismantling of the entire column would be necessary. Those facts encourage our further studies to consider the homogeneous catalysis, aiming to overcome some of the complexities presented.

The disadvantage on considering the homogeneous catalyst is the restriction imposed on some column configurations. The separation sections can only exist above the homogeneous catalyst feed stage, as a result of its low volatility – in the case of some organic acids – and thus its presence in all the stages from its feed location to the bottom of the column. This condition will be respected and the simulation model will be adapted for the work in further chapters.

FOURTH PART

IV. CONTROLLABILITY METHODOLOGY

7.	The indices-based controllability analysis	111
8.	Controllability study of a column configuration	125

The combination of separation and reaction in a single apparatus generates important complexities regarding process dynamics, control and supervision, hindering the successful operation of reactive columns. By considering an indices-based analysis methodology, the objective is to identify some criteria to quantify and to qualify the system controllability at early design steps, for different control structures. Conventional distillation columns have two degrees of freedom, so two different variables have to be controlled to ensure separation specifications. In the case of reactive distillation columns, the conversion rate is also a variable of control interest. In the column configuration proposed, a third control loop with a measured variable inside the reaction zone can address the reaction conditions by manipulating a third degree of freedom given by the ratio of the two separated feed flows. The three loops are designed to exhibit high sensitivity, good balance and small interference. Chapter 7 presents the controllability methodology. The first steps are obtained through steady state simulations, with the calculation of the Sensitivity Matrix, the Singular Value Decomposition, the Condition Number and the Intersivity Index. Then, the dynamic simulation of the system is studied, by considering the properly chosen control loops with the Integral of the Squared Errors calculations. Chapter 8 applies the methodology to a reactive distillation for the production of ethyl acetate, highlighting the specific sensitivities of this system and the best control configurations.

La Partie IV présente la méthodologie proposée pour l'analyse de la contrôlabilité des colonnes de distillation réactive et l'applique à une configuration typique de colonne, pour illustrer les calculs.

En adoptant la méthode séquentielle avec des indices qui anticipent le comportement du système, l'objectif du Chapitre 7 est d'identifier des critères pour qualifier et quantifier la contrôlabilité et de les adapter au procédé de distillation réactive. Les critères doivent permettre la comparaison de différentes structures de contrôle et différentes configurations de colonne dès la phase de conception du procédé. Pour assurer un schéma de contrôle fiable, avec des variables contrôlées bien choisies et bien couplées avec les variables manipulées respectives, les boucles de contrôle doivent avoir une haute sensibilité, une bonne stabilité et robustesse et montrer de faibles interactions.

Les premiers pas pour étudier la contrôlabilité du système sont conduits avec le modèle de simulation en régime permanent. Les informations concernant la sensibilité sont obtenues avec un modèle basé sur des calculs d'équilibre par étage théorique, et permettent de produire la Matrice de Sensibilité (*Sensitivity Matrix*), dans laquelle chaque élément représente un gain en régime permanent d'une variable mesurée en relation avec une variable manipulée. Puis, les valeurs propres de la matrice sont calculées par la méthode connue comme Décomposition en Valeurs Singulières (*Singular Value Decomposition*), pour identifier les mesures les plus sensibles. Un critère quantitatif, connu comme Nombre de Conditionnement (*Condition Number : CN*), est calculé comme le ratio de la valeur propre la plus élevée sur la plus petite. Il fournit une indication de l'équilibre entre les sensibilités dans un système multi variable. Les systèmes les mieux équilibrés sont représentés par une valeur de *CN* proche de l'unité. Le couplage du *CN* avec la plus petite des valeurs propres donne un nouvel indice : l'Indice d'Intensivité (*Intersivity Index : I*), qui quantifie la sensibilité et l'équilibre du système. La valeur désirée pour *I* est la plus grande possible. Pour analyser les interactions entre les boucles de contrôle et définir le meilleur couplage des variables contrôlées et manipulées, le Vecteur des Gains Relatifs (*Relative Gain Array*) est calculé. L'analyse du système continue par sa simulation en régime dynamique, en considérant cette fois-ci les boucles de contrôle sélectionnées dans l'étape précédente. Le comportement du procédé est étudié à la suite de potentielles perturbations et la réponse dynamique est analysée en fonction des objectifs de commande, de stabilité, de vitesse, de robustesse et du respect des spécifications de production. L'Intégrale de l'Erreur au Carré (*Integral Square Error*) est enfin calculée comme l'intégrale de la différence entre la consigne et la variable contrôlée au carré.

Table 7.1. Récapitulatif des critères de contrôlabilité

Mesure	Equation	Définition	Valeur désirée
Sensibilité :	$\Sigma = \begin{bmatrix} \sigma_1 & 0 \\ 0 & \sigma_2 \end{bmatrix}$	Σ : matrice des valeurs propres	
Equilibre :	$CN = \frac{\sigma_{\text{highest}}}{\sigma_{\text{smallest}}}$	CN : indication numérique de l'équilibre des sensibilités dans un système multi variable	↘
Equilibre et sensibilité :	$I_{i,j} = \frac{\sigma_{\text{smallest}}}{CN_{i,j}}$	I : considère l'équilibre des gains et la sensibilité des boucles multi variables	↗
Interactions :	$\Lambda = \begin{bmatrix} \lambda_{11} & \lambda_{12} \\ \lambda_{21} & \lambda_{22} \end{bmatrix}$	RGA : mesure les interactions et définit les couplages	~ 1
Réponse dynamique :	$ISE_N = \frac{\int_0^{\infty} (e(t))^2 dt}{x_{(t=0)}}$	ISE : intégrale de l'erreur au carré des comportements dynamiques	↘

Le Chapitre 8 illustre les calculs dans le cas d'une colonne réactive utilisée pour la production d'acétate d'éthyle par esterification de l'éthanol avec l'acide acétique. La configuration présente 28 étages théoriques, numérotés vers le bas, avec deux alimentations : l'acide est alimenté à l'étage n°9 et l'alcool est alimenté à l'étage n°24. Les étages numérotés de n°1 à 8, en tête de colonne, sont dédiés uniquement à la séparation. Trois spécifications industrielles de production sont à respecter.

L'étude des critères de contrôlabilité montre qu'un contrôle de composition conduit à de meilleures performances par comparaison avec contrôle de température. Néanmoins, les capteurs de température présentent l'avantage d'être moins coûteux et d'un contrôle fiable à intégrer dans la zone de séparation.

De plus, pour atteindre les trois spécifications de production, trois boucles de contrôle sont nécessaires. En comparaison avec les colonnes de distillation conventionnelles, où deux boucles de contrôle garantissent les performances de séparation, une boucle additionnelle peut être utilisée pour assurer les performances de la réaction, en contrôlant une mesure dans la zone réactive et en manipulant le débit de l'éthanol. Cela est possible dû au fait qu'un degré de liberté additionnel est géré dans une colonne avec double alimentation, par le ratio entre les débits des alimentations. Les critères définis démontrent qu'il est possible d'avoir une mesure fiable de la contrôlabilité dès la phase de conception des colonnes réactives.

A Parte IV apresenta a metodologia proposta para a análise da controlabilidade de colunas de destilação reativa e a aplica a uma configuração típica, com o objetivo de exemplificar os cálculos.

Adotando os métodos sequenciais com índices que antecipam o comportamento do sistema, o objetivo do Capítulo 7 é identificar os critérios para qualificar e quantificar a controlabilidade e os adaptar ao processo de destilação reativa. Os critérios devem permitir a comparação de diferentes estruturas de controle e diferentes configurações de coluna desde a etapa de projeto do processo. Para garantir um esquema confiável de controle, com variáveis controladas bem escolhidas e bem emparelhadas com as respectivas variáveis manipuladas, as malhas de controle devem ter forte sensibilidade, boa estabilidade e mostrar fracas interações.

Os primeiros passos para estudar a controlabilidade do sistema são conduzidos com o modelo de simulação em estado estacionário. As informações relativas à sensibilidade são obtidas com um modelo baseado em cálculos de equilíbrio por estágio teórico, e resultam na Matriz de Sensibilidade (*Sensitivity Matrix*), na qual cada elemento representa um ganho em estado estacionário de uma variável medida com relação a uma variável manipulada. Os valores singulares dessa matriz são calculados pelo método conhecido como Decomposição em Valores Singulares (*Singular Value Decomposition*), para identificar as medidas mais sensíveis. Um critério quantitativo, conhecido como Número de Condicionamento (*Condition Number : CN*), é calculado como a fração entre o maior e o menor valor singular e fornece uma indicação do equilíbrio entre as sensibilidades em um sistema multivariável. Os sistemas com melhor equilíbrio são representados por um valor de *CN* próximo à unidade. A consideração simultânea do *CN* e do menor valor singular resulta em um novo índice: o Índice de Intersensibilidade (*Intersivity Index : I*), que quantifica a sensibilidade e o equilíbrio do sistema. O valor desejado para *I* é o maior possível. Para analisar as interações entre as malhas de controle e definir o melhor emparelhamento entre as variáveis controladas e manipuladas, a Matriz de Ganhos Relativos (*Relative Gain Array*) é calculada. A análise do sistema continua com sua simulação em regime dinâmico, considerando agora as malhas de controle selecionadas na etapa precedente. O comportamento do processo é estudado após perturbações potenciais e a resposta dinâmica é analisada com relação aos objetivos do controle, à estabilidade, às velocidades, à robustez e ao respeito das especificações de produção. A Integral dos Erros ao Quadrado (*Integrated Square Error*) é enfim definida como a diferença entre os valores medidos da variável controlada e seu valor desejado, ao quadrado.

Tabela 7.1. Recapitulação dos critérios de controlabilidade

Medição	Equação	Definição	Valor desejado
Sensibilidade:	$\Sigma = \begin{bmatrix} \sigma_1 & 0 \\ 0 & \sigma_2 \end{bmatrix}$	Σ : matriz de valores singulares	
Equilíbrio:	$CN = \frac{\sigma_{\text{highest}}}{\sigma_{\text{smallest}}}$	CN : indicação numérica do equilíbrio das sensibilidades de um sistema multi-variável	↘
Equilíbrio e sensibilidade:	$I_{i,j} = \frac{\sigma_{\text{smallest}}}{CN_{i,j}}$	I : considera o equilíbrio dos ganhos e a sensibilidade das malhas multi-variáveis	↗
Interações:	$\Lambda = \begin{bmatrix} \lambda_{11} & \lambda_{12} \\ \lambda_{21} & \lambda_{22} \end{bmatrix}$	RGA : mede as interações e define os emparelhamentos	~ 1
Resposta dinâmica:	$ISE_N = \frac{\int_0^{\infty} (e(t))^2 dt}{x_{(t=0)}}$	ISE : integral do erro ao quadrado dos comportamentos dinâmicos	↘

O Capítulo 8 ilustra os cálculos no caso de uma coluna reativa usada para a produção de acetato de etila pela esterificação de ácido acético e etanol. A configuração apresenta 28 estágios teóricos, numerados a partir do topo da coluna, com duas alimentações: o ácido é alimentado no estágio nº9 e o álcool é alimentado no estágio nº 24. Os estágios numerados de nº1 à 8, no topo da coluna, são dedicados exclusivamente à separação. Três especificações de produção devem ser respeitadas.

O estudo dos critérios de controlabilidade mostra que o controle de composição conduz a desempenhos melhores do que o controle de temperatura. Entretanto, os sensores de temperatura apresentam a vantagem de serem menos custosos e de que a sua instalação pode ser considerada confiável na zona de separação. No mais, para atender às 3 especificações de produção, 3 malhas de controle são necessárias. Em comparação com as colunas de destilação convencionais, onde duas malhas de controle garantem o desempenho de separação, uma malha adicional pode ser utilizada para garantir o desempenho da reação, controlando uma variável medida na zona reativa e manipulando a vazão de alimentação de etanol. Esse fato é possível, pois um grau de liberdade adicional aparece em colunas com dupla alimentação, definido pela razão entre as vazões das alimentações. Os critérios definidos demonstraram que é possível ter uma estimativa confiável da controlabilidade desde a etapa de projeto de colunas reativas.

The indices-based controllability analysis

7.1 SELECTING CONTROLLED VARIABLES

The controllability analysis procedure consists in obtaining the sensitivity of all the process measured outputs with respect to the inputs available for control, so as to propose structures that perform the key control tasks. The steady state variations of the measured variables with respect to changes on the manipulated variables are then generated. The outputs with the highest sensitivities are selected as candidate variables to be used for the different control loops. In addition, as the control structure has multiple loops, different indices are calculated to measure balances and interferences between variables. The control structures proposed are subjected to validation via dynamic simulations, in which additional indices are introduced to measure the system closed-loop behavior. Finally, all the indices presented compose the controllability criteria to compare different control structures and column configurations. The methodology adopted for controllability analysis sequentially considers the existing calculation approaches and adapts them to the considered reactive distillation system.

This section begins with a representative literature research concerning the selection of control variables, with the purpose of introducing the sensitivity approach.

Kienle and Marquardt (1991) state that control systems design consists of two main steps. The first step is the selection of the control structure, which includes the choice of suitable manipulated and controlled variables as well as their pairings in multivariable system case. The second step is the design and the parameterization of some control algorithm, which defines the computation of the required values of the manipulated variables from the measurements and given set points.

Newell and Lee (1988) established qualitative criteria as guidelines for the selection of controlled and manipulated variables, driven by plant and control objectives. Seborg et al. (1989) discussed the selection of measured variables. The criteria are as follow.

Selection of controlled variables:

- Select variables that are not self-regulating,
- Select outputs that are direct measures of the product quality or that strongly affect it,
- Choose output variables with favorable static and dynamic responses to the available manipulated variables,
- Choose output variables that would exceed equipment or operation constraints without control.

Selection of manipulated variables:

- Select inputs that significantly affect the controlled variables,
- Select inputs that rapidly affect the controlled variables,
- Prefer variables that affect the controller variables directly rather than indirectly,
- Avoid recycling disturbances.

Selection of measured variables:

- Reliable, accurate measurements are essential for good control,
- Select measurement points that are sufficiently sensitive,
- Select measurement points that minimize time delays and time constants.

When selecting the control variables, the understanding of the process degrees of freedom is made necessary. Conventional distillation columns have two degrees of freedom, and they thus show the need of manipulating two different input variables in order to ensure separation specifications. In the case of reactive distillation columns, the conditions regarding the reaction should also be controlled and the expected conversion, essential for operation quality, is therefore of control interest.

As far as the ethyl acetate system is concerned, a reactive column with double feed configuration was adopted. At the same time that additional disturbances can independently occur in each feed flow, one additional degree of freedom is given by the feed ratio and may provide another manipulated variable. Three different control loops are of interest to ensure both separation and reaction performances. This hypothesis is validated in section 8.1.

This chapter presents the methodology adopted to select the most appropriate control variables (controlled and manipulated variables) and the calculation of criteria to measure the column controllability.

7.2 STEADY STATE SIMULATIONS

By considering all the given conditions for selecting a controlled variable, and in order to ensure a good control scheme, the defined control loops must show:

- High sensitivity
- Good balances
- Small interferences

The first steps in studying the system controllability are obtained by extracting information from simulations run at steady state. The sensitivity information can be acquired from any simulated model based on stage-to-stage calculations. The commercial process simulator Aspen Plus[®] has been used to perform these steady-state simulations and the resulting values are then processed by software or macroinstructions developed in Matlab[®] and Microsoft Excel.

7.2.1 The Sensitivity matrix

Moore (1992) defines loop sensitivity as a measure of how the control sensor responds at steady state to changes in the manipulated variable. Mathematically, the loop sensitivity can be defined as the partial derivative of the sensor signal with respect to changes in the signal of the manipulated variable:

$$\text{Loop sensitivity} = \frac{\partial S_i}{\partial M_j}$$

S_i : Signal from control sensor i , expressed as a percentage of the maximum signal

M_j : Signal to manipulated variable j , expressed as a percentage of the maximum signal

The types and locations of the sensors are critical to the sensitivity problem. Their selection should consider detailed analytical techniques. The Model Sensitivity Analysis tool of Aspen Plus[®] is used to compute these partial derivatives: one operational parameter can be changed in a given interval, by a chosen step, and the resulting values of the selected output variables are obtained. The different computed partial derivative values are then organized into a matrix named the system sensitivity matrix K and defined as:

$$K_{n \times m} = \begin{bmatrix} \frac{\partial S_1}{\partial M_1} & \dots & \frac{\partial S_1}{\partial M_j} & \dots & \frac{\partial S_1}{\partial M_m} \\ \dots & \dots & \dots & \dots & \dots \\ \frac{\partial S_i}{\partial M_1} & \dots & \frac{\partial S_i}{\partial M_j} & \dots & \frac{\partial S_i}{\partial M_m} \\ \dots & \dots & \dots & \dots & \dots \\ \frac{\partial S_n}{\partial M_1} & \dots & \frac{\partial S_n}{\partial M_j} & \dots & \frac{\partial S_n}{\partial M_m} \end{bmatrix}$$

with: S_i : i^{th} measured variable in the column

M_j : j^{th} manipulated variable

m : number of manipulated variables

n : number of measured variables

The sensitivity matrix may also be called gain matrix, because each component of the matrix represents the steady-state gain of one measured variable with respect to one manipulated variable. Steady-state gains are computed through simulations by acting on each input, one at a time.

In order to compare the sensitivities between them, it is necessary to quantify the sensitivity of each measured variable according to a real measurement device and to normalize them regarding the range of possible values of this real device. The measurable variables are the temperature and the mass compositions of each component at each stage of the column. Hence, the specific equations to define the loop sensitivities in the studied system can be discretized as:

$$\frac{\partial T_i}{\partial M_j} \approx \frac{\frac{\Delta T_i}{(T_{\max} - T_{\min})}}{\frac{\Delta M_i}{(M_{\max} - M_{\min})}} \quad \frac{\partial c_i}{\partial M_j} \approx \frac{\frac{\Delta c_i}{(c_{\max} - c_{\min})}}{\frac{\Delta M_i}{(M_{\max} - M_{\min})}}$$

It must be underlined that the definition of each measurement range strongly influences the sensor locations selection, as the sensitivity to the input perturbation strongly depends on this range. This choice should then be made carefully and with a good knowledge of the real analyzers. The discussion of this key point is further developed in section 8.2.3.

Once matrix K that better represents the system interactions is defined, it becomes the basis for the Singular Value Decomposition method.

7.2.2 Singular Value Decomposition

The dynamic analysis of multivariable systems is influenced by some important properties, such as the zeros, the poles, and the singular values of the system. The zeros and poles values are roots obtained directly from the process model. The singular values are calculated from the method known as Singular Value Decomposition (*SVD*).

In linear algebra, *SVD* is a factorization of a rectangular matrix. Its application in process control typically involves square, invertible matrices and it is proved to be a useful tool in analyzing and designing multivariable control systems. Nowadays efficient computer programs are available, and commonly used, for *SVD* calculations. MATLAB[®] was adopted in this work. *SVD* decomposes one matrix into three unique component matrices. For any real $n \times m$ matrix K , it is always possible to find orthogonal matrices U and V such that:

$$U^T \cdot K \cdot V = \Sigma \quad \text{where } \Sigma = \begin{bmatrix} S & 0 \\ 0 & 0 \end{bmatrix}; \quad \text{with } S = \begin{bmatrix} \sigma_1 & 0 & \dots & 0 \\ 0 & \sigma_2 & \dots & 0 \\ \dots & \dots & \dots & \dots \\ 0 & 0 & \dots & \sigma_m \end{bmatrix}$$

U is a $n \times n$ unitary matrix and V is a $m \times m$ unitary matrix

By applying the properties of these orthogonal matrices U and V , the following relation is obtained:

$$K = U \cdot \Sigma \cdot V^T$$

where it can be understood that:

- The columns of V form a set of orthonormal input or analyzing basis vector directions for K ; these are the eigenvectors of $K^T K$ and may be called the right singular vectors,
- The columns of U form a set of orthonormal output basis vector directions for K ; these are the eigenvectors of $K K^T$ and may be called the left singular vectors,
- The diagonal values in matrix Σ are the singular values, which can be thought of as scalar gain controls by which each corresponding input is multiplied to give a corresponding output; these are the square roots of the eigenvalues of $K K^T$ and $K^T K$ that correspond to the same columns in U and V . The singular values are scalars organized in descending order such that $\sigma_1 \geq \sigma_2 \geq \dots \geq \sigma_m \geq 0$.

Moore (1992) adopts the *SVD* calculations for studies on temperature and composition sensors placement in a conventional distillation column. This methodology is adapted here to a reactive distillation column, and simultaneously considering all the sensors sensitivities.

The interest in using the *SVD* calculations to analyze and to design multivariable control systems can be better understood when the physical interpretation of the component matrices is discussed. The objective with this decomposition is to address the sensor placement problem, because matrices U and K are both measures of sensor sensitivity. In the following paragraphs the physical interpretation of each component matrix reported by Moore (1992) is listed and extended to reactive distillation:

$U = U_1 : U_2 : \dots : U_n$: the left singular vectors are the most important component matrix. It provides a sensor coordinate system for viewing the sensitivity of the column regarding changes in the manipulated variables. This coordinate system is such that U_1 indicates the vector direction that is most responsive to changes in the manipulated variables. U_2 indicates the next most responsive vector

direction. The third vector U_3 is the next most responsive, and so on. The properties of U provide that each vector direction is orthogonal to the other vector directions.

If these considerations are taken from the reactive distillation system point of view, U_1 indicates the most sensitive combination of tray temperatures or compositions in the column. The major component of the U_1 vector is the most sensitive location for a temperature/composition sensor in the column. U_2 indicates the next most sensitive combination of measurable variables, orthogonal to the variables represented in U_1 . The main components of U_2 represent location sensitivity and exhibit the least possible interactions with the primary sensors. However, it should be highlighted that even if this method searches for vectors leading to the least interactions, some systems may have considerable interactions between all sensors.

$V = V_1 : V_2 : \dots : V_n$: the right singular vectors are not directly used in the analysis of the sensors placement problem; however, their interpretation is helpful to complete the physical picture provided by the SVD. The right singular vector provides a manipulated variable coordinate system for viewing the sensitivity of the column. This coordinate system is such that V_1 indicates the combination of control actions that affects the column the most, V_2 indicates the next most effective combination of control actions, etc. Vectors V are also orthogonal.

$\Sigma = \sigma_1 : \sigma_2 : \dots : \sigma_n$: the scalar singular value provides an indication of the multivariable gains in a decoupled process. This information is useful to evaluate the difficulty of a proposed multivariable control system. As given above, the singular values compose the matrix S .

7.2.3 Condition number

The results from the sensitivity analysis are rearranged to provide indicators of the reactive column controllability; the different calculations are presented in the following sections.

The ratio the largest and the smallest singular value of matrix S is known as the condition number (CN) of K :

$$CN(K) = \frac{\sigma_{highest}}{\sigma_{smallest}}$$

The condition number is a positive number used as an indication of how ill-conditioned the gain matrix K is. In other words, it provides a quantitative indication of the balance of sensitivities in a multivariable system. Extremely large, but finite, values of condition numbers indicate that the matrix is close to singularity, or ill conditioned, reflecting an imbalance in the multivariable gains. Conversely, low condition numbers evidence that the multivariable gains are well balanced and the system should have enough degrees of freedom to meet the control objectives.

Thus, if the methodology searches for the best controllable systems, the expected values of condition number are those closer to unity. The $CN = 1$ indicates that the degrees of freedom of the system are saturated, having the same sensitivity in each vector direction. Consequently, a small value of condition number is related to good control system robustness.

In the case of systems with high CN values, problems in one loop can easily propagate through the entire system; these consequences can be even more complicated on a multi-loop control configuration.

According to Moore (1992), with respect to the question of multiple sensor placements, there are two levels of SVD analysis: an overall analysis and a specific analysis. The condition number already presented concerns the overall analysis and it is helpful to gage the magnitude of the multivariable control problem. The specific condition number is determined so as to represent the process a dual-ended control system (i.e. 2 manipulated and 2 controlled variables) would actually experience. Moreover, the author's approach is also adapted to represent a system with three control loops.

Actually, a column configuration has one single representative value of overall CN , because all inherent variables are considered, but can show different values of specific CN for each control variables selected. The calculations of specific matrices and condition numbers can be conducted for several choices of control structures and they can be compared as a function of their specific criteria values. Through the comparison of the specific CN values, it is possible to define which choice represents the best controllable configuration.

For example, based on the sensitive variables proposed by the U vectors, if the chosen sensors are the acid composition at one stage and the alcohol composition at another stage of the column the overall gain matrix is reduced to a specific $K_{2 \times 2}$, where new singular values and condition number can be calculated as a function of the 2 control loops. In the case of the selection of three sensitive sensors, the new gain matrix becomes a $K_{3 \times 3}$.

7.2.4 Intersivity index

In addition to the calculations of the condition number, which measures the balance of the system degrees of freedom, other specific criteria can be defined. It was already accepted that the singular values of the system quantify the multivariable sensitivity. Moore (1992) claims that, in terms of placing sensors for maximum sensitivity, the focus should be on the weakness of the subsystem and this weakness is reflected in the smallest of the singular values.

Therefore, if one aims to find subsystems with both high sensitivity and balance, the Intersivity Index (I) can be considered. The calculation of the Intersivity index associates the values of the condition number and the smallest singular value:

$$I_{i,j} = \frac{\sigma_{i,j \text{ smallest}}}{CN_{i,j}} = \frac{(\sigma_{i,j \text{ smallest}})^2}{\sigma_{i,j \text{ largest}}}$$

with: i : i^{th} measured variable in the column
 j : j^{th} manipulated variable

The systems with better sensitivity and balance are represented by important I values.

This criterion is calculated when considering specific sensors, in function of the specific gain matrix K and the specific CN . The objective is to quantitatively compare different choices of sensors placement. In addition, due to the fact that a high value of the Intersivity index is sought, it is possible to perform an optimization by identifying which specific group of sensors results in the highest value of I among all measurable parameters of the column. The required codes have been implemented in Matlab[®] and are presented in Appendix IV.

7.2.5 Loops pairing

When applying a control strategy in multivariable systems, the first aim is to search for multiple and independent single-loop controllers so as to avoid complexity of the controller structure. In our case, each loop uses one input variable to control one assigned output variable. The advantage of this configuration is that each loop can be designed as if it was in a SISO (single input - single output) system. Although this approach may simplify the process control design, in multivariable systems, the variables are not always independent from each other and significant interactions can occur among them in the closed-loop configuration.

So, if the process control of a multivariable system is based on multiple single-loop design, the pairings of manipulated and controlled variables should be carefully chosen to minimize interaction effects. To achieve this minimization, these interactions should be analyzed and the Relative Gain Array (RGA) of the system is calculated.

To begin the approach, the relative gain λ_{ij} between output y_i and input m_j should be defined:

$$\lambda_{ij} = \frac{\text{process gain as seen by a given loop with all other loops open}}{\text{process gain as seen by a given loop with all other loops closed}}$$

The value of the relative gain provides a quantitative information about the influence extent of process interactions when the manipulated variable m_j is used to control y_i , in steady-state conditions.

The physical interpretation is:

- $\lambda_{ij} < 1$: there is interaction in the system and its effect has the opposite direction of the main effect. The consequence is a total effect smaller than the main effect, and therefore a larger controller action is required to achieve a change of a system output in the closed loop than in the open loop.
- $\lambda_{ij} = 1$: the main effect of m_j on y_i , measured when all loops are opened and the total effect, measured when other loops are closed, are identical. In this case, there are no interaction effects in the loop, and m_j should be paired with y_i .
- $\lambda_{ij} > 1$: there is interaction in the loop and it affects the system in the same direction as the main effect.
- $\lambda_{ij} = 0$: variable m_j has no effect on y_i ; a loop pairing of these variables has no significance.
- $\lambda_{ij} < 0$: the interaction effect has opposite direction and larger value than the main effect.

So, the recommendation is to pair the controlled and manipulated variables so that the corresponding relative gains are positive and as close to unity as possible.

When the relative gain is calculated for all input/output combinations of a multivariable system, the RGA (also called Bristol array) is obtained:

$$RGA = \begin{bmatrix} \lambda_{11} & \lambda_{12} & \dots & \lambda_{1n} \\ \lambda_{21} & \lambda_{22} & \dots & \lambda_{2n} \\ \dots & \dots & \dots & \dots \\ \lambda_{n1} & \lambda_{n2} & \dots & \lambda_{nn} \end{bmatrix}$$

This is the RGA approach ideally conceived for linear systems, in which the sum of the relative gains in any row or column is equal to 1. Since the *RGA* is based on the assumption of perfect control, the results are independent of controller tuning or sophistication. For this reason, this matrix is a reliable measure for screening alternative flowsheets at the conceptual design step of a process, considering only its steady state simulation. However, if *RGA* provides information about the steady-state interaction in a linear process system, the dynamic factors are not taken into consideration.

Due to the fact that reactive distillation is a nonlinear process, some assumptions and approximations are made necessary in *RGA* application. One possible approach would be the linearization of nonlinear systems around steady-state operation conditions. The calculations of the matrix elements consider also only the process open loop gains, which are supposed to be constant and the common characteristics of the *RGA* would be thus respected. With these assumptions, the calculation of the elements of a 2x2 matrix, for example, relies only on the knowledge of the four open loop gains.

It should be noted that the nature of nonlinear systems is to have different characteristic parameters at different steady-state conditions and thus, the *RGA* for nonlinear systems may consist of non-constant elements that change in function of the steady-state operation. With the purpose of preserving the nonlinearity and the interaction information, the concept of *RGA* has been extended for non-linear systems, and the Derived-*RGA* is proposed.

7.2.6 *Derived-RGA for nonlinear systems*

The definitions and objectives remain similar, but the calculation of the relative gains change; the model is no longer linearized around a nominal regime. The numerator of each element (the process gain as seen by a loop with all other loops open) remains the same but the denominator (the process gain as seen by a loop with all other loops closed) is now determined by using the nonlinear steady-state simulator, assuming that all controllers are perfect: the output variables are forced to remain at their nominal value by the definition of a steady-state simulation specification that acts on the related manipulated variable. Now, the matrix property regarding the sum of the relative gains in any row or column to equal 1 is no longer valid and each matrix element should be individually calculated.

As in the case of conventional RGA, well controllable systems will then have the Derived-RGA diagonal values close to unity. Different choices of sensor placements can be compared as a function of their Derived-RGA diagonal values.

Another interest of this new approach is that it is possible to anticipate the difficulty to pair the proposed variables. When the simulation to calculate a specific element does not converge, even with larger relaxation or smaller iteration steps, it means that the specifications defined are not achievable and the mass and energy new balances may not be physically possible.

7.3 DYNAMIC SIMULATIONS

Once the steady state behavior and all the sensitivities are analyzed, the dynamic simulation of the system, by considering the control loops, need to be studied to better understand the system behavior. The dynamic performances in relation to control objectives, system stability, response velocities and meeting of specifications can be predicted by simulation in the software Aspen Plus Dynamics®.

To initialize the dynamic simulation, some hydraulic characterizations of the column become necessary. Although parameters such as reboiler design, diameter of the column, height of theoretical stages or liquid holdup are very important to the dynamic analysis, their values are not often easily obtained, and a small deviation can induce errors in the sensitivities, the instabilities and the responses of the process. The definition of these parameters should be obtained by both experiments in a pilot plant and validation by simulation. In the chapter 6 of this manuscript, experimental studies aiming at understanding and acquiring these parameters have been reported.

Once the dynamic simulation is correctly initialized in the software, the inventory control concerning the levels and the column pressure are automatically introduced in order to ensure the column operability and safety and will be always present in practice. Thus, in the following, we will only discuss the introduction of the quality control loops, so as to meet the process objectives.

7.3.1 PID tuning

First, the dynamic model operates under open-loop control conditions, i.e. the controllers are set into manual mode, the manipulated variables have fixed values and no output information is considered. The simulation gives important information on the process responses if no quality control is acting.

Then, the new quality controllers are added to the system. As the objective of this study is to analyze the controllability of the column based on different sensors placements, we prefer to adopt linear controllers that are frequently mentioned in the literature for the control of reactive distillation processes (Huang et al. 2004, Cheng and Yu 2005, Kaymak and Luyben 2006, Lai et al. 2007, Lee et al. 2007, Kumar and Kaishta 2009, Sumana and Venkateswarlu 2010) and commonly used in industrial applications. The control loops introduced in the column are linear PI controllers.

It is worth mentioning that some authors presented better performances of nonlinear controllers in comparison to linear controllers for reactive distillation processes (Gruner et al. 2003, Kawathekar and Riggs 2007, Vora and Daoutidis 2001), but their use would require more complex developments and would change the focus of this study. To develop the interest in different controller configurations a little further, an overview of advanced controllers design is given in Appendix II.

Once the pairing of the manipulated and the controlled variables for each single loop is conducted by the Derived-RGA method, the respective PI controllers must be tuned to run the dynamic simulation.

The information obtained with the open-loop simulation is used to tune the controllers through Internal Model Control (IMC) method. The IMC method is based on the process model, relating the model parameters to the controller settings in a straightforward manner. IMC is commonly used to select PID controller settings based on process dynamic response criteria (Rivera et al. 1986).

7.3.2 Quantitative errors measurement

With the introduction of the controllers, the simulation of the closed-loop system allows the qualitative and the quantitative evaluation of the control configuration design performance. The qualitative analysis is obtained by the observation of the system responses to different perturbations. For the quantitative analysis, the most widely used criteria are the calculations of indices known as Integral Absolute Error (*IAE*) or Integral of the Squared Error (*ISE*). The *IAE* is an integral measure of the error signal $e(t)$, which calculates the absolute difference between the set point and the measurement over the entire closed-loop response. The *ISE* calculates the square value of the difference between the set point and the measurement.

$$IAE = \int_0^{\infty} |e(t)| dt \qquad ISE = \int_0^{\infty} (e(t))^2 dt$$

$$\text{where } e(t) = x_{measured}(t) - x_{setpoint}(t)$$

For PID controller design, some relations are developed that minimize this integral error criterion for simple process models under some type of load (disturbance) or set point change. The tuning of controllers based on the optimization of the *IAE* or *ISE* would also be possible.

The *ISE* is adopted to quantify the errors of the control loops considered. In order to make a realistic comparison among the calculated values for variables of different nature – the temperature and the compositions, for example –, the normalized *ISE* is considered as the original *ISE* divided by the value of the controlled variable at steady state. An additional controllability criterion has thus been defined as the *ISE* normalized value for each controller performance.

$$ISE_N = \frac{\int_0^{\infty} (e(t))^2 dt}{x_{(t=0)}}$$

$$\text{where } e(t) = x_{measured}(t) - x_{setpoint}(t)$$

7.4 CONTROLLABILITY CRITERIA

Finally, we defined different criteria to qualify and to quantify the system controllability, by considering steady state and dynamic behaviors. Measures of sensitivity, balance and interference can now be compared for different control strategies, or for different column configurations.

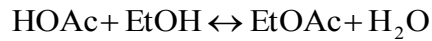
Table 7.1. Recapitulation of the controllability criteria

Measurement	Equation	Definition	Ideal value
Sensitivity:	$\Sigma = \begin{bmatrix} \sigma_1 & 0 \\ 0 & \sigma_2 \end{bmatrix}$	Σ : singular values matrix	
Balance:	$CN = \frac{\sigma_{highest}}{\sigma_{smallest}}$	CN : numerical indication of the balance of sensitivities in a multivariable system	↘
Balance and sensitivity:	$I_{i,j} = \frac{\sigma_{smallest}}{CN_{i,j}}$	I : considers the multivariable gains balance and loop sensitivities	↗
Interferences:	$\Lambda = \begin{bmatrix} \lambda_{11} & \lambda_{12} \\ \lambda_{21} & \lambda_{22} \end{bmatrix}$	RGA : measures the interferences and defines the pairing	~ 1
Dynamic responsiveness:	$ISE_N = \frac{\int_0^{\infty} (e(t))^2 dt}{x_{(t=0)}}$	ISE : Integrated square error of the dynamic behavior	↘

Controllability study of a column configuration

8.1 APPLICATION EXAMPLE

In order to exemplify the calculations presented in Chapter 7, a real column configuration is used for the controllability analysis. At this moment, control structures are compared, but the column design is fixed. The reactive distillation of the heterogeneous catalyzed esterification of ethanol (EtOH) and acetic acid (HOAc) to ethyl acetate (EtOAc) and water (H₂O) is studied. The reaction considered is written as:



With the objective of ensuring separation and reaction performances, the possible manipulated variables are: heat duty, reflux ratio or reflux rate, and the ethanol feed flow rate. The acid feed flow rate acts as a throughput manipulator to determine production rates.

The reactive distillation column has 28 theoretical stages, which are numbered from top to bottom. Stage n°0 accounts for the condenser and stage n°28 represents the reboiler. Two feed streams are present: the acid feed stream is injected at stage n°9, together with the homogenous catalyst, and the alcohol feed stream is injected at stage n°24. The stages above the acid feed, i.e. stages numbered from 1 to 8, are only for separation, without a reaction taking place. The column is schematized in Figure 8.1:

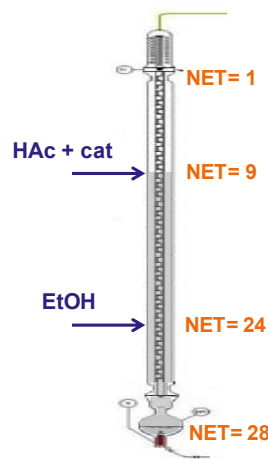


Figure 8.1. Reactive distillation column scheme for the sensitivity analysis

This column design is proposed for an industrial application, in which the meet of three production specifications is to be controlled:

- 100ppm of acetic acid at the distillate
- 1% wt of acetic acid at the bottom
- 1.3%wt of ethanol at the distillate

This section focuses on the response to one specific system perturbation: the increase of the water composition in the ethanol feed flow. This perturbation is coherent with the industrial conditions, because the ethanol used is produced from sugar cane, and the raw material usually presents some variability in composition. Chapter 10 analyzes other possible perturbations that the system may face.

The measurable variables are the temperature and the mass compositions (of each component: acid, alcohol, ester or water) on each stage, which leads to $28 \times 5 = 140$ possible sensor locations.

First, control configurations with two quality control loops are considered. This approach is the most widely discussed in the literature with the purpose of respecting and saturating the two degrees of freedom of a conventional distillation column. Then, the consideration of three quality control loops is compared in order to ensure also the reaction conversion. It is thus necessary to choose two or three of the measurable variables to pair with the manipulated variables so as to define the control loops.

It can be assumed that the composition values range from 0 to 1, and that the temperatures measurement range from 60 to 120°C. Equations presented in section 7.1.1 are considered.

8.2 TEMPERATURE INFERENCE CONTROL

The first approach in studying the column sensitivity considers the temperature inferential control as a reliable alternative to control by composition analyzers. This fact is commonly cited in the literature (Kumar and Kaistha 2008, Lee et al. 2007, Luyben and Yu 2008). Inferential control is based on temperature measurements to infer the product compositions. For the separation of multi-component mixtures, algebraic correlations based on process models and plant data are developed to relate the mole fraction of the heavy component to several different tray temperatures.

The advantages of measuring temperature against measuring composition online are of great importance. Online composition analyzers are typically more expensive both in terms of installation and maintenance cost. Moreover, most analyzers are relatively slow, with time delay between two sample points, and they should be adapted and well calibrated for each application. It is also important to note that, for a good performance of the composition control, the composition analyzers need to be very sensitive and they must rapidly recognize the changes in the variables, which is not always possible at real industrial devices.

Inferential control is well adapted for conventional distillation processes. However, when chemical reaction is present among the system components, a constant temperature can hide important changes in compositions, as in the case of equilibrium limited reactions, for example. The control of temperature should be carefully considered in the case of intensified processes.

To understand the impacts of inferential control in the system, the controllability approach begins with the consideration of only temperature measurements. The sensitivity of the reactive column is analyzed with the values of the 28 temperature sensors responses to perturbations of -2.5% at each of the three manipulated variables: heat duty, reflux ratio, and ethanol feed flow rate. The values of the matrix K coefficients are represented graphically in Figure 8.2. The horizontal axis accounts for the column theoretical stage, the vertical black lines represent the feed locations and the reactive section is colored in gray (stages n°9 to 28).

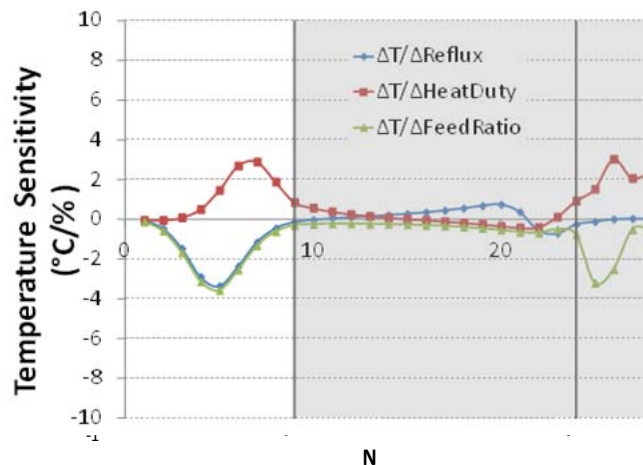


Figure 8.2. Sensitivity matrix considering only temperature sensors

Highly sensitive measurements are observed to be located between the feed locations and the outputs of the column. The top separation section is highly sensitive to changes in all inputs – reflux rate, heat duty and ethanol feed flow rate – and the bottom section is mainly sensitive to heat duty and ethanol feed flow rate. As a consequence of the stable temperatures imposed by the equilibrium-limited reaction, the reactive section between the two feed locations shows a flat sensitivity profile.

The temperature sensitivity profile is in agreement with the observations made during the experiments presented in Chapter 6. Figure 6.15 showed the stronger temperature gradient inside the separation zones and suggested the higher responsiveness of these measurements to changes in the column operational parameters. The difference when comparing the actual configuration with the column presented in Chapter 6 is the absence of a separation section at the bottom of the column. This fact is the

result of the homogenous catalysis adopted here, which forces reaction to occur in all the stages below the catalyst feed. However, even when there is no separation-only section at the bottom of the column, the most sensitive sensors are located below the lower feed position.

The values of K are the input for the Singular Value Decomposition. The SVD method decomposes the matrix into three orthogonal vectors, which are graphically presented in Figure 8.3.

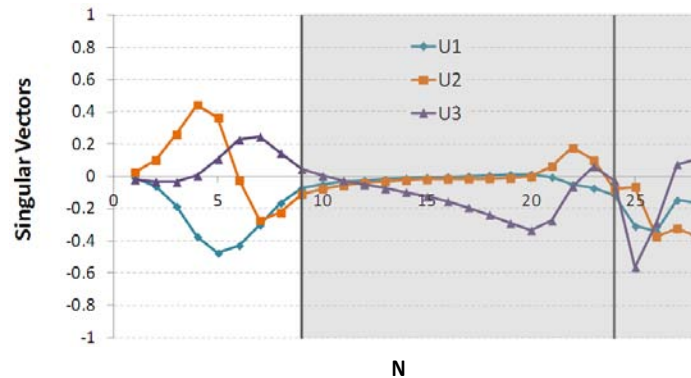


Figure 8.3. Singular vectors matrix considering only temperature sensors

The singular vectors present the sensors with higher sensitivities, but also consider the possible interactions among them. The responsiveness of the measures in sections between feed positions and column outputs are verified and new responsive measurements are identified between the two feed locations. This section of the column is the one where reaction mainly occurs.

The criteria are calculated for the column overall inferential control:

$$S_{only T} = \begin{bmatrix} 10.14 & 0 & 0 \\ 0 & 4.62 & 0 \\ 0 & 0 & 2.91 \end{bmatrix}$$

$$CN_{only T} = \frac{10.14}{2.91} = 3.5$$

Dual-ended control

Now, the analysis is performed with the specific sensors selection for production quality control purposes. First, the consideration of a dual-ended control is studied and a proper configuration for the control system is the choice of the reflux rate and the heat duty as the two manipulated variables.

In Figure 8.3, if two temperature sensors should be chosen, the first two left singular vectors – U_1 and U_2 – are to be considered. The proposition of Kaymak and Luyben (2006), which states that the

locations of the temperature control trays should be chosen such that the two temperature controllers both have direct action (an increase in temperature increases feed in return), which requires negative open-loop process gains for both loops, is preferably respected. The two temperature sensors with higher sensitivity are selected at stages n°5 and n°26. Both sensors are located between a feed location and the end of the column, at the top or at the bottom sections. It endorses the fact that between the two feed positions, the equilibrium-limited reaction is more likely to occur and the temperatures are less representative of column operation changes. A specific matrix K is composed for these temperatures and the SVD calculation results in:

$$S_{T5\ T26} = \begin{bmatrix} 4.02 & 0 \\ 0 & 2.53 \end{bmatrix}$$

$$CN_{T5\ T26} = 1.6$$

$$I_{T5\ T26} = 1.6$$

The value of the specific condition number is lower than the one calculated for the system with all the measured variables, which suggests that the dual temperature control problem should result on better performance than the overall analysis. The CN value close to unity suggests that there are few interactions between the two controlled variables. This is the consequence of their distance in the column. The Bristol array can also be obtained as defined in the precedent chapter:

$$\text{Derived-RGA} = \begin{array}{c} \text{Reflux} \quad \text{Heat Duty} \\ T5 \left| \begin{array}{cc} 1.040 & -0.343 \\ 0.004 & 0.406 \end{array} \right| \\ T26 \end{array}$$

The Derived-RGA proposes the pairing of the reflux ratio to control the temperature at stage n°5 and the heat duty to control the temperature at stage n°26. This result is physically coherent, due to the proximities of the controlled and manipulated variables.

Moreover, the value of $\lambda_{T5, \text{Reflux}} = 1.04$, close to unity, is observed to reflect an ideal pairing of the temperature at stage n°5, at the column top separation section, with the reflux rate and that there is no interaction with the other loop. As a consequence, the temperature at stage n°26 is paired with the heat duty, but the value of $\lambda_{T26, \text{Heat Duty}} = 0.406$ provides the information that there is interaction in the measurement. This observation is also shown by the curves intersection in this zone (Figure 8.3).

The system steady state model is then exported to the dynamic simulation and the two quality controllers are introduced. PI controllers are considered and tuned by the Internal Model Control method (Garcia and Morari, 1982). The dynamic simulation represents an increase in water composition in the ethanol feed from 7 %wt to 8 %wt after 1 hour. The evolution of the controlled and the manipulated variables are presented in Figure 8.4. The PID tuning is shown in the figures, as well as the normalized values of ISE for each control loop after the perturbation.

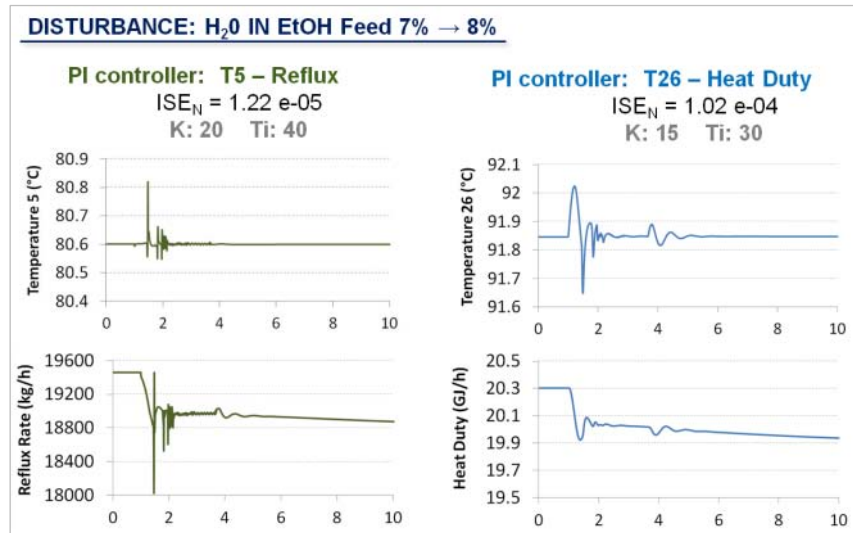


Figure 8.4. Dual-ended inferential control variables after an increase of water in the ethanol feed flow

The chosen temperatures are observed to be controlled by acting on the reflux and the heat duty, and remain constant after approximately 4 to 5 hours. In addition, it is important to verify the meet of product specifications after the perturbation:

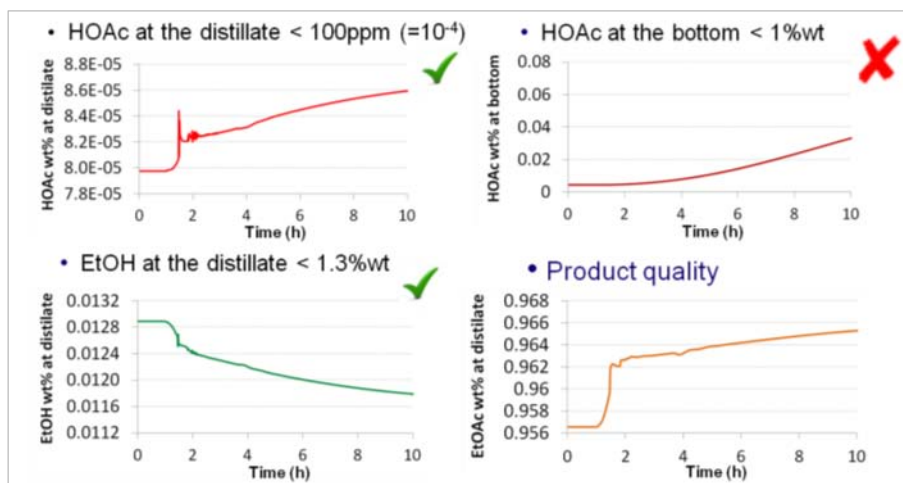




Figure 8.5. Dual-ended inferential control product specifications after an increase of water in the ethanol feed flow

In the graphs which show the evolution of the product specifications, a  or a  are added so as to judge if their values remain acceptable after the perturbation, under the proposed control structure.

The control configuration is verified to perform well with respect to the controlled variables; the temperatures selected return to their nominal values by manipulating the reflux and the heat duty. However, it is not possible to abide for the three different specifications after a perturbation when there are only two control loops for the quality of the system. The acid composition at the bottom of the column strongly increases when the water composition is higher in the ethanol feed flow, and its value is not controlled by the proposed configuration. The specification of 1%wt is no longer respected.

The evaluation of the control configuration regarding product specification is very important in an industrial context. The classical approach, checking mainly the return of the controlled variables to their operating value, ensures the column regulation and operability, but is not sufficient to meet production requirements.

The separation performance of the distillation column can be quantified by analyzing the output values. In order to have a good representation of the reaction performance, it is worth calculating the conversion of the limited reactant. The column configuration presented in Figure 8.1 was conceived so as to provide an acid conversion of 99.9% at normal operating conditions. This value should also be calculated after the perturbation, in the new regime that results from the new manipulated variables conditions. With the dual-ended temperature control configuration presented above, the new acid conversion after the perturbation decreases to 97.8% which would not be acceptable from an industrial point of view.

It can be presumed that, in order to meet the three product specifications and to maintain the reaction conversion, three different control loops are required. In comparison to conventional distillation columns, where two control loops ensure the separation performance, the additional control loop can be used to maintain the reaction conditions.

Because the reactive distillation system considered operates with a two-feed configuration, one additional control loop may be introduced into the column without over-specifying its degrees of freedom. The controllability approach is thus performed for a triple-ended control configuration.

Triple-ended control

A third temperature control loops is introduced and the controlled variable is chosen in function of the calculations presented in Figures 8.2 and 8.3. The three sensors with higher sensitivity are to be chosen one at each vector of U , so as to minimize interactions. A possible choice considers the measured variables already selected such as temperatures at stages n°5 and n°26, with the addition of temperature at stage n°20 to be controlled by the alcohol feed flow rate.

The new sensor is selected within the reactive zone. This fact is different from all the previous assumptions that suggest that sensitivity is significant only above and below both feed streams. The temperature selected is located a few stages above the lower feed position.

The specific values for the matrix S , CN and I are obtained for the proposed control structure:

$$S_{T5 \ T20 \ T26} = \begin{bmatrix} 5.95 & 0 & 0 \\ 0 & 2.55 & 0 \\ 0 & 0 & 0.91 \end{bmatrix}$$

$$CN_{T5 \ T20 \ T26} = 6.5$$

$$I_{T5 \ T20 \ T26} = 0.14$$

		Reflux	Heat Duty	FEtOH
$Derived-RGA$	=	T5	0.874	-
		T20	1.732	0.973
		T26	46.061	0.841
				-

Some of the gains that compose the Derived-RGA were very difficult to be obtained, or even impossible. This is a result of the calculation definition of these values in Aspen Plus[®]. For example, to calculate the $\lambda_{T5, \text{Heat Duty}}$ in a SISO configuration, the other two control loops should be defined as the reflux to be controlled by the temperature at stage n°20 and the ethanol feed flow rate to be controlled by the temperature at stage n°26. These loops do not perform well and the simulation that considers this control configuration does not converge. Thus, when the representative gain of a control loop is not obtained, this loop is not considered as a possibility for pairing since it may result in difficulty in control experimentally.

Results propose to pair the temperature at stage n°5 with the reflux rate, the temperature at stage n°20 with the ethanol feed flow rate and the temperature at stage n°26 with the heat duty. This pairing

configuration is coherent with the one presented for the dual-ended control; the two previous control loops are maintained and the new controlled temperature is paired with the new manipulated variable.

The dynamic behavior of the system under the new control configuration is presented for the same perturbation of water in the feed stream. For an increase of water composition at the ethanol feed, the system takes approximately 10h to stabilize and some oscillations are observed.

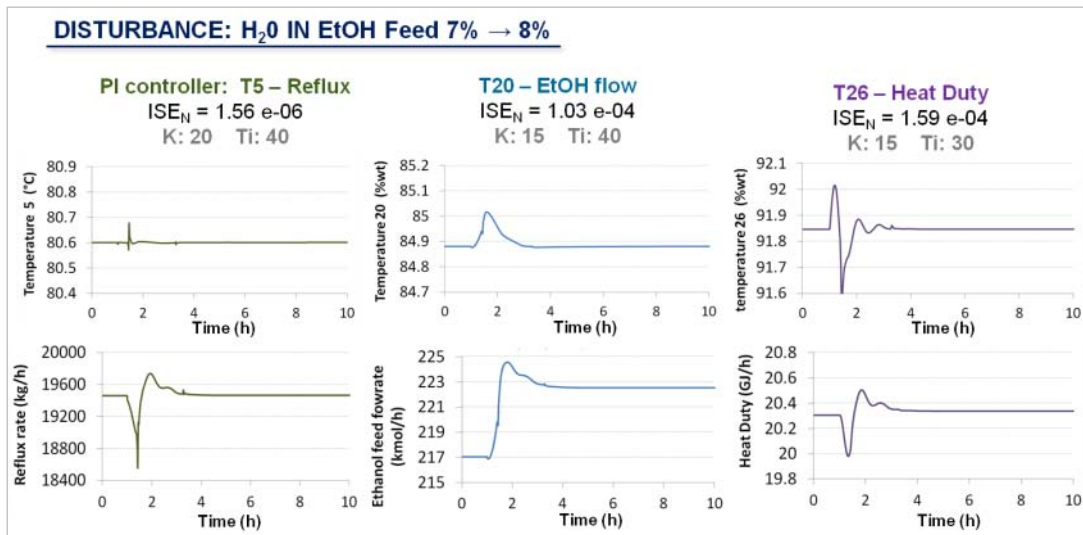


Figure 8.6. Triple-ended inferential control variables after an increase of water in the ethanol feed flow

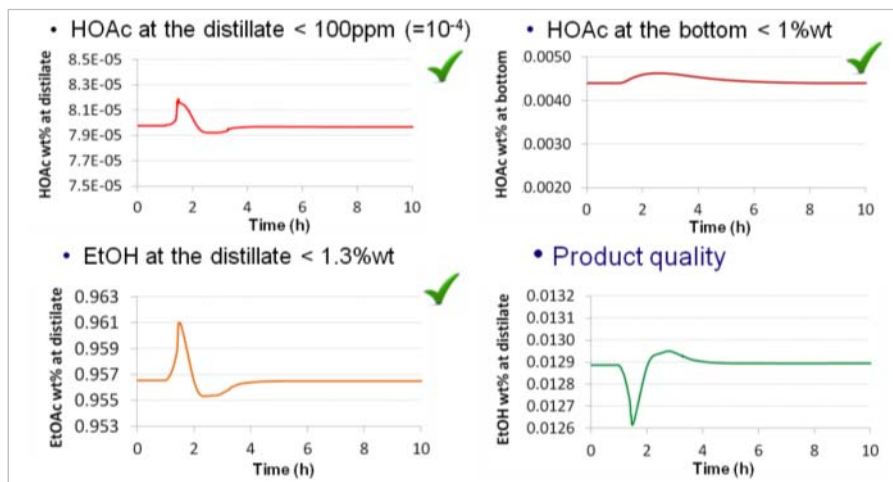


Figure 8.7. Triple-ended inferential control product specifications after an increase of water at the ethanol feed flow

The coexistence of three PI controllers on temperatures through the columns shows that it is possible to abide for all the specifications along with the production quality, showing the better performance of the triple-ended control schemes for the selected reactive distillation column design.

Actually, an additional control loop with a measured variable inside the reactive zone to be controlled by the ethanol feed flow rate helps to maintain the reaction conditions. For the same

perturbation, in the same column configuration with the same steady-state regime, the target operational acid conversion of 99.9% was maintained with the new triple-ended control configuration.

8.3 COMPOSITION CONTROL

If the compositions can be measured online, new control schemes can be considered. So, now, all temperatures and components compositions are assumed to be possibly measured.

The values obtained for matrix K , when three manipulated variable are changed by a perturbation of -2.5% are calculated with respect to the composition of each of the four components, in the 28 theoretical stages of the column. They can be analyzed with graphics for each measured variable in Figure 8.8. The horizontal axis accounts for the column theoretical stage, the vertical lines represent the feed locations and the gray section is where reaction occurs.

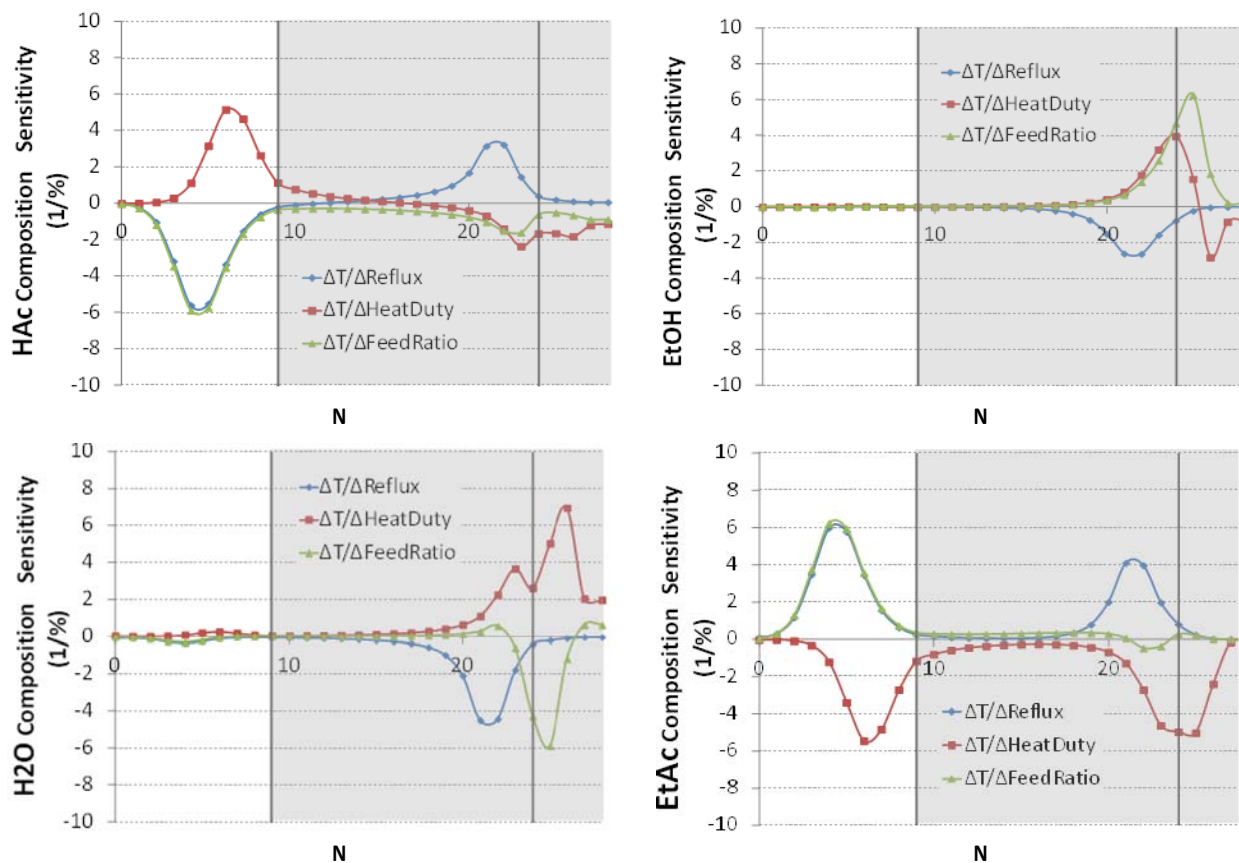


Figure 8.8. Sensitivity matrix considering each component compositions sensors

Stages corresponding to pure separation section shows strong sensitivity of acid and ester compositions. However, in this section the reiss strong interference between reflux and ethanol feed effects. At the bottom of the column, a stronger sensitivity of heat duty is verified. The stages located around the lower feed position show a second region of high sensitivity. The sensors locations that show

stronger sensitivity are the compositions of acid and ester in the separation section, and the compositions of alcohol, ester and water near the lower feed position.

The singular value decomposition of matrix K is calculated and the results are the matrices $U_{140 \times 140}$, $S_{3 \times 3}$ and $V_{3 \times 3}$. The three first columns of the left singular values matrix U are considered and their scalar values are plotted in Figure 8.9. So as to compare the sensitivity between all the possible measured variables, the horizontal axis accounts for temperatures and composition of each component at each stage location, numbered from top to bottom. The maximum absolute values of the U vectors indicate the locations of the main components.

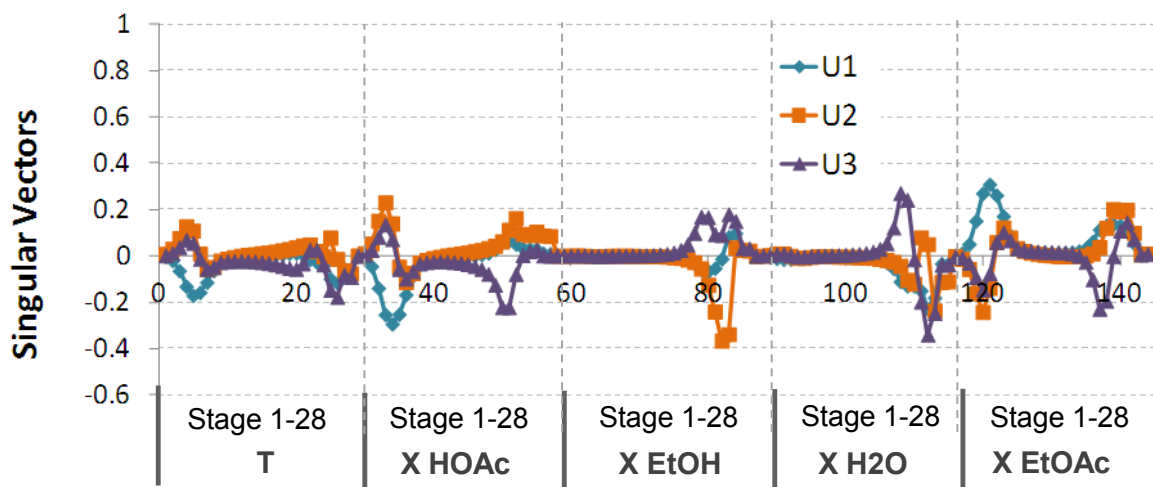


Figure 8.9. Singular vectors matrix considering all column sensors

The calculated matrix S , with the system singular values and the CN are calculated:

$$S_{all\ measures} = \begin{bmatrix} 27.85 & 0 & 0 \\ 0 & 16.55 & 0 \\ 0 & 0 & 12.48 \end{bmatrix}$$

$$CN_{all\ measures} = \frac{27.85}{12.48} = 2.2$$

The criteria values suggest that the triple-loop composition control may show better performance than the triple-loop temperature control, due to its smaller value of overall CN .

The SVD results considering the composition measurements propose a new control configuration. If we chose to place three control loops, the three vectors U_1 , U_2 and U_3 should be observed. The measured variables considered are the acid composition at stage n°5, the ethanol composition at stage n°23 and the water composition at stage n°25. The specific controllability criteria are calculated:

$$S_{HOAc5 EtOH23 H2O25} = \begin{bmatrix} 10.86 & 0 & 0 \\ 0 & 4.47 & 0 \\ 0 & 0 & 3.85 \end{bmatrix}$$

$$CN_{HOAc5 EtOH23 H2O25} = 2.8$$

$$I_{HOAc5 EtOH23 H2O25} = 1.36$$

$$\text{Derived-RGA} = \begin{array}{c|ccc} & \text{Reflux} & \text{Heat Duty} & \text{FEtOH} \\ \hline \text{HOAc5} & 0.855 & -0.138 & -0.137 \\ \text{EtOH23} & 0.499 & 1.103 & 1.114 \\ \text{H2O25} & - & 0.652 & - \end{array}$$

Through Derived-RGA results, it can be observed that both heat duty and ethanol feed stream could be satisfactory paired with the ethanol composition at stage n°23, but the only loop gain calculated to control the water composition at stage n°25 was the one with heat duty manipulation. Consequently, the best variables pairing is obtained when the reflux rate controls the composition of acid at stage n°5, the heat duty controls the composition of water at stage n°25 and the ethanol feed stream controls the ethanol composition at theoretical stage n°23. Once again, this result is coherent with the physical proximity of these variables in the column.

Once the three PI controllers are tuned as described previously (IMC rules), it is possible to run a dynamic simulation of the behavior of the system. In Figures 8.10 and 8.11 the results obtained after a perturbation in the water content in the ethanol feed stream are drawn:

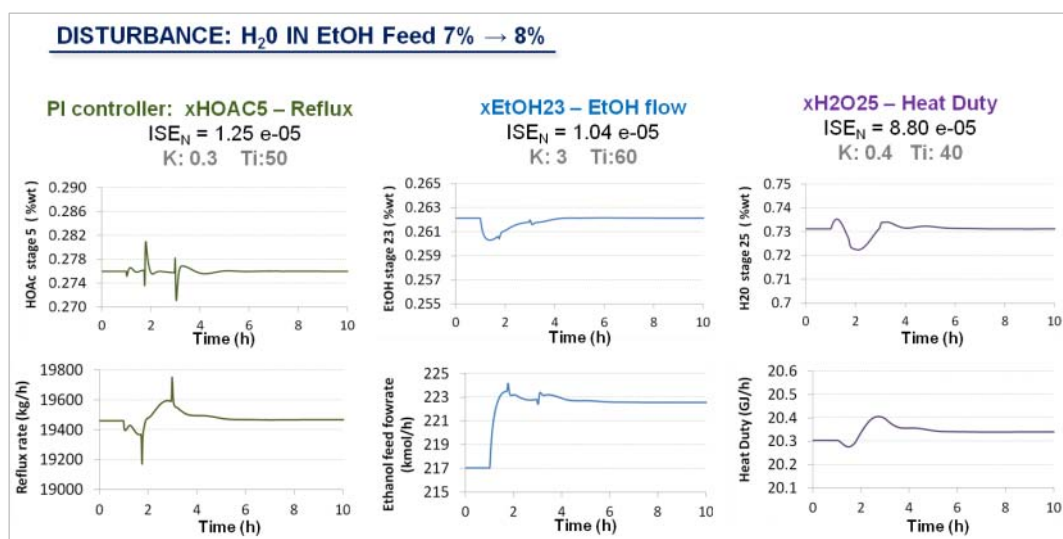


Figure 8.10. Composition control variables after an increase of water in the ethanol feed flow

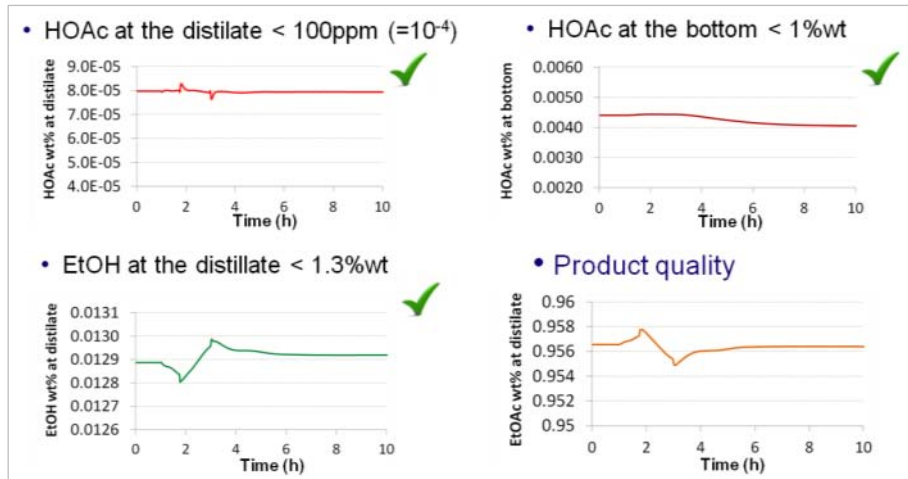


Figure 8.11. Composition control product specifications after an increase of water in the ethanol feed flow

The selected compositions are observed to be well controlled by the manipulation of the reflux, the ethanol feed flow and the heat duty, and the product specifications are respected. The acid conversion of 99.9% is maintained after perturbation.

The triple-ended composition control can be compared with the triple-ended temperature control. The specific values of CN and I suggest that the composition control performs better than the temperature control. Values of composition-loops ISE were also smaller than temperature loops, except for the control of temperature at stage n°5, at the separation section. This result supports the idea that inferential control is valuable to be used in separation sections and that compositions could be better to be measured where reaction occurs in the distillation column.

8.3.1 Simultaneous control of temperature and composition

The better performance of the composition control compared to the temperature control has been shown. However, online composition analyzers are more expensive and require detailed implementation. With the objective of finding a compromise between these controller types, a structure that mixes both temperature and composition sensors can be analyzed.

The sensitivity of temperature in the separation section is analyzed together with the compositions measured near the bottom of the column. The controlled variables are selected as the temperature at stage n°5, the ethanol composition at stage n°23 and the water composition at stage n°25.

The specific controllability criteria are calculated:

$$S_{T5 \text{ EtOH}23 \text{ H}2\text{O}25} = \begin{bmatrix} 8.86 & 0 & 0 \\ 0 & 4.41 & 0 \\ 0 & 0 & 3.85 \end{bmatrix}$$

$$CN_{T5 \text{ EtOH}23 \text{ H}2\text{O}25} = 2.9$$

$$I_{T5 \text{ EtOH}23 \text{ H}2\text{O}25} = 1.09$$

$$\text{Derived-RGA} = \begin{array}{c|ccc} & \text{Reflux} & \text{Heat Duty} & \text{FEtOH} \\ \hline T5 & 0.874 & -0.319 & - \\ \text{EtOH}23 & 0.888 & 1.055 & 1.139 \\ \text{H}2\text{O}25 & 0.034 & 0.983 & - \end{array}$$

The values of specific CN and I are better than the specific values calculated for the triple-ended temperature control and are closer, but little worse, than the values calculated for the triple-ended composition control. It can be concluded that this control performance should be similar to the one when only composition controllers are considered and that a composition control loop at the column separation section can be reliably replaced with a temperature inferential control. This fact is confirmed by the dynamic simulation. The results are plotted in Figures 8.12 and 8.13.

The acid conversion after the perturbation remains at 99.9%.

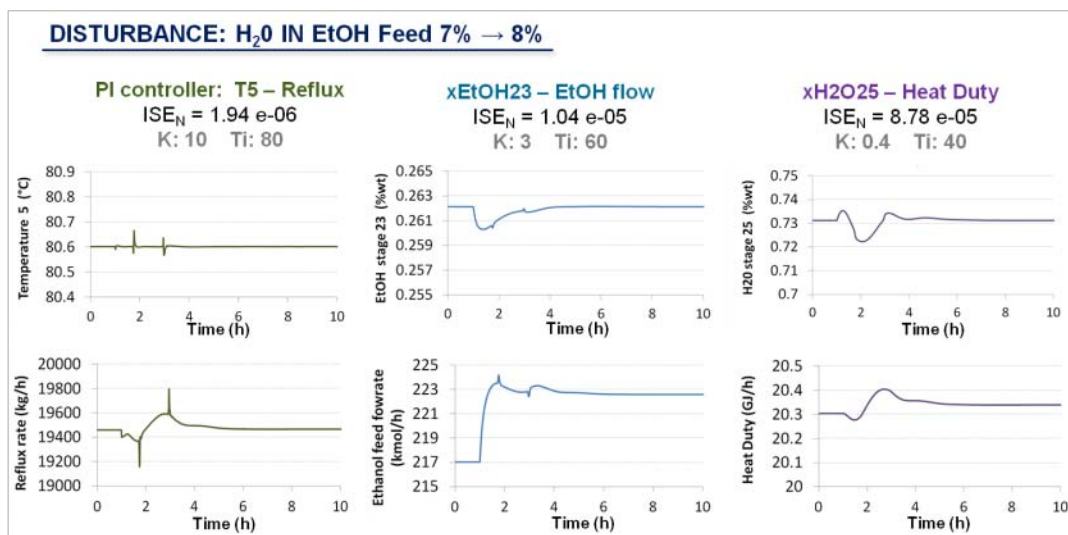


Figure 8.12 Temperature and composition control variables after an increase of water in the ethanol feed flow

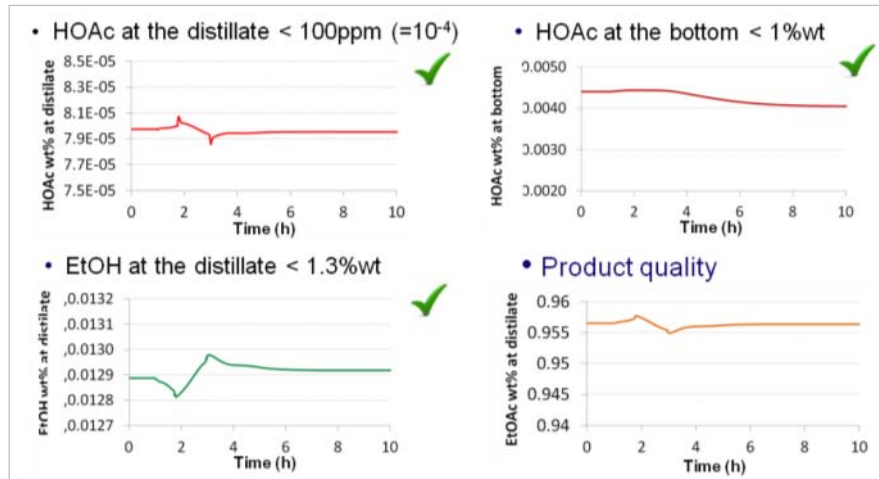


Figure 8.13. Temperature and composition control product specifications after an increase of water in the ethanol feed flow

8.3.2 Controlling the product specifications directly

The key control task of the industrial reactive column is the meet of the output specifications in order to ensure production quality. Special attention should be necessarily given to the composition of acetic acid and ethanol in the distillate, and to the composition of acetic acid in the residue flow. Thus, one may question why not to directly control these compositions. The response is given by the controllability analysis of this configuration.

First, when observing the sensitivity values of the column (Figure 8.8), the output compositions do not show important sensitivities. Second, the controllability criteria are calculated for this specific loops choice:

$$S_{HOAc1\ EtOH1\ H2O28} = \begin{bmatrix} 1.44 & 0 & 0 \\ 0 & 0.32 & 0 \\ 0 & 0 & 0.01 \end{bmatrix}$$

$$CN_{HOAc1\ EtOH1\ H2O28} = 101.5$$

$$I_{HOAc1\ EtOH1\ H2O28} = 0.00014$$

$$\text{Derived-RGA} = \begin{array}{c|ccc} & \text{Reflux} & \text{Heat Duty} & \text{FEtOH} \\ \hline HOAc1 & 0.552 & 1.108 & - \\ EtOH1 & - & - & - \\ HOAc28 & 2.442 & 0.164 & - \end{array}$$

The CN value is very high and the I value is extremely low, previewing a weak performance of the control configuration. The dynamic simulation after a perturbation of water in the feed stream presents a system with low ISE values, but with small-amplitude oscillations and offsets, and that takes approximately 20h to stabilize (Figure 8.14).

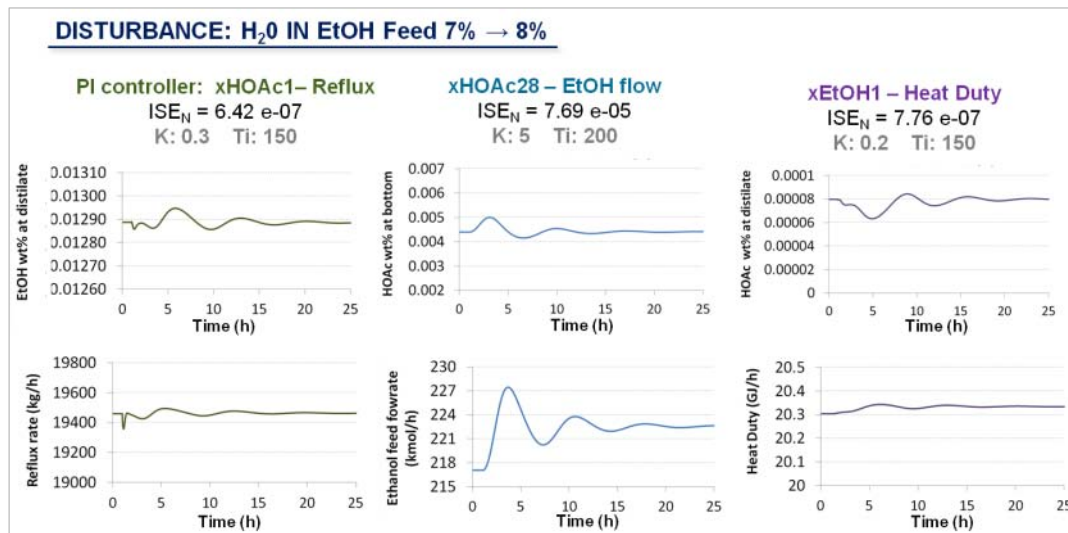


Figure 8.14. Specification control variables after an increase of water in the ethanol feed flow

This behavior can be understood because the controlled variables have strong interferences between them. For example, both alcohol and acid are measured in the distillate stream and these values are correlated. Moreover, the ethanol feed flow rate and the heat duty are manipulated variables located near the bottom of the column and one of them should control a composition in the distillate, because there is only one controlled variable at the bottom. The physical distance between the manipulated and the controlled variable may strongly affect the loop dynamics.

In a SISO configuration (i.e. single input – single output) the structure that directly considers the product compositions as controlled variables does not provide successful column operability. One additional possibility would be the use of a Model Predictive controller that does not need to assign SISO loops. However, the development of high-complexity controller is out of the scope of this work, because they would bring some further difficulties due to its tricky tuning and robustness issues. So, further studies will be undertaken considering the controlled variables proposed by the sensitivity approach, located at the stages inside the column.

The acid conversion after the perturbation remains at 99.9%.

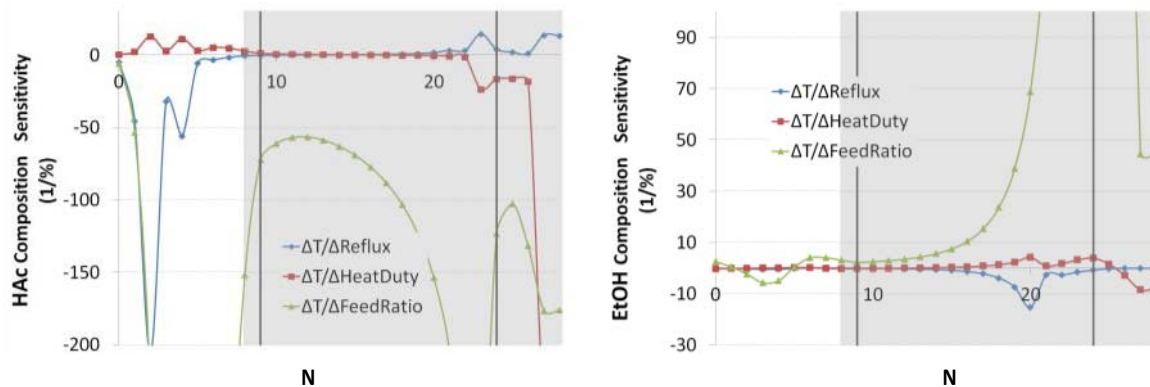
8.3.3 Impact of the composition analyzers sensitivity

The measurement of the composition analyzers was assumed so far to range from 0 to 1. However, it is verified that, throughout the column, there are small values of composition and so it may be of interest to get more precise measurement. For example, the acid concentration at the distillate has the magnitude of some ppms and there is a stringent process constraint to this quantity to be below 100ppm in order to avoid corrosion and allow the further purification of the final product. The range of the acid composition analyzer at this stage may be smaller with the purpose of providing more precise representative values.

With this objective, three different types of analyzers are considered for the column measurements. They differ as to the limits (saturation) for the composition values:

- C_1 : 0 to 5000ppm
- C_2 : 0 to 0.1
- C_3 : 0 to 1.0

The choice of which analyzer to be used for each measured variable is defined by its value at steady-state conditions. If the target operating value is below 5000ppm, analyzer C_1 is used. If the target operating value is between 5000ppm and 0.1, analyzer C_2 is used. Analyzer C_3 is considered for other measures. The same discretization equations presented in section 7.1.1 are considered and the new sensitivity matrix is provided. Each composition can be analyzed through the column, in function of its theoretical stages in Figure 8.15. The temperatures sensitivities do not change.



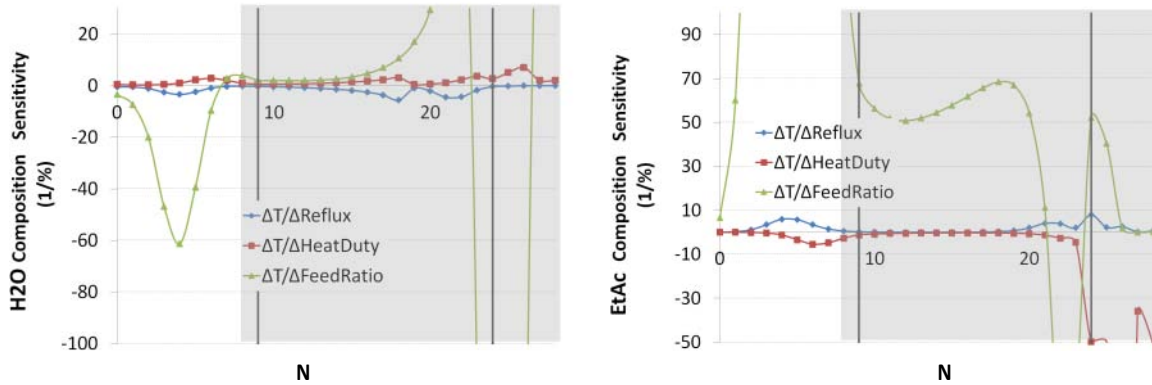


Figure 8.15. Sensitivity matrix considering each component compositions sensors with 3 types of analyzers

Now, more sensitivity is observed on the output compositions: the distillate and the bottom compositions are more sensitive and a stronger influence of the ethanol feed flow rate is verified. These results exemplify the fact that the definition of the measurement range of each composition analyzer strongly influences the sensors locations.

The sensitivity matrix K with consideration of the different ranges for composition analyzers is the base for SVD calculations. The left singular vectors are presented in Figure 8.16.

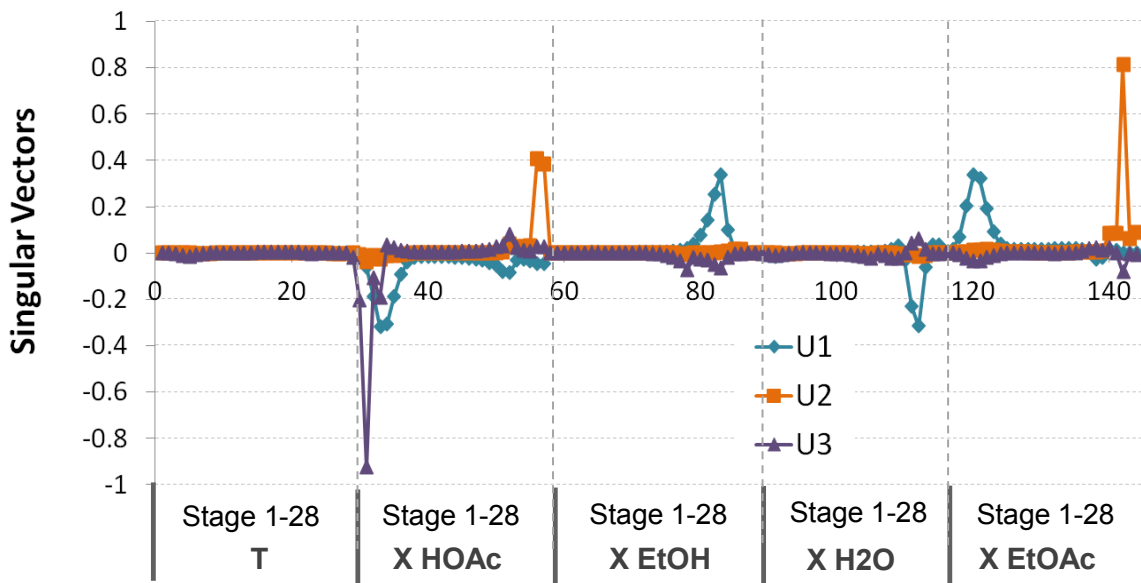


Figure 8.16. Singular vectors matrix considering all column sensors with 3 types of analyzers

Now, the sensors locations that show stronger sensitivity are the compositions of acid and ester in the separation section, and the compositions of the four components at the bottom of the column. The temperatures and the section between the two feed stages show significant smaller sensitivity.

The matrix S , with the system singular values, and the CN are calculated:

$$S_{3 \text{ analyzers}} = \begin{bmatrix} 3714.10 & 0 & 0 \\ 0 & 593.10 & 0 \\ 0 & 0 & 218.80 \end{bmatrix}$$

$$CN_{3 \text{ analyzers}} = \frac{3714.10}{218.80} = 17.1$$

The analysis of the SVD calculations affirms the different results as a function of the sensors definition. When compared with the criteria calculated for the control with one single type of analyzers, the control can be conclude to be more difficult for the case in which analyzers are more sensitive. This observation is coherent due to the fact that higher sensitivity requests higher control efficiency.

For the sake of comparison, the control configuration proposed by the coexistence of three different types of composition analyzers is verified. When analyzers of different precisions can be used, different results may be obtained for the variables sensitivities.

From the observing the left singular vectors of Figure 8.16, if one sensitive sensor is chosen at each vector in order to minimize interactions, the proposed measured variables are the acetic acid composition at stage n°2, the ethanol composition at stage n°23 and the ethyl acetate composition at stage n°26.

Although the sensitivity matrices show higher sensitivity of the output compositions when three types of analyzers are present, the results of the SVD calculations identify as reliable sensors the compositions in the separation section and near the lower feed position. This result is qualitatively similar to the one obtained through the analysis of one single type of composition analyzer.

The quantitative values calculated for the proposed configuration are presented:

$$S_{HOAc2 \ EtOH23 \ EtOAc26} = \begin{bmatrix} 574.52 & 0 & 0 \\ 0 & 481.32 & 0 \\ 0 & 0 & 185.90 \end{bmatrix}$$

$$CN_{HOAc2 \ EtOH23 \ EtOAc26} = 3.1$$

$$I_{HOAc2 \ EtOH23 \ EtOAc26} = 60.15$$

	Reflux	Heat Duty	FEtOH
$Derived-RGA = HOAc2$	0.589	0.928	–
$EtOH23$	–	0.545	1.263
$EtOAc26$	–	0.967	–

The values of the condition number and the Intersivity index show that the proposed composition control structure may have a weaker performance when compared to the previous composition control loops proposed. More Derived-RGA gains were difficult to calculate, and the possible configuration is to pair the composition of acetic acid at stage n°2 with the reflux, the ethanol at stage n°23 with the ethanol feed flow rate and the ethyl acetate at stage n°26 with the heat duty. The controllers are introduced at the column simulation, tuned, and the dynamic behavior after an increase of the water composition in the ethanol feed stream is simulated.

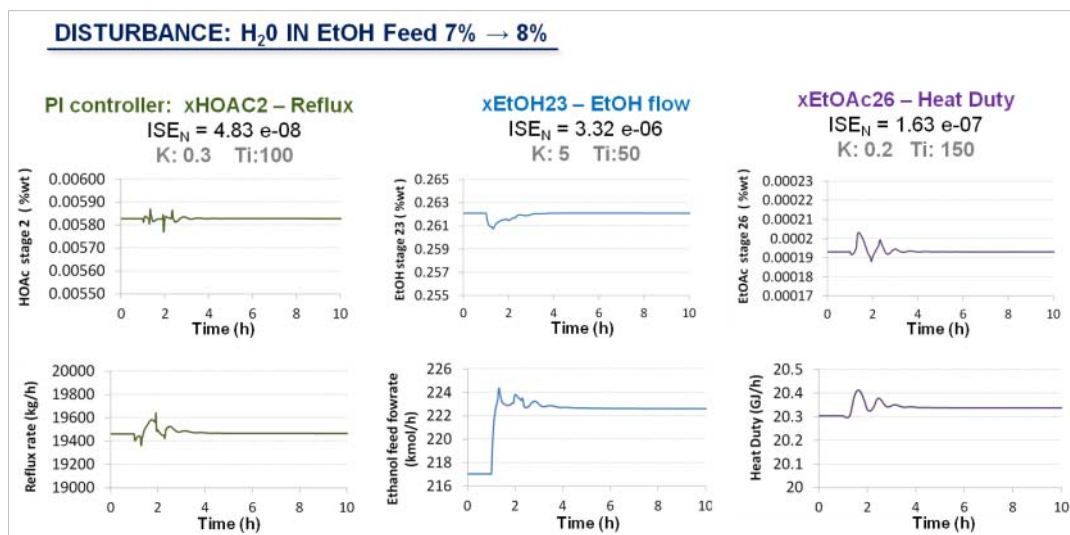


Figure 8.17. Three-analyzer composition control variables after an increase of water in the ethanol feed flow

The control variables show oscillations, but compositions are well controlled, they return to their nominal value far before 5h. The ethanol feed control loop shows the slower dynamics. Product specifications are met and the acid conversion after the perturbation remains at 99.9%.

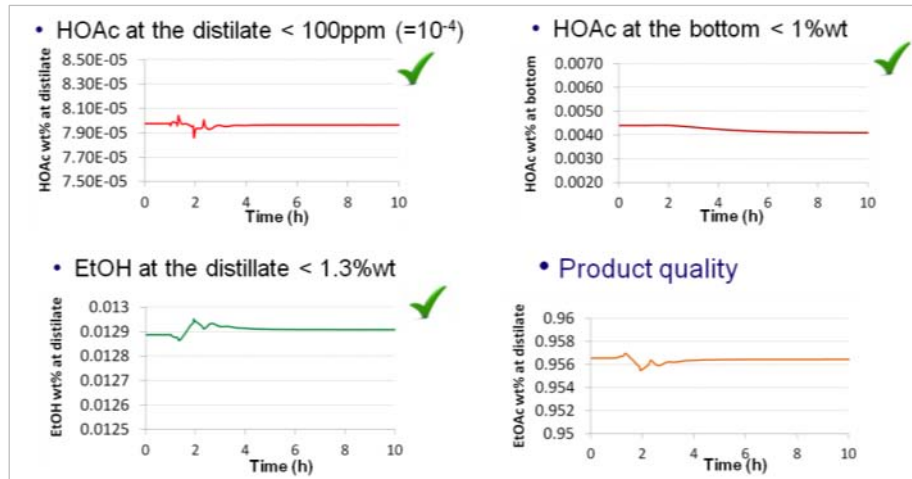


Figure 8.18. Three-analyzer composition control product specifications after an increase of water in the ethanol feed flow

Finally, the system dynamic responses are very similar with the presence of one or three types of composition analyzers. It seems that the dynamic behavior shows a little more oscillation in the latter case, but the response velocities have the same magnitude. It can be concluded that both approaches result in a controllable proposition of sensors placement and the investment need to implement three types of analyzers with different sensitivities is not really necessary.

8.4 CONCLUSIONS

The indices-based methodology proposed considers different qualitative and quantitative criteria to address the controllability of distillation processes. The calculations are adapted for the reactive columns and the production of ethyl acetate by esterification of acetic acid and ethanol is studied.

It was observed that, to comply with the three product specifications, three different control loops are required. In comparison to conventional distillation columns, where two control loops ensure the separation performance, one additional control loop that controls a measurement inside the reactive zone and manipulates the ethanol feed flow rate can be used to maintain the reaction conditions, due to the additional degree of freedom given by the feed ratio in a double-feed column configuration.

Actually, in the control structure proposed by Tang et al. (2005b) for their plantwide scheme (c.f. chapter 2), two product specifications are met in the first column with two control loops, and a third control loop was introduced in the stripper column. In the approach proposed in this chapter, three loops could be introduced directly in the RD column to meet three specifications, achieving the same performance of the plant-wide scheme.

The study considers the overall analysis, with all the possible measured variables, and the specific approach, with only the selected controllers. The overall analysis shows that composition control performs better than temperature control. The calculated specific criteria show that temperature sensors may be used to a reliable and less expensive inferential control in the separation stages.

It can be concluded that the criteria defined show reliable measurement of the system controllability and the results were acknowledged by the simulated dynamic responses to an increase of the water composition in the ethanol feed stream, which represents an industrial perturbation of real concern.

It is worth mentioning that the results from the dynamic behavior of the system are very dependent on the tuning of the PI controllers. Although the *IMC* method proposed values for the gain and the period of each controller, an improvement of the tuning values was necessary so as to obtain better results. Due to the fact that this improvement is implemented based solely on observation – it is neither a schematic nor an automatic approach yet – special attention should be paid.

In the next chapters different reactive column configurations are simulated, with different number of theoretical stages for reaction or for separation and consequently different feed positions. Through steady-state and dynamic simulations, the controllability criteria presented are useful to detect some heuristic rules and to suggest column characteristics that provide better controllability.

FIFTH PART

V. CONTROLLABILITY ANALYSIS AS FROM THE DESIGN STEP

9.	Design methodology for the ethyl acetate system	155
10.	Controllability analysis of the ethyl acetate system	171
11.	Experimental understanding of the controllability approach	203

Once the methodology for the identification of controllability criteria is stated, the objective of Part V is to conceive a reactive distillation column for the production of ethyl acetate, considering controllability aspects as from the conceptual design step. Several steps are performed, sequentially increasing the process complexity. Chapter 9 presents the thermodynamic and kinetics data of the esterification system, and uses the methodology developed at the LGC for the pre design of reactive columns. The steps of feasibility analysis, synthesis and conceptual simulation are conducted and two feasible column configurations are proposed which attain desirable reaction and separation performances. Chapter 10 conducts the sensitivity analysis and calculates the controllability criteria of each column designed. One configuration is selected and improved in order to attain the stringent industrial specifications, which are only possible due to the addition of a decanter in the top output stream, resulting in a reflux composed only by the distillate organic phase. Then, some new configurations are analyzed, by changing some structural parameters of the industrial configuration. The comparison of the controllability criteria, the control structures and the closed-loop dynamic behaviors allows the identification of some heuristic key rules and column characteristics which provide better operability. In chapter 11, an experimental study was performed, in which the understanding of the process degrees of freedom was discussed so as to adapt the controllability approach and well operate the pilot plant.

Dans la Partie V, la méthodologie de conception qui considère des aspects de contrôlabilité est appliquée à la production de l'acétate d'éthyle, avec prise en compte de spécifications réelles de production et des potentielles perturbations du système.

La méthodologie présentée au Chapitre 4 est appliquée dans le Chapitre 9, pour proposer des configurations possibles de la colonne en régime permanent. L'étude thermodynamique utilise les modèles NRTL pour représenter l'équilibre entre phases et Hayden-O'Connell pour la dimérisation de l'acide en phase vapeur. Les modèles prédisent trois azéotropes binaires avec des points minimaux d'ébullition et un azéotrope ternaire avec points minimaux d'ébullition, correspondant à la température minimale dans l'espace des compositions. L'estérification est donnée comme une réaction réversible et les deux sens de la réaction sont contrôlés par une loi cinétique de type premier ordre d'Arrhenius.

L'étape d'analyse de faisabilité calcule et étudie les courbes de résidu réactives et les courbes extractives réactives : il est possible d'obtenir un résidu avec une forte concentration d'eau mais dû à la présence des azéotropes, il n'est pas possible d'avoir un distillat pur en acétate d'éthyle. La composition accessible du distillat est un mélange ternaire, riche en acétate d'éthyle avec de l'eau et de l'éthanol, proche de la composition de l'azéotrope ternaire.

L'étape de synthèse identifie les paramètres opératoires et propose des structures de colonne. L'étape de conception simule ces structures de colonne, en considérant les phénomènes thermiques. Deux configurations possibles de colonne sont proposées : une colonne avec 16 étages théoriques, l'alimentation inférieure étant placée 5 étages au-dessus du pied de colonne et un taux de reflux égal à 1.0, appelée *Design16*, et une colonne avec 21 étages théoriques, l'alimentation inférieure étant placée 7 étages au-dessus du pied de colonne et un taux de reflux égal à 1.22, appelée *Design21*.

L'objectif du travail est alors de choisir une configuration en fonction de sa contrôlabilité. Le Chapitre 10 regarde les sensibilités des colonnes, calcule les critères de contrôlabilité et sélectionne la colonne *Design16* comme la plus facilement contrôlable. Dû aux contraintes industrielles pour la configuration de la colonne, qui n'ont pas pu être considérées aux étapes antérieures, la colonne *Design16* est adaptée, avec l'ajout d'un décanteur dans le courant du distillat et de quelques étages théoriques pour atteindre les spécifications de production plus strictes, avec maintien de l'alimentation placée 5 étages au-dessus du pied de colonne. La nouvelle structure possède 28 étages théoriques et est appelée *Design28*.

Basée sur la colonne industrielle proposée, une étude est menée sur différentes configurations en changeant le nombre d'étages théoriques dans chaque section de colonne et, par voie de conséquence, la position relative des alimentations. L'analyse de contrôlabilité est réalisée en regardant les comportements stationnaires et dynamiques des procédés, et quelques règles heuristiques sont identifiées pour la conception de colonnes les plus contrôlables.

Les résultats montrent que, même si le nombre d'étages théoriques et les positions des alimentations changent, la position relative des variables contrôlées sélectionnées reste similaire pour les différentes configurations: un capteur est sélectionné au milieu de la section de séparation dans le haut de la colonne, un deuxième capteur est placé quelques étages au-dessus de l'alimentation inférieure et un troisième capteur est sélectionné dans la section inférieure de la colonne, entre l'alimentation inférieure et la sortie en pied. Ce résultat peut être considéré comme une règle heuristique pour le placement des variables contrôlées dans une colonne à deux alimentations.

Si une sensibilité plus grande est recherchée dans une section spécifique, des étages théoriques doivent être ajoutés, mais les performances de contrôle ne sont pas affectées. L'addition d'étages entre les deux alimentations, cependant, améliore la contrôlabilité et l'opérabilité de la colonne parce que le régime opérationnel nominal a plus de flexibilité pour le changement des compositions en sortie, tout en respectant le maintien des spécifications de production. La colonne finalement sélectionnée comme la plus contrôlable est appelée *Design30c*, et correspond à *Design28* avec deux étages additionnels au milieu de la colonne. L'étude du comportement dynamique du procédé s'est avérée importante pour prévoir les conditions du système et concevoir une colonne adaptée aux perturbations potentielles. Les critères de contrôlabilité sont des mesures fiables de l'opérabilité de la colonne réactive.

Enfin, une deuxième étude expérimentale est conduite pour illustrer les calculs de contrôlabilité. Le Chapitre 11 examine l'importance de la bonne sélection des variables manipulées, en insistant sur la compréhension des degrés de liberté du pilote. La colonne présentée dans le Chapitre 3 est utilisée. L'approche expérimentale regarde la sensibilité et la stabilité du procédé. La méthode d'analyse de contrôlabilité est menée et quelques remarques importantes sont qualitativement discutées. Le régime opératoire est stabilisé grâce à l'addition des boucles de contrôle proposées par la méthode. L'importance d'avoir les variables manipulées bien découplées est surlignée et la méthodologie de contrôlabilité se montre fiable quand elle repose sur le calcul en fonction des bons degrés de liberté du procédé.

Na Parte V, a metodologia de projeto que considera os aspectos de controlabilidade é aplicada à produção de acetato de etila, levando em conta especificações reais de produção e potenciais perturbações do processo industrial.

A metodologia apresentada no Capítulo 4 é aplicada no Capítulo 9, para propor configurações viáveis de colunas em estado estacionário. O estudo termodinâmico usa modelos NRTL para representar o equilíbrio entre fases e Hayden-O'Connell para a dimerização do ácido acético em fase vapor. Os modelos preveem 3 azeótropos binários com pontos mínimos de ebulição e 1 azeótropo ternário também com ponto mínimo de ebulição, correspondendo à temperatura mínima do espaço de composições. A esterificação é definida como uma reação reversível e os dois sentidos de reação são controlados por uma lei cinética de tipo Arrhenius de primeira ordem.

A etapa de análise de viabilidade calcula e estuda as curvas de resíduo reativas e as curvas extrativas reativas: é possível obter um resíduo com forte concentração de água mas, como consequência da presença dos azeótropos, não é possível obter um destilado puro em acetato de etila. A composição acessível no destilado é uma mistura ternária, rica em acetato de etila com água e etanol, próxima da concentração do azeótropo ternário.

A etapa de síntese identifica os parâmetros operatórios e propõe estruturas de coluna. A etapa de concepção simula essas estruturas de coluna, considerando os fenômenos térmicos. Duas configurações possíveis de coluna são propostas: uma coluna com 16 estágios teóricos, alimentação inferior localizada 5 estágios acima do fundo da coluna e taxa de refluxo igual a 1.0, chamada *Design16*, e uma coluna com 21 estágios teóricos, alimentação inferior localizada 7 estágios acima do fundo da coluna e taxa de refluxo igual a 1.22, chamada *Design21*.

O objetivo do trabalho é então escolher uma configuração em função de sua controlabilidade. O Capítulo 10 observa as sensibilidades das colunas, calcula os critérios de controlabilidade e seleciona a coluna *Design16* como a que é mais fácil de controlar. Por causa das restrições industriais para a configuração de coluna, que não puderam ser consideradas nas etapas anteriores, a coluna *Design16* é adaptada, com a adição de um decantador na corrente de destilado e de alguns estágios teóricos para atingir as especificações de produção mais severas, com a manutenção da alimentação inferior 5 estágios acima do fundo da coluna. A nova estrutura possui 28 estágios teóricos e é chamada *Design28*.

Baseado na coluna industrial proposta, um estudo foi conduzido sobre diferentes configurações, mudando a quantidade de estágios teóricos em cada seção de coluna e, conseqüentemente, mudando a posição relativa das alimentações. A análise de controlabilidade foi realizada observando os comportamentos estacionários e dinâmicos do processo, e algumas regras heurísticas foram identificadas para o projeto de colunas mais controláveis.

Os resultados mostram que, mesmo se a quantidade de estágios teóricos e a posição das alimentações mudam, a posição relativa das variáveis controladas selecionadas continua similar para diferentes configurações: um sensor é selecionado no meio da seção de separação no topo da coluna, um segundo sensor é posicionado alguns estágios acima da alimentação inferior, e um terceiro sensor é selecionado na seção inferior da coluna, entre a alimentação inferior e a corrente de saída de fundo. Esse resultado pode ser interpretado como uma regra heurística para o posicionamento das variáveis controladas em uma coluna com duas alimentações.

Se uma sensibilidade maior é esperada em uma seção específica, mais estágios teóricos devem ser adicionados, mas o desempenho do controle não é afetado significativamente. A adição de estágios entre as duas alimentações, entretanto, melhora a controlabilidade e a operabilidade da coluna porque o regime operatório nominal ganha maior flexibilidade para as mudanças de composição nos produtos, respeitando assim a manutenção das especificações de produção. A coluna finalmente selecionada como a mais controlável é chamada *Design30c*, e corresponde à coluna *Design28* com dois estágios adicionais no meio da coluna. O estudo do comportamento dinâmico do processo se mostrou importante para prever as condições do sistema e conceber uma coluna adaptada a responder às potenciais perturbações. Os critérios de controlabilidade são medidas confiáveis da operabilidade da coluna reativa.

Enfim, um segundo estudo experimental foi conduzido para exemplificar os cálculos de controlabilidade. O Capítulo 11 examina a importância da seleção adequada de variáveis manipuladas, insistindo na compreensão dos graus de liberdade do piloto. A coluna apresentada no Capítulo 3 é usada. A abordagem experimental observa a sensibilidade e a estabilidade do processo. O método de análise de controlabilidade é aplicado e algumas observações importantes são qualitativamente discutidas. O regime operatório é estabilizado graças à inserção de malhas de controle propostas pelo método. A importância de que as variáveis manipuladas sejam bem desacopladas é realçada e a metodologia de controlabilidade se mostra confiável quando baseada em cálculos em função dos graus de liberdade adequados ao sistema.

Design methodology for the ethyl acetate
reactive system

9.1 THE DESIGN METHODOLOGY

The methodology presented in the Chapter 4, is applied to propose a preliminary design of a feasible reactive distillation column configuration for the production of ethyl acetate. The different steps of the procedure are reminded in Figure 9.1.

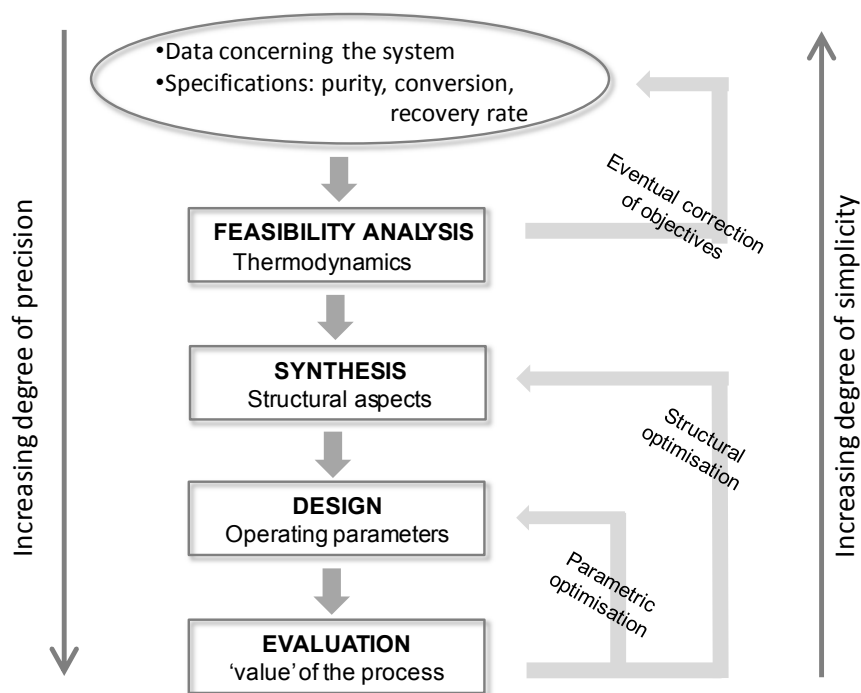


Figure 9.1. General principle of the design methodology

9.2 THERMODYNAMIC STUDY

In reactive distillation, the reaction is superimposed upon the distillation; both phase equilibrium and chemical equilibrium are simultaneously respected. The first steps of the design methodology are thus based on the acquisition of reliable physical and thermodynamic data.

9.2.1 Phase equilibrium

To account for non-ideal vapor-liquid equilibrium and possible vapor-liquid-liquid equilibrium for the quaternary system, the NRTL model is used for liquid phase. Table 9.1 provides the binary parameters used for the ethyl acetate system. The only vapor phase non-ideality considered is the dimerisation of acetic acid as described by Hayden-O'Connell second virial coefficient model. The Aspen Plus[®] built-in association parameters are used to compute fugacity coefficients.

Table 9.1. Binary parameters for the NRTL model

i j	HOAc EtOH	HOAc H ₂ O	HOAc EtOAc	EtOH H ₂ O	EtOH EtOAc	H ₂ O EtOAc
aij	0	-1.976	0	-0.9852	1.817306	3.853826
aji	0	3.329	0	3.7555	-4.411293	-2.34561
bij (K)	-252.482	609.889	-235.279	302.2365	-421.289	-4.42868
bji (K)	225.476	-723.888	515.821	-676.0314	1614.287	1290.464
cij	0.3	0.3	0.3	0.3	0.1	0.3643

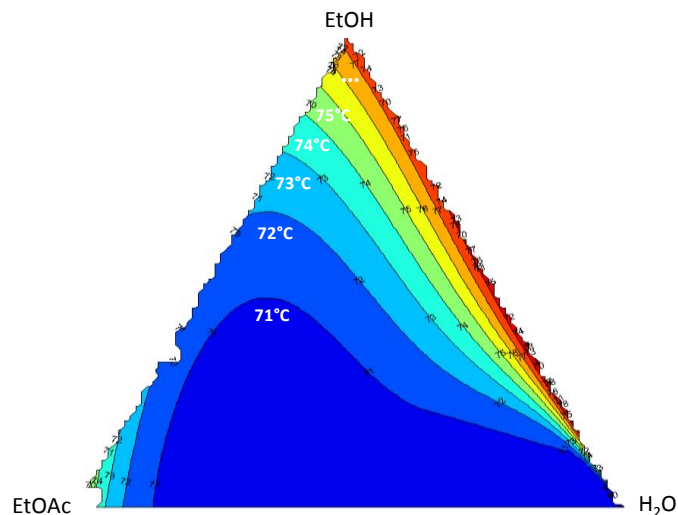
Luyben and Yu (2008) emphasized that the quality of the model parameters is essential to generate a correct process flowsheet of reactive distillation processes. A small deviation of thermodynamic data can result on important errors in the process design. Correct description of the azeotropes existence and ranking of azeotropic temperatures lead to the generation of a correct residue curve map and, consequently, to the proposition of a feasible column configuration.

The model predicts three minimum boiling binary azeotropes and one minimum boiling ternary azeotrope, which is the minimum temperature in the composition space.

Table 9.2. Azeotropic data

	Composition			Temperature
	EtOH	EtOAc	H ₂ O	(°C)
azeo B1	0	0.687	0.313	70.52
azeo B2	0.457	0.543	0	72.10
azeo B3	0.902	0	0.098	78.18
azeo T	0.107	0.607	0.286	70.28

A deeper analysis of the ternary azeotrope is conducted. Figure 4.2 displays the ternary EtOH-EtOAc-H₂O diagram showing the iso-temperature lines in the molar composition space.

Figure 9.2. Iso-temperature lines for the ternary mixture EtOH-EtOAc-H₂O

The bubble temperature of the mixture is shown to have a very flat profile and all the compositions within the greater dark area have a bubble temperature between 70.2 and 71°C. As a consequence, if a precision of 1°C is assumed for temperature measurement in the column top product, where the ternary mixture EtOH-EtOAc-H₂O is mainly present, a large part of the composition space is confused. For precise identification of the distillate product, a composition analyzer should be desired.

Moreover, the possibility of liquid-liquid phase splitting should also be mentioned. Figure 9.3 (Tang et al. 2005a) presents the liquid-liquid envelopes for the four ternaries present in the ethyl acetate system.

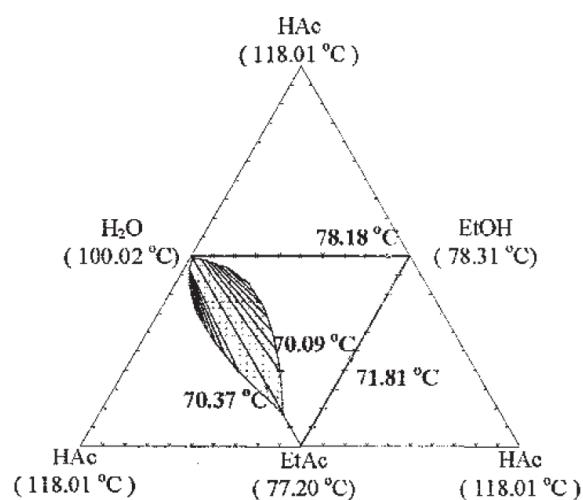


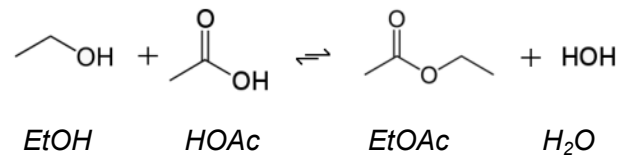
Figure 9.3. Liquid-liquid envelopes for the ternary mixtures (Tang et al. 2005a)

Luyben and Yu (2008) also described the liquid-liquid envelope for the ethyl acetate system and observed that the ternary minimum boiling azeotrope lies close to the liquid-liquid envelope edge. This conclusion suggests that relatively pure water can be recovered from the liquid-liquid separation of the ternary mixture EtOH- EtOAc- H₂O. This fact proposes the use of a decanter at the top product of the column, which is often encountered in esterification reactive distillation systems (Kloker et al. 2003, 2004, Tang et al. 2005, Lai et al. 2008). As a consequence of the compositions present inside the column, the liquid phase splitting is not considered in its theoretical stages.

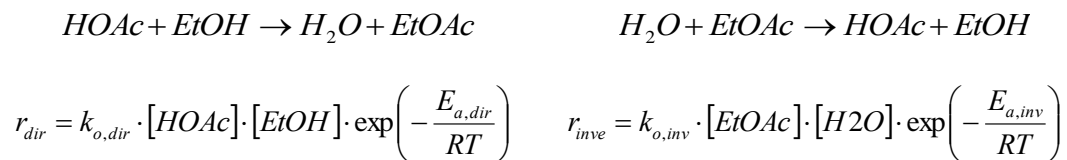
Due to the fact that the pre-design methodology adopted was conceived for the study of single reactive distillation columns, the introduction of a decanter will be further solved as an improvement of the resulting column configuration (cf. chapter 10), but not considered as from the feasibility step.

9.2.2 Kinetics data

The esterification of acetic acid with ethanol can be generally expressed as follows:



The esterification is considered as a reversible reaction, in which the chemical equilibrium is not instantaneously reached. The model requires two different reactions, one to account for the direct production of ethyl acetate and the other to account for the reverse direction. Both reactions are controlled by a first order Arrhenius type kinetic law (equations 9.3 and 9.4):



The homogeneous-catalyzed reaction kinetics is studied so as to avoid the complexities regarding the heterogeneous catalyst, as presented in Chapter 6. The liquid catalyst is sulfuric acid, which is fed to the column mixed with the acetic acid feed stream.

The reaction rates are expressed in the pseudo-homogeneous model and with components represented in terms of molar composition:

$$r = k \cdot e^{\left(-\frac{E}{RT}\right)} \cdot \prod_{i=1}^{N_c} C_i^{\alpha_i}$$

Where	r : reaction rate	T : absolute temperature (K)
	k : pre-exponential factor (m ³ /kmol/s)	N_c : number of components
	E : activation energy (kJ/kmol)	C_i : composition of each component
	R : gaz constant (J/K/mo l)	α_i : coefficient of each component

The values for pre-exponential factors and activation energies are obtained from Solvay previous studies and given in Table 9.3.

Table 9.3. Kinetic data

	<i>direct</i>	<i>reverse</i>
k (m ³ /kmol/s)	1170.245	259.810
E (kJ/kmol)	33595.3	33704.4

9.3 FEASIBILITY ANALYSIS

The results of the feasibility analysis based on an ∞/∞ analysis are commented below.

9.3.1 Reactive residue curves

In reactive residue curve maps, temperature always increases along with the residue curve line, and the singular points can be stable nodes, unstable nodes or saddle nodes. Each rRCM links one unstable node (the lowest boiling point) to one stable node (the higher boiling point), possibly passing closed to saddle nodes. In the case of reactive systems, additional points can be found in the diagram, corresponding to reactive azeotrope. A reactive azeotrope occurs when liquid composition and temperature remain constant due to the compensation of the phenomena of reaction and separation.

The reactive residue curves map (rRCM) of the ethyl acetate system is calculated under 1 atm and is presented in Figure 9.4. All the feasibility analysis graphs are plotted in function of the transformed variables defined by Ung and Doherty (1995), as previously presented in chapter 4. So, all points in the square formed by transformed coordinates of the pure products are at chemical equilibrium.

It can be observed that two stable nodes appear: the pure components HOAc and EtOH. There is one unstable node inside the diagram, which is the lightest product and can be understood as a reactive azeotrope with high influence of the physical azeotropes, composed by a mixture of these azeotropes compositions. All reactive residue curves start at this unstable node and two distillation zones appear. The majority of the curves end at the representative point of pure HOAc but some of them end at the EtOH node. The pure components EtOAc and H₂O and the two binary azeotropes EtOH-EtOAc (azeo B2) and EtOH-H₂O (azeo B3) are saddle nodes. The physical ternary azeotrope of EtOH-EtOAc-H₂O (azeo T) and the binary azeotropes EtOAc-H₂O (azeo B1) are no longer singular points in the system. Actually, they are formed by components which react, so the liquid-vapor equilibrium limitation caused by these azeotropes no longer exists in the reactive system.

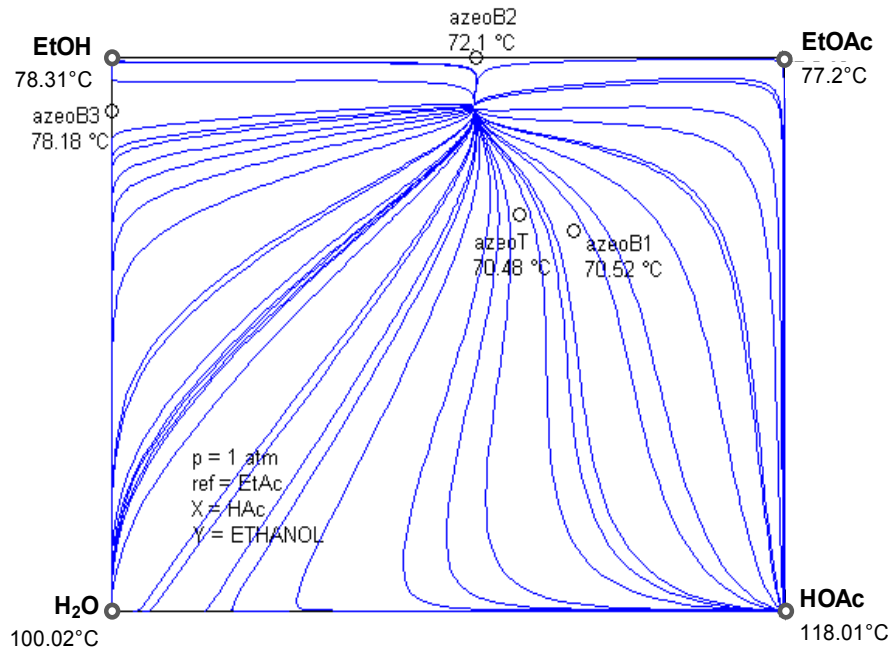


Figure 9.4. rRCM of the system $\text{HOAc} + \text{EtOH} \rightleftharpoons \text{EtOAc} + \text{H}_2\text{O}$

Previously, Kenig et al. (2001) presented a similar rRCM for the ethyl acetate system. Recently, Zheng et al. (2013) also proposed a residue curve map of the ethyl acetate synthesis reaction, with very similar curves characteristics. The latter authors performed a study on the influence of the Damköler number (D = a ratio of phase equilibrium strength to the reactive equilibrium strength) and observed that without reaction the ternary azeotrope is the unstable node of the quaternary system. The addition of reaction influences the EtAc-EtOH- H_2O azeotropic compositions and a new unstable node appears. The consistency of the results among the works reveals the reliability of the thermodynamic data adopted in this study.

The sensitivity of the stable node to the system pressure is plotted in Figure 9.5. The influence of the operating pressure is interesting to be analyzed, so as to imagine feasible process configurations under different pressure values. The atmospheric pressure, 1 atm, is selected for further calculations.

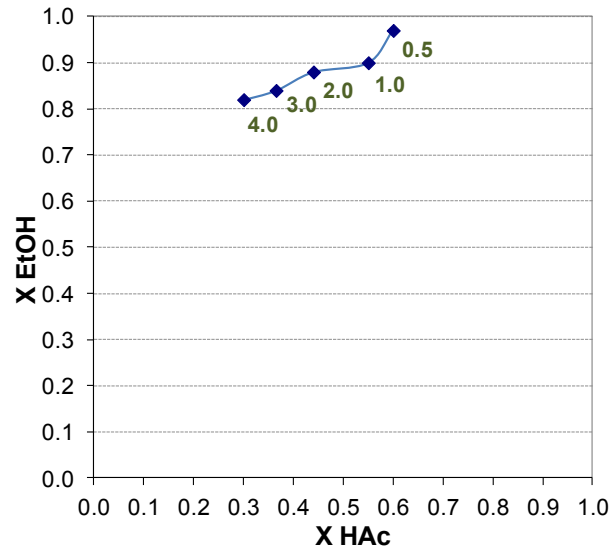


Figure 9.5. Locus of the rRCM unstable point for different values of pressure

9.3.2 Extractive residue curves

For double-feed configuration columns, whereas the reactive residue curves can be seen as an approximation of the composition profiles in the rectifying and stripping sections of a reactive column operating at total reflux, the reactive extractive curve approximates the liquid compositions in the reactive middle section of the same column.

A reactive extractive curve is obtained by the locus of liquid composition through the resolution of mass balances for given: initial composition, value of the ratio between the upper feed flowrate and the vapor flowrate (F_U/V) parameter and composition of the upper feed.

Assuming an upper feed consisting of almost pure acetic acid (0.01% H_2O) and a F_U/V value of 0.3, the reactive extractive curves map (rExCM) is calculated and plotted in Figure 9.6. These assumptions are to be confirmed later, at the simulation step. To our knowledge, the calculation of rEXCM of the ethyl acetate system has never been published in the literature, although it is showed to give important information for the design of the double feed column considered.

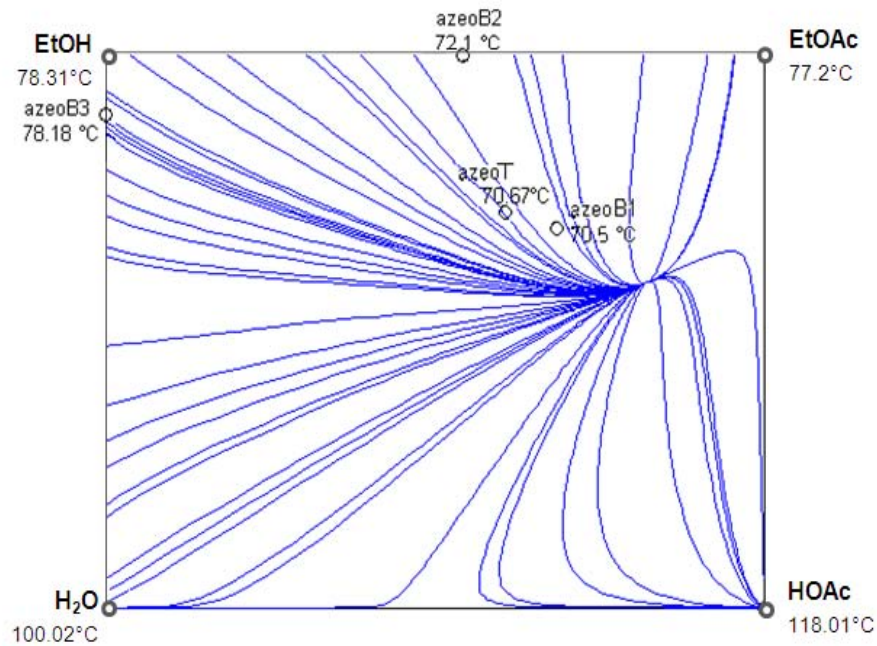


Figure 9.6. *rExCM* of the system $\text{HOAc} + \text{EtOH} \rightleftharpoons \text{EtOAc} + \text{H}_2\text{O}$

The *rExCM* also exhibits fixed points (stable node, unstable node and saddles). The unstable node is again a point inside the diagram, which corresponds to the attainable composition at the top of the middle section. This means that, for a F_U/V , = 0.3 and whatever the initial composition, extractive profile will end at this point. The sensitivity of the unstable extractive point to the F_U/V is given in Figure 9.7.

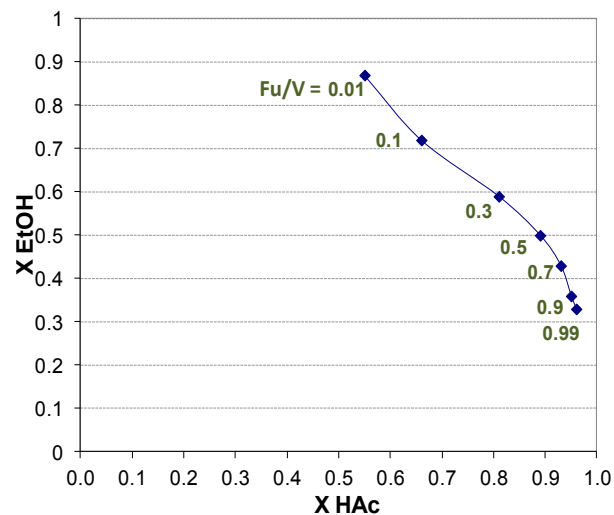


Figure 9.7. Locus of the *rExCM* unstable point for different values of F_U/V

It can be observed that, for high values of F_U/V the attainable point lies close to the edge corresponding to the binary HOAc-EtOAc. At lower values of F_U/V , the attainable point becomes closer to the composition of the ternary azeotrope. Actually, this parameter should be better understood as a result of the system than of a manipulated variable.

9.3.3 Feasible steady states

The simultaneous analysis of the rRCM and rExCM allows assessing the feasibility of reactive distillation process. Given the singular points and the distillation boundaries, the following rules enable to determine the most favorable feed composition and the column structure necessary to obtain the desired product (They et al. 2012):

Rule n°1: The points representing the distillate, the bottom and the equivalent feed of an entirely reactive column must satisfy the material balance, i.e. being aligned in the diagram.

Rule n°2: Single feed entirely reactive distillation is a feasible and probably an economic operation if both products (bottom and distillate) are connected by a reactive distillation curve.

Rule n°3: If one or both products are saddle points, the concentration profile can be shifted into the direction of the saddle point by using a entirely reactive column with two feed stages.

Rule n°4: A necessary condition for the feasibility of entirely reactive double-feed distillation columns is the possibility of drawing a continuous path from the bottom to the distillate thanks to a reactive residue curve (reactive rectifying section), a reactive extractive curve (reactive middle section) and another reactive residue curve (reactive stripping section).

Rule n°5: If it is necessary to separate a product that cannot exist alone in equilibrium mixture, a section with non-reactive distillation trays must be added.

Due to the fact that the ethyl acetate is a saddle point, a double-feed configuration is adopted for the reactive column. A small excess of alcohol is preferred to facilitate the acid consumption to meet stringent acid specifications (cf chapter 10). Hence, a molar excess of EtOH/HOAc = 1.03 is considered. Given the boiling point of the two reactants, the heaviest reactant (HOAc) is preferably fed in the upper location and the lightest reactant (EtOH) in the lower location. The feed compositions are considered as:

EtOH: 93.0%wt EtOH + 7.0%wt H₂O or 83.9%mol EtOH + 16.1%mol H₂O

HOAc: 99.9%wt HOAc + 0.1%wt H₂O or 99.7%mol HOAc + 0.3%mol H₂O

Graphical feasibility analysis is demonstrated in Figure 9.8. First, the points representing the feed configurations are placed and they are connected by a straight continuous black line. The single point representative of the double feed composition is placed as a dark circle in this line and is defined from a mass balance considering the molar proportion of the feed flows.

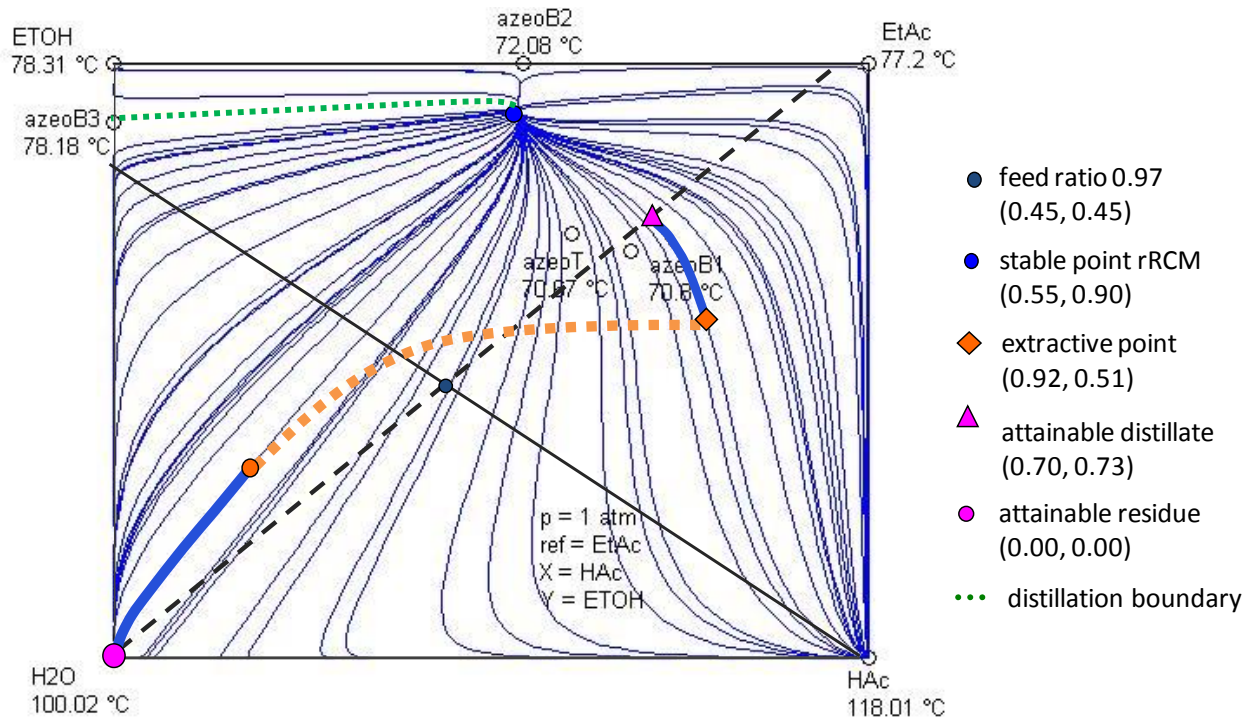


Figure 9.8. Feasibility analysis of the double-feed configuration

So as to respect the material balance, the representative points of the feed, the distillate and the residue are required to be aligned in the diagram (*Rule n°1*). Thus, the straight dotted black line is drawn. In order to achieve high acid conversion, the attainable residue is supposed to be pure H₂O. The attainable distillate (pink triangle) could be placed in any position of the dotted line.

Then, to respect *Rule n°4*, a continuous path among reactive residue curves and an extractive residue curve should be found. Starting from the bottom representative point (pure H₂O), the liquid composition profile in the stripping section would follow a residue curve (continuous blue line); then the profile in the middle section would follow an extractive curve (dotted orange line). The previous rExCM analysis showed a limit for the profiles in the middle section, which is represented by the orange diamond in the diagram. The composition profile in the rectifying reactive section would start in the diamond and follow a residue reactive curve until the distillate representative point, which is a pink triangle.

Klöker et al. (2004) stated that due to the presence of minimum boiling azeotropes, it is not possible to obtain high purity ethyl acetate at the top of the column, but rather a ternary mixture with water as a by-product and some non-converted ethanol. This fact is confirmed in Figure 9.8.

So, the feasibility analysis thus suggests a column where it is possible to have a bottom with high concentration of H₂O and a distillate represented inside the diagram, with a composition close to the ternary azeotrope. The transformed compositions are converted into molar compositions, and the attainable products are given in Table 9.4.

Table 9.4. Attainable product compositions provided in the Feasibility Analysis step

	transformed coordinates		molar coordinates			
	X HOAc	X EtOH	x HOAc	x EtOH	x H ₂ O	x EtOAc
residue	0.00	0.00	0.000	0.000	1.000	0.000
distillate	0.70	0.73	0.17	0.20	0.10	0.53

The example above has an EtOAc molar purity of 53% at the column distillate. Actually, Lee et al. (2007) showed that one single double-feed column cannot produce pure EtOAc, and further purification is needed. This aspect will be considered in the further steps of the design methodology.

The feasibility methodology then confirms then if the expected objectives for the system are physically attainable by a reactive distillation process, but it is not sufficient to define the configuration and size of the process. The methodology moves forward through the synthesis step.

9.4 SYNTHESIS STEP

The synthesis step is based on the Boundary Value Design method introduced by Barbosa and Doherty (1987). The specifications required for the synthesis, such as distillate, bottom and feed compositions and the column structure are inherited from the previous feasibility analysis.

The composition profiles in the rectifying, middle and stripping sections are obtained considering an entirely reactive column, and calculating the mass balance between the top of the column and a rectifying stage and between the bottom of the column and a stripping stage respectively. Because the profiles depend on the reflux ratio, a sensitivity analysis is performed by changing the reflux ratio and the position of the lower feed. When the rectifying, middle and stripping profiles intersect, a feasible steady state is identified. As the synthesis step computes the profile stage by stage, the number of stages required in each section of the column can be estimated.

For the system studied, two feasible configurations were found. The first column proposed has 16 theoretical stages, obtained when the lower feed is located 5 stages from the bottom of the column and

the reflux ratio is 1.0. It should be mentioned that other configurations could also be feasible, by increasing the lower feed position. So as to avoid too big columns, these two configurations were selected and they are sufficient to exemplify the application of the entire design methodology.

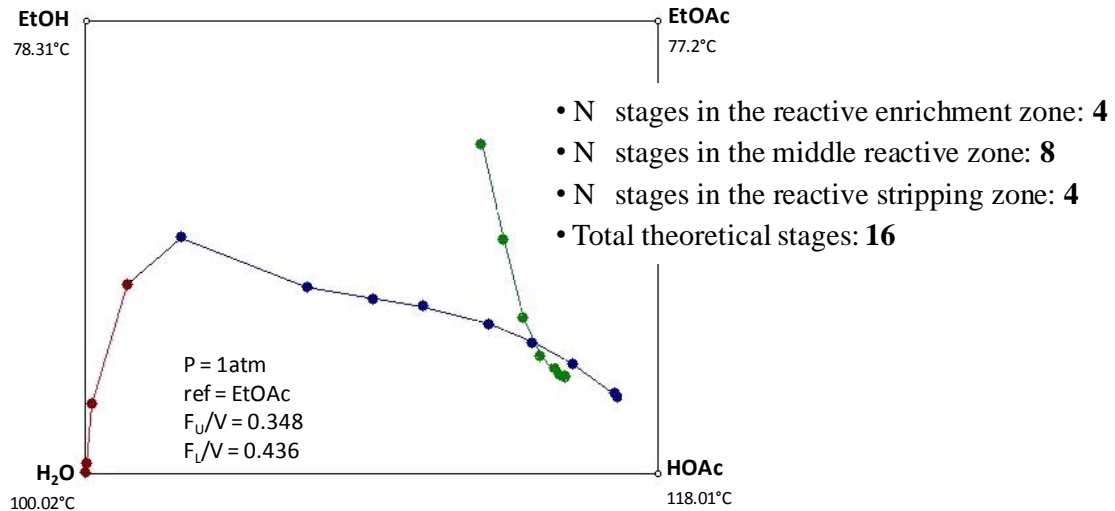


Figure 9.9. Composition profiles obtained from Synthesis step, column with 16 stages

The second configuration proposed has 21 theoretical stages, obtained when the lower feed is located 7 stages from the bottom of the column and the reflux ratio is 1.22.

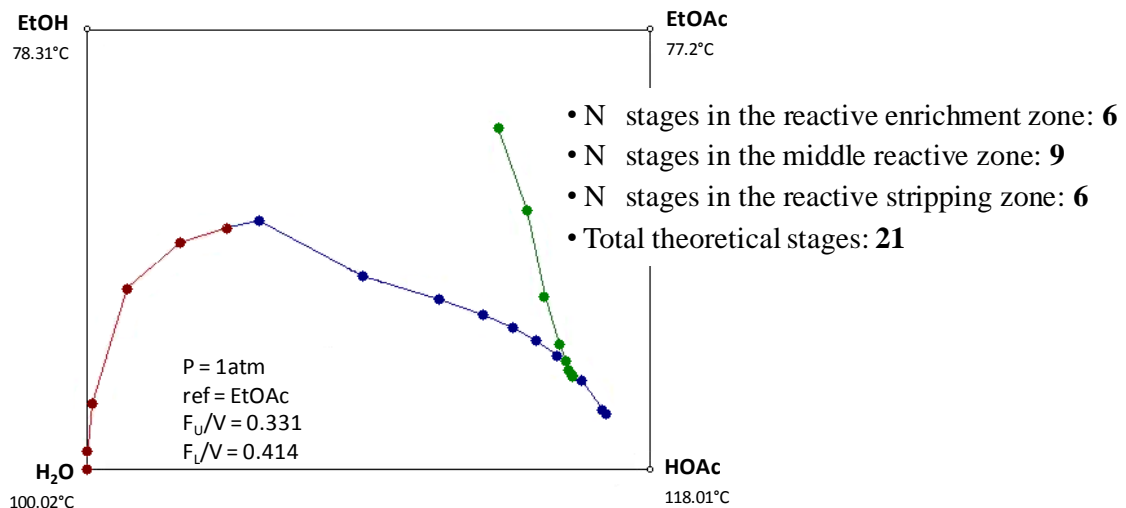


Figure 9.10. Composition profiles obtained from Synthesis step, column with 21 stages

Different configurations are possibly feasible; so that the engineer can choose the best configuration according to his/her own specifications (lower investment, lower operating costs, better operability, etc.). The objective of the work is to choose the configuration in function of its controllability. The comparison of the columns in function of controllability criteria will be performed in chapter 10.

9.5 CONCEPTUAL DESIGN STEP

So far, the column configurations have been drawn up from the mass balances only. The conceptual design step consists in adjusting the operating parameters taking into account the overall complexity of the process, such as the thermal phenomena (heat of reaction, thermal loss, heat of mixture, etc.).

The parameters obtained from synthesis step are inserted into the simulation software Aspen Plus[®]. The number of plates and feed positions are considered, and the attainable compositions are used to initialize the column. Once the pressure (1atm), the feed composition and the column configuration are given, the degree of freedom of the MESH equations is 2; the software choices to saturate these degrees of freedom are:

- liquid distillate flow rate and reflux flow rate
- liquid distillate flow rate and heat given to reboiler
- heat given to reboiler and reflux rate

The last option was selected; the operating parameters were defined so as to provide the best attainable conversion. Figures 9.11 and 9.12 present the profiles obtained for the production of ethyl acetate on both feasible reactive column configurations.

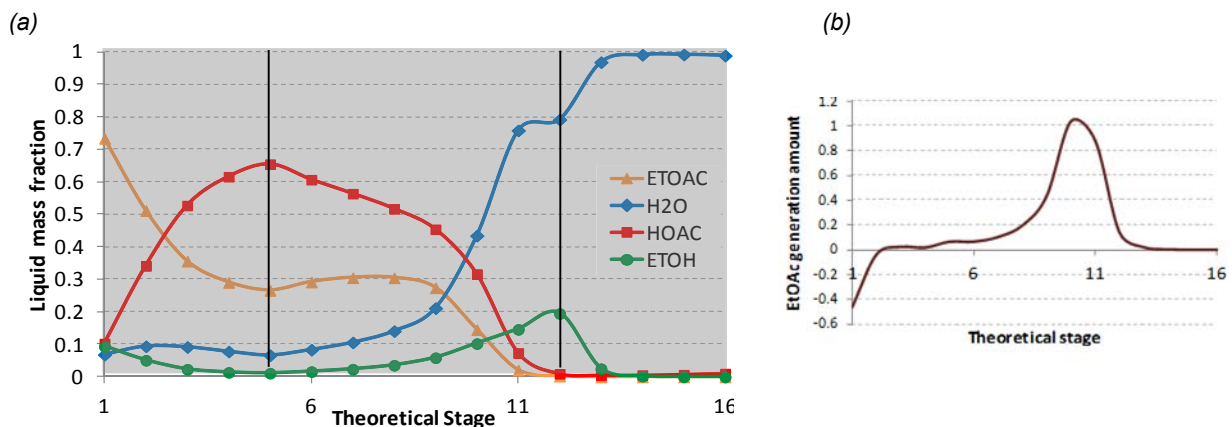


Figure 9.11. (a) composition and (b) EtOAc generation profiles from Conceptual Design step, column with 16 stages

The resulting purity of ethyl acetate at the distillate of the 16-stage column is 52.2%mol, or 73.0%wt, which is close to the value calculated at the synthesis step, assuring its reliability. The conversion rate of the acid is 82.8%.

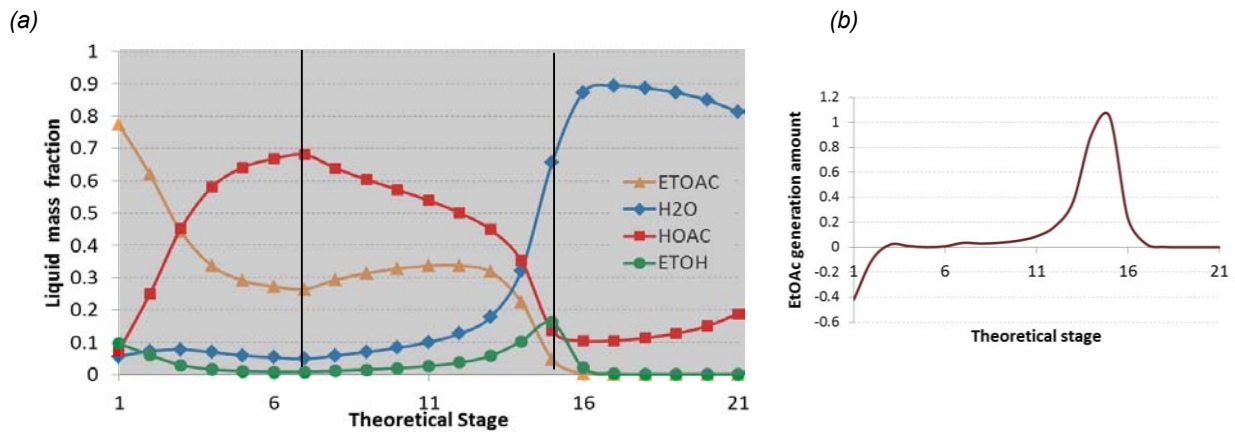


Figure 9.12. (a) composition and (b) EtOAc generation profiles from Conceptual Design step, column with 21 stages

The resulting purity of ethyl acetate at the distillate of the 21-stage column is 57.7%mol, or 77.1%wt. The acid conversion is 83.3%. The resulting configurations from the conceptual design step are a reliable initialization condition for further optimizing the process. This optimization step can be based on a more rigorous model including non-equilibrium equations for the LV equilibrium, for example, but more data would be necessary to describe the transfer phenomena (Rouzineau, 2002 and Higler, 1998).

From the Figures 9.11 (b) e 9.12 (b), it can be observed that the generation of EtOAc is negative in the first stages, on the top section of the column. Actually, the esterification reaction occurs in a reverse direction at these stages due to the high content of EtOAc and the presence of catalyst; the equilibrium is displaced and the hydrolysis reaction occurs, hindering the acquisition of higher contents of EtOAc at the distillate stream. In order to avoid this behavior, the configurations can be improved by changing the catalyst feed position from the top of the column to the acetic acid feed location. Now, both acids are fed together and the top separation section, located above the acid feed position, is dedicated solely to separation. This modification confirms the heuristic key rule of the feasibility analysis step that stated that, to obtain high concentrations of EtOAc at the distillate, a separation-only section would be required.

The new composition profiles are presented in Figures 9.13 and 9.14. They show higher conversion of acid: 97.8% for the configuration with 16 stages and 99.2% for the configuration with 21 stages, with higher contents of EtOAc at the distillate and no hydrolysis reaction.

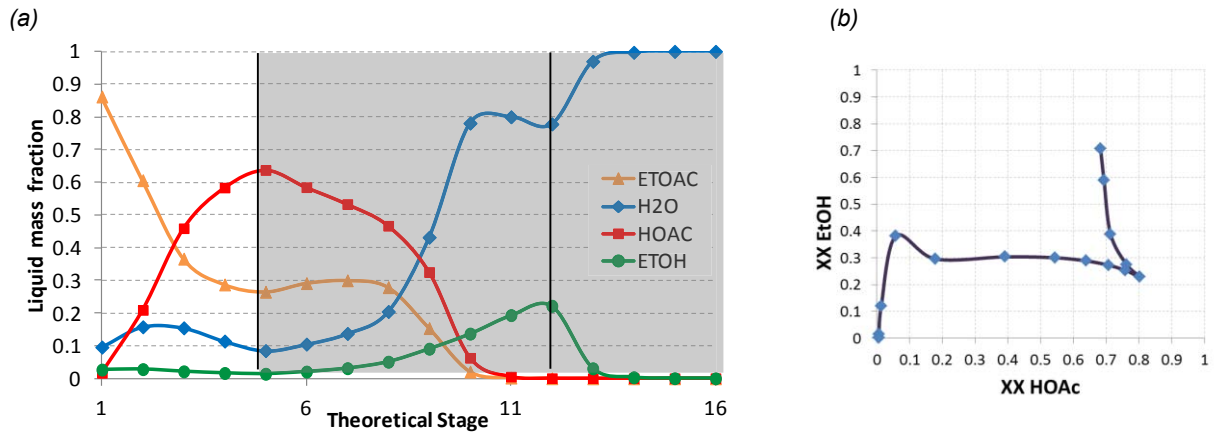


Figure 9.13. (a) molar and (b) transformed composition profiles from Conceptual Design step, column with 16 stages

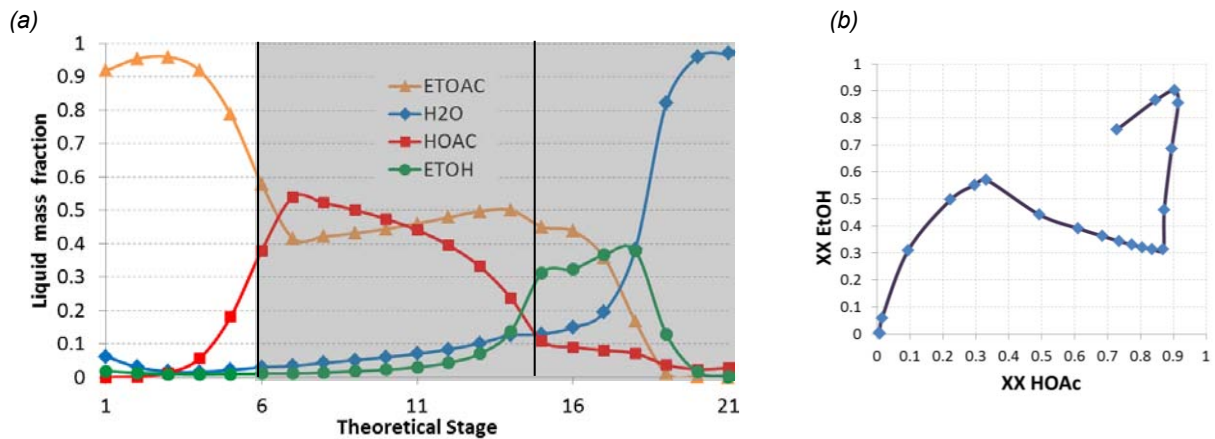


Figure 9.14. (a) molar and (b) transformed composition profiles from Conceptual Design step, column with 21 stages

At this moment, all the analysis based on steady-state conditions was performed and two feasible reactive column configurations were proposed, which attain the process specifications in function of reaction and separation requirements.

However, it was discussed in chapter 1 that although reactive distillation process is really promising, the interactions existing between reaction and separation functions lead to non-linearity which strongly complicates the dynamics and control of such processes. Special attention should be given and there exists an important concern about complementing the design methodology presented by integrating controllability and diagnosability aspects.

The feasible column configurations will then be analyzed in terms of controllability and diagnosability in next chapters. New approaches are proposed and they consider the dynamic behavior of the ethyl acetate system as from the conceptual design step.

Controllability analysis of the ethyl
acetate reactive system

10.1 INTRODUCTION

At the synthesis step level of the reactive column design methodology (sections 4.1.2 and 9.4), the configuration proposition has two degrees of freedom: the reflux ratio and the position of the lower feed stage. As a result, various configurations may be feasible depending on the values of these two parameters. To discriminate between these configurations, different criteria can be considered.

The criterion used was usually either a lower investment or lower operating costs, reflecting a choice of a feasible column with the smallest number of theoretical stages, or the smallest reflux ratio. This choice was based on a static analysis, regarding only economics and environmental criteria.

As it has already been discussed that, due to the present nonlinearities and variables couplings, when the conceptual design of a reactive distillation process is optimally obtained without consideration of its dynamic behavior, the result may be a unit very difficult to control. It is thus appropriate to now consider controllability criteria as from the conceptual step and this is the objective of the present chapter.

This section presents the controllability analysis performed to discriminate the two feasible configurations proposed in section 9.4, from an operability standpoint. The configuration selected is then adapted to respect the required industrial configuration for the ethyl acetate production. In fact, as it will be discussed later in this chapter, the industrial process requires a decanter on the distillate output, and it cannot be taken into account in the preliminary design procedure. Later, other column configurations are modeled with different number of theoretical stages for reaction and for separation, changing the relative feed positions. Through steady-state and dynamic simulations, the controllability criteria are calculated and compared. The main objective is to establish heuristic key rules and column characteristics that would provide better controllability performance. These characteristics should be directly identified in later synthesis-step approaches when choosing among several possible column configurations.

10.2 CHOICE OF THE COLUMN CONFIGURATION IN FUNCTION OF CONTROLLABILITY

The design methodology presented in chapter 9 proposed two possible column configurations for the ethyl acetate production. The first one, which will be referenced as *Design16*, consists of 16 theoretical stages, with the lower feed located on the fifth stage from the bottom and operates with a reflux ratio equals to 1.0 (Figure 10.1). The second column configuration, which will be referenced as

Design21, consists of 21 theoretical stages, with the lower feed located on the seventh stage from the bottom and operates with a reflux ratio equals to 1.22 (Figure 10.5).

Column Design16 controllability analysis

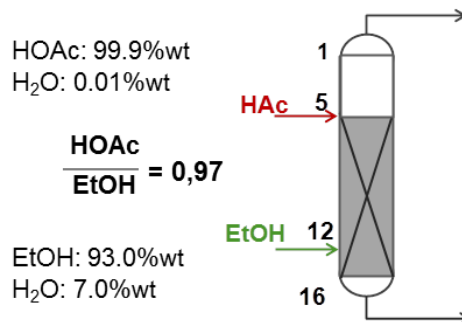
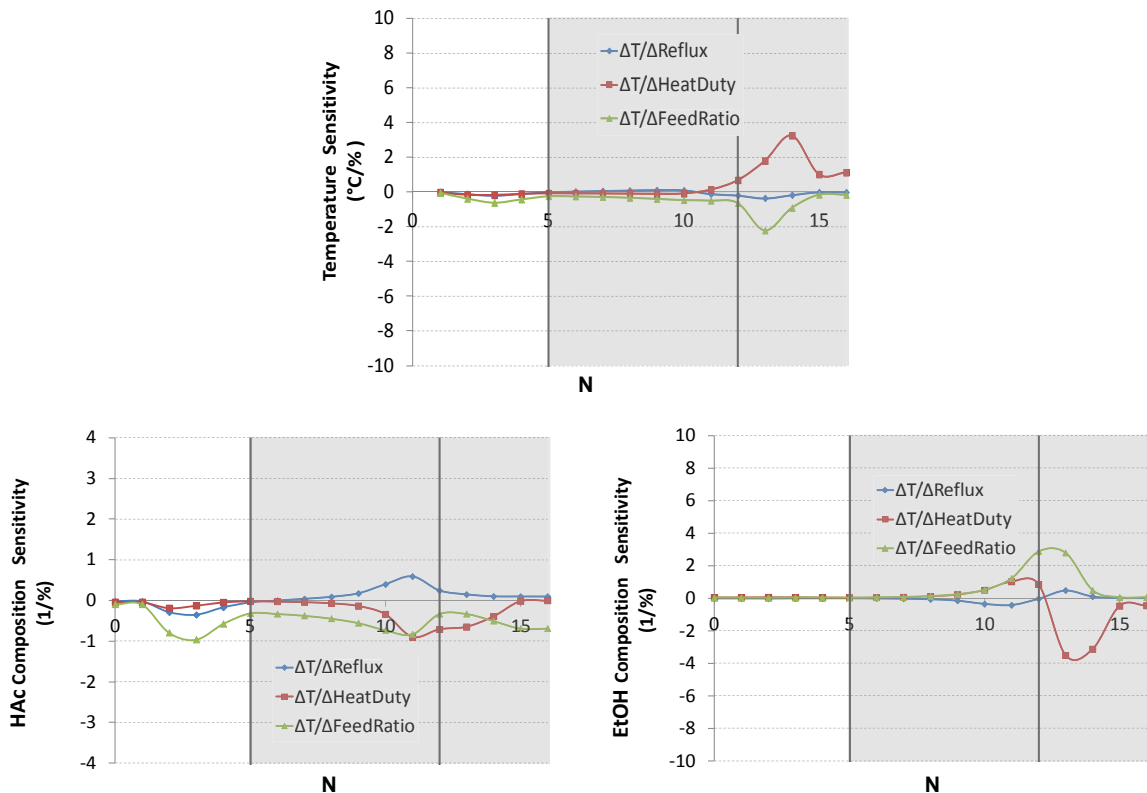


Figure 10.1. Column Design16 scheme

To begin with, the controllability analysis is performed on the column Design16. The sensitivity matrix *K* is calculated through steady state simulations and the gains are presented in Figure 10.2. The vertical lines account for feed locations and the catalyst, so reaction occurs in the gray zone.

It can be observed that the sensitivity of this column is concentrated near the lower feed position and that the heat duty is the most impacting manipulated variable.



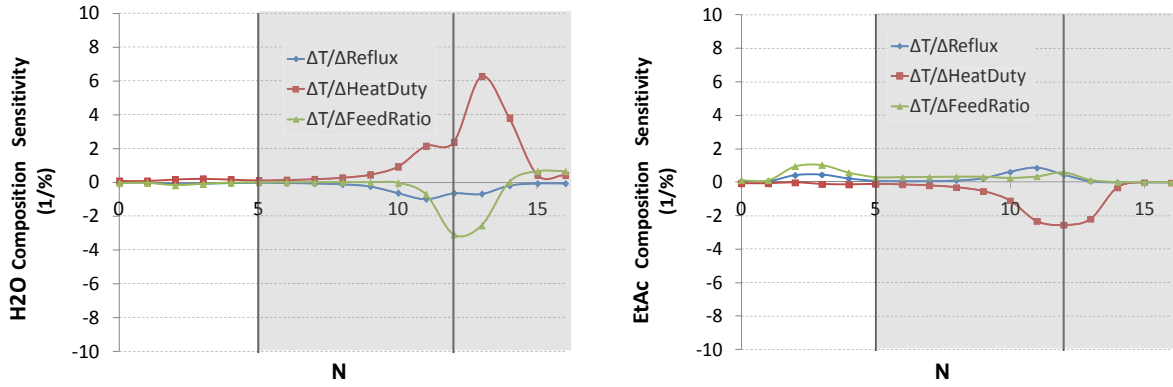


Figure 10.2. Sensitivity matrices of column Design16

The Singular Value Decomposition is first performed considering only temperature sensors and then with additional consideration of composition sensors. Although the K matrices do not show sensitivity at the section dedicated solely to separation at the top of the column, the SVD calculations show a better distributed influence on the temperature sensors through the entire column, by the decomposition of the singular vectors.

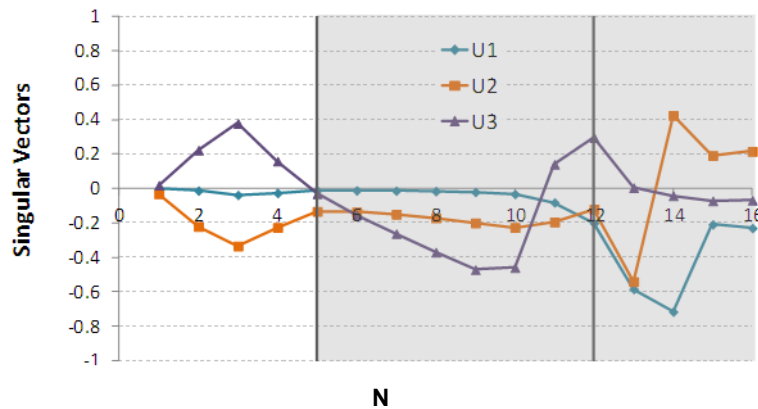


Figure 10.3. Singular vectors matrix considering only temperature sensors, column Design16

When only temperature inferential control is considered, the singular values and the overall condition number are:

$$S_{onlyT} = \begin{bmatrix} 4.58 & 0 & 0 \\ 0 & 1.93 & 0 \\ 0 & 0 & 0.32 \end{bmatrix}$$

$$CN_{onlyT} = 14.3$$

Figure 10.4 reports the results obtained when both temperature and composition control are simultaneously considered. The new singular values and the overall condition number are also calculated.

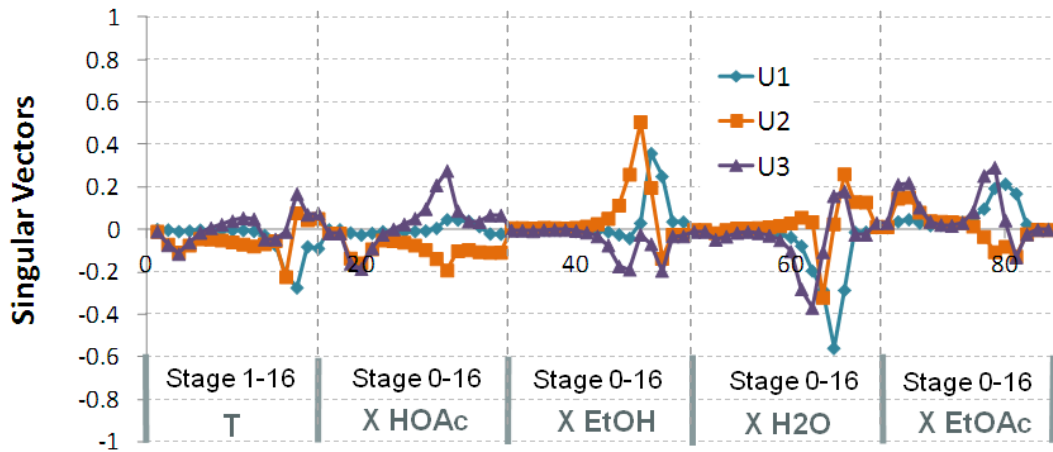


Figure 10.4. Singular vectors matrix considering all sensors, column Design16

$$S_{all\ measures} = \begin{bmatrix} 12.17 & 0 & 0 \\ 0 & 5.89 & 0 \\ 0 & 0 & 1.78 \end{bmatrix}$$

$$CN_{all\ measures} = 6.8$$

It is reminded that the *CN* provides a quantitative indication of the sensitivities balance in a multivariable system and values close to unity reflect that the multivariable gains are well balanced and the system should have enough degrees of freedom to meet the control objectives.

When only temperature control is considered, the configuration meet the control tasks in a more difficult way than when all the sensors are used, as shown by the lower *CN* obtained for the latter case. This result is in agreement with the observations made in chapter 8.

Column Design21 controllability analysis

The controllability analysis is now performed on the second feasible configuration: *Design21*.

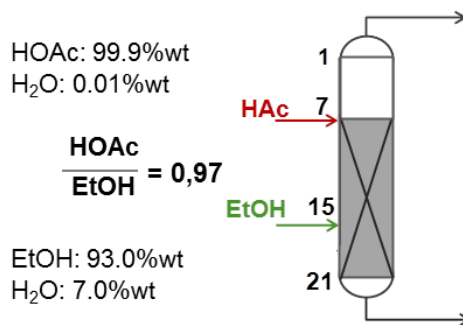


Figure 10.5. Column Design21 scheme

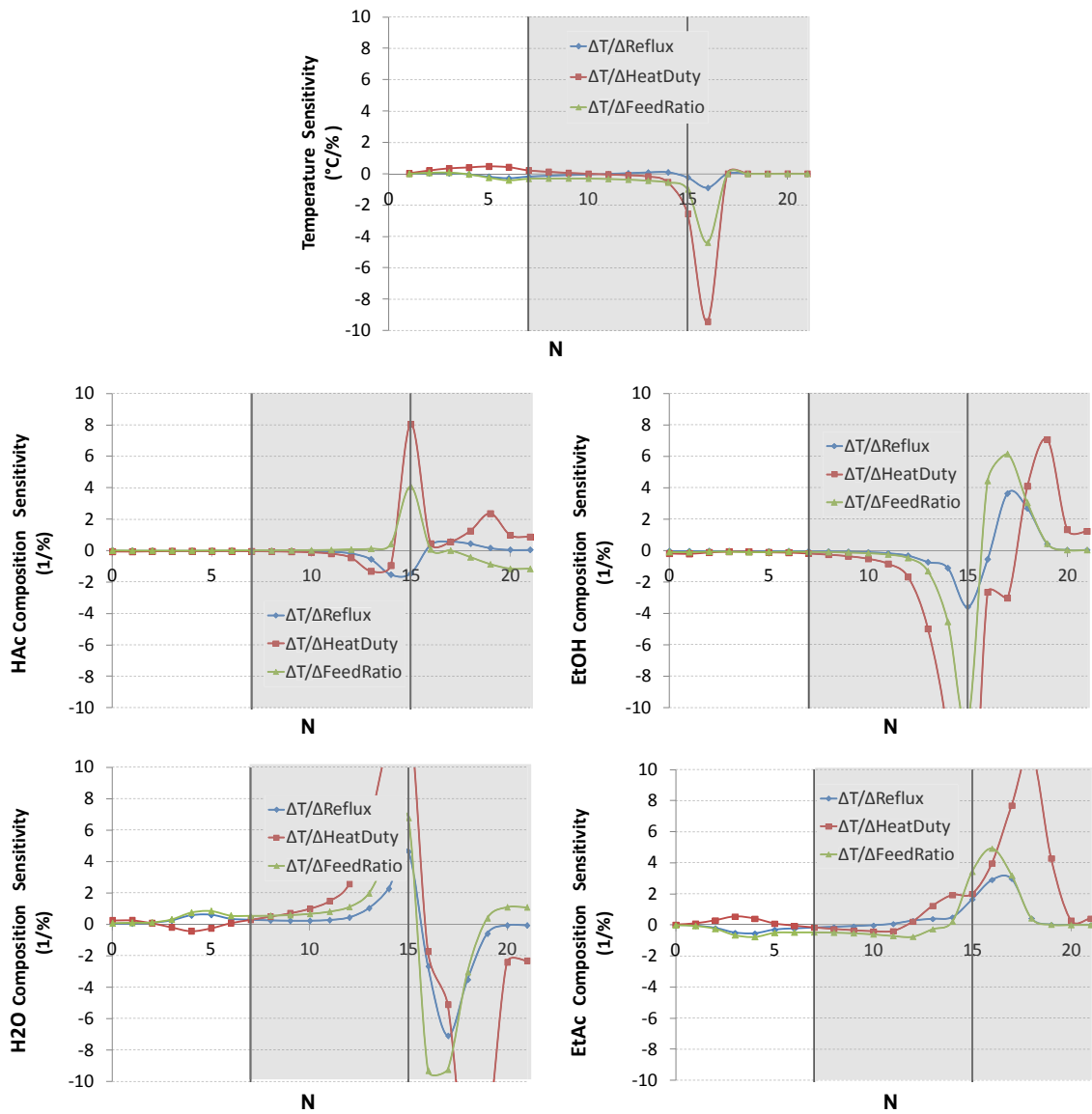


Figure 10.6. Sensitivity matrices of column *Design21*

The sensitivity analysis of the column *Design21* also shows small sensitivity at the top section of the column. The sensitivity around the lower feed position has greater values than the ones calculated for the column *Design16*. The singular values (Figure 10.7) and the condition number have been calculated in the case of only temperature inferential control is considered.

SVD calculations are also performed and the singular vectors show relevance of all sensors from stage $n^{\circ} 5$ to stage $n^{\circ} 16$ in the reactive column. The overall *CN* calculated with consideration of all temperature sensors is equal to 27.6, showing higher value than in the case of column *Design16*.

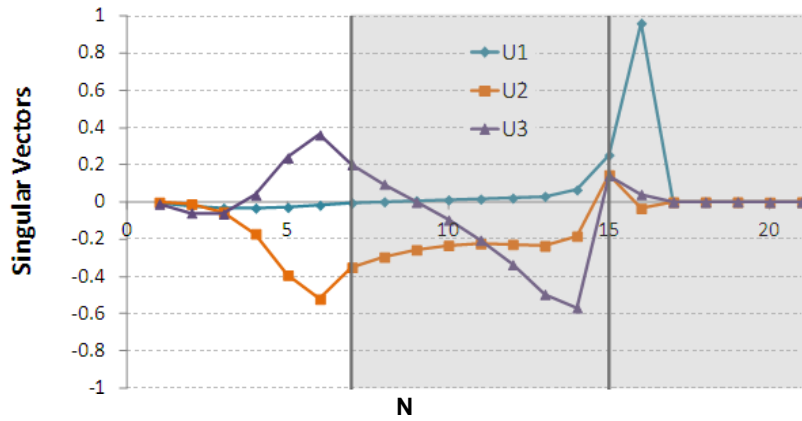


Figure 10.7. Singular vectors matrix considering only temperature sensors, column Design21

$$S_{onlyT} = \begin{bmatrix} 10.85 & 0 & 0 \\ 0 & 1.17 & 0 \\ 0 & 0 & 0.39 \end{bmatrix}$$

$$CN_{onlyT} = 27.6$$

Figure 10.8 reports the results obtained when both temperature and composition control are considered. The singular values and the respective CN are also calculated, showing better controllability when composition sensors are considered in addition to the temperature sensors, due to the smaller criterion value.

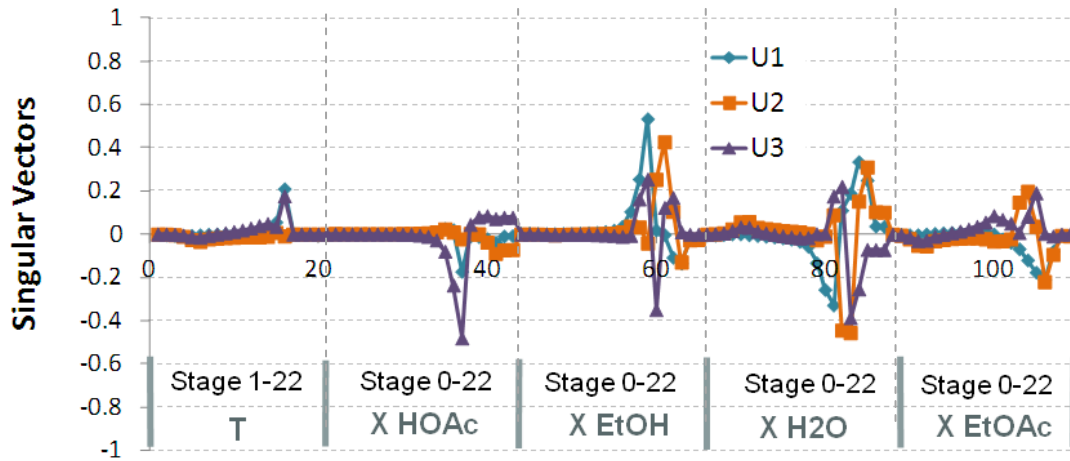


Figure 10.8. Singular vectors matrix considering all sensors, column Design21

$$S_{all\ measures} = \begin{bmatrix} 49.49 & 0 & 0 \\ 0 & 18.14 & 0 \\ 0 & 0 & 6.57 \end{bmatrix}$$

$$CN_{all\ measures} = 7.5$$

The two feasible column configurations *Design16* and *Design21* differ mainly in the position of the lower feed. In the previous design, there were 4 theoretical stages between the lower feed position and the bottom of the column. In the present configuration, this section consists in 6 stages. As a consequence, the total number of theoretical stages and the reflux ratio also changed so as to maintain high reaction and separation efficiencies. As it can be observed in Figures 10.2 and 10.6, the sensors sensitivities have different magnitudes for the two column configurations, and the higher differences occur near the lower feed. For both configurations, the top separation section has 4 stages and small sensitivities appear.

Column *Design16* appears to be better controllable than column *Design21* due to the lower *CN* values for all cases ($CN_{only T} = 14.3$ and $CN_{all measures} = 6.8$ for *Design16* against $CN_{only T} = 27.6$ and $CN_{all measures} = 7.5$ for *Design21*).

It seems important to remember that the calculations in chapter 9 showed that column *Design21* performs a little better than column *Design16* with respect to acid conversion (82.8% for *Design16* against 83.3% for *Design21*). However, the comparison of the two different column configurations here in chapter 10 concludes that column *Design16* is better controllable than column *Design21*. This controversial proposition shows the interest of the controllability analysis at the design phase of intensified processes. A judicious trade-off should be performed. Moreover, the smaller quantity of theoretical stages of column *Design16* should request lower investment costs. Due to the small difference in acid conversion, the lower investment required and the significant difference in *CN* values, the column configuration *Design16* is chosen as the most appropriate RD column configuration given by the conceptual design step from an operability point of view.

In the next sections, we adapt this configuration to the industrial application specifications and a sensitivity study on some structural parameters is presented.

10.3 INDUSTRIAL SPECIFICATIONS

The reactive column resulting from the conceptual design step (sections 9.3 and 10.2) shows high acid conversion of 98.8%, with good production of ethyl acetate at distillate. However, for the industrial application, some more stringent product specifications must be met. The configuration proposed must be improved to achieve an operating regime that respects:

- HOAc at the distillate < 100ppm wt
- EtOH at the distillate < 1.3%wt
- HOAc at the bottom < 1.0%wt

So as to ensure a better and coherent acid conversion, the column hydraulic holdup must be sufficient for the reaction requirements. The bubble-cap trays technology is then adopted for the reactive stages. The Koch-Glitsch bubble cap trays are suitable for the application due to their important weir height, providing the required holdup in reactive sections.

For the separation-only stages, the Mellapak packing is adopted. The packing enlarges the internal surface and promotes turbulences so that the mass transfer between the liquid and the vapor phase is increased and the separation is enhanced, with smaller pressure drop than trays.

In the existing industrial configuration consisting of a sequence of a reactor and a conventional distillation column, a decanter is placed at the top of the column for water removal. It is an additional important device used to separate aqueous phase from organic phase. We consider the same device on the distillate output of the reactive column. It operates at room temperature. This configuration with column and decanter continuously operating was also proposed by other authors in the literature (Kloker et al, 2004, Kolena et al, 2004, Lai et al, 2008). The design methodology presented and applied before cannot take into account this decanter. However, as it was already presented, the main interest of the methodology lies in the sequential and progressive introduction of process complexity; the introduction of the decanter is a refinement made in the present step.

To respect the constraints regarding coherent holdups and product specifications, a new column configuration is proposed. The decanter is introduced on the top stream, four stages are added into the separation section and eight stages are introduced between the two feed positions. These values were obtained by exhaustive simulation in order to find the minimum number of additional stages necessary to achieve the specifications. Due to the presence of the decanter, the reflux ratio is constituted mainly by part of the distillate organic phase and has the value of 1.15.

The final column consists in a total of 28 theoretical stages, where both acetic and sulfuric catalyst acids are fed on the top of the reactive section, stage n°9, and industrial-grade ethanol is fed at stage n°24, respecting the proposition of the synthesis step for *Design16* (5 stages from the bottom). Stages remain numbered from the top to the bottom of the column.

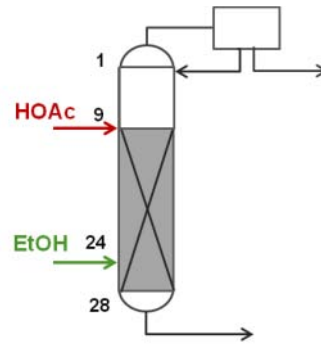


Figure 10.9. Column Design28 scheme

The operational parameters, such as heat duty and reflux rate, were adapted and the proposed industrial configuration, now called *Design28*, delivers 99.9% of acid conversion. The composition profiles are plotted in Figure 10.10. Distillate composition lies near the ternary azeotrope.

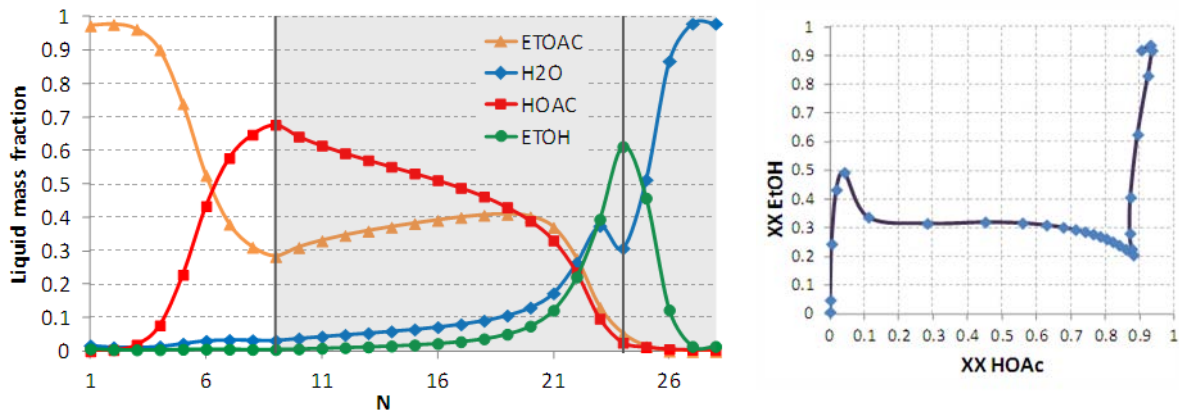


Figure 10.10. Mass compositions and transformed composition column Design28 profile

The profile plotted in Figure 10.10 in the transformed compositions space represents the separation section as almost a vertical straight line, clearly showing its important role in purifying the acid content and approaching the ethyl acetate composition (the right-up edge).

Now, to study the dynamic controllability of the RD column, the geometric and hydraulic parameters should also be defined.

The sizes of the reboiler and of the decanter were considered from Solvay documents. The reboiler is a thermo-siphon, defined into Aspen Plus[®] with the specification of vapor fraction equals 1.

The steady-state operating regime calculated for a slight excess of acetic acid in the feed, is detailed in Figure 10.11. It is used as an initialization point for the dynamic simulations.

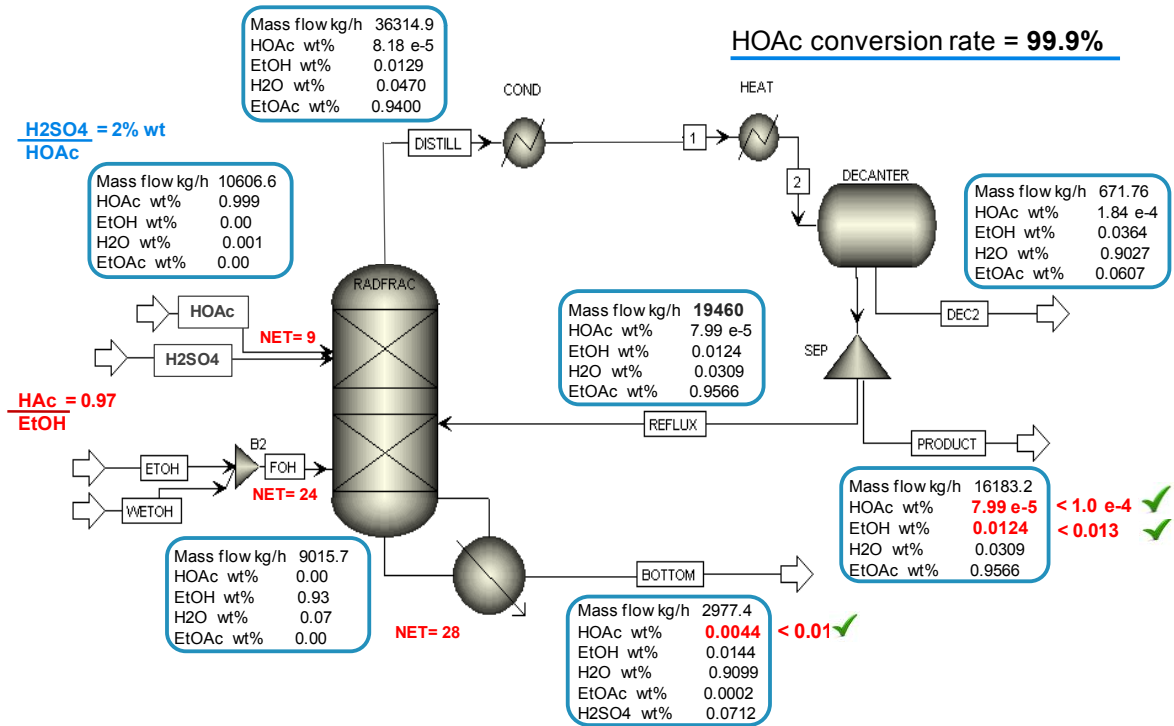


Figure 10.11. Steady state regime details for column Design28

Now the controllability methodology can be applied to the column *Design28*. Actually, it is the configuration already presented in the example of chapter 8. The overall controllability criteria are recalled here:

$$CN_{only T} = 3.5$$

$$CN_{all measures} = 2.2$$

In chapter 8, different control configurations were proposed based on the most sensitive and better balanced sensors. The system dynamic responses were observed after a perturbation of the water content in the alcohol feed flow rate.

In this chapter, the dynamic analysis is improved considering a perturbation on the acid feed flow rate. The acid feed flow rate is the throughput manipulative disturbance and the control structure should be robust to its changes. The throughput perturbation has a stronger impact on the system than the perturbation of water in the ethanol feed stream.

For the selected control configurations, the evolution of the system after a decrease of 2.5% on the acid feed flow rate is presented, with temperature inferential control loops (Figures 10.12 and 10.13), and with composition control loops (Figures 10.14 and 10.15):

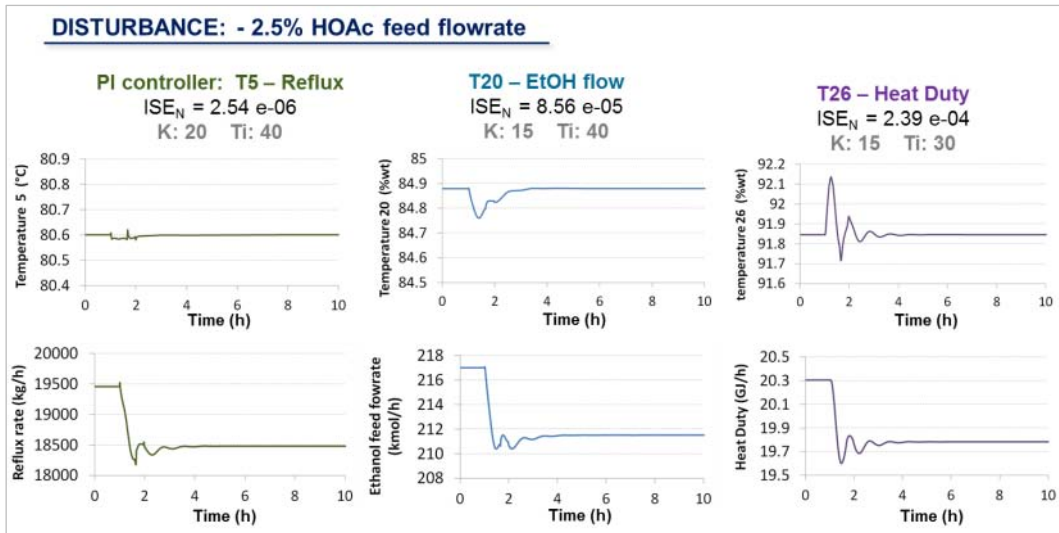


Figure 10.12. Inferential control variables after a decrease of acid feed flow rate, column Design28

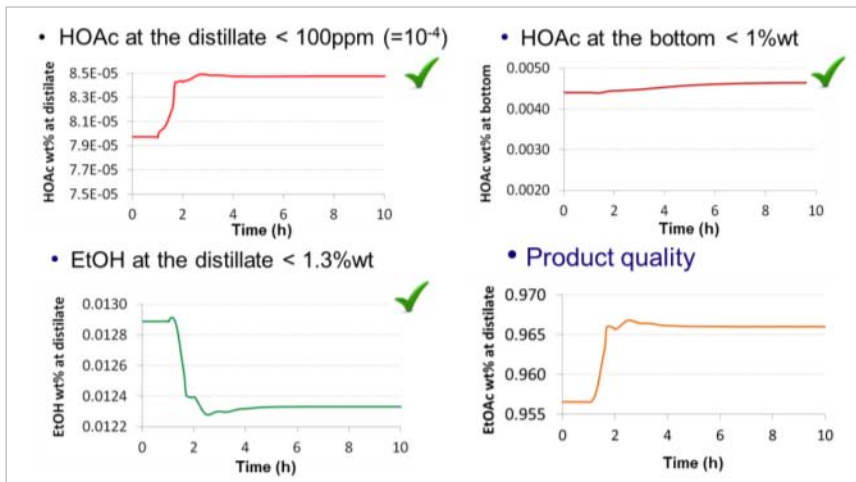


Figure 10.13. Inferential control specifications after a decrease of acid feed flow rate, column Design28

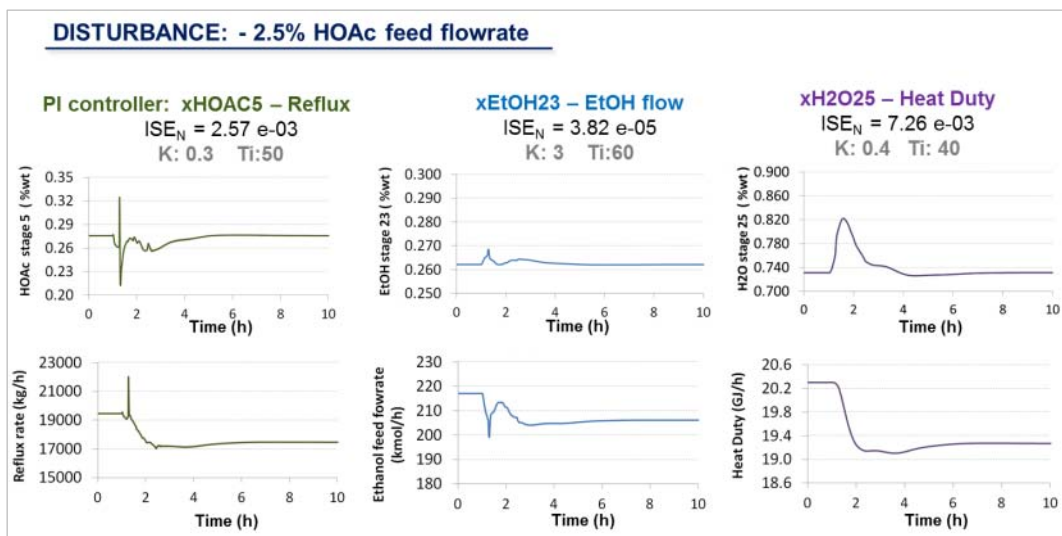


Figure 10.14. Composition control variables after a decrease of acid feed flow rate, column Design28

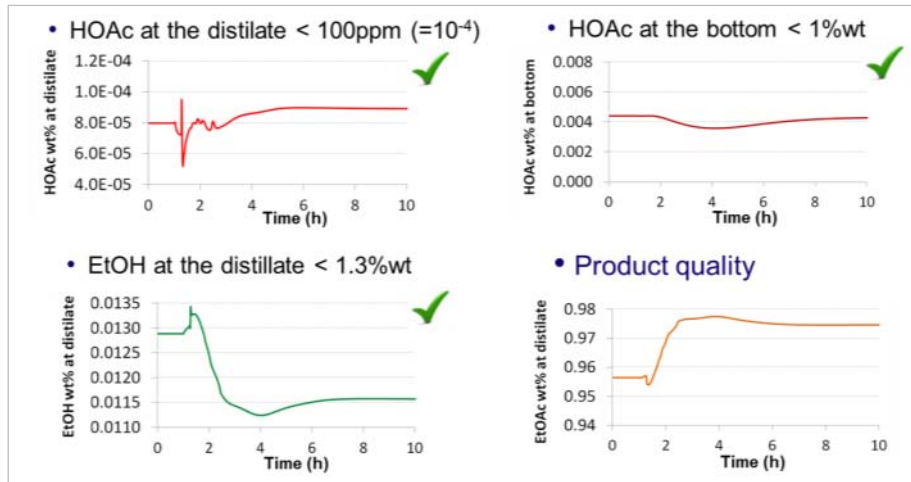


Figure 10.15. Composition control specifications after a decrease of acid feed flow rate, column Design28

A decrease in the acid feed stream results in a new steady-state, with lower production rate and higher ester content in the distillate. The control configuration ensures the reaction conversion of 99.9% of the acetic acid, by reducing the heat duty, the reflux rate and the ethanol feed flow rate.

The same analysis is performed for an increase of 2.5 % of the acid feed stream, for both temperature and composition control loops (Figures 10.16 to 10.19).

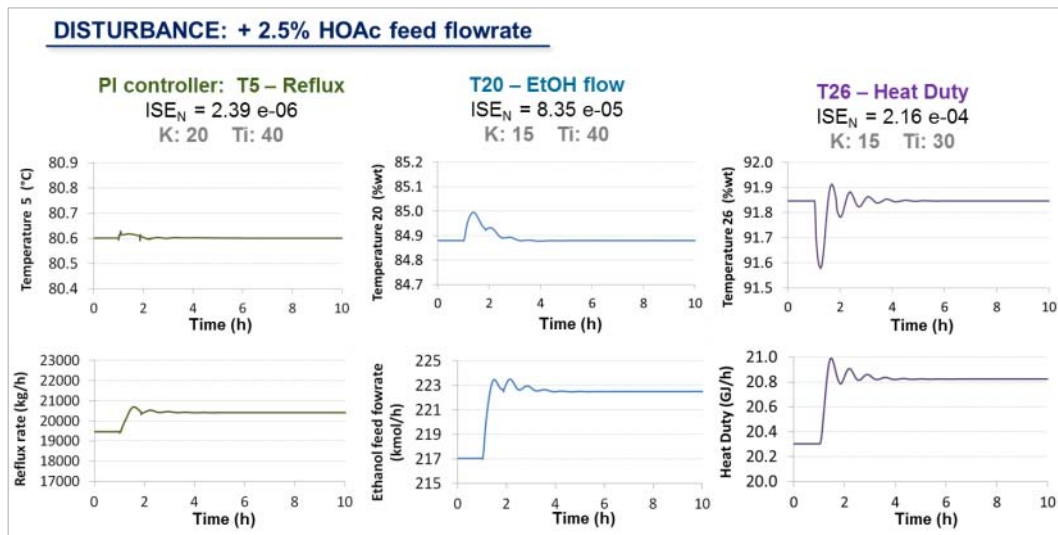


Figure 10.16. Inferential control variables after an increase of acid feed flow rate, column Design28

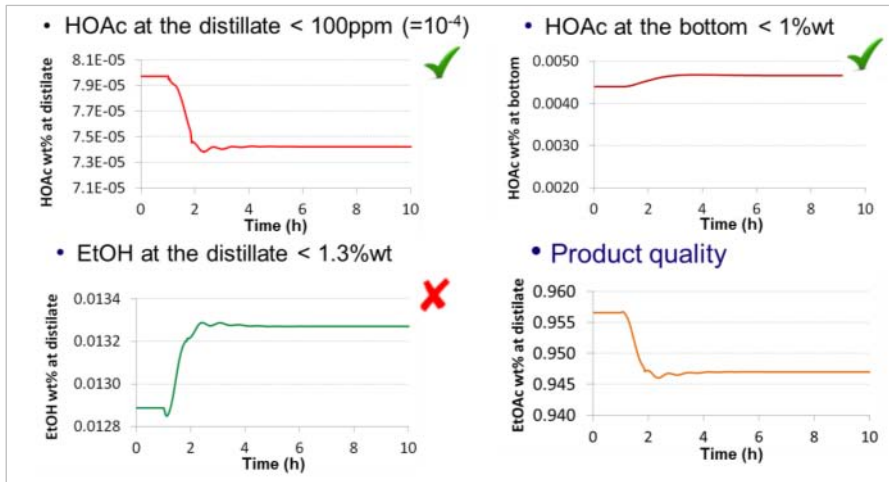


Figure 10.17. Inferential control specifications after an increase of acid feed flow rate, column Design28

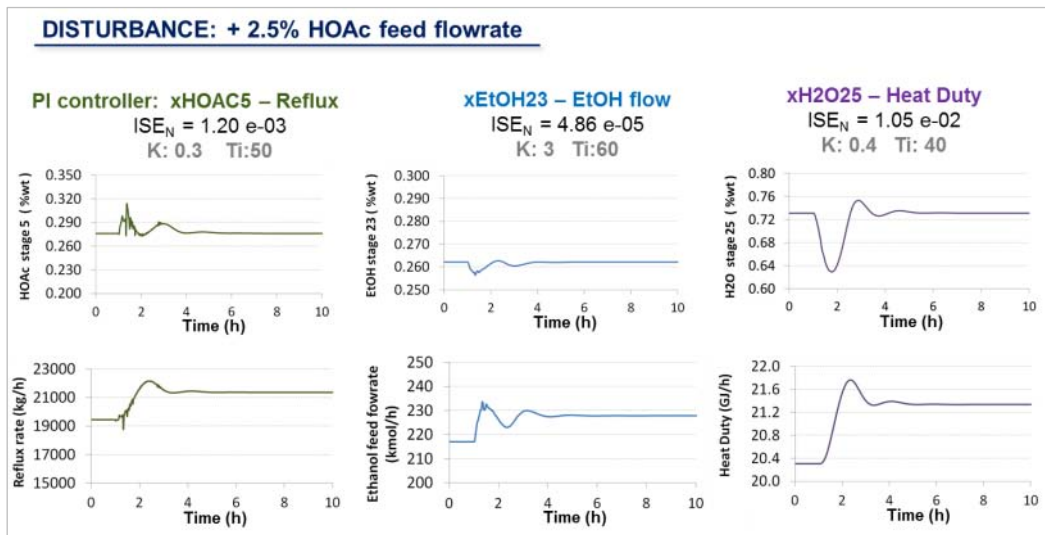


Figure 10.18. Composition control variables after an increase of acid feed flow rate, column Design28

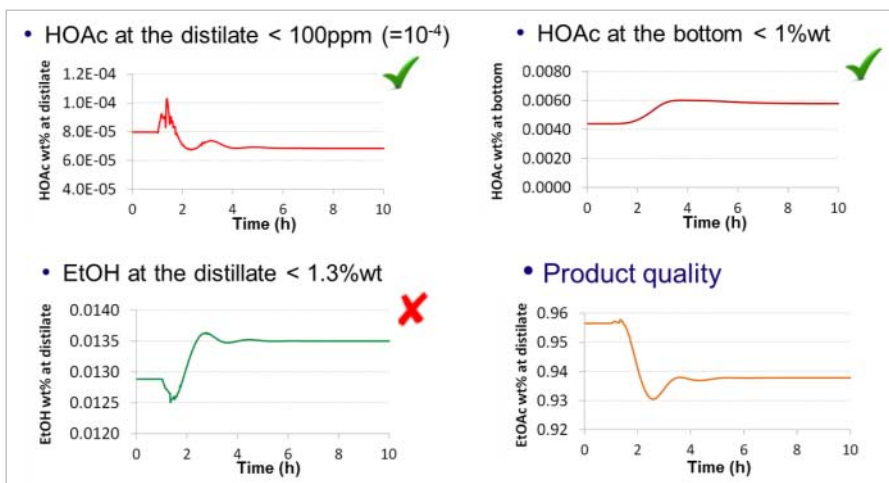


Figure 10.19. Composition control specifications after an increase of acid feed flow rate, column Design28

The increase in the acid feed flow rate strongly affects the esterification reaction. The excess of ethanol decreases, and the control system should compensate its effects, by increasing the heat duty, the reflux rate and the ethanol feed flow rate. However, this new steady-state does not respect of the three product specifications. The control configuration succeeds in maintaining the acid conversion at 99.9%, but the actions required to achieve this objective consequently increase the ethanol content in the distillate and the inherent product specification is no longer respected. The new regime shows higher production rate and smaller ester content in the distillate.

In the present configuration, the PI controllers are concluded to perform well, but the triple-ended control configuration is not sufficient to respect the three specifications after the perturbation that increases the throughput manipulator.

10.4 COMPARISON OF DIFFERENT COLUMN CONFIGURATIONS

In order to generalize the approach and identify some heuristics regarding structural parameters that could provide a better controllability, the methodology is applied to different column configurations. Their comparison is made through the indices values, the dynamic responses and the respect of product specifications.

The further sections present different columns structures, operating under the same nominal regime. These configurations are based on the column *Design28*, with the addition of some stages into each column section, resulting on different relative feed locations.

In order to maintain coherence and an acceptable comparison between the columns, the boil-up ratio was maintained constant for the different configurations. The operating reflux ratio and heat duty were adapted so as to provide a nominal regimes which meet the same product specifications. As a consequence, the similar operating parameters show small difference between the operation costs of the column configurations.

The control of all columns proposed meet the product specifications after the perturbations which increase the water content in the ethanol feed flow and decrease the acid feed flow rate, with accepted response time and few oscillations. We focus in this chapter on the behavior observed after the increase of the acid feed flow rate. The dynamic simulations of different perturbations for each configuration are presented in Appendix V.

10.4.1 Adding separation stages above upper feed stream

If two stages are added in the separation section, the column *Design30a* is obtained. The controllability approach, considering both steady state sensitivities and dynamic responses, is performed.

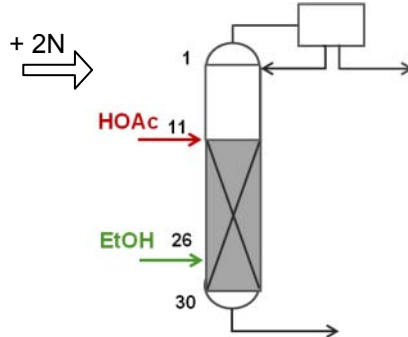


Figure 10.20. Column *Design30a* scheme

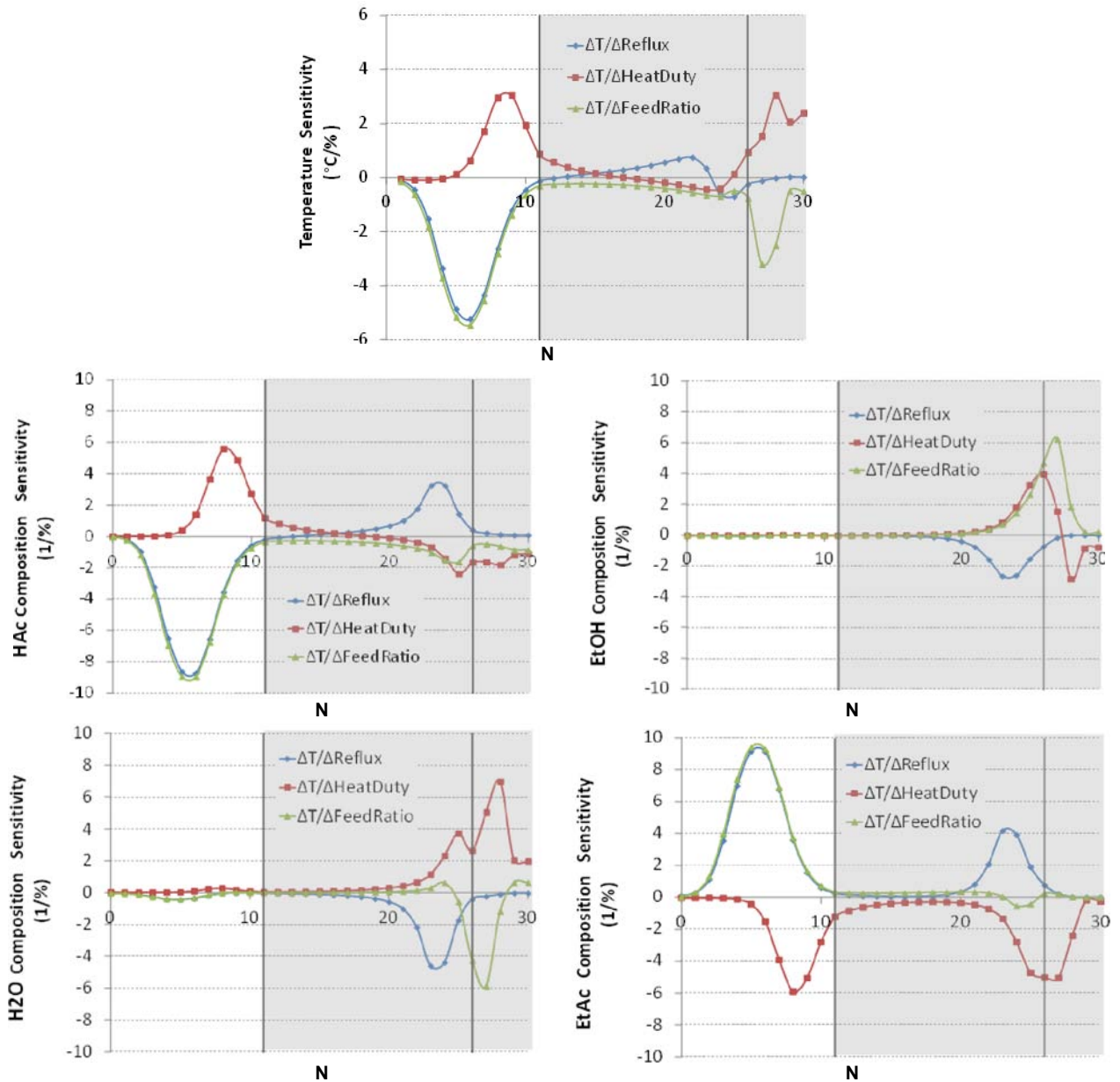


Figure 10.21. Sensitivity matrices of column *Design30a*

When comparing Figure 10.21 to Figures 8.2 and 8.8, which show the sensitivity of column *Design28* sensors, the curves are qualitatively similar, with a higher sensitivity at the separation section of column *Design30a*, which is composed of more stages.

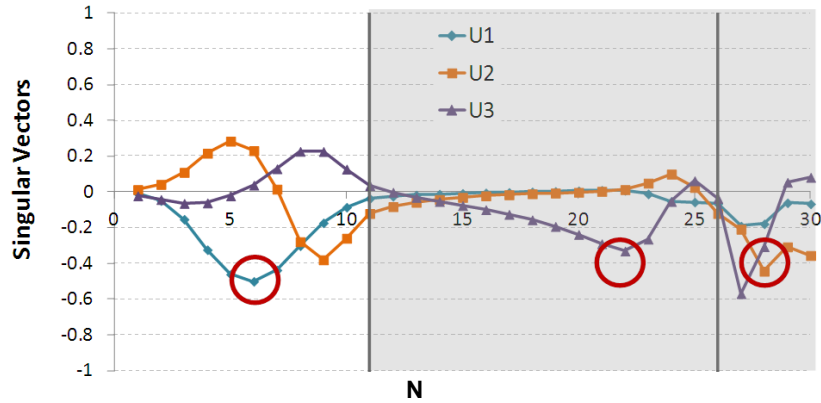


Figure 10.22. Singular vectors matrix considering only temperature sensors, column *Design30a*

$$S_{\text{only } T} = \begin{bmatrix} 14.94 & 0 & 0 \\ 0 & 6.24 & 0 \\ 0 & 0 & 2.97 \end{bmatrix}$$

$$CN_{\text{only } T} = 5.0$$

The temperature sensors located on stages $n^{\circ} 6$, 22 and 28 are selected. Their relative positions are the same as those previously selected for column *Design28*, i.e. one sensor is located at the center of the separation section, a second sensor is few stages above the lower feed position and the third sensor is selected between the lower feed and the bottom of the column. Actually, due to the addition of two stages at the top section, the previous sensors located on stages $n^{\circ} 20$ and 26, are the same measures now located at stages $n^{\circ} 22$ and 28. The specific criteria are calculated:

$$CN_{T6 \ T22 \ T28} = 8.2$$

$$I_{T6 \ T22 \ T28} = 0.12$$

The specific criteria are here calculated in order to give more information about the control structure proposed, because they change as a function of the sensors selected. It is important to mention that the comparison of the column configurations is performed based on the values of the overall criteria. Each configuration has 2 values of overall *CN* – for the consideration of all temperature sensors or all composition and temperature sensors – which remain constant and independent of the control structure selected.

The pairing of the manipulated and the control variables in chapter 8 was obtained from Derived-RGA calculations. Some gains were observed to be difficult, or even impossible, to obtain by the process simulation. However, the results available from the different Derived-RGAs always proposed the same relative configuration: the sensor in the separation section is to be paired with the reflux rate, the sensor located above the ethanol feed position is to be paired with this feed flow rate and the sensor in the bottom section is to be controlled by the heat duty. As a consequence, new Derived-RGAs are not necessarily calculated, but the controlled variables follow the same pairing rules.

The dynamic simulation with the inferential control is reported in Figures 10.23 and 10.24:

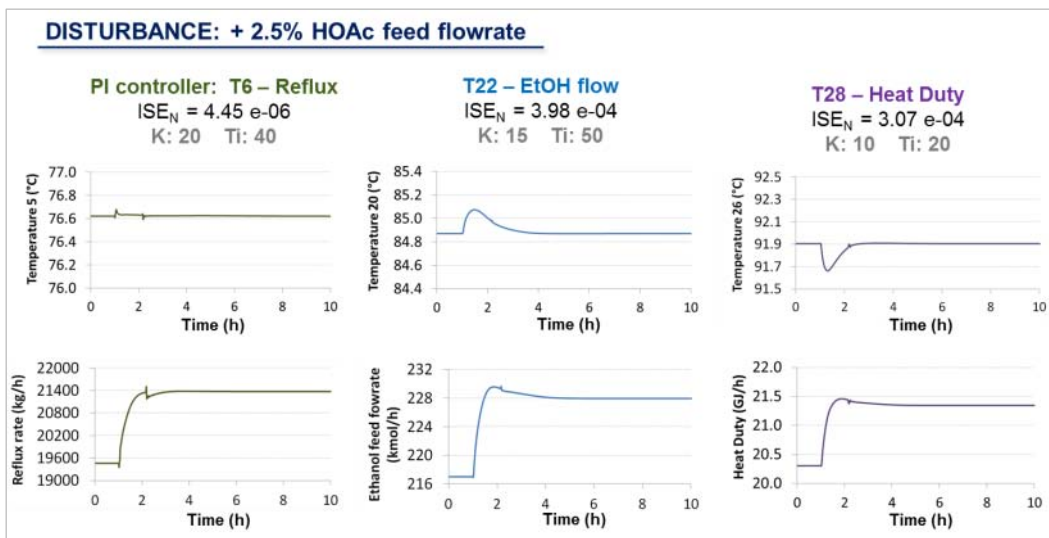


Figure 10.23. Inferential control variables after an increase of acid feed flow rate, column Design30a

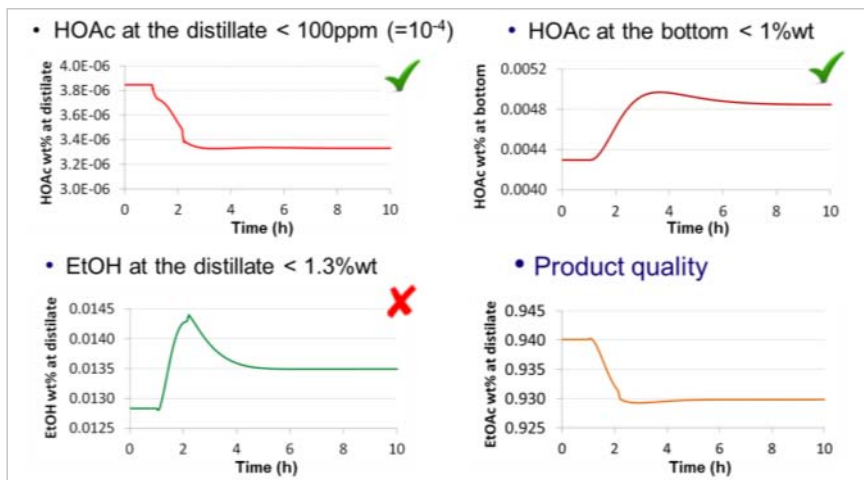


Figure 10.24. Inferential control specifications after an increase of acid feed flow rate, column Design30a

The results of the analysis with the composition sensors are plotted in Figure 10.25:

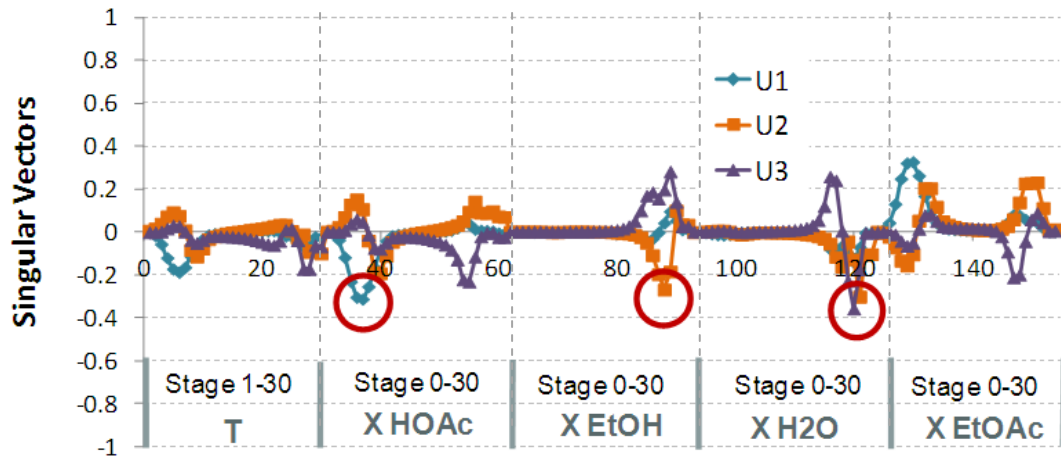


Figure 10.25. Singular vectors matrix considering all sensors, column Design30a

$$S_{all\ measures} = \begin{bmatrix} 39.63 & 0 & 0 \\ 0 & 20.07 & 0 \\ 0 & 0 & 13.05 \end{bmatrix}$$

$$CN_{all\ measures} = 3.0$$

$$CN_{HOAc6\ EtOH25\ H2O27} = 3.2$$

$$I_{HOAc6\ EtOH25\ H2O27} = 1.35$$

The compositions sensors selected are also similar to the ones from the column with 28 stages.

Overall and specific controllability criteria values show greater values than the previous column, reflecting a worse control performance. The addition of separation stages does not really improve the column operability nor the respect of the specifications (Figure 10.26 and 10.27).

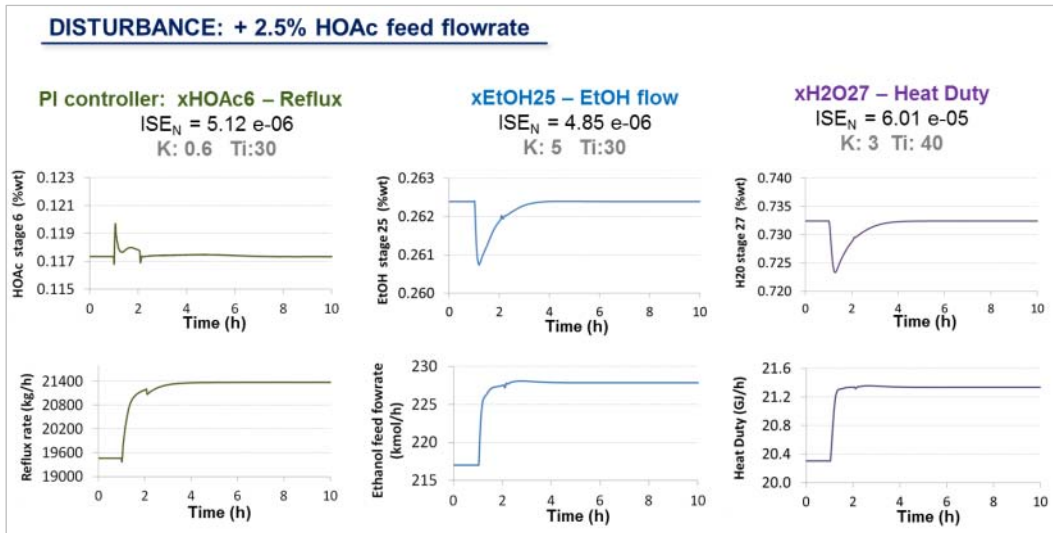


Figure 10.26. Composition control variables after an increase of acid feed flow rate, column Design30a

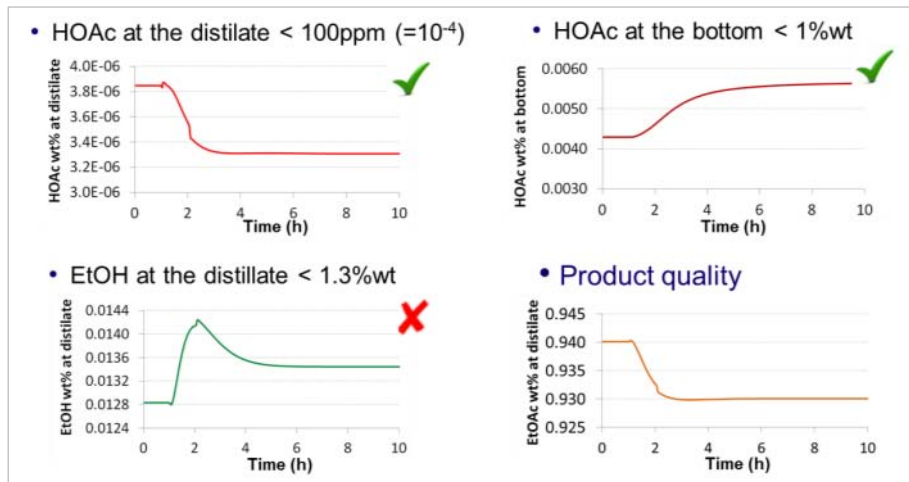


Figure 10.27. Composition control specifications after an increase of acid feed flow rate, column Design30a

10.4.2 Adding reactive stages below the lower feed stream

Another feasible configuration is obtained when two stages are added at the column bottom section, between the lower feed position and the residue output. It is called Design30b (Figure 10.28).

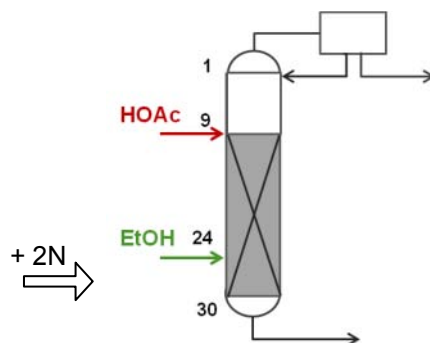


Figure 10.28. Column Design30b scheme

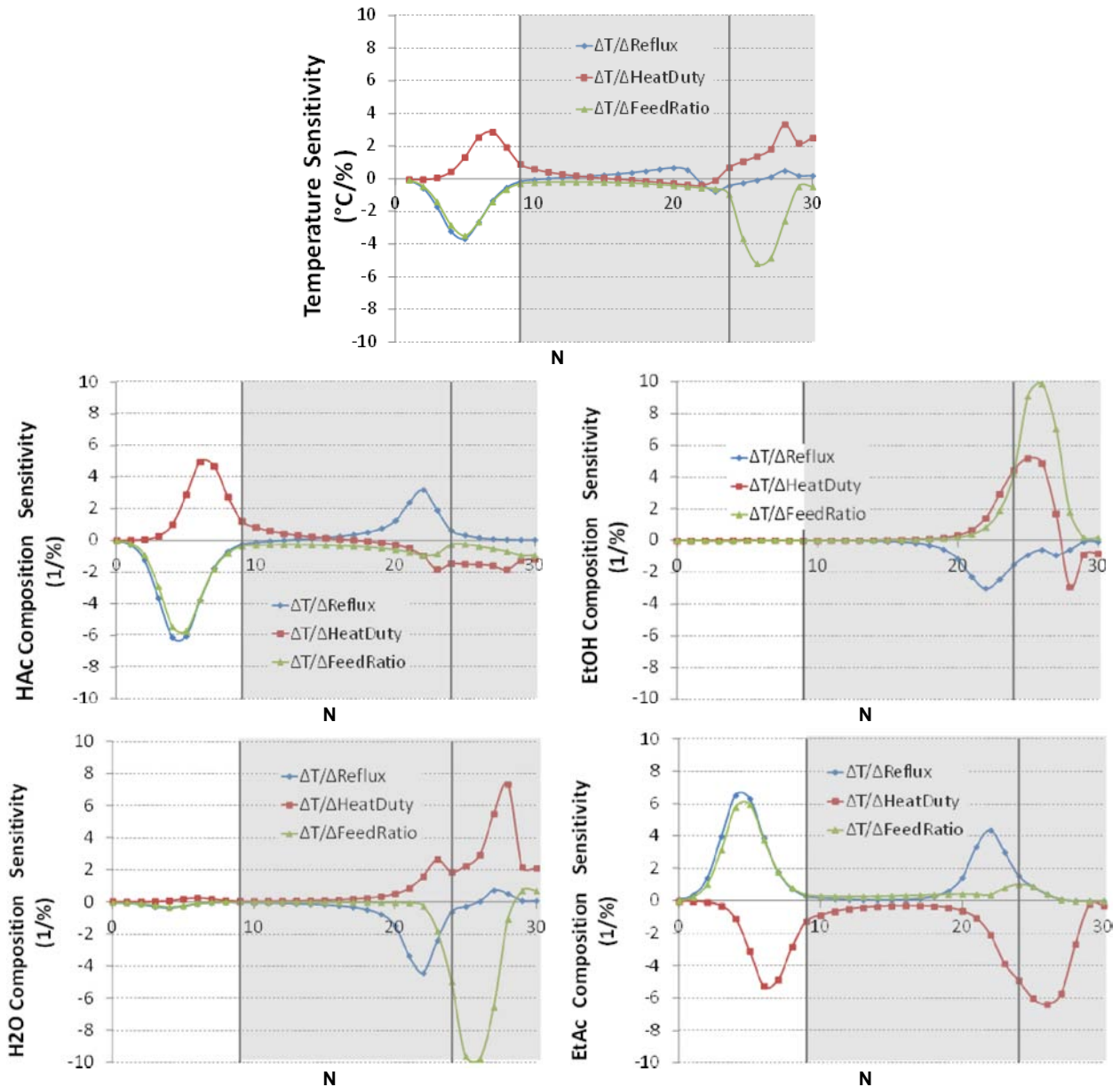


Figure 10.29. Sensitivity matrices of column Design30b

Accordingly to previous observations, when more stages are present in a specific section, the sensitivity of each stage in this section increases. Here, a more important sensitivity is verified at the bottom section of the column. The locations of the selected temperature sensors are similar to those of the other columns. The inferential analysis proposes to control the measures at stages n° 5, 21 and 28.

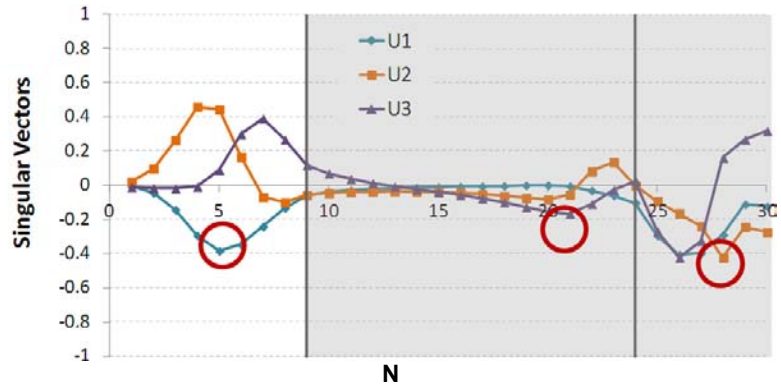


Figure 10.30. Singular vectors matrix considering only temperature sensors, column Design30b

$$S_{onlyT} = \begin{bmatrix} 12.16 & 0 & 0 \\ 0 & 5.24 & 0 \\ 0 & 0 & 4.57 \end{bmatrix}$$

$$CN_{onlyT} = 2.7$$

$$CN_{T5\ T21\ T28} = 7.5$$

$$I_{T5\ T21\ T28} = 0.10$$

The controllability criteria for the inferential control forecast a worse performance than the one in column Design28.

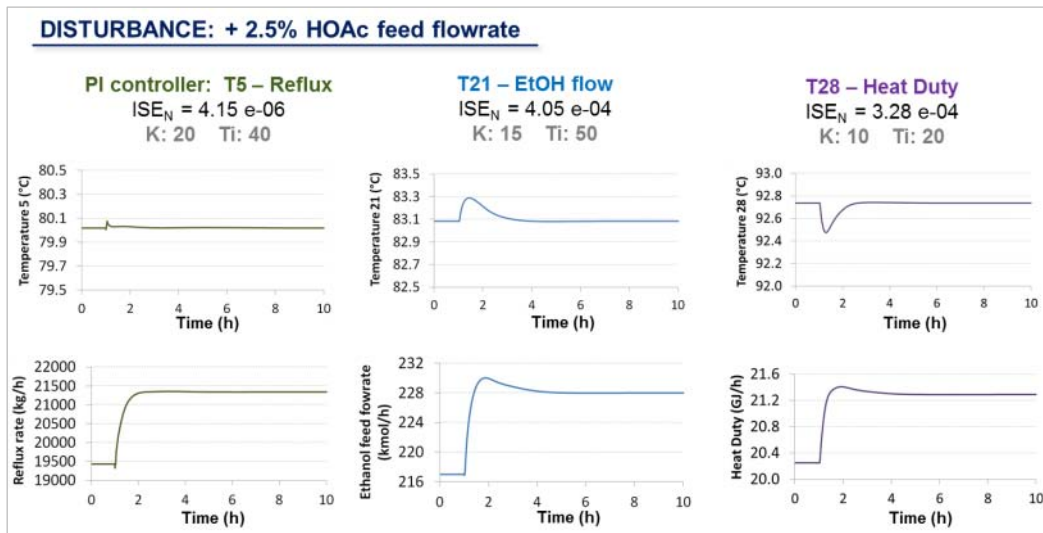


Figure 10.31. Inferential control variables after an increase of acid feed flow rate, column Design30b

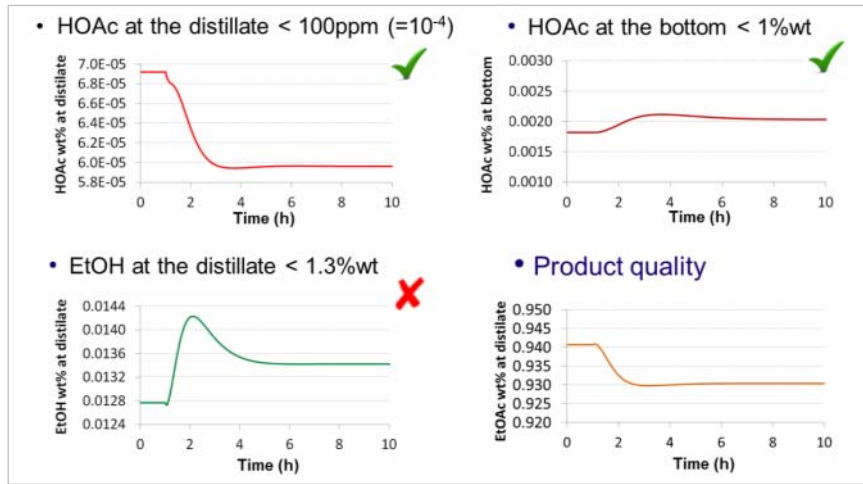


Figure 10.32. Inferential control specifications after an increase of acid feed flow rate, column Design30b

The analysis that considers all measures, however, proposes different sensor locations than the previous approach. Although the stages selected remain near the previous ones, now the water and the ester contents measurements are chosen.

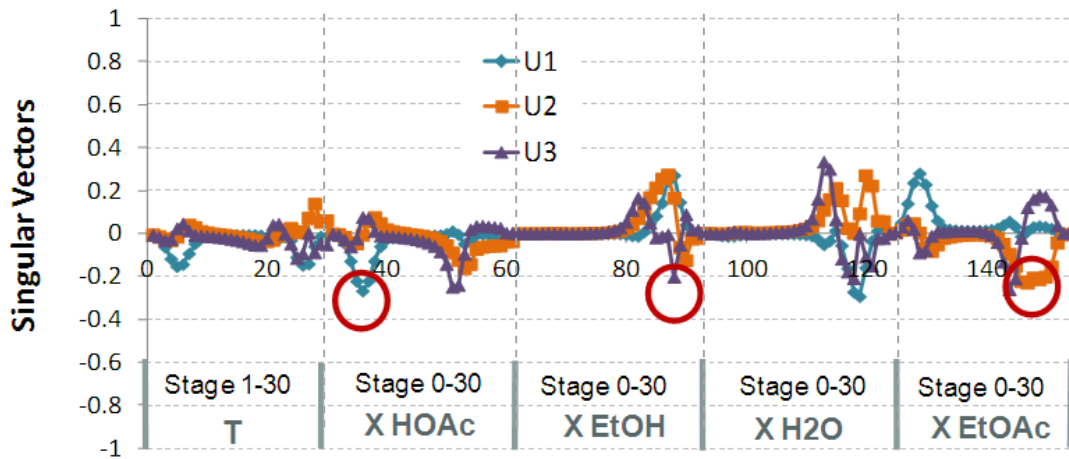


Figure 10.33. Singular vectors matrix considering all sensors, column Design30b

$$S_{all\ measures} = \begin{bmatrix} 32.05 & 0 & 0 \\ 0 & 23.41 & 0 \\ 0 & 0 & 15.40 \end{bmatrix}$$

$$CN_{all\ measures} = 2.1$$

$$CN_{HOAc6\ H2O22\ EtOAc26} = 4.4$$

$$I_{HOAc6\ H2O22\ EtOAc26} = 0.51$$

This control configuration exhibits more oscillations than the previous cases, the controller variables processes back to their set points and the production responses remain similar, i. e. ethanol specification in the distillate is not kept after an increase in the throughput manipulator.

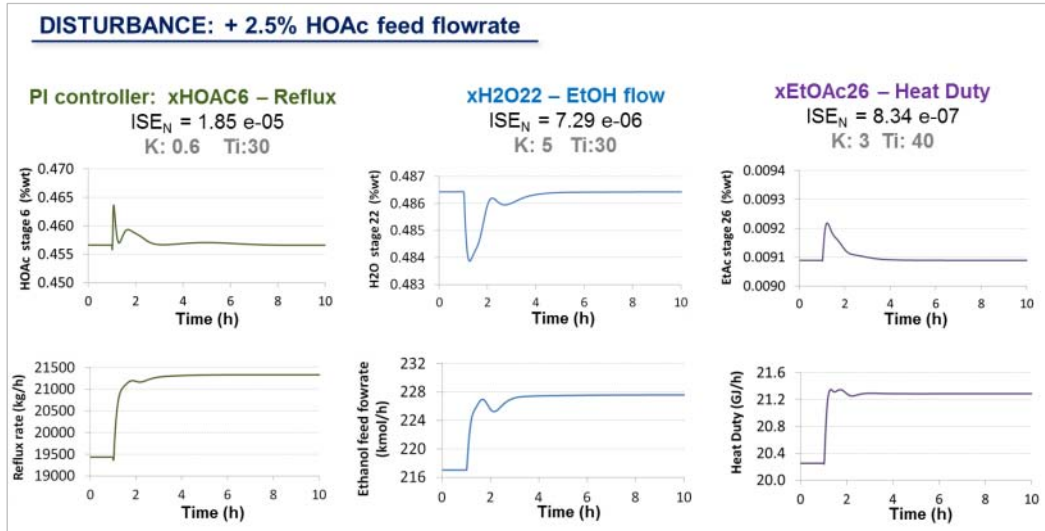


Figure 10.34. Composition control variables after an increase of acid feed flow rate, column Design30b

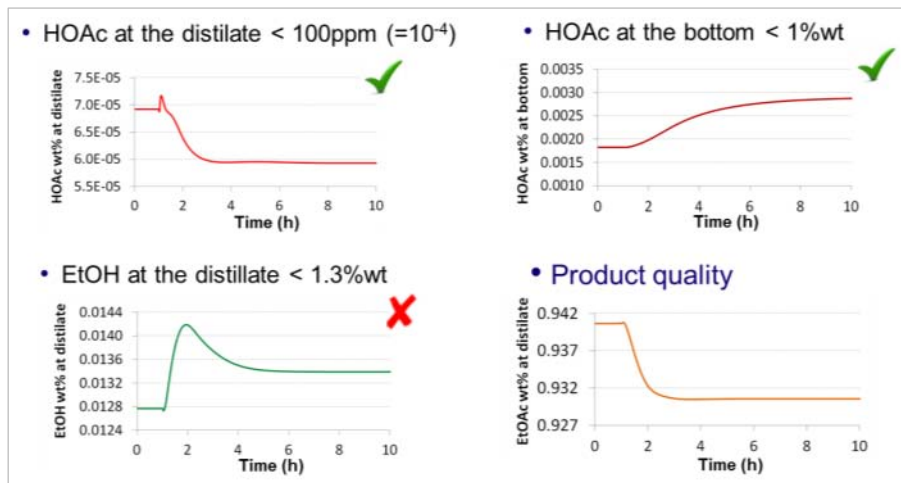


Figure 10.35. Composition control specifications after an increase of acid feed flow rate, column Design30b

The addition of the two stages at the stripping section resulted in a change of lower feed position, which is now located seven stages from the column bottom. Actually, this configuration is similar to column Design21 proposed from the LGC methodology. The action of improving the number of stages at the bottom of the column does not present a better controllability of this RD column. Accordingly, the previous choice of column Design16 as more controllable than column Design21 is validated.

10.4.3 Adding reactive stages between feed stages

Two stages are added between the feed locations, the zone where the reaction mainly occurs. The new configuration is referenced as *Design30c* (Figure 10.36).

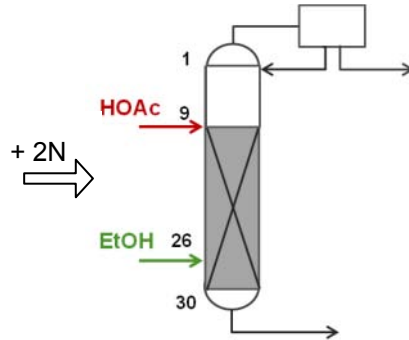


Figure 10.36. Column Design30c scheme

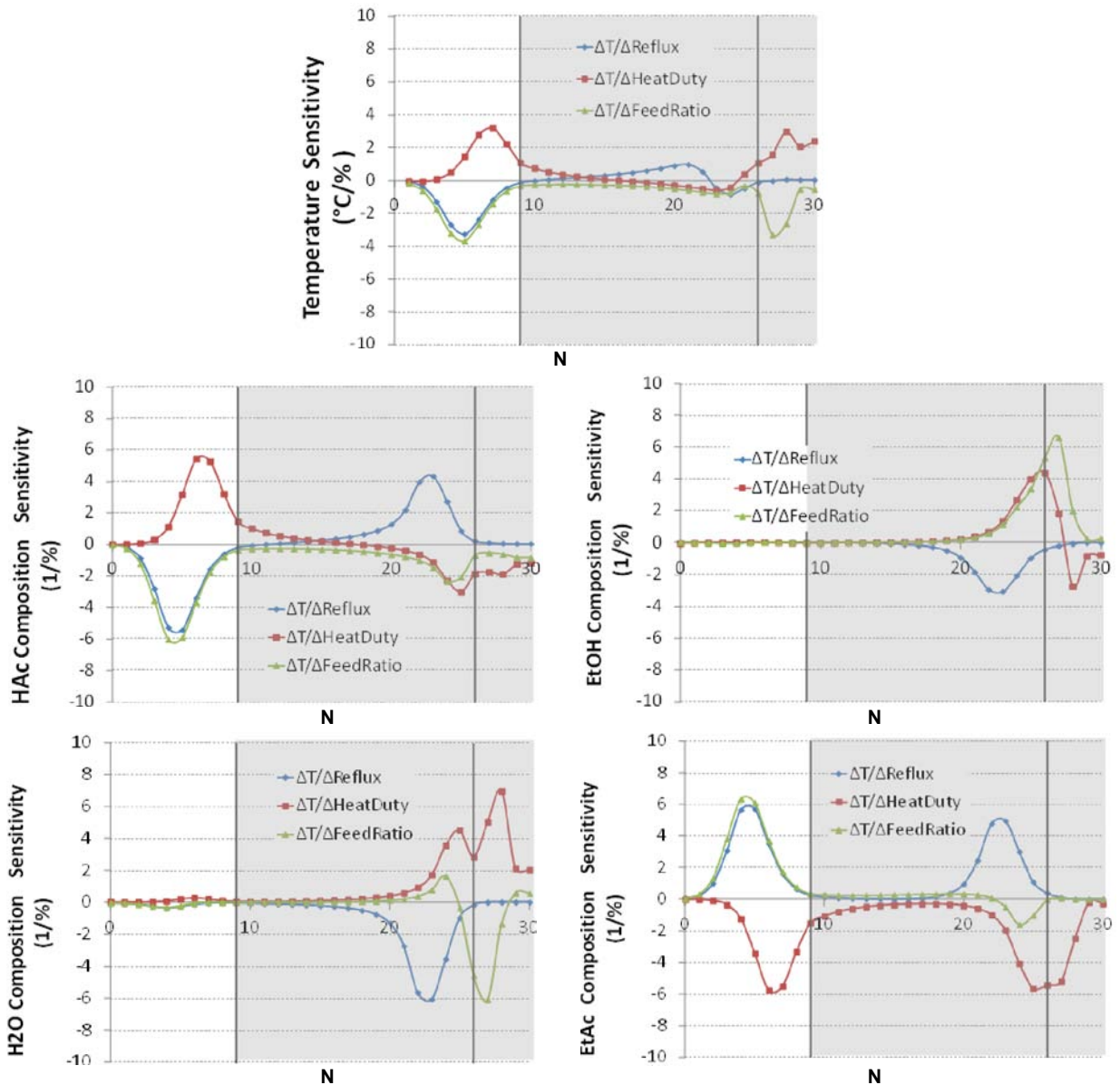


Figure 10.37. Sensitivity matrices of column Design30c

Temperature sensors are selected at stages n° 5, 21 and 28. Both overall and specific controllability criteria reveal a better performance of this new configuration, as verified by the low *ISE* values calculated from the dynamic simulations.

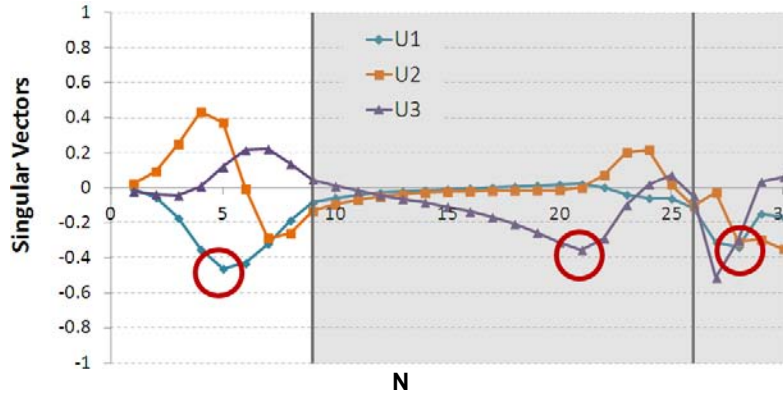


Figure 10.38. Singular vectors matrix considering only temperature sensors, column Design30c

$$S_{onlyT} = \begin{bmatrix} 10.39 & 0 & 0 \\ 0 & 4.86 & 0 \\ 0 & 0 & 3.34 \end{bmatrix}$$

$$CN_{onlyT} = 3.1$$

$$CN_{T5\ T21\ T28} = 5.6$$

$$I_{T5\ T21\ T28} = 0.19$$

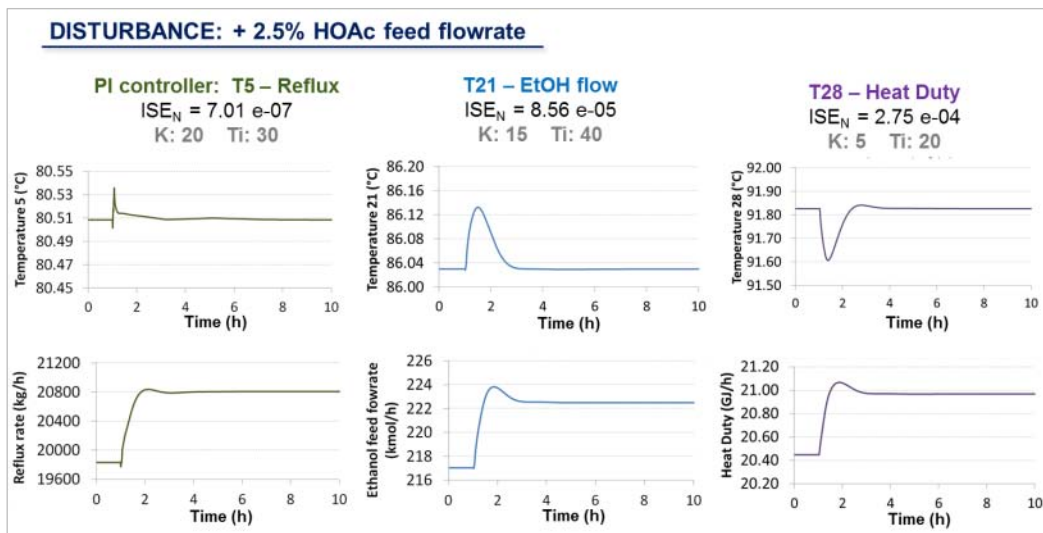


Figure 10.39. Inferential control variables after an increase of acid feed flow rate, column Design30c

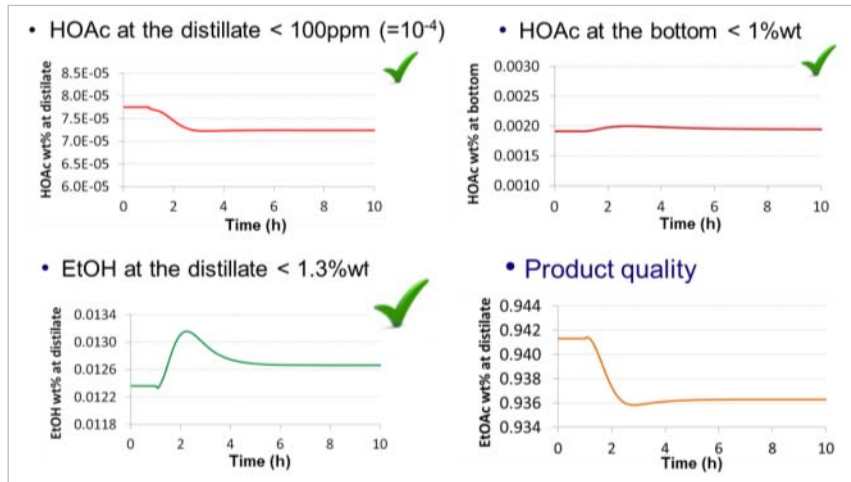


Figure 10.40. Inferential control specifications after an increase of acid feed flow rate, column Design30c

The ethanol specification is still met after the perturbation, showing a better operability of the Design30c configuration. Actually, the addition of reactive stages in the middle section of the column results in a nominal operating regime with more relaxed constraints, providing flexibility for the key compositions to receive the column perturbations.

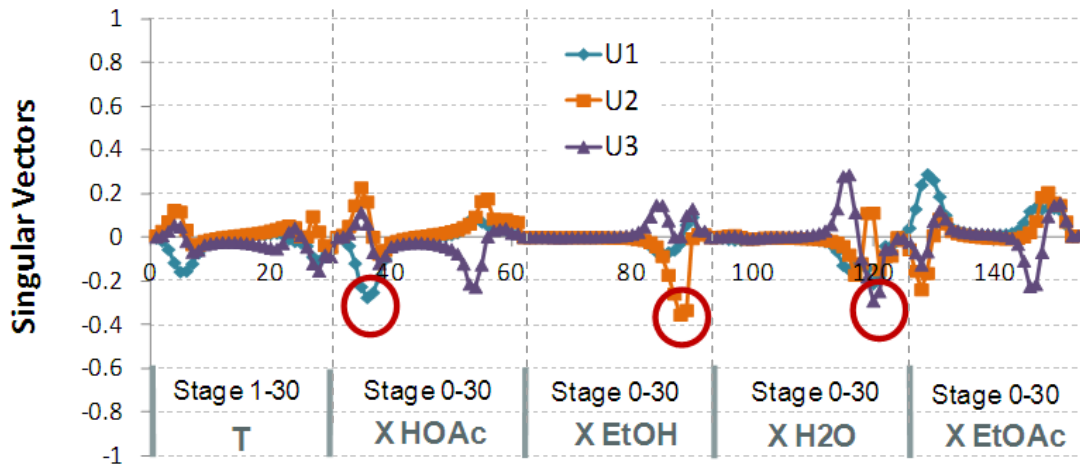


Figure 10.41. Singular vectors matrix considering all sensors, column Design30c

$$S_{all\ measures} = \begin{bmatrix} 29.08 & 0 & 0 \\ 0 & 19.35 & 0 \\ 0 & 0 & 15.22 \end{bmatrix}$$

$$CN_{all\ measures} = 1.9$$

$$CN_{HOAc5\ EtOH25\ H2O27} = 2.7$$

$$I_{HOAc5\ EtOH25\ H2O27} = 1.47$$

The overall criteria for all the measures and the specific criteria which consider a set of compositions also provide better controllability. The ethanol content specification in the distillate is also met after the perturbation under composition control.

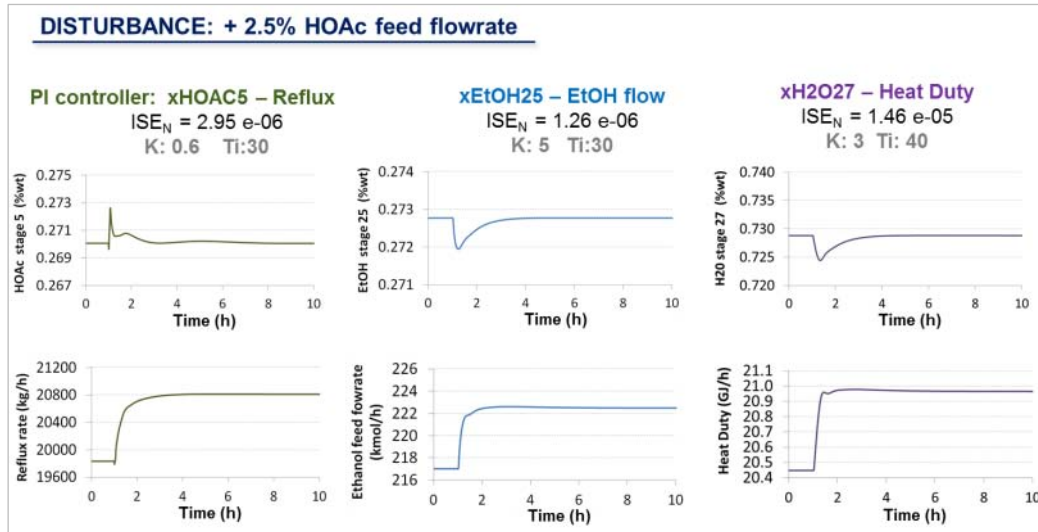


Figure 10.42. Composition control variables after an increase of acid feed flow rate, column Design30c

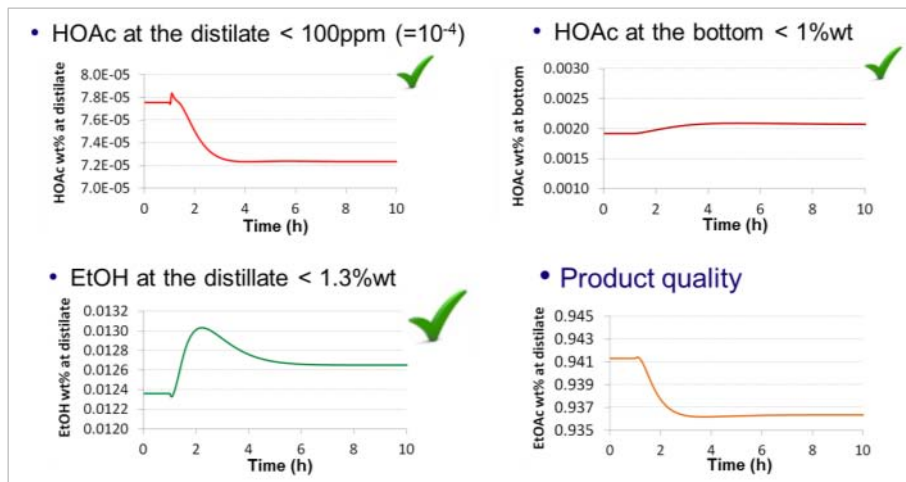


Figure 10.43. Composition control specifications after an increase of acid feed flow rate, column Design30c

Furthermore, Section 8.2.1 proposed a control configuration with a temperature measure at the top separation section and two composition control loops at the bottom of the column. It was verified that a temperature sensor may reliably replace a composition control in the separation stages. This control configuration also shows good performance for the column *Design30c*.

$$CN_{T5 \text{ EtOH25 H2O27}} = 2.9$$

$$I_{T5 \text{ EtOH25 H2O27}} = 1.04$$

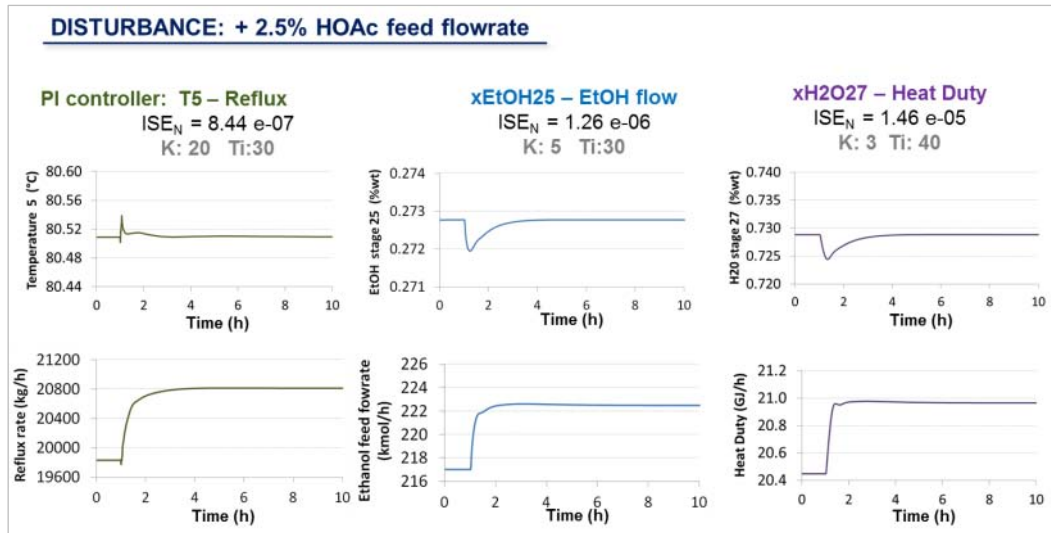


Figure 10.44. Temperature and Composition control variables after an increase of acid feed flow rate, column Design30c

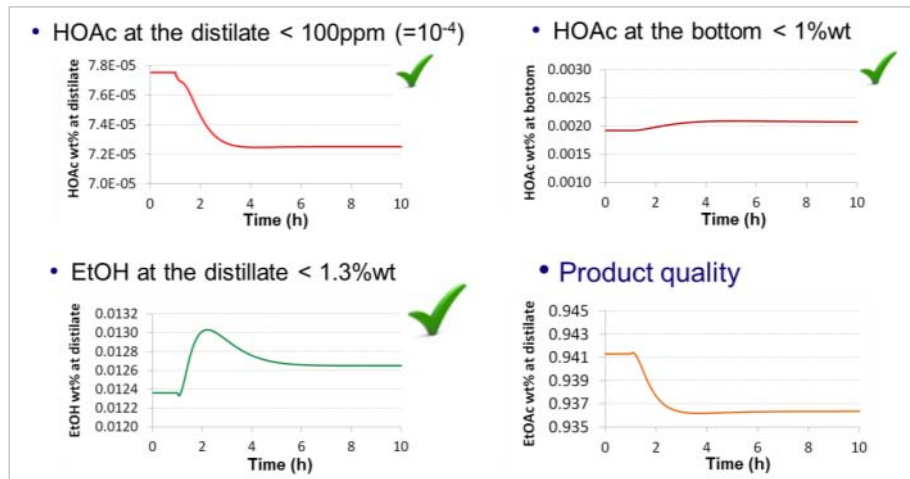


Figure 10.45. Temperature and Composition control specifications after an increase of acid feed flow rate, column Design30c

10.5 CONCLUSIONS

Chapter 10 shows the interests of the suggested controllability methodology described in Part IV. One of the PhD concerns, considering controllability aspects as early as the design step of reactive distillation columns is fully applied here to the ethyl acetate case study. Different feasible configurations were proposed as the result of the pre design methodology, and the calculation of the controllability criteria allows the choice of one configuration, anticipating its performance in plant operation.

An industrial configuration is then determined, in which a decanter is added and stringent specifications have to be met. By changing the number of stages in each column's section, the relative feed positions change and new configurations have been studied. The controllability methodology, considering both steady-state and dynamic behaviors, was conducted for all configurations and some key heuristic rules that provide better controllable columns were identified.

The details of each column configuration, operating parameters and sensors selected are reminded in Table 10.1. The configuration which showed the best controllability was column *Design30c*.

Table 10.1. Controllability criteria for the column configuration analysis

Column configuration	Total number of theoretical stages	HOAc feed position	EtOH feed position	Number of reactive stages	Number of separation stages	Reflux ratio	Heat duty (kW)	Selected temperature sensors	Selected composition sensors
<i>Design28</i>	28	9	24	20	8	1.15	5635	T 5 T 20 T 26	HOAc 5 EtOH 23 H ₂ O 25
<i>Design30a</i>	30	11	26	20	10	1.16	5635	T 6 T 22 T 28	HOAc 6 EtOH 25 H ₂ O 27
<i>Design30b</i>	30	9	24	22	8	1.15	5625	T 5 T 21 T 28	HOAc 6 H ₂ O 22 EtOAc 26
<i>Design30c</i>	30	9	26	22	8	1.18	5680	T 5 T 21 T 28	HOAc 5 EtOH 25 H ₂ O 27

The calculated criteria are presented in Table 10.2:

Table 10.2. Controllability criteria for the column configuration analysis

Column configuration	Overall CN	Specific CN	Specific I
<i>Design28</i>	$CN_{\text{onlyT}} = 3.5$ $CN_{\text{all measures}} = 2.2$	$CN_{T5, T20, T26} = 6.5$ $CN_{\text{HOAc5, EtOH23, H2O25}} = 2.8$	$I_{T5, T20, T26} = 0.14$ $I_{\text{HOAc5, EtOH23, H2O25}} = 1.36$
<i>Design30a</i>	$CN_{\text{onlyT}} = 5.0$ $CN_{\text{all measures}} = 3.0$	$CN_{T6, T22, T28} = 8.2$ $CN_{\text{HOAc6, EtOH25, H2O27}} = 3.2$	$I_{T6, T22, T28} = 0.12$ $I_{\text{HOAc6, EtOH25, H2O27}} = 1.35$
<i>Design30b</i>	$CN_{\text{onlyT}} = 2.7$ $CN_{\text{all measures}} = 2.1$	$CN_{T5, T21, T28} = 7.5$ $CN_{\text{HOAc6, H2O22, EtOAc26}} = 4.4$	$I_{T5, T21, T28} = 0.10$ $I_{\text{HOAc6, H2O22, EtOAc26}} = 0.51$
<i>Design30c</i>	$CN_{\text{onlyT}} = 3.1$ $CN_{\text{all measures}} = 1.9$	$CN_{T5, T21, T28} = 5.6$ $CN_{\text{HOAc5, EtOH25, H2O27}} = 2.7$ $CN_{T5, \text{EtOH25, H2O27}} = 2.9$	$I_{T5, T21, T28} = 0.19$ $I_{\text{HOAc5, EtOH25, H2O27}} = 1.47$ $I_{T5, \text{EtOH25, H2O27}} = 1.04$

Although the number of theoretical stages and feed positions change, the relative position of the selected controlled variables remains the same for the different column configurations: one sensor is located in the middle of the top separation section, a second sensors is located few stages above the lower feed position and a third sensor is selected at the bottom section, between the lower feed position and the residue output. This result could become a heuristic key-rule to design reactive distillation columns with double-feed configuration.

If higher sensitivity is sought in a specific column section, additional stages should be added, but the resulting control performance does not show important improvements. The addition of stages between the two feed positions, however, clearly improves the controllability and operability of the column, because the nominal operating regime gives more flexibility for the specifications to change and to continue to meet the production requirements.

This approach regarding the process dynamic behavior is shown to be important on forecast process conditions and designing a column adapted for the most important perturbations the system may encounter. The controllability criteria are reliable measures of the column operability and the proposed method can be added to the LGC methodology for the design of reactive distillation columns.

Experimental understanding of the
controllability approach

The success of the controllability and diagnosability studies is based on the correct selection of the controlled and of the manipulated variables. The previous chapters gave special attention to the impacts of the controlled variables, by observing their sensitivities, balances and interferences. This chapter will also detail the importance of good selection of the manipulated variables.

The real reactive distillation column presented in chapter 3 was used for an experimental study regarding the process sensitivity and stability. The controllability methodology is applied and some important remarks are qualitatively analyzed.

11.1 UNDERSTANDING THE PROCESS DEGREES OF FREEDOM

The degree of freedom of a process is defined by the number of process variables that need to be specified so as to determine the remaining unknown (output) variables. When the number of specified variables equals the number of independent equations, the system is said to be uniquely specified. If an incorrect number of manipulated variables is chosen, multiple or inconsistent solutions or no solution at all will be found (Henley and Seader, 1981). The process degree of freedom can thus be determined by:

$$N_{Degree} = N_{Variable} - N_{Equation}$$

N_{Degree} : degrees of freedom

$N_{Variables}$: number of process variables

$N_{Equation}$: number of independent equations that describe the process

The number of independent manipulated variables can be expressed:

$$N_{Manipulated} = N_{Degree} - N_{External} = N_{Variables} - N_{Equations} - N_{External}$$

$N_{Manipulated}$: number of manipulated variables

$N_{External}$: number of state variables externally defined by the environment, which are constrained and not free to be manipulated by the control system

$$N_{Manipulated} \geq N_{Controlled}$$

$N_{Controlled}$: number of controlled variables

Seider et al. (1999) stated that when a control loop is introduced by pairing a manipulated variable with a controlled output, the manipulated variable degree of freedom is transferred to the output set point, which becomes the new independent variable. As a result, a reliable controllability study of a reactive distillation process needs to carefully understand the system degree of freedom and identify the appropriate manipulated variables.

The reactive distillation process studied so far has been presented in a double-feed configuration, with three degrees of freedom. Thus, the three manipulated variables chosen were the heat duty, the reflux ratio and the flow rate of the ethanol feed stream. The controllability methodology developed in chapters 7, 8 and 10 focuses on the selection of the most sensitive compositions or temperature measures to be paired with each manipulated variable in the three control loops.

Actually, in the major industrial columns, the operating regime is defined by manipulating the heat duty, the reflux ratio or reflux rate, and the flow rate of some of the feed streams. This configuration is presented in Figure 11.1. During an operating regime, heat is brought to the reboiler and, as a function of the vaporization enthalpy of the inner solution, vapor is produced from the boiling liquid. The vapor flows upward into the column, going through the distillation trays, and is condensed at the top. As a consequence of the fixed reflux ratio and the level regulation in the sump, the distillate flow rate is determined as an output variable. At the bottom of the column, there is also a level control, so that the flow rate of the outlet stream changes by respecting the column mass balance. Moreover, due to the double-feed configuration, the ratio of the inlet streams is one additional operating parameter to be defined. In conclusion, the three manipulated variables – heat duty, reflux ratio and inlet feed stream – are the independent degrees of freedom.

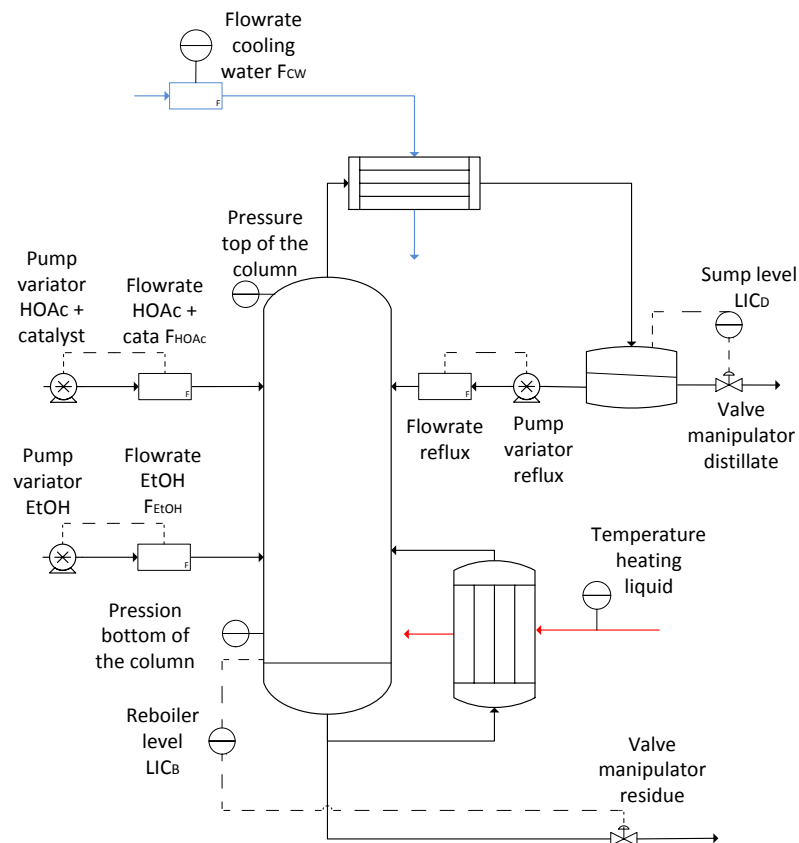


Figure 11.1. Configuration and instrumentation of a typical industrial distillation column

However, some column configurations might differ from the characteristics presented above. As the objective of this chapter is to better understand the controllability analysis through an experimental approach, the first step is the comprehension of the underspecified variables in the real column. The pilot configuration and instrumentation is presented in Figure 11.2.

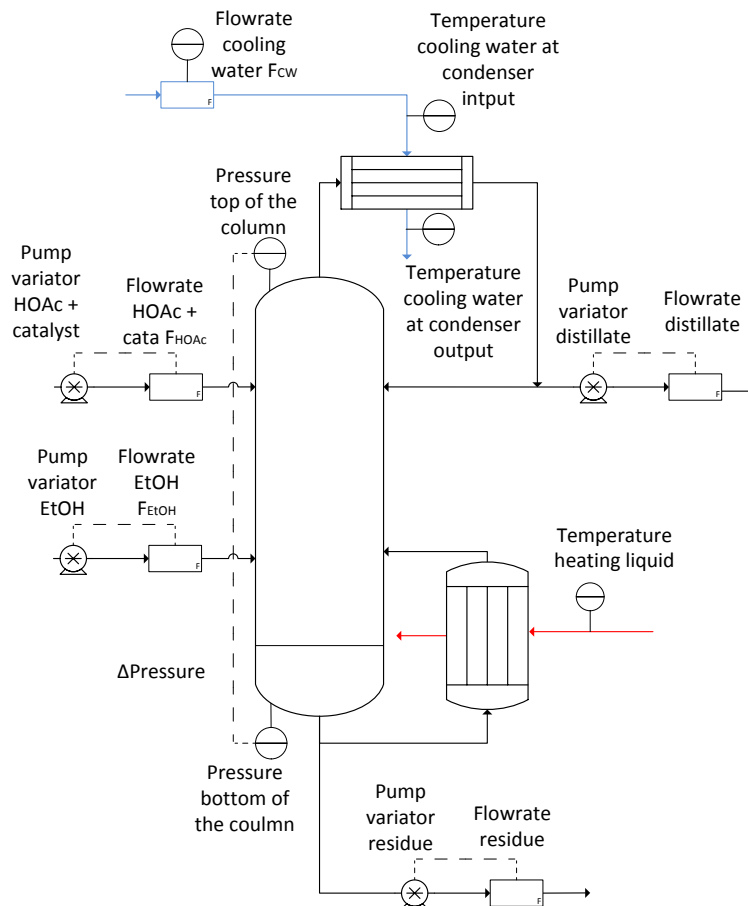


Figure 11.2. Configuration and instrumentation of the pilot distillation column

Actually, the pilot configuration at our disposal for this experimental part is not similar to the column presented in Figure 11.1 and this understanding is crucial for a good system operation. The main differences are that the distillate flow rate is now defined by the pump flow variations and there is no level regulation in the reboiler. Hence, if a similar reasoning is conducted, the heat given to the reboiler produces vapor, which flows upward into the column and condenses at the top. As the distillate outlet flow is fixed, the reflux rate is a consequence of the amount of liquid coming from the condenser and the sump level regulation. The reboiler liquid level may change, but the bottom stream flow rate is directly defined by the pump flow variation so as to meet the column mass balance. Thus, the three independent operating variables to be determined are heat duty, distillate flow rate and an inlet feed stream.

In both column configurations (typical industrial and pilot plant), pump flow variations determine the flow of inlet streams and the energy transfer in the reboiler and in the condenser are given by the heating liquid and the cooling water, respectively.

Both configurations would perform well during steady state regimes. However, when the system is under transient behavior, the second configuration shows higher difficulty in reaching stabilization. In fact, when compositions in the reboiler evolve, vaporization enthalpies change and a constant heat duty will result in different amounts of vapor produced. In the first configuration, the reflux rate is fixed so the changes on vapor flow will affect the distillate flow rate; the dynamic behavior is reflected on an output parameter and the column stabilizes in a new regime. In the second configuration, the distillate flow rate is fixed, so the changes on vapor flow will affect the column reflux, one operating parameter directly related to the attainable compositions; for example, a higher reflux increases the lighter component content inside the column and, as a consequence, a constant heat duty will provide more vapor, which results in higher reflux and so on; the system will not stabilize. This phenomenon was experimentally verified.

Figure 11.3 shows an unstable behavior during approximately 50h of experiment, when the three degrees of freedom – heat duty, distillate flow rate and ethanol feed flow – were kept constant.

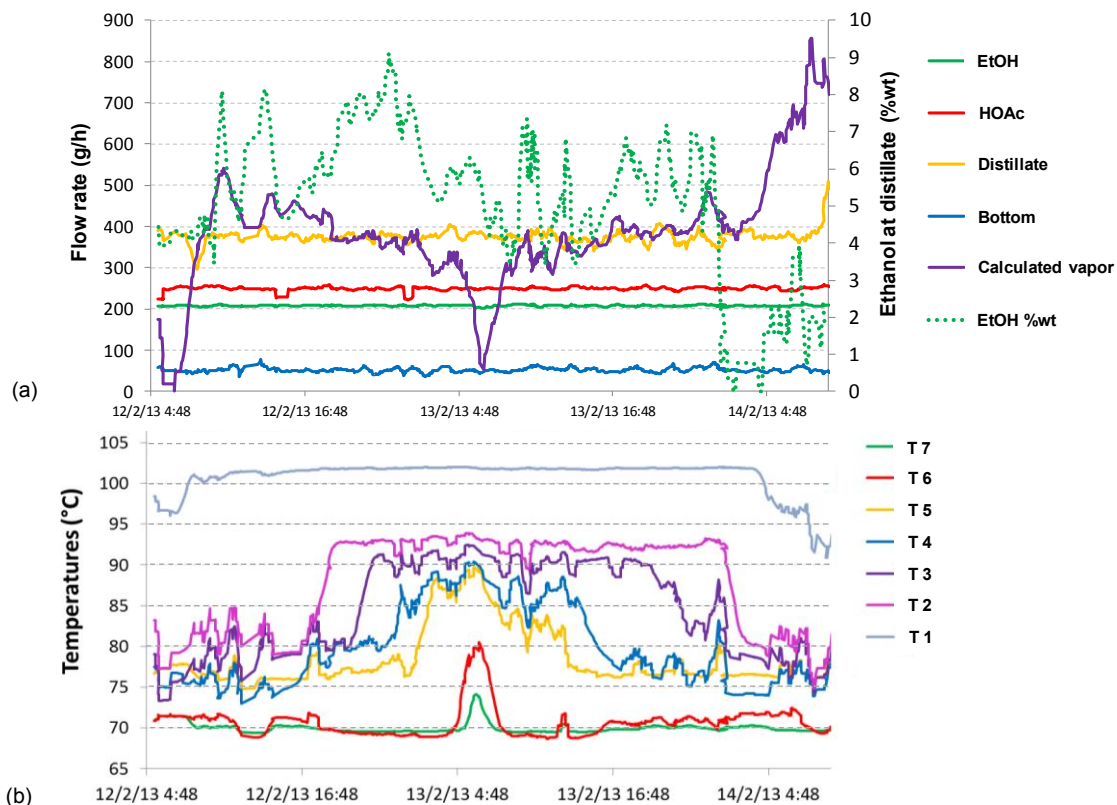


Figure 11.3. Experimental unstable behaviors of (a) streams flow rates and (b) column temperatures

As presented in chapter 3, the column has six modular sections and one liquid distributor on the top of each section, where a measurement of temperature is performed. The pilot was schematized in Figures 3.7 and 3.10. An additional temperature measurement is located in the reboiler liquid, which results in seven temperature measurements, numbered from the bottom to the top of the column. The two top sections are dedicated to separation, no reaction occurs in these parts. The acid and the homogeneous catalyst are fed at the liquid distributor n°5 and the alcohol is introduced below at distributor n°2.

The experimental unstable behavior suggests some comments. The pilot instrumentation allows the introduction of control loops to manipulate the three independent variables.

The first system operability improvement was conducted by introducing a control loop that calculates the vapor produced, in function of the distillate compositions and condenser inlet and outlet temperatures, and manipulates the heat duty. The objectives are to keep a constant vapor flow rate and to balance the impacts of the reboiler composition on the vaporization ratio; the reboiler composition may change but the heat provided will be manipulated so as to produce a constant amount of vapor.

Now the vapor produced is fixed by the control loop and the distillate rate is fixed by the pump flow variation. Thus, the reflux rate becomes a fixed value given by the mass balance. As a result, the column disturbances cannot change the top streams flow; the consequences will be seen on its compositions. Under this configuration, the column is better operated, but the production quality is not mastered.

The second improvement on operability can be expected by the introduction of another control loop to regulate the distillate flow rate. The column dynamic disturbances can influence the flow rate of the distillate, and the production quality can be maintained. The controllability methodology proposed is thus applied for selecting the appropriate controlled variable.

11.2 APPLICATION OF THE CONTROLLABILITY CALCULATIONS

The controllability methodology defined in the previous chapters was conceived based on the dynamic response of the process to some disturbances; the objective was the return of the system to its nominal steady state. The same approach can be applied here; the objective is now the stabilization of the system with respect to unstable operating conditions. The analyses are adapted to the pilot configuration and the sensors sensitivities are identified.

First, a representative simulation model was obtained for the pilot. The software Aspen Plus[®] was used and the definition of the model parameters considered the approach presented in chapter 6. The intrinsic parameters such as the thermodynamics and kinetics were the ones presented in chapter 9. The operational variables such as flow rates, pressure and heat duty were adapted from the experiment conditions. The column was filled with bubble cap trays so as to enhance the liquid holdup for homogeneous catalyst. The values given by the manufacturer propose the column representation by 35 theoretical equilibrium stages, and the geometric calculation plus pilot observations result in about 20ml of liquid holdup per stage.

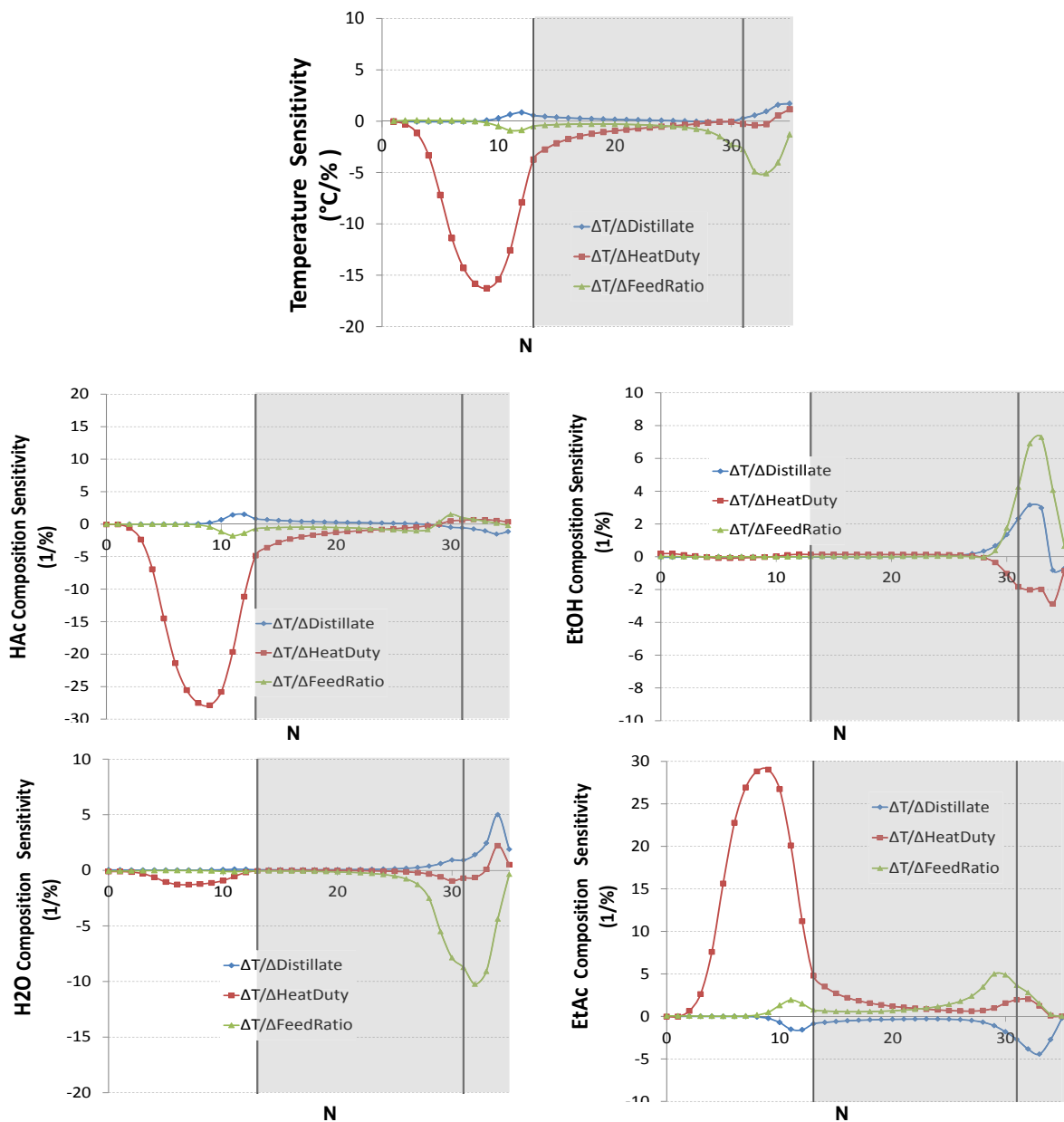


Figure 11.4. Sensitivity matrices of the pilot column

The pilot sensitivity is to be calculated in function of the existing degrees of freedom. Hence, the calculations are adapted to consider the heat duty, the distillate flow rate and the ethanol feed flow rate.

Figure 11.4 shows the sensitivity of each possible measurement. The grey area accounts for the reactive section and the feed positions are represented by a dark vertical line.

The RD column sensitivity results are coherent to those presented in the previous chapters. The pilot plant is also a hybrid reactive column, with a rectifying section solely dedicated to separation. The most sensitive measurements are the temperatures and the contents of acetic acid and ethyl acetate in the separation section, and the temperatures and the contents of ethanol and water around the lower feed position.

Online composition measurements were only available at the output streams. As online temperature measurements were present on each liquid distributor, the following steps of the controllability study will consider only temperature variables. The Singular Value Decomposition is presented in Figure 11.5. The physical locations of the temperature sensors are pointed by the vertical arrows, by supposing a linear distribution of the theoretical stages.

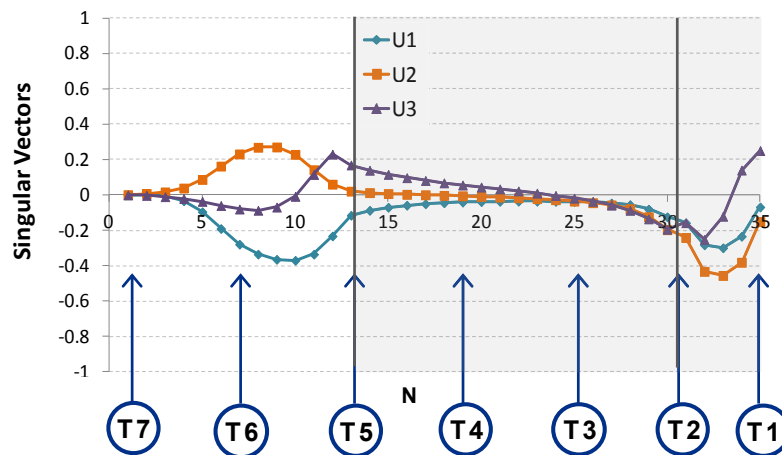


Figure 11.5. Singular vectors matrix considering the temperature sensors of the pilot column

The singular values matrix S and the condition number are also calculated.

$$S_{\text{temperatures}} = \begin{bmatrix} 12.17 & 0 & 0 \\ 0 & 10.78 & 0 \\ 0 & 0 & 1.97 \end{bmatrix}$$

$$CN_{\text{temperatures}} = 6.2$$

The value calculated for the Condition Number can be compared with the values calculated for the industrial columns designed in chapter 10. The previous values of CN considering only temperature measurements were around 3. Because higher CN values reflect more difficult controllability, the present pilot is confirmed to be more difficult to operate than the conventional industrial configuration.

From the simultaneous observations of the simulated sensitivity matrices and the SVD calculations, three different temperature measurements can be identified as the most relevant to be controlled: T6, T2 and T1. However, from the observation of the experimental transient behavior (Figure 11.3b), temperatures T6, in the middle of the separation zone, and T1, in the reboiler, show low sensitivities to the system unstable conditions.

The relative stability of the sensor T6, located in the middle of the separation zone, can be explained if the representative theoretical stage in the simulation is not exactly n°7, as pointed out in Figure 11.5. For example, if one or two bubble caps are not efficient in the top section, the temperature sensor would be better represented by a location at a lower-numbered theoretical stage, which could show less sensitivity to the column disturbances – this is the case of theoretical stages n°4 or n°5. This bad robustness of the temperature measurement could be balanced by the introduction of additional sensors through the separation zone; this fact will be discussed in depth in chapter 12.

The temperature given by sensor T1, in the reboiler, would be suitable to be controlled by the manipulation of the heat duty, but this variable is already considered in the first control loop.

The temperature measured by sensor T2 is then selected as a reliable and sensitive controlled variable for the new controller. The additional loop is introduced so as to keep T2 constant, by manipulating the distillate flow rate.

Both controller set points were selected so as to maintain the stable nominal regime found by the process simulation.

Figure 11.6 presents approximately 40 hours of experimental results after the introduction of the two control loops. Actually, the vapor regulation acts on the heat duty value and the T2 regulation defines the distillate flow rate, and, as a result, the reflux ratio; the manipulated degrees of freedom are decoupled and the system stable operation is clearly observed.

The production quality, represented by the ethanol mass content in the distillate, was also plotted in the experimental results. It can be seen that it is strongly related to the operating parameters. Thus, one additional step for the system operability improvement could be implemented by a better choice of the controller set points. The system can be oriented to another regime with better production quality by finding the optimal operating parameters. Within the laboratory time constraints, it was not possible to reach this objective which remains as a potential perspective for future work.

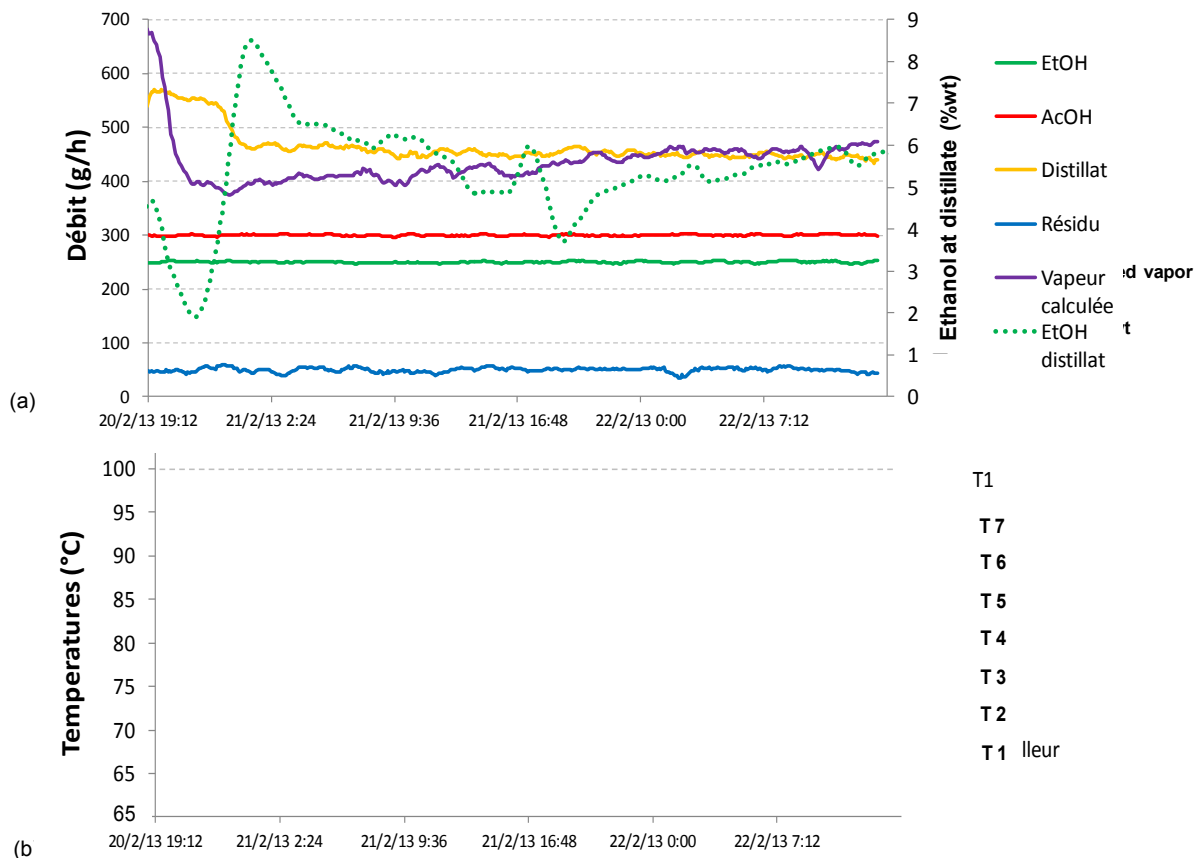


Figure 11.6. Experimental stable behaviors of (a) streams flow rates and (b) column temperatures

Finally, the rearrangement of the pilot operation variables was possible by the introduction of the correct control loops. The new degrees of freedom are the controller set points and the three operating parameters – reflux ratio, heat duty and feed ratio – are independent from each other. This approach highlights the importance of having well decoupled manipulated variables and shows that the controllability methodology is reliable when calculated in function of the real process degrees of freedom.

SIXTH PART

VI. DIAGNOSABILITY METHODOLOGY

3.	The diagnosability analysis	219
----	-----------------------------	-------	-----

The objective of process diagnosis is to rapidly detect abnormal operating conditions so as to avoid performance reduction and to promote a more secured operation regarding human skill and surroundings. The diagnosability analysis as from the conceptual step of processes is important to identify the most relevant sensors types and locations. The diagnosis technique is based on the sequence of the behavioral model definition, the sensors placement method and the online recognition of the operating situation. It is possible to analyze the data given by the process without any previous classification or already with an interpretation determined by an expert. Chapter 12 applies a quantitative diagnosability analysis, based on fuzzy-logic classification methods, concerning the reactive distillation column structure proposed for the production of ethyl acetate.

L'objectif du diagnostic des procédés est de détecter rapidement les conditions opérationnelles anormales afin d'éviter des réductions de performance et de favoriser une opération plus sûre pour l'opérateur humain et son environnement. Dans le cadre des méthodes de diagnostic basées sur la logique floue, utilisant des données historiques du procédé, la technique LAMDA (*Learning Algorithm for Multivariable Data Analysis*) s'avère intéressante pour l'analyse des systèmes complexes.

Le Chapitre 12 applique une analyse quantitative de diagnosticabilité à la configuration de colonne réactive proposée dans le Chapitre 10 pour la production d'acétate d'éthyle : *Design30c*. La méthode de classification basée sur la logique floue et utilisant les concepts et techniques présentés dans le Chapitre 5 est utilisée.

D'abord, différents scénarios de fonctionnement normal et anormal (présence de fautes) du procédé sont simulés dans Aspen Plus Dynamics® et une grande quantité de données est disponible, qui sont représentatives du fonctionnement normal et des défaillances les plus probables. Dans un autre contexte, ces données pourraient être acquises à partir des mesures réalisées en ligne pendant un intervalle de temps de fonctionnement du procédé réel.

Dans le cadre de la distillation réactive considérée, trois scénarios réalistes de défaillance peuvent être définis pour adresser la diagnosticabilité : une dérive d'une mesure de température sensible (décalage de la température sensible mesurée de -1°C), un encrassement du bouilleur, ce qui limite la charge qui peut être fournie par le bouilleur (diminution du coefficient d'échange thermique au bouilleur) ou une saturation de la charge au condenseur (dérive de la chaleur évacuée au condenseur).

La technique de classification LAMDA est alors utilisée dans le logiciel P3S®, avec l'historique des mesures obtenues dans la colonne pendant ces scénarios. Lors de l'approche hors ligne, l'analyse des données conduit à une étape d'apprentissage. La méthode de classification gère plusieurs classes représentatives de différentes situations de fonctionnement du procédé. Après l'étape d'apprentissage, la phase de reconnaissance est menée : les données sont analysées et les classes établies peuvent être identifiées et interprétées comme représentation des possibles conditions opératoires de fonctionnement du procédé. Cette interprétation est faite à l'aide de l'intervention de l'expert.

La première approche considère le diagnostic avec tous les capteurs existants dans la colonne. Due à la complexité élevée et aux coûts élevés de mesures en ligne de composition, une deuxième approche élimine les capteurs de composition et considère uniquement les températures le long de la

colonne. Les résultats montrent que les mesures de composition fournissent plus de pertinence que les mesures de température pour le diagnostic, mais la difficulté de leur utilisation peut être surmontée par l'utilisation d'un nombre plus important de capteurs de température, i.e. le même degré de reconnaissance est obtenu avec 3 mesures de composition ou 10 mesures de température.

La troisième approche sélectionne alors uniquement les 10 capteurs de température les plus pertinents. En fait, la considération des mesures dans tous les étages théoriques n'est souvent pas possible d'un point de vue pratique. Une bonne reconnaissance de 88% des différents états fonctionnels est obtenue.

Les méthodes de classification et de sélection de capteurs concluent que la section d'enrichissement en tête de colonne, dédiée uniquement à la séparation, est une zone fiable pour le diagnostic, si les capteurs sont placés de façon séquentielle dans ces étages. De plus, l'observation simultanée de ces capteurs dans le haut de la colonne et d'autres proches de la position de l'alimentation inférieure permet une bonne identification des états fonctionnels du procédé.

Ces conclusions sont en cohérence avec les résultats proposés par l'analyse de sensibilité (Chapitres 8 et 10) et doivent être considérées dès la phase de conception des colonnes de distillation réactive. L'analyse de diagnosticabilité et l'identification des placements des capteurs les plus pertinents dès la phase de conception sont importantes parce que l'installation de capteurs après la construction de l'unité est ensuite infaisable.

L'approche définie pour étudier la diagnosticabilité se montre donc intéressante pour des procédés en particulier pour les procédés intensifiés.

O objetivo do diagnóstico de processos é detectar rapidamente as condições operatórias anormais a fim de evitar perdas de desempenho e favorecer uma operação mais segura para o operador humano e seu ambiente. No contexto dos métodos de diagnóstico baseados em lógica difusa, usando dados históricos de processo, a técnica LAMDA (*Learning Algorithm for Multivariable Data Analysis*) se mostra interessante para analisar sistemas complexos.

O Capítulo 12 aplica uma análise quantitativa de diagnosticabilidade à configuração de coluna reativa proposta no Capítulo 10 para produção de acetato de etila: *Design30c*. O método de classificação baseado em lógica difusa, utilizando os conceitos e técnicas apresentados no Capítulo 5, é usado.

Inicialmente, diferentes cenários de funcionamento normal e anormal (presença de falhas) do processo são simulados em Aspen Plus Dynamics® e uma quantidade grande de dados é gerada, representativos do funcionamento nominal e das falhas mais prováveis. Em outro contexto, esses dados poderiam ser obtidos a partir de medições realizadas online durante um intervalo de tempo de funcionamento do processo real.

No caso da destilação reativa considerada, três cenários realistas de falhas podem ser definidos para abordar a diagnosticabilidade: um desvio de uma medição de temperatura sensível (variando o valor de temperatura medido em -1°C), um entupimento na tubulação do refeedor, o que limita a troca de calor fornecida pelo equipamento (diminuição do coeficiente de troca térmica no refeedor) ou uma saturação do resfriamento no condensador (variação da quantidade de calor evacuada no condensador).

A técnica de classificação LAMDA é então usada no software P3S®, com o histórico de medidas obtidas na coluna durante esses cenários. Na abordagem off-line, a análise dos dados constitui uma etapa de aprendizagem. O método de classificação gera várias classes representativas de diferentes situações de funcionamento do processo. Após a etapa de aprendizagem, a fase de reconhecimento é conduzida: os dados são analisados e as classes estabelecidas podem ser identificadas e interpretadas como a representação de possíveis condições operatórias do processo. Essa interpretação é feita com a ajuda e intervenção de um perito.

A primeira abordagem considera o diagnóstico com todos os sensores existentes na coluna. Graças à complexidade elevada e aos altos custos de medição online de composição, uma segunda abordagem elimina os sensores de composição e considera somente as temperaturas ao longo da coluna. Os resultados mostram que as medições de composição fornecem maior pertinência para o

diagnóstico em comparação com as medições de temperatura, mas a dificuldade necessária de instalação pode ser compensada pelo uso de uma quantidade maior de sensores de temperatura, i.e. o mesmo grau de reconhecimento obtido com 3 medições de composição é obtido com 10 medições de temperatura.

A terceira abordagem seleciona somente os 10 sensores de temperatura mais pertinentes. De fato, a consideração de medições em todos os estágios teóricos é frequentemente impossível de um ponto de vista prático. Um reconhecimento adequado de 88% dos diferentes estados funcionais é obtido.

Os métodos de classificação e de seleção de sensores mostram que a seção de enriquecimento no topo da coluna, dedicada exclusivamente para separação, é uma zona confiável para o diagnóstico, se os sensores forem posicionados em estágios sequenciais. Além disso, a observação simultânea desses sensores no topo da coluna e de outros próximos da localização da alimentação inferior permite uma boa identificação dos estados de funcionamento do processo.

Essas conclusões são coerentes com os resultados encontrados na análise de sensibilidade (Capítulos 8 e 10) e devem ser consideradas desde a etapa de projeto de colunas de destilação reativa. A análise de diagnosticabilidade e a identificação da localização dos sensores mais pertinentes na etapa de projeto são importantes porque a instalação de sensores depois da construção dos equipamentos pode ser inviável.

A abordagem proposta para estudar a diagnosticabilidade mostra-se assim de interesse para os processos químicos, particularmente para os processos intensificados.

The diagnosability analysis

12.1 THE SYSTEM BEHAVIORAL MODEL

Diagnosis aims at detecting the existence of a fault in the process, finding its cause and determining the procedure to follow in order to ensure its optimal operating conditions. The need to detect faulty operating conditions and to find solutions adapted for each process have motivated scientific researches on prior detection of faults, automatic diagnosis and operator assistance for decision making. Within the fuzzy diagnosis methods based on historical data, the LAMDA (Learning Algorithm for Multivariable Data Analysis) classification technique has great importance to complex systems diagnosis.

Based on the concepts and methods presented in chapter 1, section 1.4 and chapter 5 of this manuscript, the diagnosability analysis of the reactive distillation process studied is explained here. First, different fault scenarii are simulated to form an historical data base, then the classification method run leads to the creation of a '*behavioral model*' based on these simulated data. Later, the most reliable and relevant sensors are selected.

12.1.1 Faults scenarios

In order to have a representative set of data for the classification approach, a great amount of measurements should be available to describe the process behavior on normal and on all possible dysfunctional operating conditions. In general, there are sufficient data available to represent the behavior of the process in normal operating conditions; however, the historical data are commonly not sufficient to represent all possible abnormal situations. In this case, information can be obtained from process dynamic simulators and in the case studied, the model previously developed in Aspen Plus Dynamics® is used to generate the missing information. The column configuration *Design30c* defined in Chapter 10 is considered. The control structure selected has three PI controllers: the temperature at stage n°5 is controlled by manipulating the reflux ratio, the temperature at stage n°21 is paired with the ethanol feed flow rate and the temperature at stage n°28 is controlled by the reboiler heat duty.

The disturbances the system may encounter can mostly be divided into two groups: instrumentation failures, such as errors in temperature, flow rates or composition measurements, and mechanical faults, such as a wrong definition of a controller set point or an exchanger fouling.

Within the reactive distillation column considered, three different realistic disturbance scenarii can be defined in order to address the diagnosability analysis:

- An abrupt change of the sensitive temperature measurement: a -1°C shift of the sensitive measurement
- A drift of the heat duty provided to the reboiler: a tubing fouling would reduce the heat exchange capacity of the heating fluid
- A drift of the heat duty taken from the condenser: a tubing fouling would reduce the heat exchange capacity of the cooling fluid

To get a good model representation of the faults impacts on the process, each situation is simulated at different time. The process is supposed to be at the same nominal regime before each disturbance, so the fault parameters are imposed to get back to their nominal value after the stabilization in the new regime. The chronological sequence of events is specified in Figure 12.1.

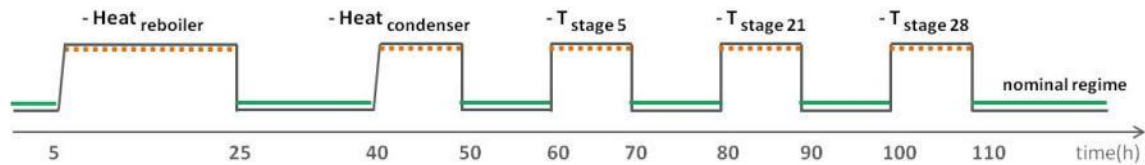


Figure 12.1. Simulated fault scenario

The disturbance of the condenser heat is modeled by a 10% decrease in the nominal duty value. In the case of the reboiler, the heat duty cannot be directly changed because it is a manipulated variable in a control loop; the heat decrease is thus carried out by a 20% change in the global heat exchange coefficient. Both changes are modeled as a one-hour ramp and they remain at the abnormal value until the system reaches a new steady-state (20h for the reboiler disturbance and 10h for the condenser). The disturbances in the controlled temperatures are modeled by subtracting 1°C from its actual measured value. The new “wrong” value is sent as the input to its respective PI controller. The system returns to its normal operating situation 10h after each temperature measurement disturbance.

The diagnosability approach is then based on classification methods of this historical data. As explained in Chapter 5, each measured element, or individual, is represented by its parameters, also called descriptors, and all the individuals have a fixed number of descriptors. For the reactive column, each individual represents a group of measurements of the system characteristics recorded every 3 minutes. All measurements are analyzed at a given time, and no time window is considered.

12.1.2 Diagnosis based on classification methods

The objective of the diagnosability analysis based on classification techniques is to determine the operating situation that best represents the process, at each measurement time. The idea is thus to establish a 'behavioral model', in which different classes represent the possible process operating conditions, for normal and abnormal situations. For each individual, its values and statistical characteristics are identified and classified using the LAMDA method, which uses fuzzy logic techniques. The classification method is based on a two-step procedure: the learning and the recognition phases, as previously presented in chapter 5.

The procedure concerning the reactive distillation studied begins by a self-learning procedure without initialization. The software P3S[®] is used and the historical data is given by the simulation described in Section 12.1.1. Along the 125 hours simulated, 2500 individuals are created with 153 descriptors each: one temperature and four compositions at each of the 30 stages plus the three manipulated variables of the control loops (reflux ratio, reboiler duty and ethanol feed flow rate). It seems interesting to consider the manipulated variables because their behaviors reflect the control actions in some possible fault situation. The active quantitative descriptors are normalized between highest and smallest value and they compose the system population. Figure 12.2 shows the form this population is presented at the software: each sensor is a continuous curve, composed by its measured values through the simulation time.

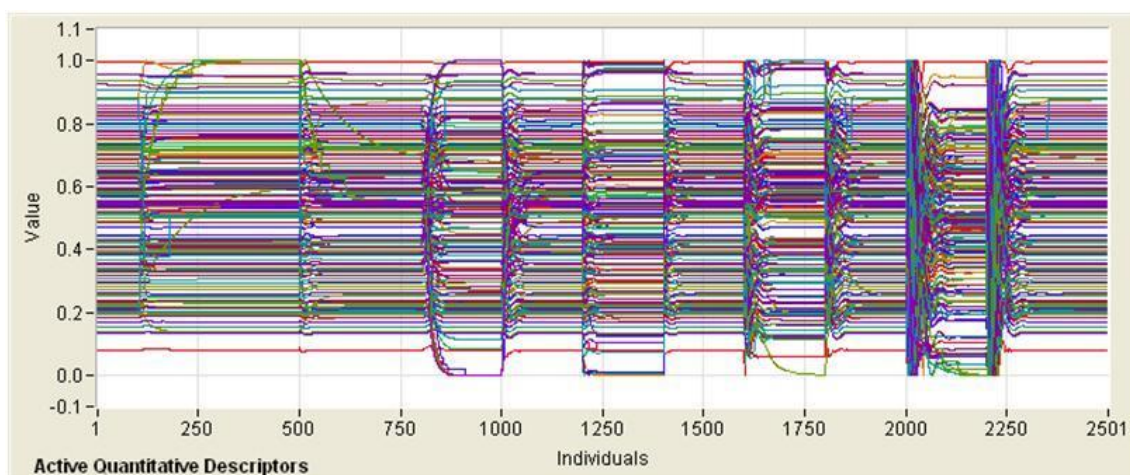


Figure 12.2. Descriptors population represented by all the system measurements

As different functions of the classification algorithms can be used (see Appendix III), human judgment is necessary to choose the one that best identifies the process situations. The algorithm called

Binomial Distance is applied here, with an exigency index of 0.8. These parameters are selected so as to result on a quantity and a partition of classes that can be physically understood by the human observation. The method identifies 14 different classes, in which 98% of the individuals (situations) are well represented. The classification is presented in Figure 12.3.

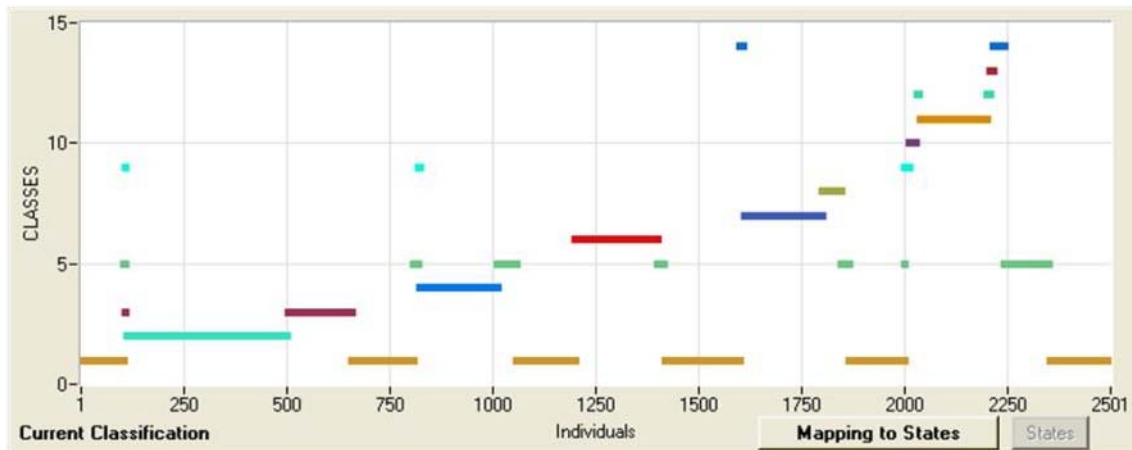


Figure 12.3. 14 classes resulting from self-learning classification of all the process sensors

The main operating situations are clearly differentiated. Human observation identifies the physical phenomena and defines the behavioral model, called '14-behavior':

- class n°1 represents the nominal regime,
- classes n°2 and 3 account for the disturbance in the reboiler heat duty,
- class n°4 represents the state with fault of the condenser heat duty,
- classes n° 6, 7 and 11 are respectively related to the disturbances in the sensitive temperatures at stages n°5, 21 and 28,
- classes n°5, 9 and 14 represent transient regimes,
- classes n° 10, 12 and 13 can be identified as alarm situations predicting the established fault on temperature measurement at stage n°28,
- class n°8 is related to a transient regime around the disturbance in temperature measurement at stage n°21. This disturbance is observed to have strong influence on the sensors.

In agreement with the approaches conducted for the controllability analysis, the system diagnosability can also be studied if the composition analyzers are not used. For the same historical data,

the population now represented only by the temperatures and the manipulated variables (33 sensors) is presented in Figure 12.4.

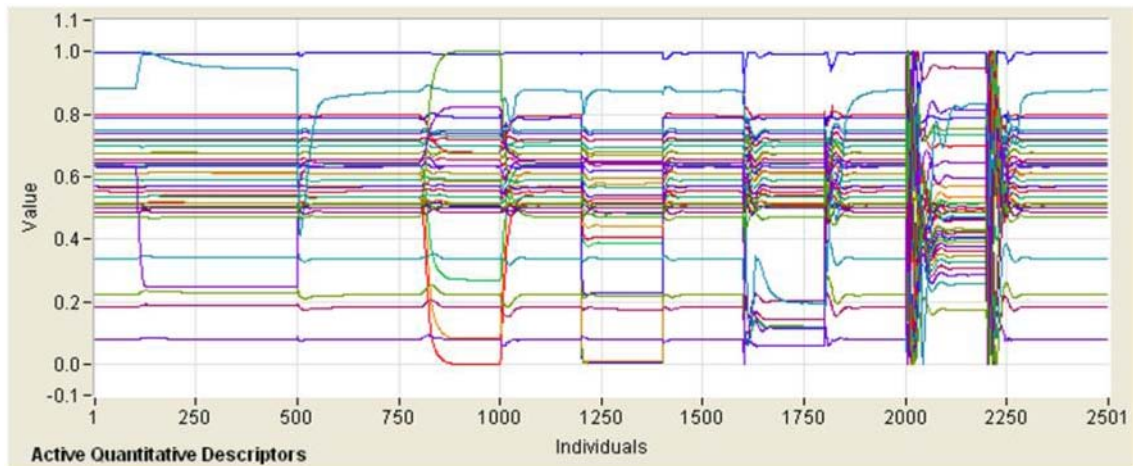


Figure 12.4. Descriptors population represented by system temperatures and manipulated variables measurements

The same Binomial Distance algorithm with an exigency index of 0.8 is selected and self-learning without initialization of classes is carried out. In Figure 12.5, 10 different classes are now sufficient to represent 98% of the individuals. A new behavioral model is thus provided and can be called '10-behavior'. The nominal steady-state and the five regimes representing the main disturbances are well recognized. However, there are fewer classes able to identify transient behaviors between these situations. The differentiation and the detection of disturbances are less judicious, due to a lower number of situations (classes) recognized.

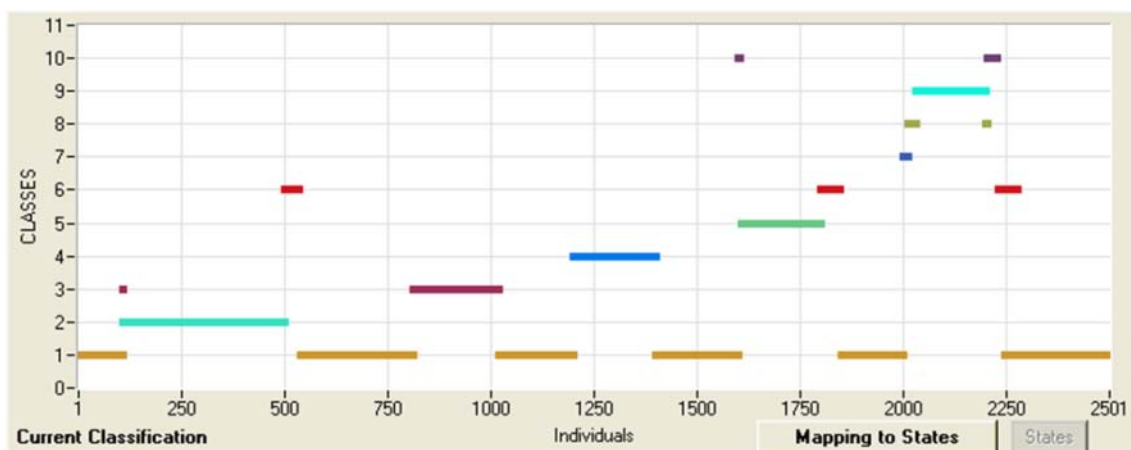


Figure 12.5. 10 classes resulting from self-learning classification without composition sensors

In Chapter 5 the learning approach was presented and a distinction was made between methods based on self-learning or based on supervised learning. It is nevertheless shown that these methods can be complementary. To improve the diagnosability analysis with only temperature descriptors, a step of

supervised learning is performed. The measurements are examined and matched to the classes identified in a previous phase. The 14 classes previously defined in *behavior-14* (Figure 12.3) are then given as input to the software and the new historical data are classified so as to obtain a satisfied partition among these existing classes. The same algorithm parameters are considered and the temperature sensors are able to classify 88% within the 2500 individuals with accuracy, i. e. to recognize the operating situation from *behavior-14*. The difference is that classes 3 and 8 are no longer related to a specific disturbance, but they represent transient regimes recognized at different historical moments.

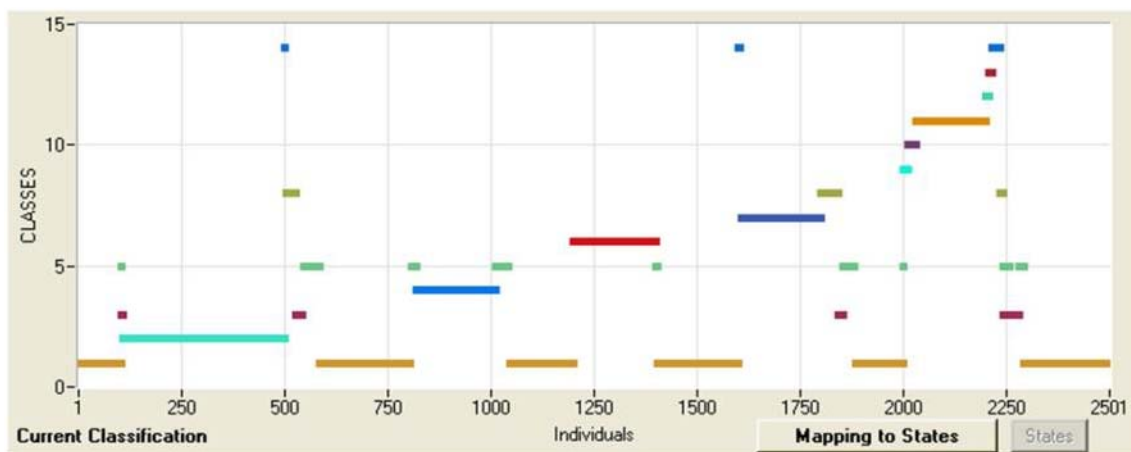


Figure 12.6. 14 classes resulting from supervised-learning classification without composition sensors

In conclusion, the consideration of only temperature and manipulated variables sensors would reduce the recognition adequacy degree – from 98% to 88% of the individuals –, but it allows a cost reduction due to the fact that expensive composition analyzers are not necessary.

12.2 SENSORS SELECTION

The LAMDA methodology formerly applied considers a substantial number of system descriptors. This approach can be refined considering a sensors selection method. The objective is to choose the most relevant descriptors which maximize the distinction between the different classes of the behavioral model, i.e. the descriptors that provide more information about detection, isolation and diagnosis of the situation represented.

Hedjazi et al. (2010b) present a sensor selection method based on the fuzzy set theory: a membership margin is defined in the membership space and then a fuzzy weight concept is introduced to

evaluate the importance of features in their new common space. The method is further explained in Appendix III and is applied here.

Assuming that the detailed recognition of transient situations is important to define alarms and promptly detect the faults, the behavioral model with 14 classes is considered to exemplify the sensors selection approach. It has been shown that it is possible to classify 98% of the process situations (individuals) with all the column sensors and 88% of the situations when composition measurements are not adopted. The ranking of the most selective descriptors and their recognition degree is given in Tables 12.1 and 12.2. For comparison purposes, only the first 33 descriptors are exhibited for the approach with all the measurements.

Table 12.1. Rank of the most relevant sensors among all the column measurements

ALL SENSORS		
n°	Descriptor	Recognition (%)
1	Stage(29).x("HOAC")	70.372
2	Stage(1).x("HOAC")	86.126
3	Stage(7).x("ETOAC")	87.285
4	Stage(6).x("ETOAC")	87.725
5	Stage(3).x("HOAC")	87.605
6	Stage(5).x("HOAC")	87.605
7	Stage(2).x("HOAC")	87.525
8	Stage(5).x("ETOAC")	87.605
9	Stage(4).x("HOAC")	87.605
10	Stage(6).x("HOAC")	87.685
11	Stage(6).T	87.605
12	Stage(4).T	87.645
13	Stage(5).T	87.645
14	Stage(4).x("ETOAC")	87.765
15	Stage(8).x("ETOAC")	88.205
16	Stage(7).T	88.165
17	Stage(7).x("HOAC")	88.205
18	Stage(6).x("H2O")	89.004
19	Stage(29).x("ETOAC")	91.723
20	Stage(9).x("ETOAC")	91.723
21	Stage(3).x("H2O")	91.923
22	Stage(3).x("ETOAC")	91.923
23	Stage(3).T	92.043
24	Stage(29).T	92.843
25	Stage(30).x("HOAC")	92.763
26	Stage(5).x("ETOH")	92.763
27	Stage(10).x("ETOH")	92.763
28	Stage(29).x("ETOH")	93.003
29	Stage(8).x("H2O")	93.003
30	Stage(11).x("HOAC")	93.003
31	Stage(30).x("ETOAC")	94.482
32	Stage(22).x("ETOAC")	94.482
33	Stage(12).x("ETOAC")	94.442

Table 12.2. Rank of the most relevant sensors among the temperature and manipulated variable measurements

WITHOUT COMPOSITION SENSORS		
n°	Descriptor	Recognition (%)
1	Stage(6).T	49.340
2	Stage(4).T	61.535
3	Stage(5).T	62.295
4	Stage(7).T	69.332
5	Stage(3).T	76.090
6	Stage(29).T	83.806
7	Stage(30).T	85.526
8	Stage(27).T	85.926
9	Stage(9).T	86.006
10	Stage(26).T	87.085
11	Stage(24).T	87.245
12	Stage(25).T	87.245
13	Stage(8).T	87.245
14	Stage(11).T	87.285
15	Stage(13).T	87.525
16	Stage(28).T	87.565
17	Stage(23).T	87.565
18	Stage(12).T	87.565
19	Stage(14).T	87.565
20	Stage(15).T	87.565
21	("REFLUX").FmR	87.565
22	Stage(1).T	87.565
23	Stage(20).T	87.565
24	Stage(16).T	87.565
25	Stage(19).T	87.565
26	Stage(17).T	87.565
27	Stage(18).T	87.565
28	Stage(21).T	87.565
29	Stage(22).T	87.565
30	Stage(2).T	87.565
31	Stage(10).T	87.565
32	("FOH").FmR	87.565
33	QRebR	87.605

When all the descriptors are available, the most important sensors for the system diagnosability are shown to be the ethyl acetate and acetic acid contents. The single measurement of the acid content at stage n°29 would be able to recognize 70% of the process situations. The addition of two composition sensors at the top of the column increases the recognition to 87%. The acetic acid content measurements from stage n°1 to stage n°6 represent a sequential section of good detection of the system behavior; this section may recognize a spatial evolution of the measures as a consequence of the system faults. Finally, 19 descriptors would be necessary to identify more than 90% of the classified situations.

Alternatively, when composition sensors are not considered, the temperature at stage n°6 is observed to be the most representative for the system diagnosis. Again, the measurements at the sequential separation stages at the top of the column – stage n°3 to stage n°7 – provide good recognition of the situation. Aiming to have a recognition degree of 87%, 10 descriptors are necessary. The descriptors of manipulated variables from the quality control loops do not show relevance to the process diagnosis.

For the hybrid column configuration, with separation and reactive sections, the descriptors placed between the two feed locations – from stage n°10 to stage n°26 –, where the reaction mainly occurs, provide little information on the system diagnosability.

The diagnosability analysis at the conceptual design stage of the studied reactive distillation process is shown to be important to plan, for example, the installation of the sensors at the top separation section. Specific sensors placements are not always possible when the column has a fixed structure and the lack of measures could jeopardize the system operation.

The comparison of the two approaches illustrates the interest in using composition sensors because three descriptors are sufficient to obtain the recognition of 87 % of the situations. The same recognition degree is only obtained with 10 temperature descriptors. However, temperature sensors are known to be easier to install and less expensive than composition ones; the use of 10 temperature descriptors can be more recommended than 3 composition measurements. A significant recognition improvement is obtained when at least 19 descriptors are considered: 15 composition and 4 temperature measures for almost 92% of good recognition. A critical human judgment is recommended to define if the attainment of a higher recognition degree is worth the implementation of the required composition sensors.

A reasonable choice of sensors for good diagnosis of the reactive distillation process studied is the selection of the 10 first temperature descriptors, located at stages n°3, 4, 5, 6, 7, 9, 26, 27, 29 and 30. This result is coherent with the column sensitivity analysis, presented in section 10.4.3, which verified a strong influence at the top separative section and the stages above the lower feed position.

Once the sensors are selected, the next step of the methodology is to redefine a behavioral model, by a classification method based only on these sensors. If the sensors were correctly chosen, the resulting classes recognized should be similar to the ones obtained when considering all the descriptors; it would be a similar classification for a smaller number of sensors, thus smaller costs and uncertainties.

Figures 12.7 and 12.8 show the population given by the 10 descriptors selected and the new behavioral model resulted from the classification method, respectively. The measured values result also on a partition of 14 classes, in agreement to the previous results from *behavior-14*. It can be concluded that the same identification of classes is possible with the consideration of fewer sensors.

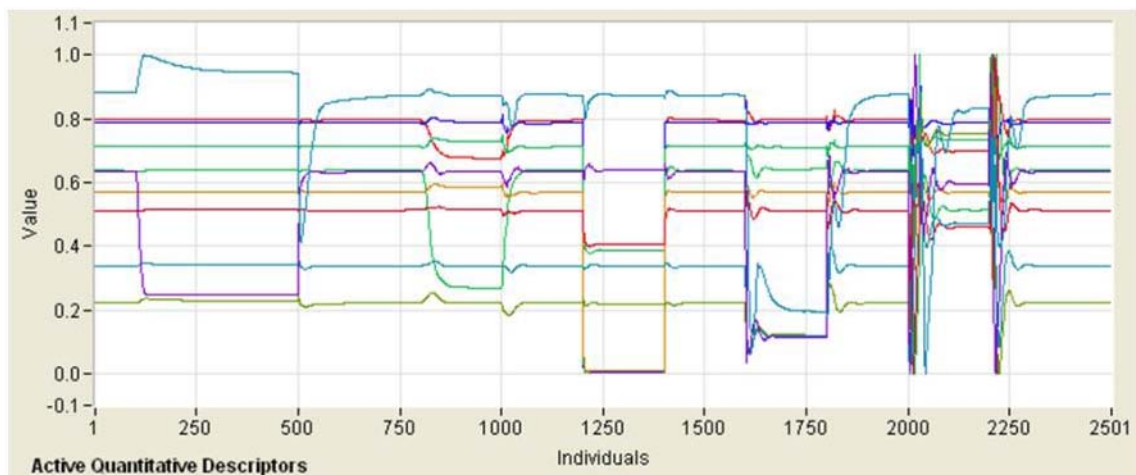


Figure 12.7. Descriptors population represented by the selected sensors

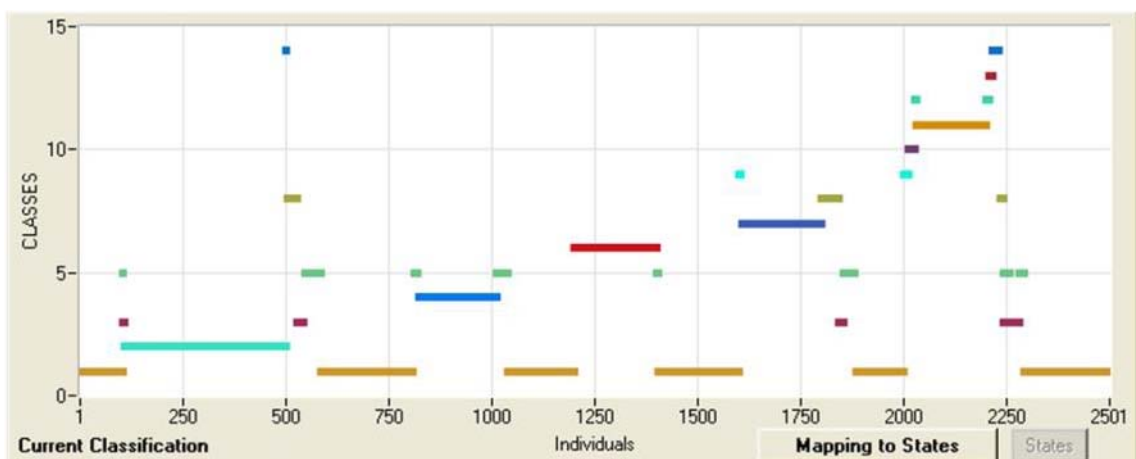


Figure 12.7. 14 classes resulting from supervised-learning classification with the sensors selected

Later, the recognition phase can deal with new data obtained online. The main interest of the approach presented here is the preparation of the system to diagnose future operating situations. Once the variables of the process are measured, the class that best represents these values will be recognized and the current situation of the process will be identified. Actually, the new measurements will be examined and matched to the classes identified in the behavioral model given by the learning phase. When an abnormal operating condition is recognized, the parameters representing this class can be identified in order to find the cause of the fault.

Finally, with few descriptors for the diagnosis, some abnormal process situations may not be detected. In this case, these situations do not match any of the proposed classes, and are part of the "NIC" class (see chapter 5). It would be therefore possible to perform a "specialized learning" by manually creating one or several classes by gathering the situations which have not been recognized.

12.3 CONCLUSIONS

Classification techniques are attractively applied to diagnosis methods, because they do not require a mathematical understanding of the process. They process historical data independently of its source or nature. The diagnosability of the reactive distillation column for the production of ethyl acetate is here studied based on the process dynamic simulation; a large number of data is available for the normal regime and each of the most probable abnormal situations of the process. Conversely, data could also be obtained from historical measurements performed during a time-window plant operation.

The classification technique LAMDA, based on fuzzy logic, was considered and the calculations were made with the software P3S[®]. During the offline phase, the data led to a learning procedure, when the knowledge of human experts was included; the classification algorithm was applied and the historical measurements were differentiated into several classes. After the learning procedure, a recognition step was conducted: the data was analyzed and the classes already established could be identified and interpreted as the representation of possible process operating conditions.

Three different approaches were conducted: the consideration of all the existing sensors, the elimination of the composition measurements and the selection of the 10 most relevant temperature sensors. The composition sensors were verified to give sound information about process diagnosis. Actually, a behavioral model was previously defined with 14 classes representing the process operating

conditions. The consideration of all composition and temperature measures would result on a good classification of 98 % of the measured situations, and the consideration of only temperature measures show a classification efficiency of 88 % instead. Conversely, if a less rigorous behavioral model, with 10 classes, can be accepted, the same temperature sensors would provide 98% of good classification.

The consideration of all process descriptors is not commonly possible, so the most representative sensors were selected. It was verified that to achieve a recognition efficiency of 87 % only 3 composition descriptors would be necessary. To still increase the percentage, an excessive large number of sensors would be required (at least 19 sensors to achieve 90% of recognition). However, the complexity of using online composition analyzers could be overcome by the use of a larger number of temperature sensors to give the same situation recognition degree, i. e. the availability of 10 temperature sensors would give the same recognition of 88 % of process situations.

The top section of the column, solely dedicated to separation, was observed to be a reliable region for diagnosis, if sensors were placed at sequential stages. The simultaneous observation of the descriptors at the top of the column and the ones near the lower feed position provide a good identification of the operating situations.

These conclusions are in agreement with the results given by the column sensitivity analysis (chapters 8 and 10) and they provide important insights to be considered in the conceptual design step of reactive column configurations.

The diagnosability approach has been shown to apply to the complex system, in which specific locations should be imagined for sensors placement, as from the process conceptual design step.

SEVENTH PART

VII. EPILOGUE

Conclusions and Perspectives	237
Nomenclature	243
References	247
Appendices	259

The last part of this work presents the main conclusions, highlighting the contribution to each laboratory, and the methodology for the design of reactive columns considering controllability and diagnosability aspects is illustrated in Figure C.1. Some perspectives for future developments are also proposed. Then, the nomenclature and the references cited in the text are given and five appendices present the binary thermodynamic data, some control basic methods, the algorithms used, the classification calculations and additional dynamic simulation results.

Une nouvelle méthodologie est proposée pour la conception de colonnes de distillation réactive en intégrant des aspects de contrôlabilité et de diagnosticabilité. Des outils méthodologiques sont appliqués à la production d'acétate d'éthyle, en identifiant les sensibilités spécifiques au système et en proposant les meilleures structures de contrôle et le placement des capteurs qui doivent être envisagés dès la phase de conception.

Basée sur la méthodologie développée au LGC pour la conception de colonnes réactives, une combinaison d'algorithmes développés en Fortran et MatLab®, connectés au serveur de propriétés thermodynamiques Simulis®, est utilisée pour l'analyse de faisabilité et les calculs de synthèse. Puis, les configurations de colonnes sont simulées dans Aspen Plus® et les paramètres opératoires les plus performants sont définis. Le régime permanent obtenu donne l'initialisation pour la simulation dynamique dans Aspen Plus Dynamics®. La simulation dynamique du procédé fournit plusieurs critères quantitatifs et qualitatifs de contrôlabilité pour la comparaison de différentes configurations de colonne et l'identification de quelques règles heuristiques. Enfin, les données de simulation sont analysées avec la procédure développée au LAAS pour la supervision, le diagnostic et le placement des capteurs sur le procédé. Deux validations expérimentales sont réalisées : une pour la validation du modèle de simulation et une autre pour la compréhension de la méthode d'analyse de contrôlabilité. La séquence des outils et méthodes est présentée ci-dessous :

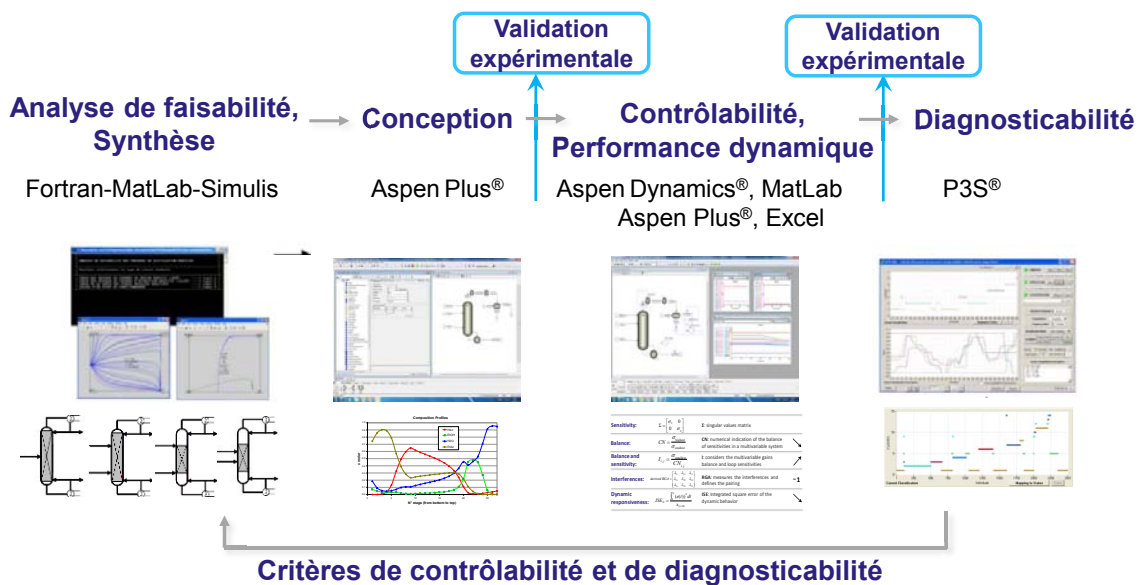


Figure C.1. Séquence d'outils et méthodes utilisés pour la méthodologie de conception

Les travaux de la thèse ont été effectués dans le cadre de plusieurs laboratoires. Donc, différents intérêts coexistent et les collaborations entre les institutions académiques et industrielles ont été renforcées. Les contributions principales pour chaque laboratoire sont décrites ci-dessous :

- La méthodologie développée au Laboratoire de Génie Chimique (LGC, France) pour la conception de colonnes de distillation réactive peut étudier différentes configurations de colonne, mais jusqu'à maintenant, uniquement le comportement en régime permanent était considéré. Il existe alors un intérêt important à prendre en compte aussi le comportement dynamique. Les travaux proposés dans la thèse améliorent cette méthodologie, avec le développement de nouveaux outils et l'identification des aspects de contrôlabilité et de diagnosticabilité qui sont intégrés pour prévoir l'opérabilité dynamique de la colonne.
- Les techniques développées pour le diagnostic des systèmes dans le Laboratoire d'Analyse et d'Architecture des Systèmes (LAAS, France) n'avaient jamais été appliqués à un procédé chimique intensifié. Les sensibilités spécifiques de la colonne de distillation réactive sont discutées et les champs d'application de la technique sont augmentés.
- Le *Centro de Estudos de Sistemas Químicos* (CESQ, *Escola Politécnica da Universidade de São Paulo*, Brésil) étudie les procédés intensifiés, mais la distillation réactive n'a jamais été adressée. Les travaux de la thèse ont augmenté leur savoir-faire dans ce domaine.
- Les outils qui ont été totalement développés lors de cette thèse, pour étudier les aspects de contrôlabilité et diagnosticabilité dès la phase de conception des procédés peuvent maintenant être utilisés dans le *Solvay Research and Innovation Center* (France). L'application cible était la production d'acétate d'éthyle par distillation réactive, mais les méthodes développées sont génériques et les calculs peuvent donc être généralisés pour tout procédé du moment qu'il dispose d'un modèle de simulation. De plus, les campagnes expérimentales ont permis d'améliorer les équipements pilotes et les instrumentations.

Les principales perspectives des travaux sont la considération de configurations de colonne plus spécifiques dès les premières étapes, telles que l'introduction du décanteur sur la ligne de reflux, la détermination d'un compromis mathématique entre les critères de contrôlabilité et les aspects liés aux coûts de la colonne, pour concevoir à la fois une colonne contrôlable et envisageable économiquement, une validation expérimentale de l'analyse de diagnosticabilité et, enfin, une validation expérimentale à l'échelle industrielle pour pouvoir implémenter le procédé de distillation réactive chez Solvay.

Uma nova metodologia foi proposta para o projeto de colunas de destilação reativa que integra aspectos de controlabilidade e de diagnosticabilidade. Ferramentas metodológicas são aplicadas à produção de acetato de etila, identificando as sensibilidades específicas do sistema e propondo as melhores estruturas de controle e posicionamentos de sensores que devem ser idealizados desde a etapa de projeto.

Baseada na metodologia desenvolvida no LGC para projeto de colunas reativas, uma combinação de algoritmos desenvolvidos em Fortran e MatLab®, conectados ao servidor de propriedades termodinâmicas Simulis®, é usada para a análise de viabilidade e os cálculos de síntese. De pois, as configurações de colunas propostas são simuladas em Aspen Plus® e os parâmetros de operação de melhor desempenho são definidos. O estado estacionário obtido gera a inicialização para a simulação dinâmica em Aspen Plus Dynamics®. A simulação dinâmica fornece vários critérios qualitativos e quantitativos de controlabilidade para a comparação de diferentes configurações de coluna e identifica algumas regras heurísticas. Enfim, os dados simulados são analisados com o procedimento desenvolvido no LAAS para a supervisão, diagnóstico e posicionamento dos sensores do processo. Duas validações experimentais foram conduzidas: uma para validação do modelo de simulação e outra para compreensão do método de análise de controlabilidade. A sequência de ferramentas e métodos é apresentada abaixo:

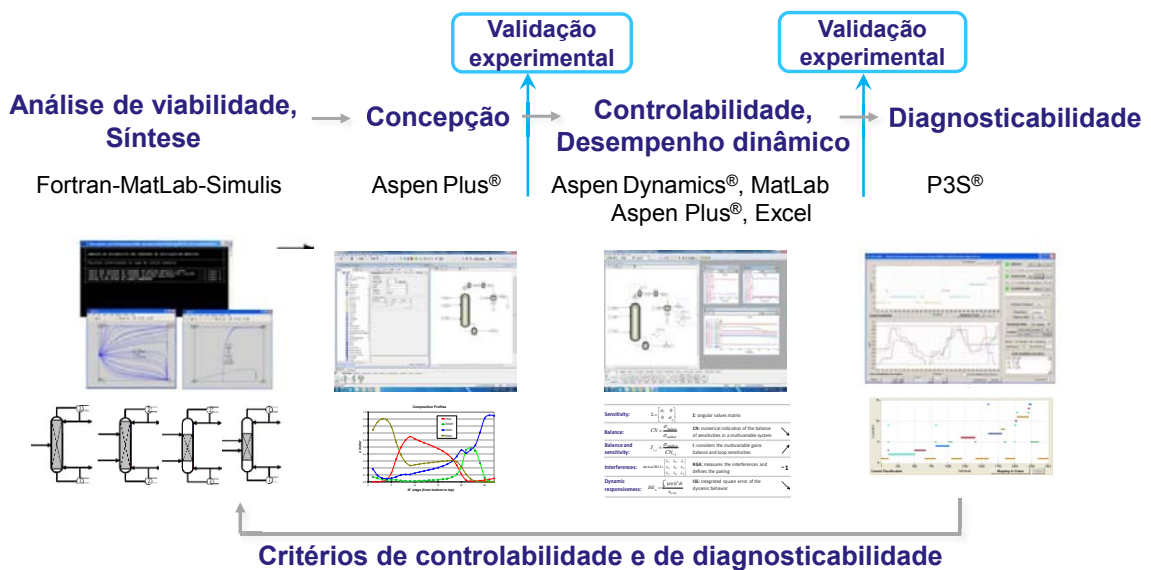


Figura C.1. Sequência de ferramentas e métodos usados na metodologia de projeto

Os trabalhos de tese foram efetuados sob supervisão e apoio de diferentes laboratórios. Assim, diferentes interesses coexistem e as colaborações entre as instituições acadêmicas e industriais foram reforçadas. As principais contribuições para cada laboratório são descritas abaixo:

- A metodologia desenvolvida no *Laboratoire de Génie Chimique (LGC, França)* para o projeto de colunas de destilação reativa estuda diferentes configurações de coluna, mas exclusivamente o comportamento em estado estacionário era considerado até hoje. Existe então um grande interesse em considerar também o comportamento dinâmico. O trabalho proposto na tese melhora essa metodologia, com o desenvolvimento de novas ferramentas e a identificação de aspectos de controlabilidade e de diagnosticabilidade que são integrados para prever a operabilidade da coluna.
- As técnicas desenvolvidas para o diagnóstico de sistemas no *Laboratoire d'Analyse et d'Architecture des Systèmes (LAAS, França)* nunca tinham sido aplicadas a um processo químico intensificado. As sensibilidades específicas à coluna de destilação reativa são discutidas e os campos de aplicação da técnica tornam-se mais abrangentes.
- O Centro de Estudos de Sistemas Químicos (*CESQ, Escola Politécnica da Universidade de São Paulo, Brasil*) estuda processos intensificados, mas a destilação reativa nunca tinha sido abordada. O trabalho da tese aumenta o conhecimento nesse campo.
- As ferramentas que foram desenvolvidas ao longo da tese, para estudar os aspectos de controlabilidade e de diagnosticabilidade desde a etapa de projeto podem agora ser usadas pelo *Solvay Research and Innovation Center (França)*. A aplicação alvo foi a produção de acetato de etila por destilação reativa, mas os métodos desenvolvidos são genéricos e os cálculos podem então ser adaptados a todos processos que possuam um modelo de simulação. No mais, os estudos experimentais permitiram melhorar os equipamentos piloto e as instrumentações.

As principais perspectivas do trabalho são a consideração de configurações de colunas mais específicas desde as primeiras etapas, como a introdução do decantador na linha de refluxo, a definição de um compromisso matemático entre os critérios de controlabilidade e os aspectos relacionados aos custos da coluna, para projetar uma coluna simultaneamente controlável e vantajosa economicamente, uma validação experimental piloto das técnicas de diagnosticabilidade e, enfim, uma validação experimental em escala industrial para poder implementar o processo de destilação reativa na Solvay.

Conclusions and Perspectives

A new methodology was proposed for the conceptual design of reactive distillation columns that integrates controllability and diagnosability aspects as from the early steps. Methodological tools are applied to the industrial production of ethyl acetate, highlighting the specific sensitivities of the system and proposing the best control structures and sensors placements to be enabled at the process design step.

The literature review discusses advantages and challenges of the reactive distillation process and outlines the interests on proposing design approaches that consider the dynamic behavior of these systems. The industrial context of the esterification system and recent advances are presented.

The first steps of the methodology are based on the pre-design approach developed at the LGC, which provides the structural and operating parameters to conceive a feasible reactive column that achieves the production specification objectives. All restrictions on thermodynamics, mass and energy balances are considered and the unit is modeled in a commercial process simulator.

At this moment, the importance of experimental validation in pilot-scale column to define reliable technological and hydrodynamic parameters is proved. The esterification open-loop system is analyzed after several perturbations and a deep discussion of the complexities regarding the heterogeneous catalysis, and the suggestion on considering the homogeneous catalysis is conducted.

Based on the process simulation, the indices-based proposed methodology considers different qualitative and quantitative criteria to address the controllability of reactive distillation columns. The vast majority of reactive columns cited in the literature uses two-point inferential control structures to ensure process performance. In the industrial case proposed in the thesis, as a double-feed configuration column has a third degree of freedom given by the feed ratio, three-point control structure is used to meet the three industrial product specifications; one additional control loop that controls a measurement placed between the two feeds and manipulates the lower feed flow rate is used to keep reaction yields. The controlled variables are always selected as follows: one at the middle of the top separation section, one above the lower feed position and one at the bottom section.

Actually, the columns distilling a reactive quaternary system, with two reactants and two products, are commonly conceived in a double-feed configuration, so the same calculations conducted here for the ethyl acetate system may be performed on other systems. As a function of their thermodynamic behaviors, the properties discussed might be used as key-rules in the reactive column design.

Controllability criteria are used to compare the performance of composition and temperature controlled variables, and different column configurations are defined by changing the number of theoretical stages in each column section and consequently changing the relative feed positions. The integrated design approach considers both steady state and dynamic aspects of the system. The criteria are calculated and compared with the purpose of detecting some heuristic rules and column characteristics that provide better controllability. The addition of theoretical stages between the two feeds positions is verified to improve the controllability of the system.

Then, the diagnosability analysis is performed with the fuzzy classification technique LAMDA. The data from the process is interpreted and classes representing normal functioning conditions and faults are generated. An analysis of the dataset provides a behavioral model of the system, which can be translated by human operators into acceptable physical conditions. The classification technique allows the analysis of all possible sensors and the selection of the ones that best identify and distinguish failures.

The ethyl acetate reactive column shows that composition sensors give reliable information about the process diagnosis, but the same results given by few composition measurements can be obtained by a larger number of temperature sensors. Good process diagnosis would be achieved by the placement of some sequential sensors at the top separation section in addition to others near the lower feed position. These conclusions are in agreement with the results given by the column sensitivity analysis.

The identification of the necessary measurements at the process design step is important because the addition of extra sensors after the process construction is often practically impossible.

Sequential tools

Based on the methodology developed at the LGC for the pre design of reactive columns, a combination of algorithms developed in Fortran and MatLab[®] connected to a thermodynamic properties server (Simulis[®]) is used for feasibility analysis and synthesis calculations. Then, the column configuration is simulated in Aspen Plus[®] and the best operating parameters are defined. The steady state regime is used to initialize dynamic simulation in Aspen Plus Dynamics[®]. The process simulation provides several quantitative and qualitative controllability criteria for comparison of different column configurations and identification of some heuristic rules. Finally, the simulation data can be analyzed by a procedure developed at the LAAS for process supervision, diagnosis and sensor placement. Two experimental validations are performed. The sequence of tools is schematized in Figure C.1:

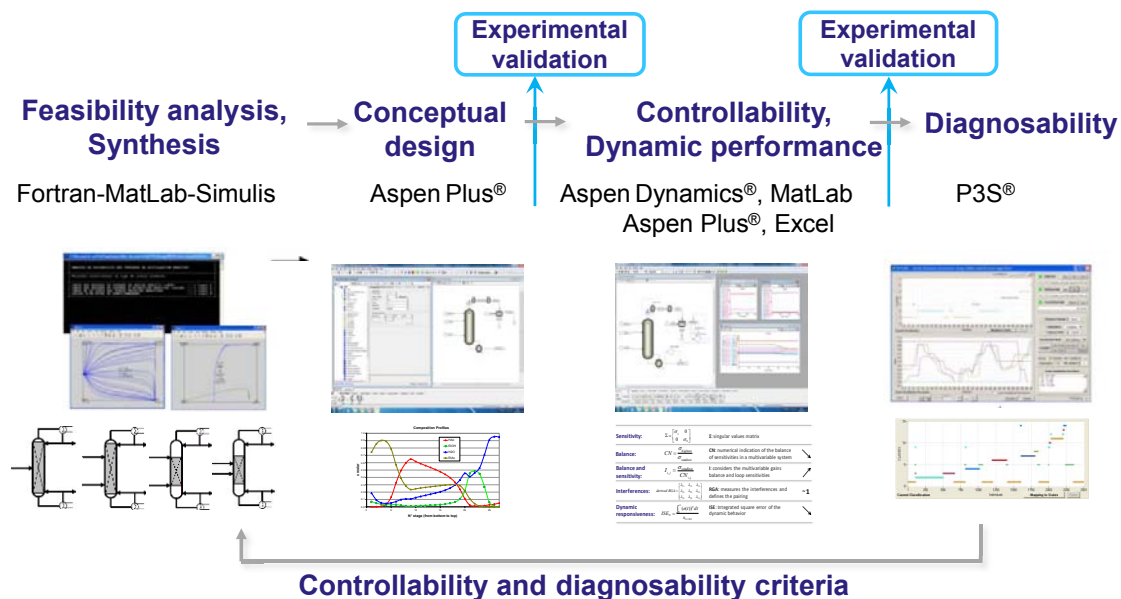


Figure C.1. Sequence of tools and methods used for the design methodology

Contributions to each laboratory

The PhD work was developed under supervision of several laboratories. So, different interests coexisted and the collaborations between the academics and the industrial institutions were strengthened. The main contributions to each laboratory are outlined:

- The methodology developed at the Laboratoire de Génie Chimique (LGC, France) for the pre design of RD columns can address different system configurations, but only the steady state behavior was considered. There existed strong interests in better understanding the dynamic behavior. The work proposed in the thesis improved this methodology, by developing new tools and by identifying controllability and diagnosability aspects that should be considered in early design steps so as to forecast the column dynamic operability.
- The techniques developed for process diagnosis at the Laboratoire d'Analyse et d'Architecture des Systèmes (LAAS, France) were unprecedentedly applied to an intensified chemical process. The specific sensitivities of the reactive distillation column were discussed and the application fields of the approach have increased.
- The Centro de Estudos de Sistemas Químicos (CESQ, Escola Politécnica da Universidade de São Paulo, Brazil) has been studying intensified processes, but the reactive distillation has not yet been addressed. The PhD thesis increased the respective know how.

- The tools developed for screening controllability and diagnosability aspects at the design step of processes can now be used in the Solvay Research and Innovation Center (France). The target application was the production of ethyl acetate by reactive distillation, but it can be generalized for any other potential process and put into practice based on its simulation model. Moreover, the experimental studies allowed the improvement of pilot devices and instrumentation.

Perspectives

An important contribution to the methodology would be the consideration of more detailed configurations as from the first steps of feasibility analysis and synthesis. Some of these developments are already being treated, such as the double-feed condition, but others are only possible to be included during process simulation and this fact restricts a representative analysis. This is the case of hybrid column, with different sections dedicated solely to separation, or, in the case of this study, the consideration of a decanter in the distillate output stream so as to provide a reflux composed only by the organic phase.

The synthesis step of the methodology proposes different feasible column configurations, from a thermodynamic point of view. The previous approach ranks the columns in function of their investment or operating costs. The approach proposed here chooses the column in function of its controllability indices values. In our case study, there was no inconsistency between these criteria. However, some application may result in controversial propositions and it may be difficult to compare processes with quite different economics and controllability indices. The final decision should be determined by the trade-off between an economic performance measure and controllability indices. To address this drawback, a mathematical optimization framework could be imagined.

With regard to the experimental approach, additional tests would be of great interest to observe the disturbance responses of the closed-loop system proposed by the controllability analysis and to validate the diagnosability approach.

Although the theoretical and experimental studies presented show the interests of the reactive distillation column for the production of ethyl acetate, the commercial implementation in Solvay requires an industrial-scale experimental validation.

Nomenclature

General

RD	Reactive distillation
LGC	Laboratoire de Génie Chimique
LAAS	Laboratoire d'Analyse et d'Architecture des Systèmes
LSCP	Laboratório de Simulação e Concepção de Processos
CESQ	Centro de Estudos de Sistemas Químicos
USP	Universidade de São Paulo
HOAc	Acetic acid
EtOH	Ethanol
H ₂ O	Water
EtOAc	Ethyl acetate
H ₂ SO ₄	Sulfuric acid

Experimental campaigns

X_i	Conversion rate
N_i	Molar flow (mol/h)
D_i	Liquid distributor
HETP	Equivalent height of theoretical stage (m)
C	Adjustable coefficient for reaction efficiency
k	Kinetics constant
R	Gas constant
FIC	Flow controller
TIC	Temperature controller

Design methodology

x_i	Molar composition
XX_i	Transformed molar compositions
rRCM	Reactive residue curves map
rExCM	Reactive extractive curves map
r	Reaction rate
T	Absolute temperature (K)
k	Pre-exponential factor (m ³ /kmol/s)
N_c	Number of components
E	Activation energy (kJ/kmol)
C_i	Composition of each component
R	Gas constant (J/K/mol)
α_i	Coefficient of each component
F_U/V	Ratio between the upper feed flowrate and the vapor flowrate

Controllability analysis

S_i	Signal from sensor i , expressed as a percentage of the maximum signal
M_j	Signal to control valve j , expressed as a percentage of the maximum signal
K	Sensitivity matrix
T_i	Temperature at stage i
C_i	Composition at stage i
<i>SVD</i>	Singular Value Decomposition
V	Right singular vectors matrix
U	Left singular vectors matrix
Σ	Singular vectors matrix
σ_i	Singular value
<i>CN</i>	Condition number
I	Intersivity index
λ_{ij}	Relative gain between output variable y_i and input variable m_j
y_i	Output control variable
m_j	Input control variable
<i>RGA</i>	Relative Gain Array
<i>Derived-RGA</i>	Derived Relative Gain Array
<i>IMC</i>	Internal Model Control
<i>IAE</i>	Integral Absolute Error
<i>ISE</i>	Integral of the Squared Error
<i>ISE_N</i>	Normalized Integral of the Squared Error
$e(t)$	Error signal
S	Singular values matrix
<i>PID</i>	Proportional-Integral-Derivative controller
<i>PI</i>	Proportional-Integral controller
<i>FEtOH</i>	Ethanol feed stream
N	Number of theoretical stages

Diagnosability analysis

<i>GAD</i>	Global Adequacy Degree
<i>MAD</i>	Marginal Adequacy Degree
X_n	Individual
x_i	Descriptor
C_k	Class
<i>NIC</i>	Non-Informative Class
$\mu(x_i C_j)$	Function of marginal relevance for descriptor x_i on class C_k

ρ_{ki}	i th parameter of class C_k
N_k	Quantity of individuals in the class C_k
Q_{ij}	Modality describing a qualitative descriptor x_i
Φ_{ij}	Probability of each modality Q_{ij} in the class C_k
s	Similarity measure between two interval descriptors
U	Universe of discourse for interval descriptors
$A = [a^-, a^+], B = [b^-, b^+]$	Examples of interval descriptors
G	Aggregation function, or fuzzy connective
α	Exigency index
μ	Arithmetic mean value of descriptors
β_n	Membership margin of individual X_n
ψ	Aggregation function
ω_f	Fuzzy feature weight
h	Indicator function

References

A

- Agar D. W. Multifunctional reactors: Old preconceptions and new dimensions. *Chemical Engineering Science*, 54, 1299, **1999**.
- Agreda V. H., Partin L. R. et Heise W. H. High-purity methyl acetate via reactive distillation. *Chemical Engineering Progress* 86 (2), 40, **1990**.
- Aguilar-Martin J. et Balssa M. Estimation récurrente d'une partition. Exemple d'apprentissage et auto-apprentissage. Technical Report LAAS-CNRS, 880139, **1980**.
- Aguilar J. and López de Mántaras R. The process of classification and learning the meaning of linguistic descriptors of concepts. *Approximate Reasoning in Decision Analysis*, North Holland Publishing Company, 165, **1982**.
- Akbaryan F. et Bishnoi P.R. Fault diagnosis of multivariate systems using pattern recognition and multisensor data analysis technique. *CCE*, **2001**.
- Al-Arfaj M. et Luyben W. Comparison of alternative control structures for an ideal two-product reactive distillation column. *Industrial & Engineering Chemistry Research* 39 (9), 3298, **2000**.
- Almeida-Rivera C. et Grievink J. Feasibility of equilibrium-controlled reactive distillation process: application of residue curve mapping. *Computers & Chemical Engineering* 28 (1), 17, **2004a**.
- Almeida-Rivera C.P., Swinkels P.L.J. et Grievink J. Designing reactive distillation processes: present and future. *Computers & Chemical Engineering* 28, 1997, **2004b**.
- Antunes B. M., Cardoso S.P., Silva C.M. et Portugal I. Kinetics of Ethyl Acetate Synthesis Catalyzed by Acidic Resins. *Journal of Chemical Education* 88 (8), 1178, **2011**.
- Avami A., Marquardt W., Saboohi Y. et Kraemer K. Shortcut design of reactive distillation columns. *Chemical Engineering Science*, 71, 166, **2012**.
- Avami A. Conceptual design of double-feed reactive distillation columns. *Chemical Engineering Technology* 36 (1), 186, **2013**.

B

- Babu K. S., Kumar M. V. P. et Kaistha N. Controllable optimized designs of an ideal reactive distillation system using genetic algorithm. *Chemical Engineering Science*, 64, 4929, **2009**.
- Barbosa D. et Doherty M.F.. Design and minimum reflux calculations for single-feed multicomponent reactive distillation columns. *Chemical Engineering Science*, 43, 1523, **1987a**.
- Barbosa D. et Doherty M.F., Design and minimum reflux calculations for double-feed multicomponent reactive distillation columns. *Chemical Engineering Science*, 43, 2377, **1987b**.
- Baur R., Higler A. P., Taylor R. et Krishna R., Comparison of equilibrium stage and nonequilibrium stage models for reactive distillation. *Chemical Engineering Journal*, 76, 33, **2000**.
- Bausa J., Watzdorf R.V. et Marquardt W. Shortcut methods for nonideal multicomponent distillation: I. Simple columns. *AIChE Journal* 44, 2181, **1998**.
- Beckmann A., Nierlich F., Popken T., Reusch D., Scala C. et Tuchlenski, A. Industrial experience in the scale-up of reactive distillation with examples from C4-chemistry. *Chemical Engineering Science*, 57, 1525, **2002**.
- Behrens M., Olujic Z. et Jansens P. J. Hydrodynamics and mass transfer performance of modular catalytic structured packings. *Chemical Engineering Research and Design*, 84 (A5), 381, **2006**.
- Behrens M., Olujic Z. et Jansens P. J. Liquid holdup in catalyst-containing pockets of a modular catalytic structured packing. *Chemical Engineering Technology*, 31 (11), 1630, **2008**.
- Bellassaoui B. Généralisation d'une approche de conception de procédés de distillation réactive : application à la production d'hydrogène par le cycle thermo-chimique I-S. Ph.D. Thesis, Institut National Polytechnique de Toulouse - Laboratoire de Génie Chimique, France, **2006**.

Bezdek J. Pattern recognition with fuzzy objective function. *Ed. Plenum Press*, **1981**.

Bezdek J., Keller J., Krisnapuram R. et Pal N. Fuzzy models and algorithms for pattern recognition and image processing. *Springer*, **2005**.

Bonet J. Contribution à l'étude de la transestérification de l'acétate de méthyle par distillation réactive. Ph.D. Thesis, Institut National Polytechnique de *Toulouse - Laboratoire de Génie Chimique*, France, **2006**.

Brehelin M. Analyse de faisabilité, conception et simulation de la distillation réactive liquide-liquide-vapeur. Application et validation expérimentale sur la production de l'acétate de n-propyle. Ph.D. Thesis, Institut National Polytechnique de *Toulouse - Laboratoire de Génie Chimique*, France, **2006**.

Burkett R.J. et Rossiter D. Choosing the right control structure for industrial distillation columns. *Process Control Instruments* 2000, 38, **2000**.

C

Calvar N., Dominguez A. et Tojo J. Vapor-liquid equilibria for the quaternary reactive system ethyl acetate + ethanol + water + acetic acid and some of the constituent binary systems at 101.3kPa. *Fluid Phase Equilibria* 235, 215, **2005**.

Chawankul N, Budman H, Douglas PL. The integration of design and control: IMC control and robustness. *Computers & Chemical Engineering* 29, 261, **2005**.

Chen F., Huss R. S., Doherty M. F. et Malone M. F. Multiple steady states in reactive distillation: kinetic effects. *Computers & Chemical Engineering* 26, 81, **2002**.

Cheng Y. et Yu C. Effects of feed tray locations to the design of reactive distillation and its implication to control. *Chemical Engineering Science* 60 (17), 4661, **2005**.

D

Darge O. and Thyron F. C. Kinetics of the liquid phase esterification of acrylic acid with butanol catalyzed by cation exchange resin. *Journal of Chemical Technology and Biotechnology* 58 (4), 351, **1993**.

Demirel B. et Kaymak D. B. Control of quaternary reactive distillation columns : Effects of number and location of temperature loops. *Industrial & Engineering Chemistry Research*, **2013**.

Dima R., Soare G., Bozga G. et Plesu V. Gas-liquid hydrodynamics in counter current columns with Katapak-S and BX structured packing. *Revue Roumaine de Chimie* 51(3) 219, **2006**.

Druart F., Reneaume J.M., Meyer M. and Rouzineau D. Simulation of catalytic distillation by a new transfer model – Application of methyl acetate production. *Canadian Journal of Chemical Engineering* 82 (5), 1014, **2004**.

Dubois D., Prade H. et Testemale C. Weighted fuzzy pattern matching. *Fuzzy Sets and Systems* 28, 313, **1988**.

Dutia P. Ethyl acetate : A techno-commercial profile. *Chemical Weekly*, 184, **2004**.

F

Fisher R.A. The use of multiple measurements in taxonomic problems. *Cambridge University Press*, 179–188, **1936**.

Fisher W.R., Doherty M.F. et Douglas J.M. The interface between design and control: 1. Process controllability. *Industrial & Engineering Chemistry Research* 27, 597, **1988**.

Fisher W.R., Doherty M.F. et Douglas J.M. The interface between design and control: 2. Process operability. *Industrial & Engineering Chemistry Research* 27, 606, **1988**.

Fisher W.R., Doherty M.F. et Douglas J.M. The interface between design and control: 3. Selecting a set of controlled variables. *Industrial & Engineering Chemistry Research* 27, 611, **1988**.

Fix E. et Hodges J.L. Discriminatory analysis. non-parametric discrimination. *Technical Report USAF School of Aviation Medicine*, 4, **1951**.

Frey T., Nierlich F., Popken T., Reusch D., Stichlmair J. et Tuchlenski A. Application of reactive distillation and strategies in process design, in: *Reactive distillation: Status and future directions*. Sundmacher K. et Kienle A. (Eds.) *Wiley-VCH Verlag GmbH & Co. KGaA*, Weinheim, **2003**.

G

Galindo M. Et Aguilar-Martin J. Interpretación secuencial de encuestas con aprendizaje lamda. aplicación al diagnostico en psicopatología. *In Workshop BERAMIA*, **2002**.

Garcia C.E. and Morari M. Internal model control. A unifying review and some new results, *Industrial & Engineering Chemistry Process Development* 21 (2), 308, **1982**.

Gehrke V. et Marquardt W. A singularity theory approach to the study of reactive distillation. *Computers & Chemical Engineering (Supplement)*, S1001, **1997**.

Georgiadis M. C., Schenk M., Pistikopoulous E. N. et Gani R. The interactions of design, control and operability in reactive distillation systems. *Computers & Chemical Engineering* 26, 735, **2002**.

Georgakis C., Vinson D.R., Subramanian S. et Uzturk D. A geometric approach for process operability analysis, in: *The integration of process design and control*. Seferlis P. et Georgiadis M. C. (Eds.) *Elsevier B. V.*, **2004**.

Giessler S., Danilov R.Y., Pisarenko R.Y., Serafimov L.A., Hasebe S. and Hashimoto I. Design and synthesis of feasible reactive distillation processes. *Computers & Chemical Engineering*, S811, **1999**.

Glasser D., Hildebrandt D. et Crowe C. A geometric approach to steady flow reactors: the attainable region and optimization in concentration space. *Industrial & Engineering Chemistry Research* 26, 1803, **1987**.

Gomez J.M. Optimisation numérique du fonctionnement, du dimensionnement et de la structure d'une colonne de distillation catalytique représentée par un modèle de transfert. PhD Thesis, *UPPA*, **2003**.

Gomez J.M., Reneaume J.M., Roques M., Meyer M. and Meyer X. A mixed integer nonlinear programming formulation for optimal design of a catalytic distillation column based on a generic nonequilibrium model. *Industrial & Engineering Chemistry Research* 45 (4), 1373, **2006**.

Gomez M.T.D., Repke J.U., Kim D.Y., Yang D.R. and Wozny G. Reduction of energy consumption in the process industry using a heat-integrated hybrid distillation pervaporation process. *Industrial & Engineering Chemistry Research* 48 (9), 4484, **2009**.

Götze L. et Bailer O. reactive Distillation with KAPATAK-S, *Sulzer Technical Review* 4, 3911, **1999**.

Götze L. et Bailer O. Sulzer Chemtech. Reactive distillation with KATAPAK®, *Catalysis Today* 69, 201. **2001**.

Grob S. et Hasse H. Reaction kinetics of the homogeneously catalyzed esterification of 1-butanol with acetic acid in a wide range of initial compositions. *Industrial & Engineering Chemistry Research* 45 (6), 1869, **2006**.

Grüner S. Nonlinear control of a reactive distillation column. *Control Engineering Practice* 11 (8), 915, **2003**.

Gurav H. et Bokade V. V. Synthesis of ethyl acetate by esterification of acetic acid with ethanol over a heteropolyacid on montmorillonite K10. *Journal of Natural Gas Chemistry* 19 (2), 161, **2010**.

H

Harbou E., Schmitt M., Parada S., Grossmann C. and Hasse, H. Study of heterogeneously catalysed reactive distillation using the D+R tray – A novel type of laboratory equipment. *Chemical Engineering Research and Design*, 89, 1271, **2011**.

Harmsen G.J., Korevaar G. et Lemkowitz S.M. Process intensification contributions to sustainable development, in: A. Stankiewicz, et al. (Eds.), *Re-engineering the Chemical Processing Plant*, Dekker, New York, **2003**.

Harmsen G.J. Industrial best practices of conceptual process design. *Chemical Engineering and Processing* 43 (5), 671, **2004**.

- Harmsen G. J. Reactive Distillation: The Front-runner of Industrial Process Intensification. A Full Review of Commercial Applications, Research, Scale-up, Design and Operation, *Chemical Engineering and Processing* 46, 774, **2007**.
- Hasanoglu A. et Dincer S. Modelling of a pervaporation membrane reactor during esterification reaction coupled with separation to produce ethyl acetate. *Desalination and Water Treatment* 35, 286, **2011**.
- Hasse H. Thermodynamics of Reactive Separations, in: Reactive Distillation: Status and Future Directions. Sundmacher K. et Kienle A. (Eds.) *Wiley-VCH Verlag GmbH & Co. KGaA*, Weinheim, **2003**.
- Hedjazi L., Kempowsky-Hamon T., Le Lann M.V. et J. Aguilar-Martin. Prognosis of breast cancer based on fuzzy classification method. In *3rd International Joint Conference on Biomedical Engineering Systems and Technologies, 1st International Conference on Bioinformatics*, **2010a**.
- Hedjazi L., Aguilar-Martin J., Le Lann M.V et Kempowsky-Hamon T.. Membership-margin based feature selection for mixed-type and high-dimensional data. *Fuzzy Sets and Systems*, **2010b**.
- Henley E. J. et Seader J. D. Equilibrium-stage separation operations on chemical engineering. *John Wiley & Sons, Inc.* **1981**.
- Higler A., Taylor R. et Krishna R. Modeling of a reactive separation process using a non equilibrium stage model. *Computer and Chemical Engineering* 22, S111, **1998**.
- Holt B.R. et Morari, M. Design of resilient processing plants. V. The effect of deadtime on dynamic resilience. *Chemical Engineering Science* 40, 1269, **1985**.
- Hu S., Zhang B.J., Hou X.Q., Li D.L. et Chen Q. L. Design and simulation of an entrainer-enhanced ethyl acetate reactive distillation process. *Chemical Engineering and Processing* 50, 1252, **2011**.
- Huang S., Kuo C., Hung S., Chen Y et Yu C. Temperature control of heterogeneous reactive distillation. *AIChE Journal* 50 (9), 2203, **2004**.
- Huang Y. S., Sundmacher K., Tulashie S. et Ernst-Ulrich S. Theoretical and experimental study on residue curve maps of propyl acetate synthesis reaction. *Chemical Engineering Science* 60 (12), 3363, **2005**.
- Huang K., Lin Q., Shao H., Wang C. et Wang S. A fundamental principle and systematic procedures for process intensification in reactive distillation columns. *Chemical Engineering and Processing: Process Intensification* 49, 294, **2010**.
- Huss R.S., Chen F., Malone M.F. et Doherty M.F. Computer aided tools for the design of reactive distillation systems. *Computer and Chemical Engineering*, 23, S955, **1999**.

I

- Isaza C. Diagnostic par techniques d'apprentissage floues : Conception d'une méthode de validation et d'optimisation des partitions. PhD thesis, *Laboratoire d'Analyse et d'Architecture des Systèmes du CNRS*, France, **2007**.
- Isaza N. C. , Le Lann M.V. and Aguilar-Martin J., Diagnosis of chemical processes by fuzzy clustering methods: new optimization method of partitions. *18th European Symposium on Computer Aided Process Engineering (ESCAPE 2008)*, Lyon (France), Juin 2008, 6p. (CD), **2008**.
- Isaza N. C. , Orantes A., Kempowsky T. and Le Lann M.V. Contribution of fuzzy classification for the diagnosis of complex systems. *SafeProcess 2009*, Barcelona, juillet **2009**.

J

- Jackson J. R. et Grossmann I. E. A disjunctive programming approach for the optimal design of reactive distillation columns. *Computer and Chemical Engineering* 25, 1661, **2001**.
- Johnson K.H. et Dallas A.B. US Patent 5348710, **1994**.

K

- Kawathekar R. et Riggs J. B. Nonlinear model predictive control of a reactive distillation column. *Control Engineering Practice* 15 (2), 231, **2007**.
- Kaymak U. et Babuska R. Compatible cluster merging for fuzzy modelling. In *IEEE Fuzzy Systems*, **1995**.
- Kaymak D. B. et Luyben W. L. Effect of chemical equilibrium constant on the design of reactive distillation columns, *Industrial and Engineering Chemistry Research* 43, 3666, **2003**.
- Kaymak D. B. et Luyben W. L. Comparison of two types of two-temperature control structures for reactive distillation columns. *Industrial & Engineering Chemistry Research* 44 (13), 4625, **2005**.
- Kaymak D. B. et Luyben W. L.; Evaluation of a two-temperature control structure for a two-reactant/two-product type of reactive distillation column, *Chemical Engineering Science*, 61, 4432, **2006**.
- Kempowsky T., Aguilar-Martin J., Subias A. et Le Lann M.V. Classification tool based on interactivity between expertise and self-learning techniques, *IFAC-Safeprocess*, Washington D.C., USA, **2003**.
- Kempowsky T. Surveillance de procédés à base de méthodes de classification : Conception d'un outil d'aide pour la détection et le diagnostic des défaillances. PhD thesis, *Institut National des Sciences Appliquées*, France, **2004**.
- Kempowsky T. P3S user's manual v1.0, **2011**.
- Kenig E, Schneider R. et Górak A. Rigorous dynamic modelling of complex reactive absorption processes. *Chemical Engineering Science*, 54 (21), 5195, **1999**.
- Kenig E., Bäder H., Górak A., Beßling B., Adrian T. et Schoenmakers H. Investigation of ethyl acetate reactive distillation process. *Chemical Engineering Science* 56 (21), 6185, **2001**.
- Keyes D. B. Esterification processes and equipment. *Industrial & Engineering Chemistry Research*, 24, 1096, **1932**.
- Kienle A. et Marquardt W., Bifurcation analysis and steady state multiplicity of multicomponent nonequilibrium distillation processes. *Chemical Engineering Science* 46 1757-1769, **1991**.
- Kienle A. et Marquardt W., Nonlinear dynamics and control of reactive distillation processes, in: *Reactive Distillation: Status and Future Directions*. Sundmacher K. et Kienle A. (Eds.) *Wiley-VCH Verlag GmbH & Co. KGaA*, Weinheim, **2003**.
- Klöcker M., Kenig E., Schmitt M., Althaus K., Schoenmakers H., Markusse P. et Kwant G. Influence of Operating Conditions and Column Configuration on the Performance of Reactive Distillation Columns with Liquid-Liquid Separators. *The Canadian Journal of Chemical Engineering* 81 (3-4), 725, **2003**.
- Klöcker M., Kenig E., Gorak A., Markusse A., Kwant G. et Moritz P. Investigation of different column configurations for the ethyl acetate synthesis via reactive distillation1. *Chemical Engineering and Processing* 43 (6), 791, **2004**.
- Kolena K., Lederer J., Mor'avek P., Hanika J., Smejkal Q. et Sk'ala D. *US Patent* 6,693,213, **2004**.
- Kookos I. K. Control structure selection of an ideal reactive distillation column. *Industrial & Engineering Chemistry Research* 50, 11193, **2011**.
- Konakom K., Saengchan A., Kittisupakorn P. et Mujtaba I.M. High Purity Ethyl Acetate Production with a Batch Reactive Distillation Column using Dynamic Optimization Strategy. *World Congress on Engineering and Computer Science* 748, **2010**.
- Konakom K., Saengchan A., Kittisupakorn P. et Mutjaba I. M. Use of batch reactive distillation with dynamic optimization strategy to achieve industrial grade ethyl acetate. *IAENG Transaction on Engineering Technologies*, Vol 6, 1373, **2011**.
- Kotora M., Buchaly C., Kreis P., Gorak A. et Markos J. Reactive distillation - experimental data for propyl propionate synthesis. *Chemical Papers*, 62 (1), 65, **2008**.
- Kramer G.J. Static liquid hold-up and capillary rise in packed beds. *Chemical Engineering Science* 53 (16), 2985, **1998**.
- Kraemer K., Harwardt A., Skiborowski M., Mitra S. et Marquardt W. *Chemical Engineering Research and Design* 89, 1168, **2011**.

- Krishna R. Hardware selection and design aspects for reactive distillation columns, in: *Reactive Distillation: Status and Future Directions*. Sundmacher K. et Kienle A. (Eds.) *Wiley-VCH Verlag GmbH & Co. KGaA*, Weinheim, **2003**.
- Kumar M. V. P. et Kaistha N. Decentralized control of a kinetically controlled ideal reactive distillation column. *Chemical Engineering Science* 63, 228, **2008**.
- Kumar M. V. P. et Kaistha N. Role of multiplicity in reactive distillation control system design. *Journal of Process Control*, 18, 692, **2008a**.
- Kumar M. V. P. et Kaistha N. Steady-state multiplicity and its implications on the control of an ideal reactive distillation column. *Industrial & Engineering Chemistry Research* 47, 2778, **2008b**.
- Kumar M. V. P. et Kaistha N. Evaluation of ratio control schemes in a two-temperature control structure for a methyl acetate reactive distillation column. *Chemical Engineering Research and Design* 87, 216, **2009**.
- Kumar M. V. P. et Kaistha N. Reactive distillation column design for controllability: A case study. *Chemical Engineering and Processing* 48, 606, **2009b**.
- Kustov A.V., Smirnova N. L. et Antonova O. A. Enthalpies and Heat Capacities of Ethyl Acetate Solutions in Water and in Several Organic Solvents at 298-318 K. *Journal of Solution Chemistry* 41 (6), 1008, **2012**.

L

- Lai I., Hung S., Hung W., Yu C., Lee M. et Huang H. Design and control of reactive distillation for ethyl and isopropyl acetates production with azeotropic feeds. *Chemical Engineering Science* 62, 878, **2007**.
- Lai I., Liu Y., Yu C., Lee M. et Huang H. Production of high-purity ethyl acetate using reactive distillation: Experimental and start-up procedure. *Chemical Engineering and Processing: Process Intensification* 47, (9-10), 1831, **2008**.
- Lee H. et Dudukovic M. P. A comparison of the equilibrium and nonequilibrium models for a multicomponent reactive distillation column. *Computers & Chemical Engineering* 23, 159, **1998**.
- Lee J.W., Hauan S. et Westerberg A.W. Graphical methods for reaction distribution in a reactive distillation column. *AIChE Journal* 46, 1218, **2000**.
- Lee J.W. et Westerberg A.W. Graphical design applied to MTBE and methyl acetate reactive distillation processes. *AIChE Journal* 47, 1333, **2001**.
- Lee J. W., Bruggemann S. et Marquardt W. Shortcut method for kinetically controlled reactive distillation systems. *AIChE Journal* 49 (6), 1471, **2003**.
- Lee H., Huang H. et Chien I. Bifurcation in the reactive distillation for ethyl acetate at lower Murphree plate efficiency. *Journal of Chemical Engineering of Japan*, 39 (6), 642, **2006**.
- Lee H., Huang H. et Chien I. Control of reactive distillation process for production of ethyl acetate. *Journal of Process Control* 17, 363, **2007**.
- Li P., Huang K. et Lin Q. A generalized method for the synthesis and design of reactive distillation columns *Chemical Engineering Research and Design* 90, 173, **2012**.
- Lim S., Loh W. et Shih Y. A comparison of prediction of accuracy complexity and training time of thirty-three old and new classification algorithms. *Machine Learning*. *Kluwer Academic Publishers*, **2000**.
- Lin Y. D., Huang H. P. et Yu C. C. Relay feedback tests for highly nonlinear processes: Reactive distillation. *Industrial & Engineering Chemistry Research* 45 (12), 4081, **2006**.
- Lin Q., Liu G., Huang K., Wang S. et Chen H. Balancing design and control of an olefin metathesis reactive distillation column through reactive section distribution. *Chemical Engineering Science* 66, 3049, **2011**.
- Lurette C. Développement d'une technique neuronale auto adaptative pour la classification dynamique de données évolutives Application a la supervision d'une presse hydraulique. PhD thesis, *Université des Sciences Technologies de Lille*, France, **2003**.
- Luyben W. L. Introduction, in: *Practical distillation control*. *Van Nostrand Reinhold*, **1992**.

- Luyben W.L. Economic and Dynamic Impact of the Use of Excess Reactant in reactive distillation systems. *Industrial & Engineering Chemistry Research* 39, 2935, **2000**.
- Luyben W. L. The need for simultaneous design education, in: Integration of process design and control. Seferlis P and Georgiadis M. C. (Eds), *Elsevier B. V.*, **2004**.
- Luyben W. L. Distillation design and control using AspenTM simulation. *John Wiley & Sons, Inc.*, **2006**.
- Luyben W. L. et Yu C. Reactive distillation design and control. *John Wiley & Sons, Inc.*, **2008**.
- Lv B.D., Liu G.P., Dong X. L., Wei W. et Jin W. Q. Novel Reactive Distillation-Pervaporation Coupled Process for Ethyl Acetate Production with Water Removal from Reboiler and Acetic Acid Recycle. *Industrial and Engineering Chemistry Research* 51 (23), 8079, **2012**.

M

- Mahdipoor H. R., Shirvani M., Nasr M. R. J. Et Shakiba S. Rigorous dynamic simulation of an industrial tray column, considered liquid flow regime and efficiency of trays. *Chemical Engineering Research and Design* 85, 1101, **2007**.
- Malone M. F. et Doherty M. F. Reactive distillation. *Industrial & Engineering Chemistry Research*, 39, 3953, **2000**.
- Mihal M., Švandová Z. et Markoš J. Steady state and dynamic simulation of a hybrid reactive separation process. *Chemical Papers* 64 (2), 193, **2009**.
- Miranda M., Reneaume J. M., Meyer X., Meyer M. and Szigeti F. Integrating process design and control: An application of optimal control to chemical processes. *Chemical Engineering and Processing: Process Intensification* 47 (11), 2004, **2008**.
- Mohideen M. J., Perkins J. D. et Pistikopoulos E. N. Robust stability considerations in optimal design of dynamic systems under uncertainty. *Journal of Process Control* 7, 371, **1997**.
- Moore C. Chapter 8, Practical distillation control. *Van Nostrand Reinhold*, edited by William L. Luyben, **1992**.
- Morari M. Design of resilient processing plants. III. A general framework for the assessment of dynamic resilience. *Chemical Engineering Science* 38, 1881, **1983**.
- Morari M. Effect of design on the controllability of chemical plants. In: *IFAC Workshop on Interactions Between Process Design and Process Control*, London, **1992**.

N

- Newell R. B. et Lee P.L. Applied Process Control. *Prentice Hall of Australia, NSW*, **1988**.
- Nikolau M. et Manousiouthakis V. Analysis of decentralised control structures for nonlinear systems. *AIChE Journal* 35, 549, **1989**.
- Noeres C., Dadhe K., Gesthuisen R., Engell S. et Gorak A. Model-based design, control and optimisation of catalytic distillation processes. *Chemical Engineering and Processing* 43 (3), 421, **2004**.

O

- Ogunnaike B. et Ray W. Process Dynamics, Modeling and Control. *Oxford University Press, Inc.*, **1994**.
- Olivier –Maget N. Surveillance des systèmes dynamiques hybrides : application aux procédés, PhD thesis , *INPT décembre*, **2007**.
- Olivier-Maget N. , Hétreux G., Le Lann J.M., Le Lann M.V, Model-based fault diagnosis for hybrid systems: Application on chemical processes, *Computers and Chemical Engineering Volume* 33 (10), 1617, **2009**.
- Olujic Z., Behrens M. et Spiegel L. Experimental characterization and modeling of the performance of a large-specific-area high-capacity structured packing. *Industrial and Engineering Chemistry Research* 46, 883, **2007**.

Orantes A., Kempowsky T. et Le Lann M.V. Classification as an aid tool for the selection of sensors used for fault detection and isolation. *Transactions of the Institute of Measurements and Control* 28 (5), 457, **2006**.

Orantes A., Kempowsky T., Le Lann M.V. et Aguilar-Martin J. A new support methodology for the placement of sensors used for fault detection and diagnosis. *Chemical Engineering and Processing* 47 (3), 330, **2007**.

P

Patel J, Uygun K, Huang YL. A path constrained method for integration of process design and control. *Computers & Chemical Engineering* 32, 1373, **2008**.

Piera N. et Aguilar J. Controlling selectivity in non-standard pattern recognition algorithms. *Transactions in Systems, Man and Cybernetics* 21, 71, **1991**.

Peng J., Edgar T. F. et Eldridge R. B. Dynamic rate-based and equilibrium models for a packed reactive distillation column. *Chemical Engineering Science* 58, 2671, **2003**.

Phung T.K., Casazza A. A., Aliakbarian B., Finocchio E., Perego P. Et Busca G. Catalytic conversion of ethyl acetate and acetic acid on alumina as models of vegetable oils conversion to biofuels. *Chemical Engineering Journal* 215, 838, **2013**.

Q

Qin S. J. and Badgwell T. An Overview of Nonlinear Model Predictive Control Applications. F. Allgöwer and A. Zheng, (Eds.), *Nonlinear Predictive Control*, Birkhäuser, p. 369, **2000**.

Qin S. J. and Badgwell T. A Survey of Industrial Model Predictive Control Technology. *Control Engineering Practice* 11, 733, **2003**.

R

Rahul M., Kumar M. V. P., Dwivedi D. et Kaistha N. An efficient algorithm for rigorous dynamic simulation of reactive distillation columns. *Computers & Chemical Engineering* 33, 1336, **2009**.

Ramzan N., Faheem M., Gani R. et Witt W. Multiple steady states detection in a packed-bed reactive distillation column using bifurcation analysis. *Computers & Chemical Engineering* 34 (4), 460, **2010**.

Reder C., Gehrke V. et Marquardt W. Steady state multiplicity in esterification distillation columns. *Computers & Chemical Engineering (Supplement)* S407, **1999**.

Reepmeyer F., Repke J.U. and Wozny G. Analysis of the start-up process for reactive distillation. *Chemical Engineering & Technology* 26 (1), 81, **2003**.

Reepmeyer F., Repke J.U. and Wozny G. Time optimal start-up strategies for reactive distillation columns. *Chemical Engineering Science* 59 (20), 4339, **2004**.

Rivera D. E., Morari M. et Skogestad S. Internal model control: PID controller design, *Industrial and Engineering Chemistry Process Development*, 25 (1), 252, **1986**.

Rock K.L. CDTECH. Selective hydrogenation of MAPD via catalytic distillation. ERTC Petrochemical Conference, Amsterdam, February **2002**.

Rosales-Quintero A. et Vargas-Villamil F. D. On the multiplicities of a catalytic distillation column for the deep hydrodesulfurization of light gas oil. *Industrial and Engineering Chemistry Research* 48, 1259, **2009**.

Rouzineau D., Meyer M., Prevost M, Meyer X., Reneaume J.M. Reactive distillation modelling and sensitivity analysis based on NEQ model. *Computer-Aided Chemical Engineering*, 20a-20b, 583, **2005**.

Rouzineau D. Simulation de techniques séparatives biphasiques multiconstituants réactives : modèle de transfert et validation expérimentale - application à la distillation réactive. PhD thesis, Institut National Polytechnique de Toulouse - Laboratoire de Génie Chimique, France, **2002**.

S

- Sakizlis V., Perkins J.D. et Pistikopoulos N. Recent advances in optimization-based simultaneous process and control design. *Computers & Chemical Engineering* 28, 2069, **2004**.
- Sandoval LAR, Budman HM, Douglas PL. Integration of design and control for chemical processes: a review of the literature and some recent results. *Annual Reviews in Control* 33, 158, **2009**.
- Schneider R., Noeres C., Kreul L. U. et Gorak A. Dynamic modelling and simulation of reactive batch distillation. *Computers & Chemical Engineering (Supplement)* S423, **1999**.
- Schoenmakers H. G. et Bessling B. Reactive distillation process development in the chemical industries, in: *Reactive distillation: Status and future directions*. Sundmacher K. et Kienle A. (Eds.) *Wiley-VCH Verlag GmbH & Co. KGaA*, Weinheim, **2003**.
- Seborg D., Edgar T. et Mellichamp D. *Process dynamics and control*, *John Wiley & Sons, Inc*, **1989**.
- Seider W. D., Seader J. D. et Lewin D. R. *Process design principles: Synthesis, analysis and evaluation*. *John Wiley & Sons, Inc.*, **1999**.
- Seferlis P. et Georgiadis M. C. Integration of process design and control – Summary and future directions, in: *The integration of process design and control*. Seferlis P. et Georgiadis M. C.(Eds.) *Elsevier B. V.*, **2004**.
- Sharifzadeh M. Implementation of a steady-state inversely controlled process model for integrated design and control of an ETBE reactive distillation. *Chemical Engineering Science* 92, 21, **2013**.
- Sharma M. M. et Mahajani S. M. Industrial applications of reactive distillation, in: *Reactive distillation: Status and future directions*. Sundmacher K. et Kienle A. (Eds.) *Wiley-VCH Verlag GmbH & Co. KGaA*, Weinheim, **2003**.
- Sharma N. et Singh K. Control of reactive distillation column : A review. *International Journal of Chemical Reactor Engineering* vol.8, **2010**.
- Siirola J.J. Industrial applications of chemical process synthesis, in: *Advances in Chemical Engineering, Process Synthesis*. J.L. Anderson (Ed.), *Academic Press*, **1996**.
- Singh A., Hiwale R., Mahajani S. M., Gudi R.D., Gangadwala J. et Kienle A. Production of butyl acetate by catalytic distillation. Theoretical and experimental studies. *Industrial and Engineering Chemistry Research* 44 (9), 3042, **2005**.
- Singh B. P., Singh R., Kumar M. V. et Kaistha N. Steady-state analyses for reactive distillation control: An MTBE case study. *Journal of Loss Prevention in the Process Industries* 18, 283, **2005a**.
- Skogestad S, Morari M. Design of resilient processing plants-the effect of model uncertainty on dynamic resilience. *Chemical Engineering Science* 42, 1765, **1987**.
- Smejkal Q., Kolena J. et Hanika J. Ethyl acetate synthesis by coupling of fixed-bed reactor and reactive distillation column-Process integration aspects. *Chemical Engineering Journal* 154, 236, **2009**.
- Sneesby M. Two-point control of a reactive distillation column for composition and conversion. *Journal of Process Control* 9 (1), 19, **1999**.
- Steger C. *Distillation discontinue extractive et réactive dans une colonne avec un bac intermédiaire*. Ph.D. Thesis, *Institut National Polytechnique de Toulouse - Laboratoire de Génie Chimique*, France, **2006**.
- Stichlmair J. et Frey T. Mixed-integer nonlinear programming optimization of reactive distillation processes. *Industrial & Engineering Chemistry Research* 40 (25), 5978, **2001**.
- Subawalla H., Gonzalez J.C., Seibert A.F. et Fair J.R. Capacity and efficiency of reactive distillation bale packing: Modeling and experimental validation. *Industrial & Engineering Chemistry Research* 36 (9), 3821, **1997**.
- Subawalla H. et Fair J.R. Design guidelines for solid-catalyzed reactive distillation systems, *Industrial & Engineering Chemistry Research* 38, 3696, **1999**.
- Sundmacher K., Uhde G. et Hoffmann U. Multiple reactions in catalytic distillation processes for the production of the fuel oxygenates MTBE and TAME: Analysis by rigorous model and experimental validation. *Chemical Engineering Science* 54, 2839, **1999**.

Sumana C. et Venkateswarlu Ch. Genetically Tuned Decentralized Proportional-Integral Controllers for Composition Control of Reactive Distillation. *Industrial & Engineering Chemistry Research* 49 (3), 1297, **2010**.

T

Tang Y. T., Huang H. P. et Chien I. L. Design of a complete ethyl acetate reactive distillation system. *Journal of Chemical Engineering of Japan*, 36, 1352, **2003**.

Tang Y., Chen Y., Huang H., Yu C., Hung S. et Lee M. Design of reactive distillations for acetic acid esterification. *AIChE Journal*, 51 (6), 1683, **2005a**.

Tang Y. T., Huang H. P. et Chien I. L. Plant-wide control of a complete ethyl acetate reactive distillation process. *Journal of Chemical Engineering of Japan*, 38, 130, **2005b**.

Tang B.H. Synthesis of Ethyl Acetate Catalyzed by Inorganic Salt. *Future Material Research and Industry Application* 455, 1060, **2012**.

Taylor R. et Krishna R. Modelling reactive distillation. *Chemical Engineering Science* 55 (22), 5183, **2000**.

Terrazas-Moreno S., Flores-Tlacuahuac A. et Grossmann I. E. Simultaneous design, scheduling, and optimal control of a methylmethacrylate continuous polymerization reactor. *AIChE Journal* 54, 3160, **2008**.

Théry R. Analyse de faisabilité, synthèse et conception de procédés de distillation réactive. PhD thesis, *Institut National Polytechnique de Toulouse - Laboratoire de Génie Chimique*, France, **2002**.

Théry R., Meyer X. M. et Joulia X. Analyse de faisabilité, synthèse et conception des procédés de distillation réactive: état de l'art et analyse critique. *The Canadian Journal of Chemistry Engineering*, 83, 242, **2005a**.

Théry R., Meyer X. M., Joulia X. et Meyer M. Preliminary design of reactive distillation columns. *Chemical Engineering Research and Design*, 83 (A4), 379, **2005b**.

Théry-Hétreux R., Meyer X. M., Meyer M. et Joulia X.. Feasibility analysis, synthesis and design of reactive distillation processes: a focus on double feed processes, *AIChE Journal*, 58, 2346, **2012**.

Tsai R. C., Cheng J. K., Huang H. P., Yu C. C., Shen Y. S. and Chen Y. T. Design and Control of the Side Reactor Configuration for Production of Ethyl Acetate. *Industrial & Engineering Chemistry Research* 47 (23), 9472, **2008**.

U

Ung S. et Doherty M.F. Synthesis of reactive distillation systems with multiple equilibrium chemical reactions. *Industrial and Engineering Chemistry Research*, 34, 2555, **1995**.

V

Vaca M. A note on the controllability of two short-cut designs for a class of thermally coupled distillation sequence. *Industrial & Engineering Chemistry Research* 48, 2283, **2009**.

Vega M. P. et Pinto J. C. Use of bifurcation analysis for development of nonlinear models for control applications. *Chemical Engineering Science*, 63, 5129, **2008**.

Venkateswarlu C. et Reddy A. D. Nonlinear model predictive control of reactive distillation based on stochastic optimization. *Industrial & Engineering Chemistry Research* 47, 6949, **2008**.

Völker M., Sonntag C. et Engell S. Control of integrated processes: A case study on reactive distillation in a medium-scale pilot plant. *Control Engineering Practices* 15 (7), 863, **2007**.

Vora N. et Daoutidis P. Dynamics and control of an ethyl acetate reactive distillation column. *Industrial & Engineering Chemistry Research* 40 (3), 833, **2001**.

W

- Wahnschafft O.M. et Westerberg A.W., The product composition regions of azeotropic distillation columns. 2. separability in two-feed columns and entrainer selection. *Industrial & Engineering Chemistry Research* 32, 1108, **1993**.
- Weissman J. Construction d'un modèle comportemental pour la supervision de procédés: Application a une station de traitement des eaux. PhD thesis, *Institut National Polytechnique de Toulouse*, France, **2000**.
- Walter E. et Pronzato L. Identification of parametric models: from experimental data. *Springer*, **2010**.
- Wang S. J., Wong D. S.H. et Yu S. W. Design and control of transesterification reactive distillation with thermal coupling. *Computers & Chemical Engineering* 32 (12), 3030, **2008**.
- Wang J., Chang Y, Wang E. Q.. et Li C. Y. Bifurcation analysis for MTBE synthesis in a suspension catalytic distillation column. *Computers & Chemical Engineering* 32 (6), 1316, **2008b**.
- Wang S.J., Huang H.P. et Yu C. C. Plantwide Design of Transesterification Reactive Distillation to Co-Generate Ethyl Acetate and n-Butanol. *Industrial & Engineering Chemistry Research* 49 (2), 750, **2010**.
- Wolff E. A., Skogestad S., Hovd M. et Mathisen K. W. A procedure for controllability analysis. *IFAC Workshop on interactions between process design and process control*, London, **1992**.

X

- Xu Y., Zheng Y., Ng F. T. T. et Rempel G. L. A three-phase nonequilibrium dynamic model for catalytic distillation. *Chemical Engineering Science* 60 (20), 5637, **2005**.

Y

- Yuan Z., Zhang N., Chen B. et Zhao J. An overview on controllability analysis for chemical processes. *AICHE Journal* 57 (5), 1185, **2011**.
- Yuan Z., Zhang N., Chen B. et Zhao J. Systematic controllability analysis for chemical processes. *AICHE Journal* 58 (10), 3096, **2012**.

Z

- Zheng H., Tian H., Zou W., Huang Z., Wang X., Qiu T., Zhao S. et Wu Y. Residue curve maps of ethyl acetate synthesis reaction. *Journal of Central South University* 20, 50, **2013**.

Appendices

The appendices are the following:

I	Thermodynamic study of the binaries	260
II	Mathematical modeling of processes and advanced control design	264
III	Classification algorithms	288
IV	Programming codes MATLAB [®]	296
V	Dynamic simulations	298

I. THERMODYNAMIC STUDY OF THE BINARIES

The design of the reactive distillation process requires reliable thermodynamic parameters for the determination of phase equilibria. In this Appendix, vapor-liquid study of the constituent binaries of the quaternary system ethyl acetate + water + ethanol + acetic acid is presented. For each binary, the xy diagram and the boiling temperature diagram were plotted. The graphics compare the equilibrium phase data provided by experimental studies to the data given by simulation with the NRTL and the NRTL-HOC models.

Actually, the NRTL activity coefficient model was considered for the phase equilibrium, with consideration of the binary parameters previously presented in the Table 9.1. The NRTL-HOC model is the simultaneous consideration of the NRTL parameters and the Hayden–O’Connell second virial coefficient model with association parameters to account for the acetic acid dimerisation in the vapor phase. The Aspen Plus[®] built-in association parameters are used to compute fugacity coefficients.

The vapor-liquid equilibria for the binaries water + acetic acid, ethyl acetate + acetic acid, water + ethanol, water + ethyl acetate and ethanol + ethyl acetate have been analyzed at 760mmHg. Due to the different availability of experimental data, the vapor-liquid equilibrium of the binary ethanol + acetic acid was analyzed at 706mmHg. Results are presented on molar compositions.

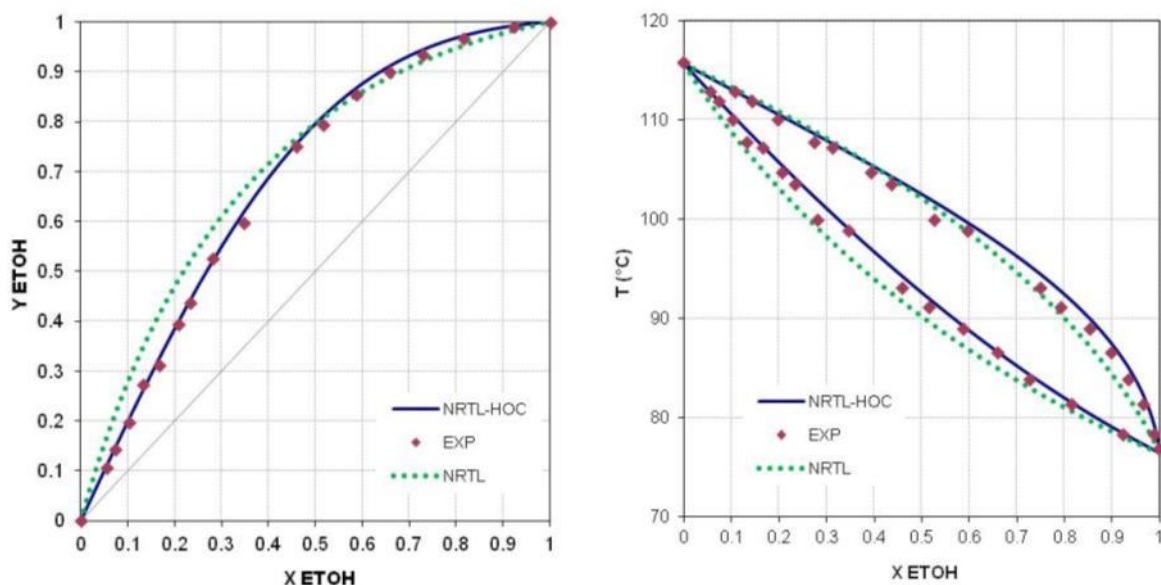


Figure A1.1. Binary xy and boiling temperature diagrams of the system ethanol – acetic acid

Experimental data for the binary ethanol – acetic acid was obtained from Rius et al. (1959).

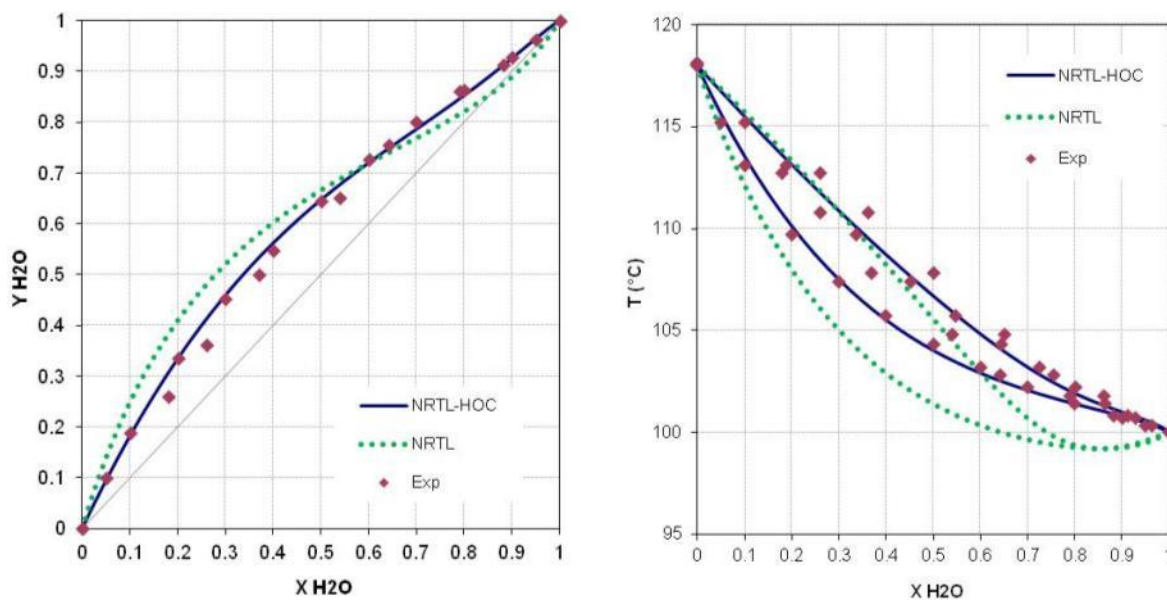


Figure A1.2. Binary xy and boiling temperature diagrams of the system water – acetic acid

Experimental data for the binary water – acetic acid was obtained from Acharya and Rao (1947), Hua Hsueh Hsueh Pao (1976) and Ramalho et al. (1964).

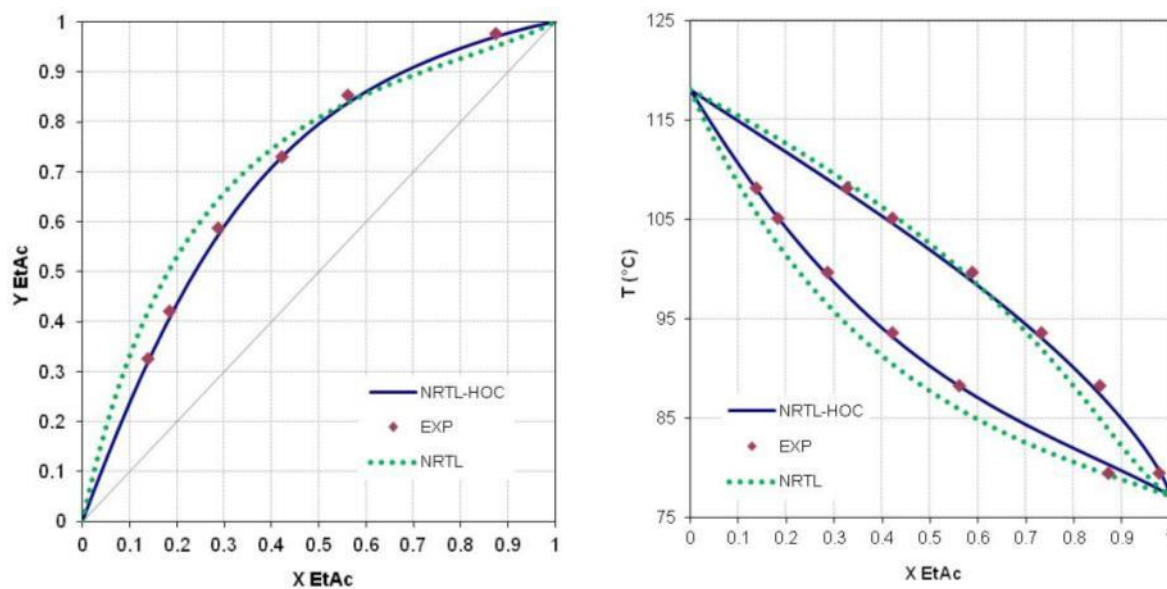


Figure A1.3. Binary xy and boiling temperature diagrams of the system ethyl acetate – acetic acid

Experimental data for the binary ethyl acetate – acetic acid was obtained from Garner et al. (1954) and Gorbunova et al. (1965).

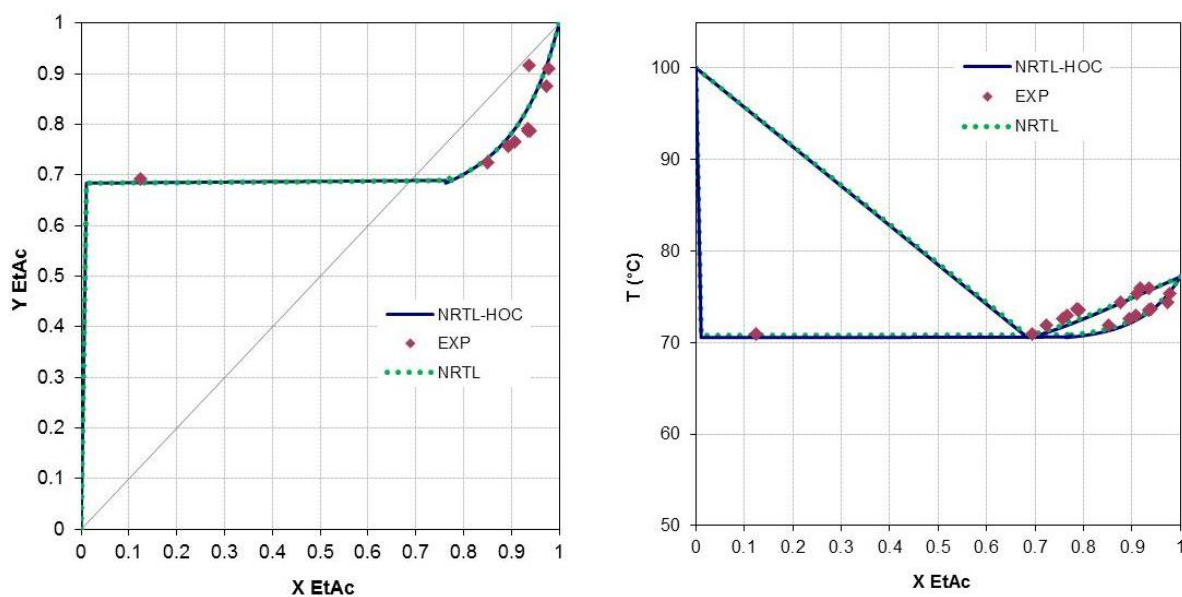


Figure A1.4. Binary xy and boiling temperature diagrams of the system ethyl acetate – water

Experimental data for the binary ethyl acetate – acetic acid was obtained from Kato et al. (1971).

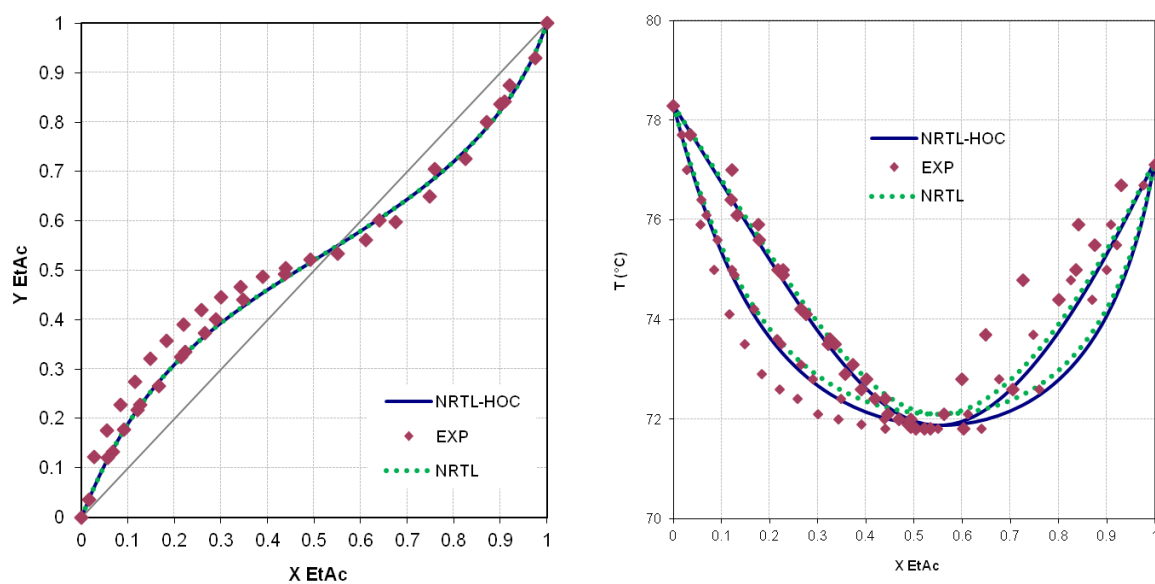


Figure A1.5. Binary xy and boiling temperature diagrams of the system ethyl acetate – ethanol

Experimental data for the binary ethyl acetate – acetic acid was obtained from Kireev et al. (1936) and Furnas and Leighton (1937).

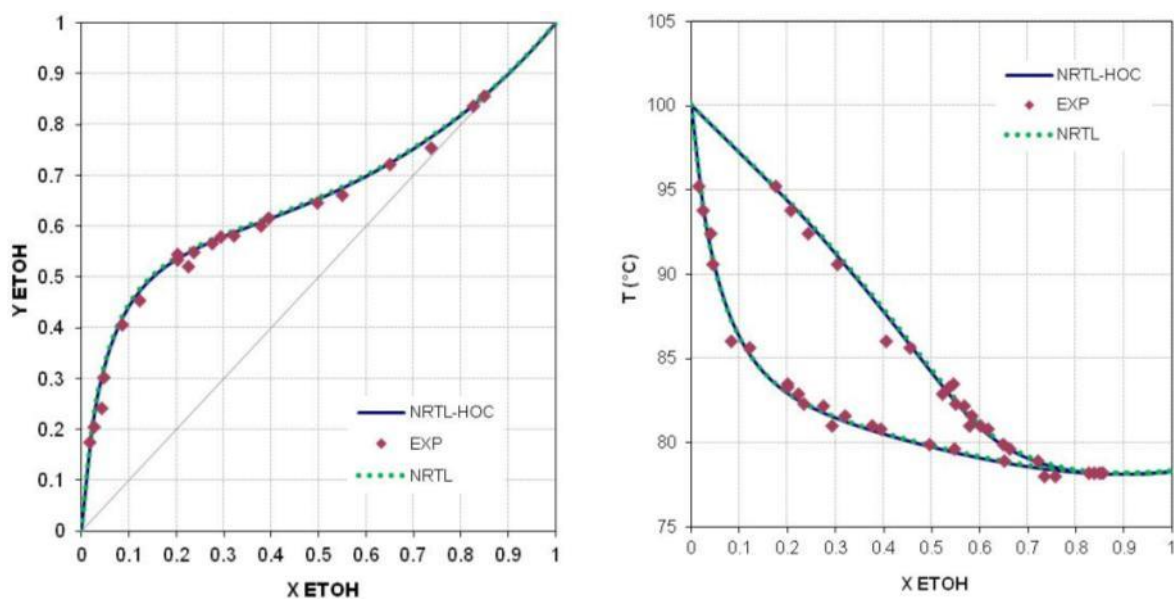


Figure A1.6. Binary xy and boiling temperature diagrams of the system ethanol – water

Experimental data for the binary ethyl acetate – acetic acid was obtained from Novella et Tarraso (1952) and Heitz (1960).

The NRTL-HOC is shown to be a reliable thermodynamic model for the representation of the binaries vapor-liquid equilibria. Actually, the consideration of the acetic acid dimerisation in the vapor phase by the Hayden–O’Connell is crucial for a good system representation.

The model predicts two minimum boiling homogeneous binary azeotropes between the components ethyl acetate – ethanol and ethanol – water, and one heterogeneous azeotrope in the binary ethyl acetate – water.

II. MATHEMATICAL MODELING OF PROCESSES AND ADVANCED CONTROLLERS DESIGN

The thesis manuscript presented several details on the reactive distillation process modeling, dynamic analysis and control aspects. The controllability studies were performed by considering the linear controllers PI (Proportional-Integral) for product purities regulation. In this appendix, the mathematical considerations of these models, the modeling of other possible controllers and some tuning methods are presented.

During mathematical descriptions of the process, the models for control will normally use the following notation:

y – the output, or controlled variable

m – the input, or measured variable

u – the input, or manipulated variable

d – the disturbance variable

x – the state variable

The mathematical models that strictly relate the output variables with the input variables are called input/output models. The mathematical models in which state variables appear explicitly along with the input and the output variables are called state-space models. Input/output models can be obtained by appropriate transformations of the state-space form, or directly from output/input data correlations. The input/output models can occur in the time domain, as well as in the frequency, Laplace or z-domain. The state-space models naturally occur in the time domain. Ogunnaike and Ray (1994) considered usual to cast these mathematical models, for any particular process, in one of four ways:

- The state-space (differential or difference equation) form; used on real-time simulation of process behavior, nonlinear dynamic analysis,
- The transform-domain (Laplace or z-transforms) form; used on linear dynamic analysis involving well-characterized input functions, control system design,
- The frequency-response (or complex variable) form; used on linear nonparametric models for processes of arbitrary mathematical structure, control system design,
- The impulse-response (or convolution) form; used on linear dynamic analysis involving arbitrary input functions, dynamic analysis and controller design for processes with unusual model structures,

- The impulse-response and the frequency-response model forms allow the creation of nonparametric dynamic models directly from experimental data, independently of mathematical relations. On the contrary, the transform-domain and the state-space models require a parametric functional form to fit experimental data.

Sometimes, it would be easier, or even necessary, to process a model different from the one that is already available. For this purpose, some relationships exist to convert one model to another.

12.3.1 State-Space Models

For the study of reactive distillation process dynamics, the state-space models are most commonly used. They allow the analysis of nonlinear system behavior and, because they are formulated with time as the independent variable, state-space models are useful on obtaining real-time behavior of process systems. For computer simulation, discrete-time formulations of the state-space models are possible. All of these conditions can be formulated by the mathematical representations presented below.

Continuous Time

For continuous time, a linear system, with a first-order differential equation, can represent a process with one input variable $u(t)$, one output variable $y(t)$ and one state variable $x(t)$:

$$\begin{aligned}\frac{dx(t)}{dt} &= ax(t) + bu(t) + \gamma d(t) \\ y(t) &= cx(t)\end{aligned}$$

Discrete Time

The process variables may be obtained at discrete points in time and their state-space model is formulated with difference equations. Some typical discrete-time models are commonly used on computer simulation. For a single-input, single-output variables linear process, the discrete model is represented:

$$\begin{aligned}x(k+1) &= qx(k) + ru(k) + \psi d(k) \\ y(k) &= cx(k)\end{aligned}$$

where $x(k)$, $u(k)$, $d(k)$ and $y(k)$ are, respectively, the state, control, disturbance and output variables at the discrete-time instant $t_k = k\Delta t$, with Δt as the sampling interval.

Wiener and Hammerstein Models

Sometimes, the dynamics of a process can be well described by a linear system, but there are static nonlinearities at the input or at the output. This phenomenon can occur if the sensors have nonlinear characteristics, for example.

A model with a static nonlinearity at the input is called a Hammerstein model, while a process with nonlinearity in the output is called a Wiener model. Their combination is known as the Wiener-Hammerstein model. For the Hammerstein case, the predicted output at a time t is given:

$$y(t) = G(q) \cdot f(u(t))$$

where $G(q)$ is the time-varying linear dynamic model and $f(\cdot)$ is the input static nonlinearity

12.3.2 Multiple-Input and Multiple-Output Systems

The most important chemical processes are often multivariable in nature. Because of the presence of multiple inputs and multiple outputs, it is known as MIMO system. The mathematical models for single-input and single-output (SISO) processes can be adapted to MIMO systems.

Models used to represent the behavior of multivariable process occur most commonly in the state-space form or in the transfer function form. Because of the presence of a multivariable system, the equations on the process model are more conveniently written in vector-matrix form.

State-space representation of MIMO processes

For a MIMO process, the mathematical representation becomes:

$$\begin{aligned} \frac{dx(t)}{dt} &= Ax(t) + Bu(t) + \Gamma d(t) \\ y(t) &= Cx(t) \end{aligned}$$

where x , u , y and d are appropriately dimensioned system vectors and

A , B , C and Γ are appropriately dimensioned system matrices

When there is an input delay α , a state delay β , an output delay η , and a disturbance delay δ , the time-domain model is on the form:

$$\begin{aligned}\frac{dx(t)}{dt} &= A_0x(t) + A_1x(t - \beta) + B_0u(t) + B_1u(t - \alpha) + \Gamma_0d(t) + \Gamma_1d(t - \delta) \\ y(t) &= C_0x(t) + C_1x(t - \eta)\end{aligned}$$

where x , u , d and y are vectors and A_0 , A_1 , B_0 , B_1 , Γ_0 , Γ_1 , C_0 and C_1 are matrices.

Nonlinear MIMO systems are represented in the form:

$$\begin{aligned}\frac{dx(t)}{dt} &= f(x, u, d) \\ y(t) &= h(x(t))\end{aligned}$$

where $f(\cdot)$ and $h(\cdot)$ are usually vectors of nonlinear functions

Multivariable processes also have representation in the discrete-time form of state-space models:

$$\begin{aligned}x(k+1) &= Qx(k) + Ru(k) + \Psi d(k) \\ y(k) &= Cx(k)\end{aligned}$$

where Q , R , Ψ and C are the appropriated matrices, and x , u , d and y are replaced by the corresponding vector quantities.

Finally, the most general form of nonlinear and discrete processes is represented:

$$\begin{aligned}x(k+1) &= f(x(k), u(k), d(k)) \\ y(k) &= h(x(k))\end{aligned}$$

Transfer-function representation of MIMO processes

The multivariable transfer function model form relates the Laplace transform of the vector of input variables to the vector of output variables. The Laplace transform is a mathematical transformation that converts differential equations to algebraic equations, what can simplify the calculation required to obtain a solution. For a m -input, n -output system:

$$y(s) = G(s)u(s) + G_d(s)d(s)$$

where $G(s)$ is the $m \times n$ transfer function matrix, with transfer function elements:

$$G(s) = \begin{bmatrix} g_{11}(s) & g_{12}(s) & \dots & g_{1m}(s) \\ g_{21}(s) & g_{22}(s) & \dots & g_{2m}(s) \\ \dots & \dots & \dots & \dots \\ g_{n1}(s) & g_{n2}(s) & \dots & g_{nm}(s) \end{bmatrix}$$

and $G_d(s)$ is an $n \times k$ transfer function matrix with analogous elements representing the disturbances of the system.

12.3.3 *Dynamic Analysis*

Once the process model is defined, the essence of dynamic analysis is the investigation of the process time-dependent response forced by the application of certain well-characterized input functions.

The typical forcing functions used are:

- The step function
- The impulse function
- The rectangular pulse function
- The ramp function
- The sinusoidal function

Dynamic analysis allows the characterization of a wide variety of actual processes into a relatively small number of well-defined categories. Depending on the process, the dynamic response could take a different form; its interpretation and classification are important for the process control design.

The mathematical tools usually considered to the study of process dynamic analysis are differential equations, numerical methods, Laplace and z-transforms, and matrices. The strategies are taken both on open-loop analysis and on closed-loop analysis.

Open-loop Dynamic Analysis

In mathematical notation, the open loop dynamic analysis of MIMO processes involves determining the process vector output $y(t)$, given the process model, and specific forms of forcing functions $u(t)$. There is no flow of information controlling back the system.

The dynamic, or transient, responses can be obtained using the state-space form or the transfer function form, in function of the problem case. For nonlinear multivariable system, as the reactive distillation, the only possible model should be in the state-space form.

For nonlinear multivariable systems, the dynamic analysis requires sophisticated mathematical tools. In order to simplification of the analysis, we will consider that approximate linear analysis, using either linearized state-space models, or equivalent transfer function matrices, are sufficient.

Open-loop dynamic analysis in state-space form

The dynamic analysis for linear systems represented in the state-space form is directly obtained: the state-space model is solved for any given form of forcing function and the nature of the resulting solution is investigated.

For non-linear systems, an approximate linear analysis is adopted, and the equations in the state-space form can also be considered as the process model:

$$\begin{aligned}\frac{dx(t)}{dt} &= Ax(t) + Bu(t) + \Gamma d(t) \\ y(t) &= Cx(t)\end{aligned}$$

where A , B , C and Γ are appropriately dimensioned system matrices

Because this equation is linear with constant coefficients, and a first-order ODE, the analytical solution can be represented:

$$\begin{aligned}x(t) &= \int_0^t e^{A(t-\sigma)} [Bu(\sigma) + \Gamma d(\sigma)] d\sigma \\ y(t) &= C \cdot \int_0^t e^{A(t-\sigma)} [Bu(\sigma) + \Gamma d(\sigma)] d\sigma\end{aligned}$$

The stability of the open-loop behavior of a multivariable process given in the state space depends on the elements of the matrix A : the process is open-loop stable if and only if all the eigenvalues of the matrix A have negative real parts.

Open-loop dynamic analysis of multivariable transfer function

The multivariable transfer function is a matrix that relates the Laplace transforms of the input vector $u(s)$ and the output vector $y(s)$:

$$y(s) = G(s)u(s)$$

This transfer function matrix $G(s)$ is also known as the transfer matrix. This matrix has similar linear properties of the single-input single-output (SISO) processes, and also has poles and zeros. These poles and zeros determine the nature of the multivariable system response. The poles of a transfer function matrix are the same as the eigenvalues of the equivalent system matrix A in the state-space form. The zeros of the multivariable system are the zeros of the determinant of the transfer function matrix $|G(s)|$.

The multivariable system outputs, or the open-loop dynamic responses, in the time domain can be obtained after carrying out a partial fraction expansion for each transfer function element, and inverting (the same manner as with SISO systems):

$$y_i = \sum_{j=1}^m \sum_{q=1}^{p_{ij}} \left(A_{ijq} e^{r_{ijq} t} \right)$$

where A_{ijq} are obtained from the partial fraction expansion, and r_{ijq} are the transfer function poles

A multivariable system is stable if all the poles of the transfer function matrix lie in the left-half plane i.e. have negative real parts. Otherwise, the system is unstable.

12.3.4 Closed-loop Dynamic Analysis

In closed-loop multivariable control systems, the output variables are measured and their values are sent to the appropriate controllers. In order to regulate the behavior of each output variable, the control actions are taken into the input, or manipulated, variables. Such arrangement gives rise to multiple control loops, with each individual loop resembling a SISO control loop.

For a closed-loop system, the transfer-function representation of MIMO processes is added by an equation for the control action $u(s)$:

$$y(s) = G(s)u(s) + G_d(s)d(s)$$

$$u(s) = G_c(s)\varepsilon(s)$$

$$\text{where } \varepsilon(s) = y_{sp} - y(s)$$

The response of the multivariable system in the closed loop to changes in the vector of set points y_{sp} and in the vector of disturbances d can be written as:

$$y(s) = \frac{\text{Adj}(I + GG_c) \cdot GG_c}{|(I + GG_c)|} y_{sp} + \frac{\text{Adj}(I + GG_c) \cdot G_d}{|(I + GG_c)|} d$$

The characteristic equation for the multivariable system is the polynomial resulting from the determinant of the return difference matrix:

$$|(I + GG_c)| = 0$$

The condition for the stability of the system is all the roots of this characteristic equation to have negative real parts.

It is important to highlight that guaranteeing stability for each individual loop provides no guarantee to the stability of the system when all loops are closed and operating simultaneously. This behavior is a consequence of possible interactions within the different controlled and manipulated variables. The choice of the best variables pairing is determinant on trying to avoid interactions.

12.3.5 Controller Design

For most control problems, the closed-loop system will be stable for a range of controller settings. Thus, it is possible to find these settings by selecting numerical values that result in desired closed-loop system performance. Some successful advanced control techniques were recently developed.

For specifying controller design and settings, different alternatives may be considered:

- Feedback Controllers
- Tuning Relations
- Multivariable Decoupling
- Direct Synthesis method
- Internal Model Control
- Optimization Approach
- Frequency Response techniques
- Computer simulation using physically-based models
- Field tuning after installation

In SISO systems, or in MIMO systems with little interaction among the variables, a single input can be paired with a single output variable by a feedback strategy. Feedback controllers are commonly used in industrial practice and the most widely applied type is the proportional-integral-derivative (PID).

In real multivariable system, the input variables are coupled to all outputs variables, resulting on important interactions among them. In this type of systems, the main input-output couplings remain desirable, but the cross-couplings, responsible for interactions, remain undesirable. Because it is commonly impossible to eliminate the cross-couplings that cause these interactions, techniques to improve the control performance should eliminate, or compensate, the effects caused by these undesirable cross-couplings. The multivariable decoupling method is the alternative most widely used.

Direct Synthesis and Internal Model Control methods are known as model-based control; what is specified a priori is the dynamic behavior desired of the closed-loop response – not the controller structure. The design technique derives the structure and the parameters of the controller that will achieve the specified desired objectives. The controller is designed by explicit use of a process model.

Model-based methods are especially useful for controller tuning since they accept simple models, and only single tuning parameters need to be specified in the calculations. In this case, the effect of all inputs on process response is considered, and there is no pairings between single variables.

When comparing, Internal Model Control has two main advantages in relation to Direct Synthesis Method: it takes model uncertainty into account and it allows the controller design to determine a good trade-off between control system performance and robustness to process changes and model errors.

The Optimization Approach specifies a desired output behavior in the form of an objective function, and the process model is used to derive the controller required to minimize this objective. The most widely technique is the Model Predictive Control, where past process dynamic behavior is used to model a quadratic objective function that relates the error between the set point and the predicted outputs.

Frequency response techniques can be applied to linear dynamic models of any order. The disadvantage of the method is that it is generally iterative in nature; hence it can be time-consuming without an effective computer program. Moreover, conservative controller settings should be employed as protection against instability.

Computer simulation can generate important information on dynamic behavior and control system performance, but a significant amount of engineering effort is needed.

Finally, field tuning of the controller after installation is often required since the process models are rarely exact.

In this section, some of these techniques are presented, based on their importance to the reactive distillation control systems, and the frequency of their use on the publications concerning this subject. The presentation begins by discussing the PID feedback controllers. The controller design to MIMO system is then explored, presenting different techniques as Decoupling, Internal Model Control, Model Predictive and Optimal Control.

These techniques are presented as they were firstly developed, concerning linear control systems designs. Later, nonlinear extensions are also discussed.

Feedback Controllers

Feedback control strategy is a widely used strategy when one input is used to control one other output. The objective is to reduce the error signal $e(t)$ between the set point $y_{sp}(t)$ and the measured value of the controlled variable $y(t)$ to zero:

$$e(t) = y_{sp}(t) - y(t)$$

The most important commercial type of feedback controllers is the proportional-integral-derivative (PID) controller. This kind of feedback control action became commercially available during the 1930s and the three basic control modes that are employed are proportional (P), integral (I) and derivative (D) control.

In proportional control P, the controller output is proportional to the error signal:

$$p(t) = \bar{p} + K_c e(t)$$

where $p(t)$: controller output

\bar{p} : bias value (value of the manipulative variable corresponding to the nominal steady state)

K_c : controller gain

The main advantages of a P controller is that the controller gain can be adjusted to make the controller as sensitive as desired to the deviations between set point and controlled variables, and that corrective action is taken as soon as the error is detected. An inherent disadvantage is its inability to eliminate steady state errors, or offsets, which may occur after a set-point change or a load disturbance.

For a system where steady-state offsets are unimportant and can therefore be tolerated, a P controller is used. Many liquid level control loops, as the reboiler or condenser in a RD column, for example, are with P control. However, when elimination of the offset is required, the integral control action I is used. Because the integral control action by itself occurs only after the error signal has persisted for some time, it is normally employed in conjunction with proportional control, resulting on the PI controller:

$$p(t) = \bar{p} + K_c \left[e(t) + \frac{1}{\tau_I} \int_0^t e(t^*) dt^* \right]$$

where τ_I : integral or reset time

The main disadvantage of using integral action is that it normally causes oscillatory response of the controlled process and thus reduces system stability. The excess of this undesirable effect can be avoided by proper tuning of the controller or by including derivative action which tends to counteract the destabilizing effects

Derivative control D considers the rate of change of the error signal and thus anticipates future behavior of the system. When all proportional, integral and derivative actions are considered, the PID controller is obtained:

$$p(t) = \bar{p} + K_c \left[e(t) + \frac{1}{\tau_I} \int_0^t e(t^*) dt + \tau_D \frac{de(t)}{dt} \right]$$

where τ_D : derivative time

Nevertheless the derivative effect is very sensitive to noisy measurements and can lead to instability behavior. Consequently, a large proportion of feedback controllers in a typical chemical plant are of the PI type. An important quantity of publications dealing with RD column control strategy use PI controllers on temperature and purity control loops.

PID controller should be used when it is important to compensate for some sluggishness in the overall system, and the process signals are relatively noise-free.

Multivariable Decoupling

A true multivariable system appears when the controllers utilize all the available process output information jointly to make decisions on how to manipulate the vector of input variables. The input variables are coupled to all output variables and the interactions among them cannot be neglected.

In this case, a multiple single-loop control configuration will not be efficient to control the process, and the Relative Gain Array method will not provide a perfect diagonal variable pairing. The design of effective multivariable controllers is a challenging problem faced by industrial control practitioners.

The most widely used multivariable controller design technique is the Decoupling. The idea of decoupling is to compensate the effects of interactions in the system, caused by the cross-coupling. The compensation is obtained by the addition of an interaction compensator between the single-loop controller and the process G .

Then, the decoupler design is based on choosing the elements of the compensator G_I to satisfy the control objective. Ogunnaike and Ray (1994) cited the following general procedure for decoupler design:

1. The process model is given by:

$$\begin{aligned} y &= Gu \\ u &= G_I v \\ \text{that gives } y &= GG_I v \end{aligned}$$

2. With the objective of eliminating all interactions, y must be related to v through a diagonal matrix, that we can call $G_R(s)$. This diagonal matrix's elements should be selected to provide the desired decoupled behavior with the simplest possible decoupler. Commonly, the diagonal elements of $G(s)$ are retained as the elements of the diagonal matrix $G_R(s)$:

$$G_R = \text{diag}[G(s)]$$

3. Finally, we may choose G_I such that:

$$\begin{aligned} GG_I &= G_R(s) \\ \text{that gives } G_I &= G^{-1}G_R \end{aligned}$$

Because decoupling design procedure is based on process model inverse, perfect decoupling is only possible when the process model is perfect and it can only be implemented if such inverses are both causal and stable. The requirement for causality in the compensator transfer function is that the time-delay structure in the $G(s)$ to be such that the smallest delay in each rows occur in the diagonal. The requirement for stability is that causality condition is satisfied and that there are no zeros with positive real part on the process $G(s)$.

This general formulation corresponds to the case of an ideal dynamic decoupler, which eliminates interactions from all loops, at every instant of time. However, this kind of decoupler is not always desirable or possible. In this case, less ambiguous approaches can be used: partial decoupling or steady-state decoupling.

Partial decoupling can be used when some of the loop interactions are weak in comparison to others. The approach focus on a subset of the control loops, where interactions are important and high performance control is necessary. The main advantage lies in the reduction of the problem dimension.

The steady-state decoupling considers only the steady-state gain portion of each transfer function element of the process, and so, it eliminates only steady-state interactions from all loops. The main

advantage is the simplification of control design and it is the decoupling technique most often applied in practice.

Although decoupling is a promising technique for multivariable effective control, its feasibility and successful implementation depend on the structure of each process. When the process is considered “ill conditioned”, it becomes a poor candidate for decoupling because of its high sensitivity to model error. The most reliable technique for assessing ill-condition, and thus decoupleability, of a process is the Singular Value Decomposition.

Besides decoupling, there exist other model-based controller design techniques that can be applied to multivariable systems. One of these techniques is the Internal Model Control.

Internal Model Control

The Internal Model Control (IMC) method (Rivera et al. 1986) is based on the process model, relating the model parameters to the controller settings in a straightforward manner. IMC is then commonly used to select PID controller settings based on process dynamic response criteria. IMC can be employed either in continuous or in discrete time. The use of IMC allows rigorous analysis in order to tune the controller and to evaluate stability and robustness of the system.

This model-based methodology considers a process whose dynamic behavior is represented by:

$$y(s) = G(s)u(s) + d$$

When perfect control is desired, we replace $y(s)$ by the desired set point $y_{sp}(s)$:

$$y_{sp}(s) = G(s)u(s) + d$$

$$\text{that gives the desired control action } u(s) = \frac{1}{G(s)} [y_{sp}(s) - d]$$

In practice, the collective effect of disturbances d is commonly unmeasured, and hence unknown, and the process model $G(s)$ may only be an approximation of the real g . It is assumed that $G'(s)$ is the best estimate of plant dynamics, the disturbance can be better estimated and $u(s)$ is recalculated:

$$d' = y - G'(s)u(s)$$

$$u(s) = \frac{1}{G'(s)} [y_{sp}(s) - d'] = Gc(s) [y_{sp}(s) - d']$$

It is important to notice that the implementation of IMC procedure assumes that the approximation of the process model is acceptable, and that its inversion is possible. To obtain those equations and design the IMC controller, different calculations are sequentially used. First, the model is factored:

$$G' = G'_+ G'_-$$

where G'_+ contains any time delays and right-half planes zeros, specified so

that its steady-state gain is one

To ensure that $Gc(s)$ is proper (the order of the denominator is equal or higher than the order of the numerator), the parameters λ and n are chosen so the filter $f(s)$ is determined as:

$$f(s) = \frac{1}{(\lambda s + 1)^n}$$

The controller is finally specified:

$$Gc(s) = \frac{1}{G'_-} f(s)$$

In the following, the procedure derived from the IMC methodology for a first order system is presented. This shows that in the case of a first order system without time delay, the optimal controller for such a system when the closed-loop desired dynamic is imposed as a faster first order system, is a classical PI controller with appropriate tuning parameter values depending of the process model parameters,

The following closed-loop system is considered:

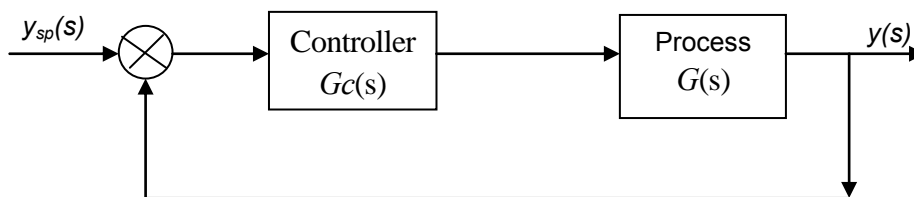


Figure AII.1: Closed-loop system used to apply the IMC methodology

The resulting closed-loop transfer function is given by:

$$\frac{y(s)}{y_{sp}(s)} = F(s) = \frac{Gc(s)G(s)}{1 + Gc(s)G(s)}$$

The transfer function of a first order system without time delay is represented by:

$$G(s) = \frac{GS}{1 + \tau s}$$

Where GS is the static gain and τ the time constant

The control objectives are expressed as follows:

- No steady-state error (which implies a static gain of the closed-loop transfer function equal)
- A resulting closed-loop dynamic of a first order system with a desired time constant τ_0 (can be expressed as a fraction of the process time constant τ : $ACCF = \tau / \tau_0$ giving the acceleration factor

In other terms, this can be traduced as defining the desired resulting closed-loop transfer function:

$$\frac{y(s)}{y_{sp}(s)} = F(s) = \frac{1}{1 + \tau_0 s}$$

By developing $F(s)$:

$$F(s) = \frac{Gc(s) \frac{GS}{1 + \tau s}}{1 + Gc(s) \frac{GS}{1 + \tau s}} = \frac{GS.Gc(s)}{1 + \tau s + GS.Gc(s)}$$

By identification:

$$F(s) = \frac{GS.Gc(s)}{1 + \tau s + GS.Gc(s)} = \frac{1}{1 + \tau_0 s}$$

so :

$$1 + \tau s + GS.Gc(s) = GS.Gc(s)(1 + \tau_0 s)$$

i.e. : $Gc(s) = \frac{1}{GS} (1 + \tau s) / \tau_0 s = \frac{1}{GS} \left(\frac{\tau}{\tau_0} + \frac{1}{\tau_0 s} \right) = \frac{1}{GS} \frac{\tau}{\tau_0} \left(1 + \frac{1}{\tau s} \right) = K_c \left(1 + \frac{1}{\tau_i s} \right)$

This is the transfer function of a PI controller with :

$$K_c = \frac{1}{GS} \frac{\tau}{\tau_0} = \frac{1}{GS} ACCF$$

where $ACCF$ is the desired acceleration factor and $\tau_0 = \tau$ the process time constant

Model Predictive Control

In model predictive control, the process model is used to predict future outputs over a predefined time period; only past values of input changes and outputs are considered to predict the future values of response. Some known techniques applied are the Dynamic Matrix Method (DMC), the Model Algorithm Control (MAC), and others with similar structure. MPC can be used for both prediction of future plant behavior and calculation of the corrective control action to ensure that the predictive response has certain desirable characteristics.

The technique is normally posed as an optimization problem, where a quadratic objective function involves the error between the set point and the predicted outputs over a finite or infinite horizon and quadratic terms on future control actions enabling the minimization of control action energy. The minimization of this objective function leads to a feedback controller, which can be designed by straightforward matrix operations. To achieve desirable performance, the controller is finally tuned.

Some typical MPC advantages were announced by Ogunnaike and Ray (1994):

- Facility to handle interactions and to be used for multivariable process systems,
- Consideration of difficult process dynamics, such as time delays and inverse response,
- There is no need for rigid process models or mathematical representations,
- Effect of measurable or unmeasurable disturbances are compensated on controller design,
- Because it is posed as an optimization problem, an optimal control effort is calculated and it may attend any possible constraints,
- The advances in computer technology and the availability of optimization software provide even more interest on its implementation.

MPC is typically best suited to processes with any combination of the following characteristics:

- Multiple input and output variables with significant interactions among the SISO loops,
- Either equal or unequal number of inputs and outputs,
- Complex or unusual dynamic behavior,
- Constraints in input or in output variables.

Even with all MPC advantages, it is important and judicious to note that processes whose variables exhibit little or no interactions, processes with normal dynamic characteristics, and those which are seldom subject to constraints will most likely not benefit from MPC: simpler techniques are just as likely to perform as well.

Before discussing the mathematical detail of predictive control methodology, it is important to define the following horizons:

- T is the model horizon, the time for the open-loop step response to reach 99%,
- V is the prediction horizon, the quantity of sampling periods to predict future behavior,
- U is the control horizon, the number of control actions that are calculated in order to affect the predicted outputs over the prediction horizon V .

Considering the horizons, the most popular model forms in conventional MPC context are the finite discrete convolution, the state-space and the transform-domain transfer function models. The conversion of one model to another is also possible, although some conversions are more straightforward than others.

Because MPC techniques are implemented by digital computers, the discrete model forms are more natural than the continuous one. In addition, the conventional MPC utilizes only linear models; the consideration of nonlinear models is recent in MPC studies (Qin and Badgwell, 2000, 2003).

In the following we present, the matrix-form representations and the Dynamic Matrix Method to design the predictive controller. The approach used on MIMO systems is also presented, followed by the possible nonlinear extensions.

Predictive Control Based on Discrete Convolution Models

For linear processes that exhibit unusual dynamic behavior, a convolution model can be applied. The convolution model is based on a discrete step or impulse response and also provides a convenient way to design a controller based on the use of optimization theory. The convolution model can be generalized by including an arbitrary number of predictions. To understand the calculations, we analyze a step response prediction model.

For the step response model, the values of the response coefficients are given by $\beta_0, \beta_1, \dots, \beta_T$ using the sampling period Δt ; we define $\beta_i=0$ for $i \leq 0$. Let \hat{y}_n be the predicted value of the output variable and u_n the value of the manipulated variable at the n th sampling instant. We also define y_n as the actual output, and $\hat{y}_n = y_n$ if there is no modeling errors or disturbances. We finally denote $\Delta u_k = u_k - u_{k-1}$.

The step-response model form is:

$$y(k) = \sum_{i=0}^k \beta(i) \Delta u(k-i)$$

Predictive Control Based on Discrete State-Space Models

The model form may be represented by:

$$y(k) = \sum_{i=0}^k a(i) y(k-i) + \sum_{i=0}^k b(i) u(k-i-\theta)$$

where the coefficients $a(i)$ and $b(i)$, and the delay θ should be obtained by fitting the model to plant data; by reason of causality, $a(0) = b(0) = 0$.

Predictive Control Based on Discrete Transfer Function Models

The transfer function model is represented by a ratio of two polynomials in the z-transform variable, along with the associated delay of m sample times:

$$y(k) = \frac{z^{-m} B(z^{-1})}{A(z^{-1})} u(z)$$

where the parameters of the transfer functions should also be determined from experimental data.

Matrix Forms for Predictive Control

Once the model is represented, we define some vectors needed for the prediction of process dynamic behavior. We note that these vectors are special, because they denote a scalar at many different time steps of the prediction horizon V , rather than a vector of different outputs at the same time instant, as commonly used. The unit step response for each discrete sampling instant n of the process may be represented by the elements of the vector β :

$$\beta = \begin{bmatrix} \beta(1) \\ \beta(2) \\ \dots \\ \beta(n) \end{bmatrix}$$

Let the current time instant be k . At absence of any control action, the output of the process may be represented by:

$$y_0^{\wedge}(k) = \begin{bmatrix} y_0^{\wedge}(k+1) \\ y_0^{\wedge}(k+2) \\ \dots \\ y_0^{\wedge}(k+V) \end{bmatrix}$$

To proceed, one applies an arbitrary sequence of m control moves $u(k)$ and considers a collective effect of unmeasured disturbances $w(k)$ on the output:

$$u(k) = \begin{bmatrix} u(k+1) \\ u(k+2) \\ \dots \\ u(k+V) \end{bmatrix} \quad w(k) = \begin{bmatrix} w(k+1) \\ w(k+2) \\ \dots \\ w(k+V) \end{bmatrix}$$

Linearity of the model is assumed and the system response is calculated:

$$y^{\wedge}(k) = \begin{bmatrix} y^{\wedge}(k+1) \\ y^{\wedge}(k+2) \\ \dots \\ y^{\wedge}(k+V) \end{bmatrix}$$

where each element were calculated by:

$$y^{\wedge}(k+1) = y_0^{\wedge}(k) + B\Delta u(k) + w(k+1)$$

$$\text{with the dynamic matrix } \mathbf{B} = \begin{bmatrix} \beta(1) & 0 & 0 & \dots & 0 \\ \beta(2) & \beta(1) & 0 & \dots & 0 \\ \beta(3) & \beta(2) & \beta(1) & \dots & 0 \\ \dots & \dots & \dots & \dots & \dots \\ \beta(V) & \beta(V-1) & \beta(V-2) & \dots & \beta(V-U+1) \end{bmatrix}$$

Controller Design by Dynamic Matrix Method

The objective of the control strategy is to find a corrected prediction $\hat{y}(k)$ that approaches the set point as closely as possible. The set point is determined by the desired response values $y^*(k)$:

$$y^*(k) = \begin{bmatrix} y^*(k+1) \\ y^*(k+2) \\ \dots \\ y^*(k+v) \end{bmatrix}$$

From the equation defined before, we should choose $\Delta u(k)$ that:

$$y_{sp}(k+1) = \hat{y}_0(k) + \mathbf{B}\Delta u(k) + w(k+1)$$

To formulate the control problem, we finally define the projected error vector $e(k+1)$, whose elements are the predicted value for the process error at v future sampling instants; it is referred to an open-loop prediction, in the absence of any control action.

$$e(k+1) = y_{sp}(k+1) - [\hat{y}_0(k) + w(k+1)] = \mathbf{B}\Delta u(k)$$

For an effective controller, the designer wants $e(k+1) = 0$. For systems in which the horizons $U \leq V$, only u future actions are calculated and \mathbf{B} is the $V \times U$ dynamic matrix. The Dynamic Matrix Control (DMC) method gives the optimal solution:

$$\Delta u(k) = (\mathbf{B}^T \mathbf{B})^{-1} \mathbf{B}^T e(k+1) = \mathbf{K}_c e(k+1)$$

where \mathbf{K}_c is the $U \times V$ matrix of feedback gains

In practice, one would calculate only the first control action $\Delta u(k)$, apply it, compare the response value with the predicted one, correct predictions, and use the above equation again, for each sampling instant. This approach gives an update and a better prediction during the horizon V .

However, when the $\mathbf{B}^T\mathbf{B}$ matrix is ill-conditioned, or singular, the control law can promote excessively large changes in the manipulated variable. An alternative solution is to moderate the changes in $\Delta u(k)$ by correctly applying some positive-definite weighting matrices in the equation:

- W_1 : weighting matrix for predicted errors
- W_2 : weighting matrix for control moves

The equation would become:

$$\Delta u(k) = (\mathbf{B}^T W_1 \mathbf{B} + W_2)^{-1} \mathbf{B}^T W_1 e(k+1) = K_c e(k+1)$$

Finally, the parameters needed to the predictive process control design are defined: the horizons T , U and V , the weighting matrices W_1 and W_2 , and the sampling period Δt . These parameters can be adjusted to adequately tune the controller, in order to promote desired control action and its consequent dynamic response. Some rules of thumbs exist to better define their values.

Multiple-output multiple-input systems

For MIMO control systems, the predictive control techniques find useful and advantageous applications, even when the system has unusual dynamic behavior or when it is crucial to meet constraints on the variables.

For systems, with m inputs and m outputs, the DMC method can be adapted by using the principle of superposition. In this case, we should select the model horizon T as the largest T_i from among all single-loop models. The mathematical representation is similar as to SISO systems, though the matrices and vectors have larger dimensions:

$$e(k+1) = \mathbf{B}\Delta u(k)$$

where $e(k+1)$: projected vector for the i th output variable, with length mV

\mathbf{B} : the dynamic matrix with dimension $mV \times mU$

B_{ij} : dynamic matrix formed from the step-response of the output variable i to the input variable j , with dimension $V \times U$

$$\mathbf{B}_{ij} = \begin{bmatrix} \beta_{ij,1} & 0 & \dots & 0 \\ \beta_{ij,2} & \beta_{ij,1} & \dots & 0 \\ \dots & \dots & \dots & \dots \\ \beta_{ij,V} & \beta_{ij,V-1} & \dots & \beta_{ij,V-U+1} \end{bmatrix}$$

In multivariable processes, it often happens that a unit change in one output variable is much more important than a unit change in another. In reactive distillation, for example, it is easily agreed that a unit change in the distillate composition (measured in mass fractions) would have much more impact than a unit change in a tray temperature over the column (measured in °C).

Thus, similarly as to SISO systems, we may want to moderate the control actions, by weighting the changes and scaling the error vector. This objective can be achieved by the introduction of the weighting matrix Γ as a tuning parameter:

$$\Delta u(k) = (\mathbf{B}^T \Gamma \mathbf{B})^{-1} \mathbf{B}^T \Gamma e(k+1)$$

Nonlinear extensions

The extension of the standard MPC concept to nonlinear systems has been the subject of intense research. Ogunnaike and Ray (1994) present essentially three approaches:

- *Scheduled Linearization*: the nonlinear model is linearized around different operating steady states and the resulting linear model is used within the linear MPC methodology.
- *Extended Linear MPC*: the basic linear MPC structure is adapted to reflect the true nonlinearities captured by an explicit nonlinear model; the control actions then become perturbations around the basic linear MPC controller recommendations. The mathematical representation of the standard MPC is only added by a vector $d^{nl}(k)$, whose elements are computed by minimizing the difference between $\hat{y}_{el}^{\wedge}(k+1)$, the output prediction obtained from the extended linear model, and $\hat{y}^{\wedge}(k+1)$, the prediction obtained from a full-scaled nonlinear model of the plant:

$$\hat{y}_{el}^{\wedge}(k+1) = \hat{y}_0^{\wedge}(k) + \mathbf{B} \Delta u(k) + w(k+1) + d^{nl}(k)$$

- *Explicit Nonlinear MPC*: the MPC problem is posed as a full-scale nonlinear problem. If y is the vector of process outputs, u is the input vector, x is the state vector, d is the disturbance vector, ξ the vector of model parameters, the current time is indicated as t_0 , and the prediction horizon remains T , the full-scaled nonlinear model would have the form:

$$\begin{aligned}\frac{dx}{dt} &= f(x, u, d; \xi) \\ y &= g(x, u, d)\end{aligned}$$

The controller is then obtained either explicitly by analytical means or implicitly as the solution of nonlinear program (NLP) complete with nonlinear model and constraints. The NLP resulting problem is:

$$\begin{aligned}\min_{u(t)} & \phi[u(t), x(t), y(t)] \\ & \frac{dx}{dt} - f(x, u, d; \xi) = 0 \\ & y - g(x, u, d) = 0 \\ \text{subject to:} & \quad h(x, u) = 0 \\ & \quad q(x, u) \leq 0 \\ & \quad x(t_0) = x_0 \\ & \quad t \in [t_0, t_0 + T]\end{aligned}$$

Optimal Control

Optimal control is a procedure different from the ones already presented; it considers the control aspects of the process since the design step of process conception, highlighting the importance of this consideration for the treatment of complex systems. It is not used to define the controller settings; instead, it is an important technique to determine optimal set points for the process control systems.

This procedure cannot be applied online in the plant, during the process operation, though it might be considered during process design calculations.

In fact, there exist cases when the conceived process design operates in a nominal steady state, but reveals an uncontrollable behavior when operation becomes transient after an external disturbance, for example. To avoid this behavior, the procedure allows the optimization in time, of a dynamic dependent criterion. The problem may be posed as the following:

$$\min_{x'(t), x(t), u(t), v, x(t_0), t_f} \Phi(x'(t_f), x(t_f), u(t_f), v, t_f)$$

$$\text{subjected to } \begin{aligned} g(x'(t_f), x(t_f), u(t_f), v, t_f, t) &= 0 \\ h_1(x'(t_f), x(t_f), u(t_f), v, t_f) &= 0 \\ h_2(x'(t_f), x(t_f), u(t_f), v, t_f) &\geq 0 \end{aligned}$$

where g : dynamic model equations

h_1 and h_2 : equality and inequality constraints

x : state variables

v : manipulated variables

u : controlled variables

This kind of problem can be solved by Pontryagin Maximum Principle, or by numerical transformations turning it into a nonlinear program (NLP). It can be considered as a Model Predictive Control (MPC) with generally infinite horizon and without constraints.

III. CLASSIFICATION ALGORITHMS

The algorithms used for the process diagnosis methodology are here detailed. First, the LAMDA technique to classify the historical data is presented, followed by the methodology used for sensors selection.

LAMDA is based on fuzzy logic calculations. The procedure to classify each individual follows the steps:

1. Calculate the Marginal Adequacy Degree (*MAD*) for each descriptor, by the application of a membership function.
2. Calculate the Global Adequacy Degree (*GAD*) of the individual, by the application of an information membership operator, the connective.
3. Evaluate the *GAD* to know if a new class has to be created. If it is the case, the new class is created and all the values of *GAD* and *MAD* from elements treated before are re-evaluated. If we consider only the classes already created, the element is assigned to the class with the higher value of *GAD* and the parameters of this class are actualized.

For an individual X_n , with its descriptors $(x_1, \dots, x_j, \dots, x_d)$, and the classes $C_1, \dots, C_j, \dots, C_k$, the calculations are organized on Figure AIII.1.

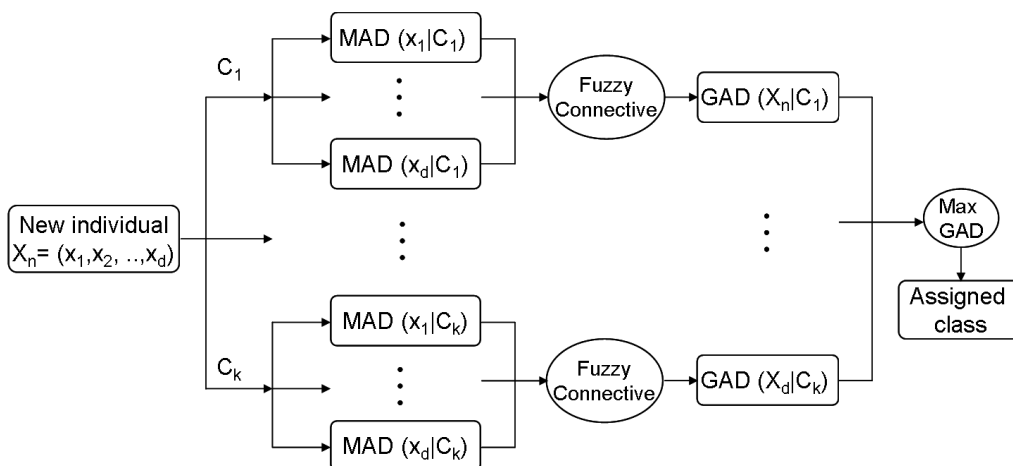


Figure AIII.1 Scheme of LAMDA calculations

The entire classification algorithm is explained with more details:

The Marginal Adequacy Degree (MAD)

For each individual, a vector of marginal adequacy degree is defined, which considers all information given by all descriptors. The vector length is the quantity of descriptors for the individual. The *MAD* is expressed as a function of marginal relevance to the C_k class:

$$\mu(x_i/C_k) = MAD(x_i/i_{th} \text{ parameter of class } C_k) = f_i(x_i, \rho_{ki})$$

This function depends thus on the descriptor x_i of the individual X and on the parameter ρ_{ki} of the C_k class. Because the fuzzy logic is considered, the following conditions are imposed:

$$0 \leq MAD(x_i/C_k) \leq 1$$

$$\exists \hat{x}_i, MAD(\hat{x}_i/C_k) \geq MAD(x_i/C_k)$$

The parameter ρ_{ki} is calculated iteratively from the i th descriptor of all individuals belonging to class C_k . This descriptor can be qualitative, quantitative, or an interval and the procedure to calculate the *MAD* depends on its type. The functions used for each case are detailed below:

- *Quantitative type descriptors:*

On LAMDA classification, the operating interval of the data is called context; it provides the maximum and the minimum values used for the normalization of quantitative descriptors. By adjusting this interval, the expert has the possibility of defining the sensitivity in which the data variations will be considered and the influence of the descriptors on the classes characterization.

The calculation of the quantitative *MAD* begins then by the normalization of the descriptors within the interval $[x_{imin}; x_{imax}]$, where the bounds are obtained from the uploaded context, so they can be the extreme values of a given dataset or independently imposed.

$$x_i = \frac{x_i - x_{i \min}}{x_{i \max} - x_{i \min}}$$

The quantitative *MAD* is calculated by selecting one of the several possible membership functions: binomial, centered binomial, distance binomial, square distance binomial or gauss.

LAMDA is a flexible methodology and the choice of the marginal function will affect the result of classification. The function is commonly chosen by heuristic considerations, thus the analysis of the

different results with the physical interpretation and opinion from an expert is recommended. The mathematical expressions described in the work of Orantes (2005) are presented below.

Binomial:

$$\mu(x_i/C_j) = \rho_{i,j}^{x_i} (1 - \rho_{i,j})^{1-x_i}$$

Centered Binomial:

$$a = \rho_{i,j}^{x_i} (1 - \rho_{i,j})^{1-x_i}$$

$$b = x_i^{x_i} (1 - x_i)^{1-x_i}$$

$$\mu(x_i/C_j) = \frac{a}{b}$$

Distance Binomial:

$$a = \max[\rho_{i,j}^{x_i}, (1 - \rho_{i,j})]$$

$$x_{dist} = 1 - abs(x_i - \rho_{i,j})$$

$$\mu(x_i/C_j) = a^{x_{dist}} (1 - a)^{(1-x_{dist})}$$

Square Distance Binomial:

$$a = \max[\rho_{i,j}^{x_i}, (1 - \rho_{i,j})]$$

$$x_{dist} = 1 - abs(x_i - \rho_{i,j})$$

$$b = x_{dist}^{x_{dist}} (1 - x_{dist})^{(1-x_{dist})}$$

$$\mu(x_i/C_j) = \frac{a^{x_{dist}} (1 - a)^{(1-x_{dist})}}{b}$$

Gauss:

$$\mu(x_i/C_j) = e^{-\frac{1}{2\sigma_{ij}^2}(x_i - \mu_{ij})^2}$$

Where μ_{ij} and σ_{ij}^2 are respectively the mean value and the variance of the descriptor i for the class j .

The parameters of each class evolve during the classification method and they can be determined in two different ways: directly when supervised learning classification is realized, or iteratively when self learning method is used.

For supervised learning, each descriptor is assigned a priori to a class by the system expert. N_k is the quantity of individuals in the class C_k . The parameters ρ for each class are obtained by calculating the mean value of the individuals that belong to this class:

$$\rho_{ki}(N_k) = \frac{1}{N_k} \sum_{t=1}^{t=N_k} x_i(t)$$

For self-learning, the iterative estimation of the parameter ρ_{kj} corresponds to the equation:

$$\rho_{ki}(N_k + 1) = \rho_{ki}(N_k) + \frac{1}{N_k + 1} (x_i(N_k + 1) - \rho_{ki}(N_k))$$

• *Qualitative type descriptors:*

Qualitative descriptors are characterized by not-ordered values that form a set of modalities:

$$x_i = Q_{i1}, \dots, Q_{ij}, \dots, Q_{iM_i}$$

The classification technique calculates the frequencies of each modality inside each class. Let Φ_j be the probability of each modality Q_j in the class C_k , the membership function of x_i is multinomial:

$$\mu_k^i(x_i) = \Phi_{i1}^{q_{i1}} * \dots * \Phi_{iM_i}^{q_{iM_i}}$$

$$\text{where } q_{ij} = \begin{cases} 1 & \text{if } x_i = Q_{ij} \\ 0 & \text{if } x_i \neq Q_{ij} \end{cases}$$

• *Interval type descriptors:*

The interval representation of data takes into account the various uncertainties and reduces large datasets, which is an important advantage on system diagnosis. The calculation of *MAD* starts with the determination of a similarity measure S between two intervals $A = [a^-, a^+]$ and $B = [b^-, b^+]$ defined on the universe of discourse $U = [\min(x^-); \max(x^+)]$ where the distance between A and B is given by $D = [\min(a^+, b^+); \max(a^-, b^-)]$ and each interval is considered as a fuzzy subset.

$$S(A, B) = \frac{1}{2} \left[\left(\frac{\sum_{x_n} (\mu_{A \cap B}(x_n))}{\sum_{x_n} (\mu_{A \cup B}(x_n))} \right) + \left(1 - \frac{\sum_{x_n} (\mu_D(x_n))}{\sum_{x_n} (\mu_U(x_n))} \right) \right]$$

This formulation allows defining the similarity between overlap or non-overlap intervals.

The class parameters are represented by a vector of intervals and they are determined by the arithmetic mean of its bounds:

$$\rho_{1k}^i = \frac{1}{m} \sum_{j=1}^m x_{ij}^- \quad \rho_{2k}^i = \frac{1}{m} \sum_{j=1}^m x_{ij}^+$$

Where m is the quantity of individuals assigned to class C_k and x_i^- and x_j^+ are normalized within the interval $[0,1]$. The MAD is the value of the similarity between the data interval x_i and the interval $\rho_k^i = [\rho_{1k}^i, \rho_{2k}^i]$ representing class C_k .

$$\mu_k^i(x_i) = MAD(x_i, \rho_k^i) = S(x_i, \rho_k^i)$$

The Global Adequacy Degree (GAD)

The GAD represents the adequacy degree of the individual X_n to the class C_k , by considering all the marginal adequacy degrees previously computed for the class C_k . The calculation of the GAD combines the MAD s by a marginal aggregation function, interpreting the system as a fuzzy set. This calculation is valid even if the descriptors are of different types (qualitative, quantitative and interval):

$$GAD(X_n/C_k) = \gamma(MAD(x_{n1}/C_k), \dots, MAD(x_{ni}/C_k), \dots, MAD(x_{nd}/C_k))$$

The aggregation functions, also called connectives, of the fuzzy logic are fuzzy versions of connectives from binary logic. They are related to logic operators among the elements:

- The *and* operator is associated to the functions known as t-norms: the product $G(a,b) = a.b$ and the minimum $G(a,b) = \min[a,b]$.
- The *or* operator is associated with the t-conorms: sum $G(a,b) = a+b - a.b$ and the maximum $G(a,b) = \max[a,b]$.

In order to obtain a classification which is neither so strict neither so permissive, the marginal aggregation function is generally chosen as a linear interpolation between fuzzy t-norm and t-conorm (Piera and Aguilar (1991)).

$$GAD(X_n/C_k) = \alpha\gamma(MAD(x_1/C_k), \dots, MAD(x_d/C_k)) + (1-\alpha)\beta(MAD(x_1/C_k), \dots, MAD(x_d/C_k))$$

Where α is called exigency index. The definition of this index is important and it gets values from 0 to 1; Orantes (2005) mentions that the most exigent classifier ($\alpha= 1$) only locates an element on a class if all of its descriptors have a high MAD to this class and the less exigent classifier ($\alpha= 0$) accepts an element in a class when at least one descriptor has a high MAD . Moreover, if α has a high value, the number of individuals assigned to the NIC is high in the supervised learning method, or the number of classes created is high in the self learning method.

Finally, all *GAD* values are analyzed and the individual is assigned to the class corresponding to the maximal *GAD*. In the case of classification by a self-learning method, it can be necessary the creation of the *NIC*, and its representation is function of the new individual that was assigned to it.

The parameters of the assigned class are then actualized:

$$\rho_{ij} = \rho_{ij} + \frac{x_i - \rho_{ij}}{N_k + 1}$$

where N_k is the quantity of individuals used for the calculation of frequencies on the class C_k .

The entire LAMDA classification algorithm is schematized on Figure AIII.2.

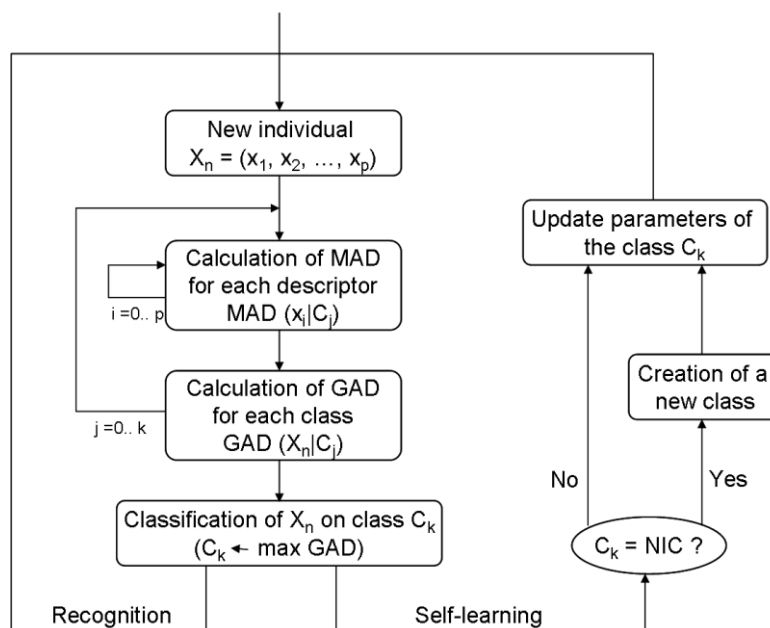


Figure AIII.2 Scheme of LAMDA classification algorithm

12.3.6 Sensors selection

To explain the sensors selection method, it is initially considered that dataset have only two classes, named C_{nc} (the correct class) and $C_{n\bar{c}}$ (the alternative class) If we assume that the individual X_n , with its respective descriptors, also known as features, $(x_1, \dots, x_i, \dots, x_d)$, is labeled by the class C_{nc} , the membership margin for this individual is defined by:

$$\beta_n = \psi(MAD(x_i|C_{nc})) - \psi(MAD(x_i|C_{n\bar{c}}))$$

Where $MAD(x_i|C_{nc})$ and $MAD(x_i|C_{n\bar{c}})$ are respectively the membership degree vectors of sample X_n to classes C_{nc} and $C_{n\bar{c}}$, and ψ is an aggregation function. Because the feature membership can be seen as

the contribution, or relevance, of this feature to a given class, the individual X_n is considered correctly classified if $\beta_n > 0$.

The aggregation function defines a compromise between membership functions and lies between union and intersection (Dubois et al. (1988)). It is given by the arithmetic mean that follows.

$$\psi(MAD(x_i/C_K)) = \sum_i \mu_k^i(x_i)$$

Hedjazi et al. (2010b) define Fuzzy Feature Weight as the relative degree of usefulness of each feature in the membership space for the discrimination between two classes. Fuzzy Feature Weight is a positive vector, referred to as ω_f , with the quantity of elements equal to the quantity of features in the individual. Fuzzy weights are then considered in the definition of the aggregation function:

$$\psi\left(\frac{MAD(x_i/C_K)}{\omega_f}\right) = \sum_i \omega_{fi} \mu_k^i(x_i)$$

In the weighted membership space, the membership margin for the individual is given:

$$\beta_n(\omega_f) = \psi\left(\frac{MAD(x_i/C_1)}{\omega_f}\right) - \psi\left(\frac{MAD(x_i/C_2)}{\omega_f}\right)$$

Therefore, it is necessary to define an appropriate procedure to estimate the weight vector ω_f . With this objective, the problem is reformulated into an optimization problem in the feature membership space:

$$\text{Min}_{\omega_f} \sum_{n=1}^N h(\beta_n(\omega_f) < 0)$$

Where $\beta_n(\omega_f)$ is the X_n margin computed with respect to ω_f and h is an indicator function. An objective function is defined to maximize the averaged membership margin in the resulted weighted feature membership space:

$$\text{Max}_{\omega_f} \sum_{n=1}^N \beta_n(\omega_f) = 1/m \sum_{n=1}^N \left\{ \sum_{i=1}^m \omega_{fi} \mu_c^i(x_i^{(n)}) - \sum_{i=1}^m \omega_{fi} \mu_{\bar{c}}^i(x_i^{(n)}) \right\}$$

$$\text{Subject to } \|\omega_f\|^2 = 1, \quad \omega_f \geq 0$$

$$\text{Where } s = \sum_{n=1}^N (MAD(x_i/C_{nc}) - MAD(x_i/C_{n\bar{c}}))$$

The constraints on ω_f are necessary so that the maximization ends up with positive and non infinite values. In the statement of this problem, it is assumed that there exists at least one feature $x_i \leq m$, such that $s_i > 0$. By solving the problem with a Lagrangian optimization approach, the final form of ω_f is obtained:

$$\omega_f = \frac{s^+}{\|s^+\|}$$

With $s^+ = [Max(s_1, 0), \dots, Max(s_m, 0)]^T$

The method was presented for two classes, but it can be easily extended for multiclass problems. Regardless the quantity of classes, an equal number of membership degree vectors is resulted and the membership function parameters of each class can also be determined from the available dataset. Thus, the margin definition for multiclass problems can be used:

$$\beta_n = Min_{C_k \neq C_l} (\psi(MAD(x_i/C_j)) - \psi(MAD(x_i/C_k)))$$

$$\text{With } s^+ = \sum_{n=1}^N Min_{C_k \neq C_l} (MAD(x_i/C_j) - MAD(x_i/C_k))$$

After solving the optimization problem also by the Lagrangian approach, the ω_f is obtained in a form analogous to the previous equation.

After all, Hedjazi et al . (2010b) verified that MEMBAS leads to s ignificant improvements of classification pe rformance in the c ase of mixed f eature-type data, due m ainly to an appropriate and similar processing for each type of data with minimal loss of information. The algorithm is schematized:

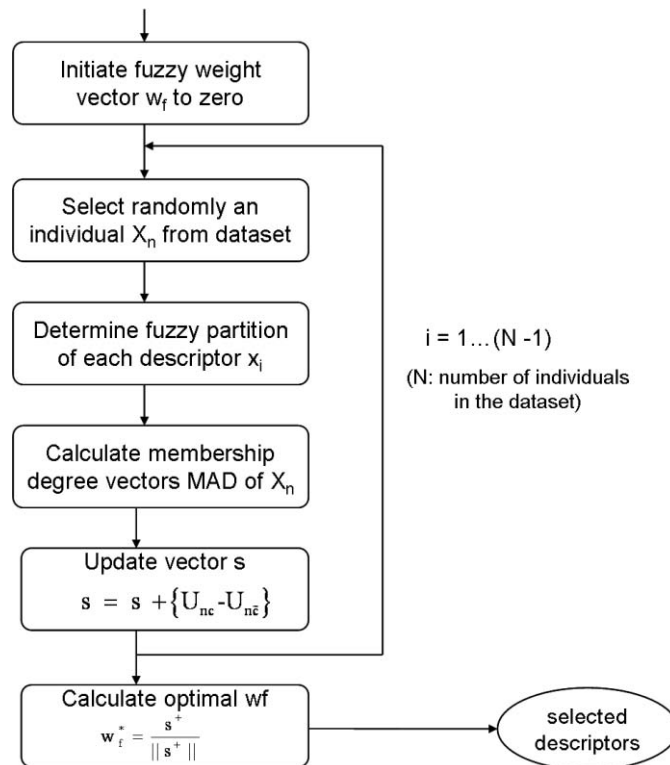


Figure AIII.3 Scheme of sensors selection by the membership margin criterion

Where $U_{nk} = [\mu_k^1(x_{n1}), \mu_k^2(x_{n2}), \dots, \mu_k^m(x_{nm})]$

IV. PROGRAMMING CODES MATLAB®

The controllability methodology explained at Chapter 7 is based on mathematical calculations that were performed in MatLab. The programming codes are presented at this appendix.

```

% Calculation of the condition number CN of a given matrix K
%   under a triple-ended control configuration
% author: Mayra FIGUEIREDO FERNANDEZ, 2012

clear all;

fileName = 'matrixK.xlsx';

K = xlsread(fileName);      % read xls file with matrix of sensitivity K
sizeK = size(K);
net = sizeK(1)
n = [1:net]';              % number of theoretical stages

[U,S,V] = svd(K);          % SVD calculation

u1 = U(:,1);               % first column of U matrix
u2 = U(:,2);               % second column of U matrix
u3 = U(:,3);               % third column of U matrix
UUU = [u1,u2,u3]

s1 = S(1,:);               % first line of S matrix
s2 = S(2,:);               % second line of S matrix
s3 = S(3,:);               % third line of S matrix
SS = [s1;s2;s3]

V

for i=1:3
    diag(i)= S(i,i);        % diagonal of matrix S, singular values
end

diag;
max_diag = max(diag);      % max singular value
min_diag = min(diag);      % min singular value
CN = max_diag/min_diag     % condition number

```

```

% Calculation of the intersivity indexes I of a given matrix K
%   under a triple-ended control configuration
% author: Mayra FIGUEIREDO FERNANDEZ, 2012

clear all;

fileName = 'matrixK.xlsx';

K = xlsread(fileName);      % read xls file with matrix of sensitivity K
sizeK = size(K);
net = sizeK(1);
n = [1:net]';              % number of theoretical stages

[U,S,V] = svd(K);          % SVD calculation

for i = 1:net
    for h = 1:net
        for f = 1:net
            for j = 1:3
                K1(j) = K(i,j);
                K2(j) = K(h,j);
                K3(j) = K(f,j);
            end

            KK = [K1;K2;K3];      % matrix (3,3)
            [D,SS,W] = svd(KK);   % SVD calculation
            SS ;

            for g = 1:3
                diagSS(g)= 0;     % clean previous values of diagK
            end
            for g = 1:3
                diagSS(g)= SS(g,g); % diagonal of matrixS
            end
            diagSS ;
            max_diagSS = max(diagSS); % max singular value
            min_diagSS = min(diagSS); % min singular value
            CN = max_diagSS/min_diagSS; % condition number
            I(i,h,f) = min_diagSS/CN; % Intersivity Index

            i;
            h;
            f;
            I(i,h,f);
        end
    end
end;

max(I(:));
[maxI idx] = max(I(:));
maxI
[x y z] = ind2sub(size(I),idx) % gives (i,h,f) of the maximum I value

```

V. DYNAMIC SIMULATIONS

Chapter 10 performed the controllability analysis for several column configurations. The dynamic behaviors of the systems were presented based on the responses after a perturbation on increasing the acid feed flow rate. This appendix presents the responses of each column to two other perturbations: an increase of water in the ethanol feed flow and a decrease of the acid feed flow rate. Results are presented for the same control structures previously selected.

Column Design30a

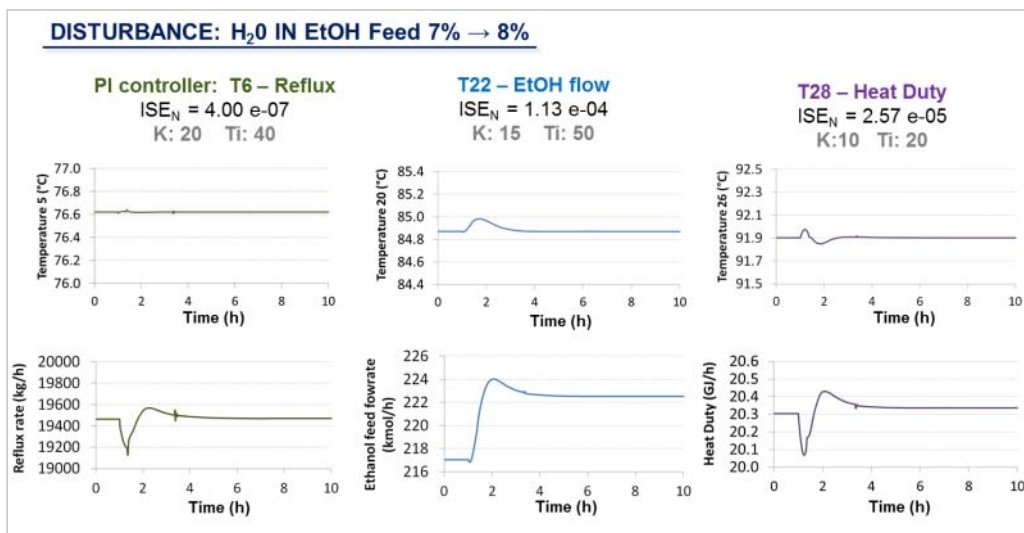


Figure AV.1. Inferential control variables after an increase of water in ethanol feed, column Design30a

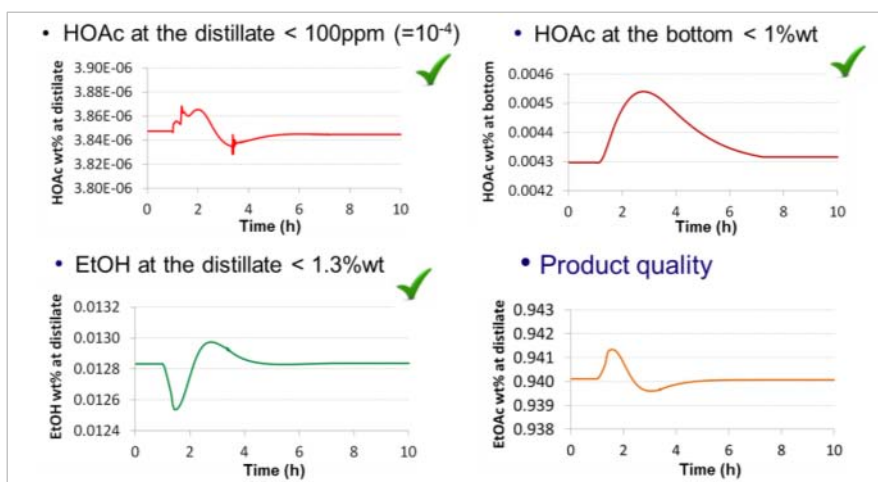


Figure AV.2. Inferential control specifications after an increase of water in ethanol feed, column Design30a

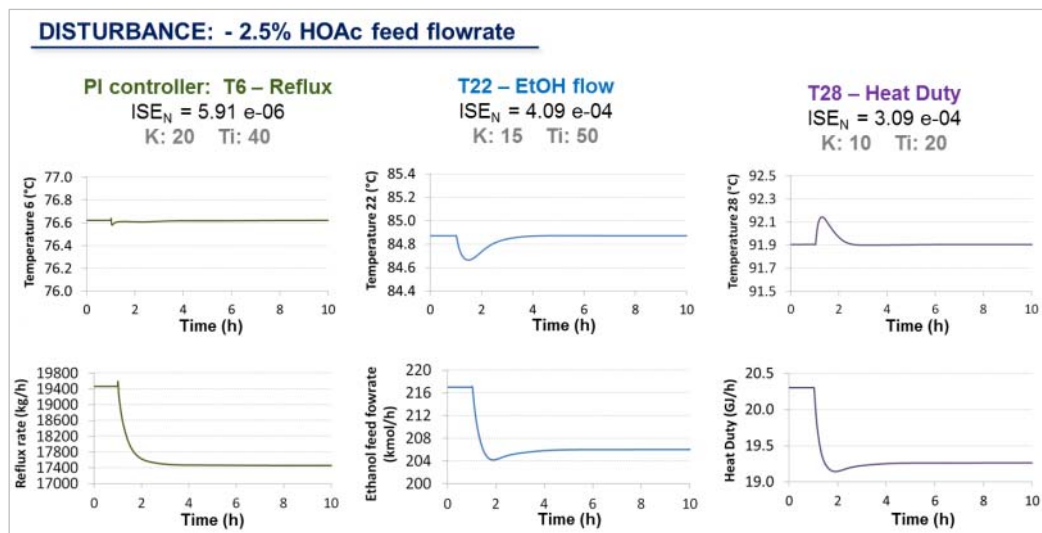


Figure AV.3. Inferential control variables after a decrease of acid feed flow rate, column Design30a

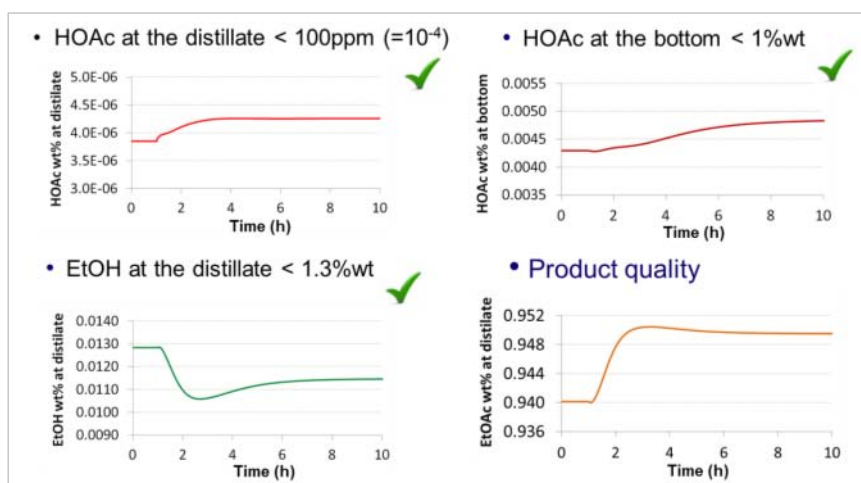


Figure AV.4. Inferential control specifications after decrease of acid feed flow rate, column Design30a

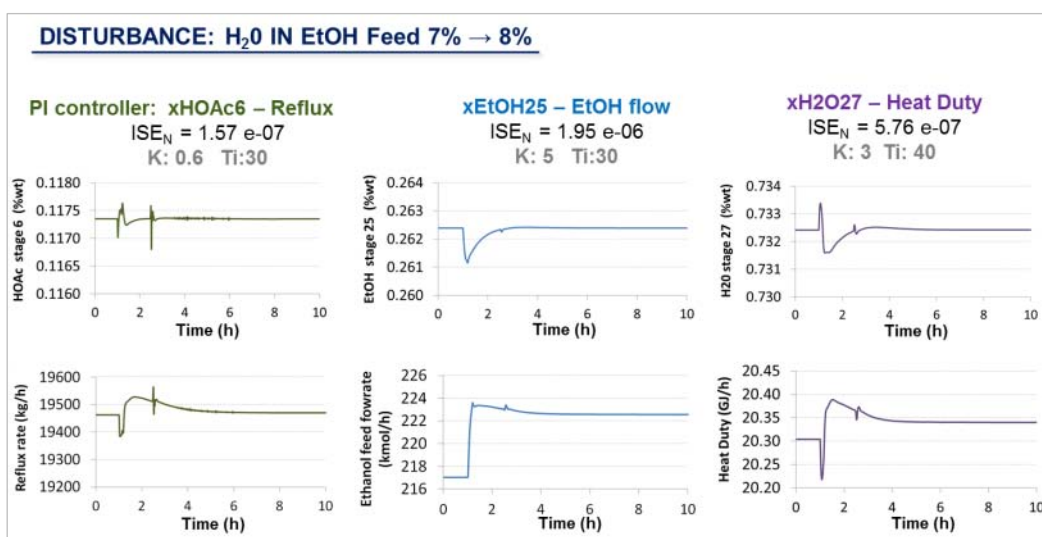


Figure AV.5. Composition control variables after an increase of water in ethanol feed, column Design30a

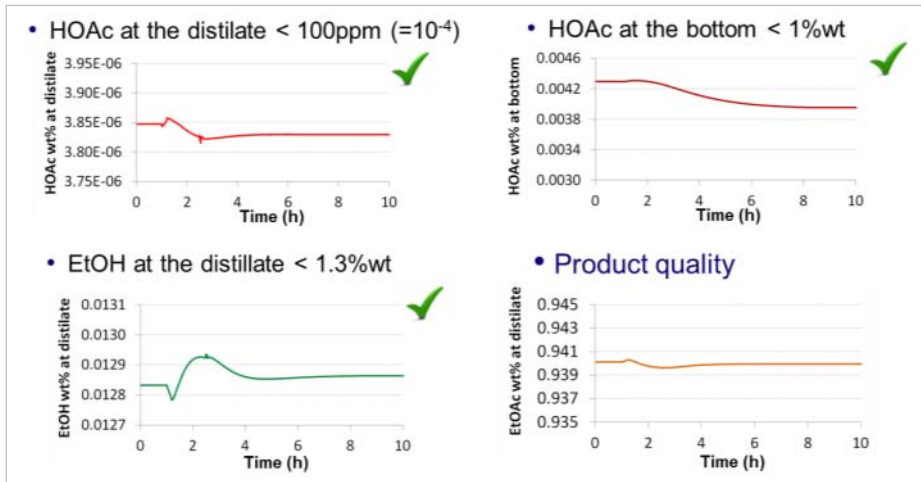


Figure AV.6. Composition control specifications after increase of water in ethanol feed, column Design30a

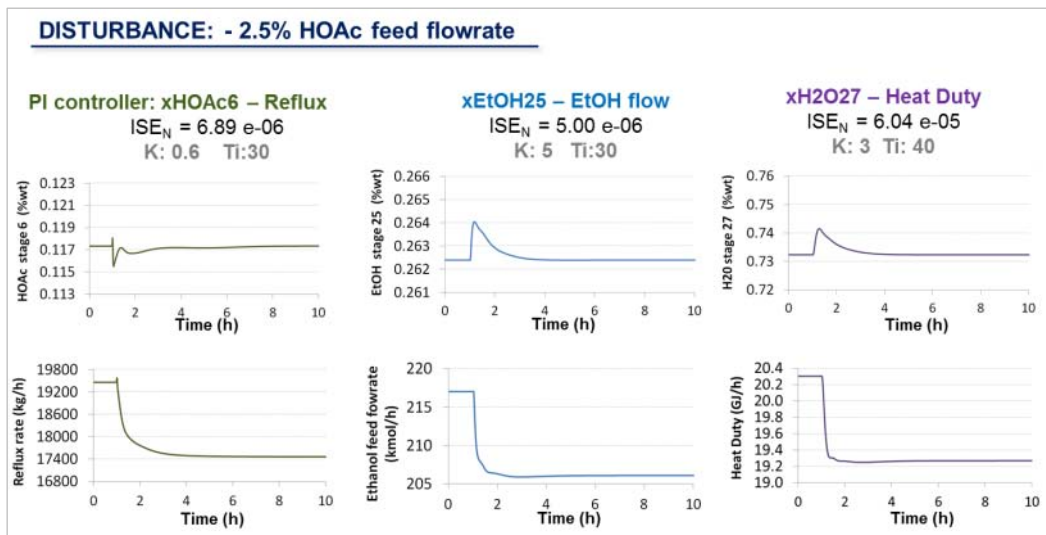


Figure AV.7. Composition control variables after a decrease of acid feed flow rate, column Design30a

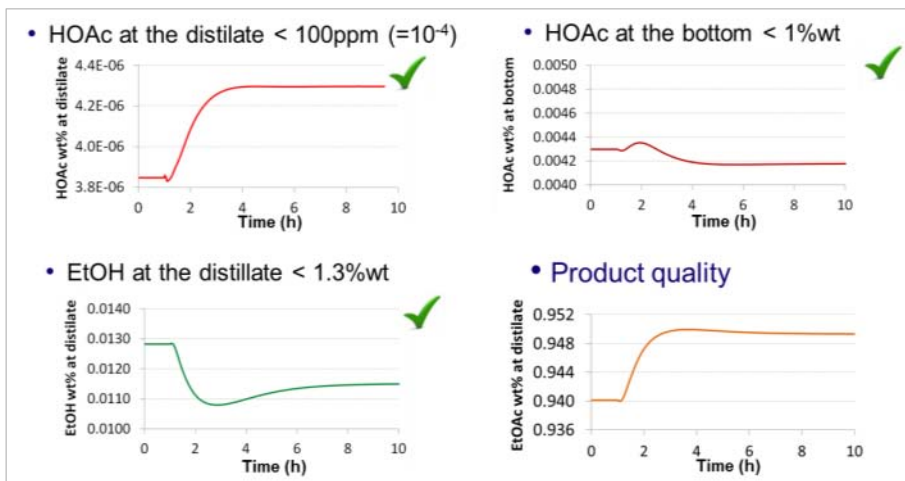


Figure AV.8. Composition control specifications after a decrease of acid feed flow rate, column Design30a

Column Design30b

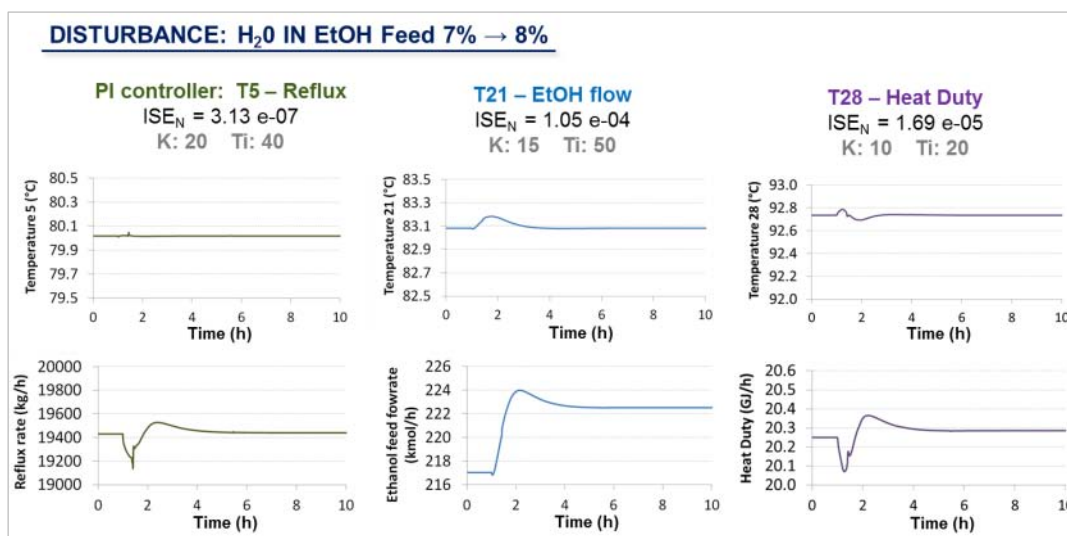


Figure AV.9. Inferential control variables after an increase of water in ethanol feed, column Design30b

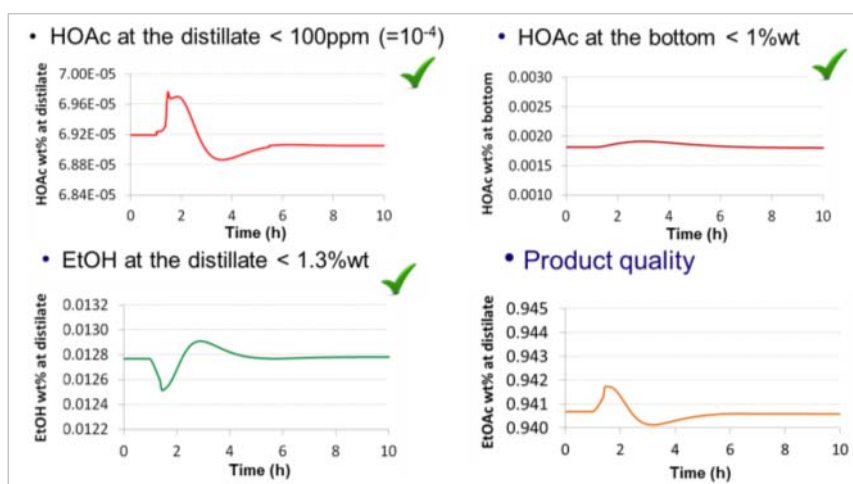


Figure AV.10. Inferential control specifications after an increase of water in ethanol feed, column Design30b

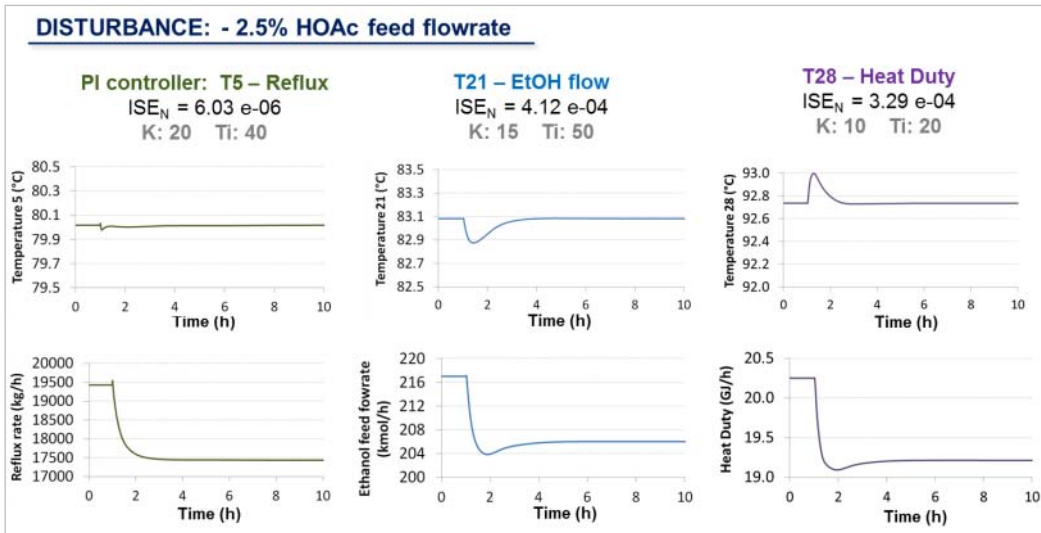


Figure AV.11. Inferential control variables after a decrease of acid feed flow rate, column Design30b

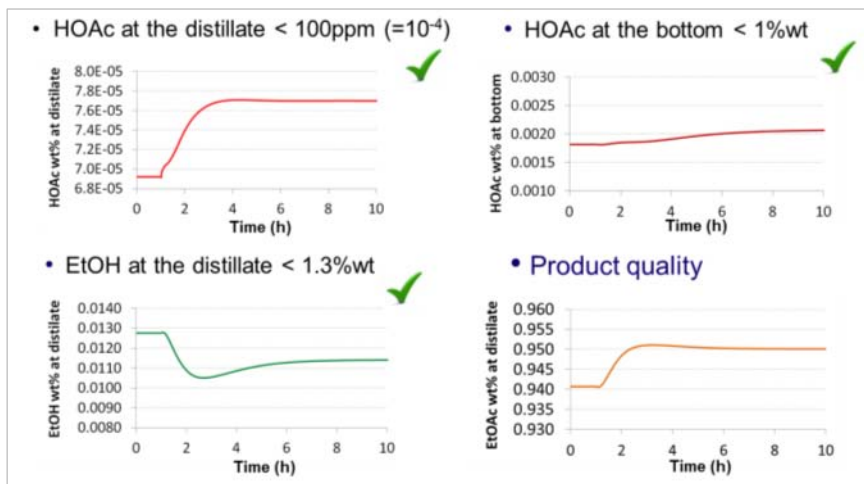


Figure AV.12. Inferential control specifications after a decrease of acid feed flow rate, column Design30b

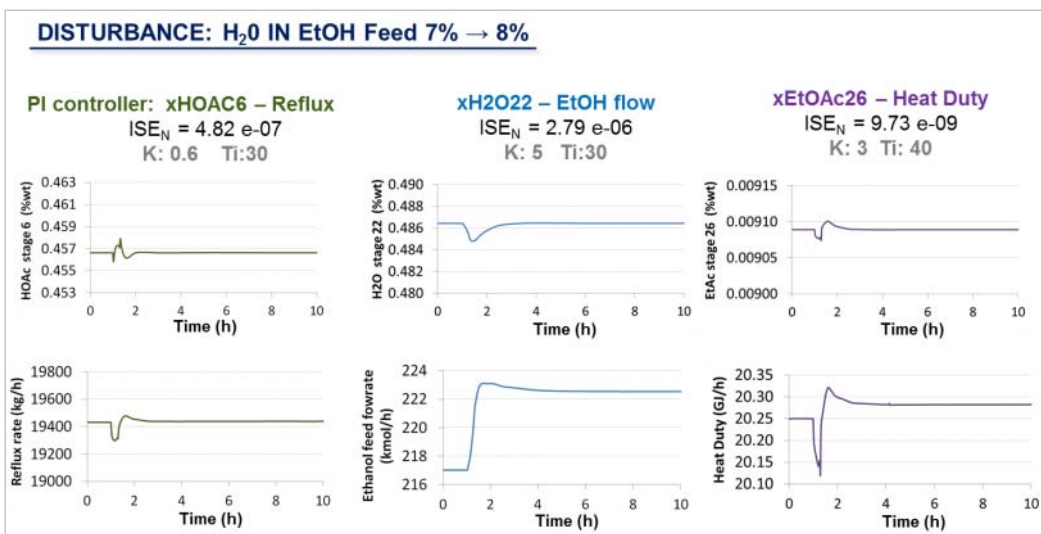


Figure AV.13. Composition control variables after an increase of water in ethanol feed, column Design30b

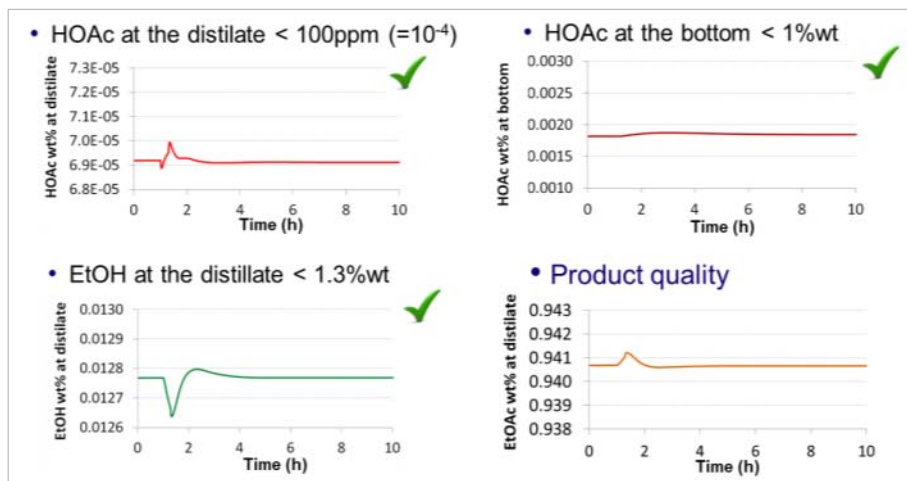


Figure AV.14. Composition control specifications after an increase of water in ethanol feed, column Design30b

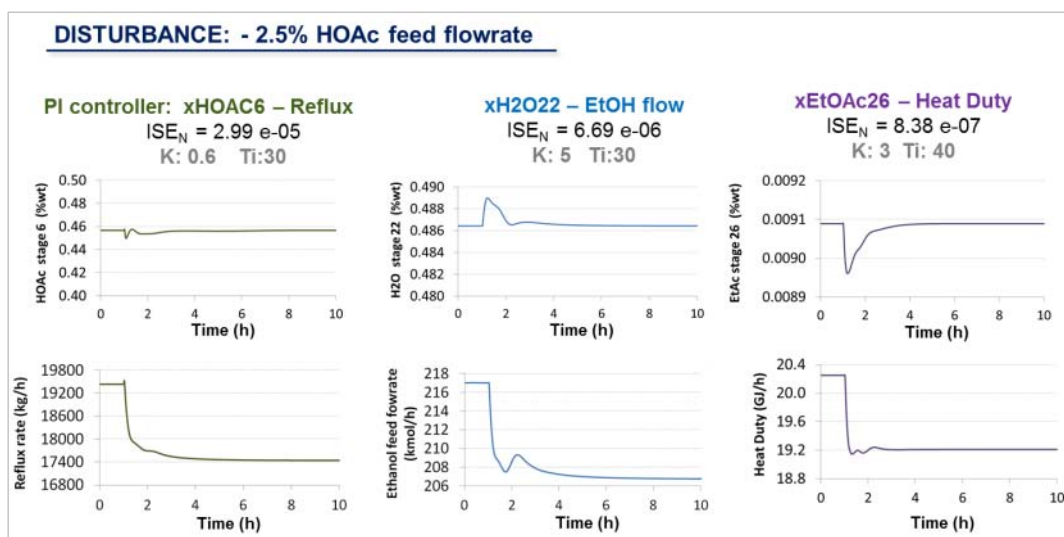


Figure AV.15. Composition control variables after a decrease of acid feed flow rate, column Design30b

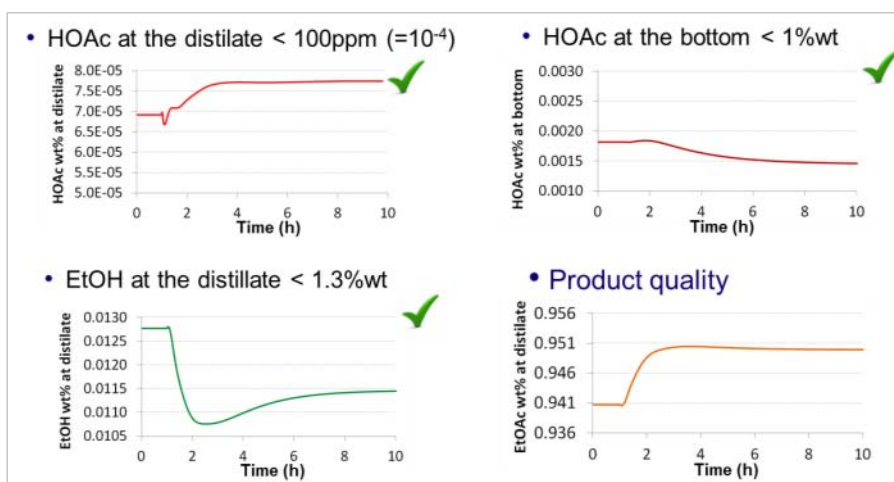


Figure AV.16. Composition control specifications after a decrease of acid feed flow rate, column Design30b

Column Design30c

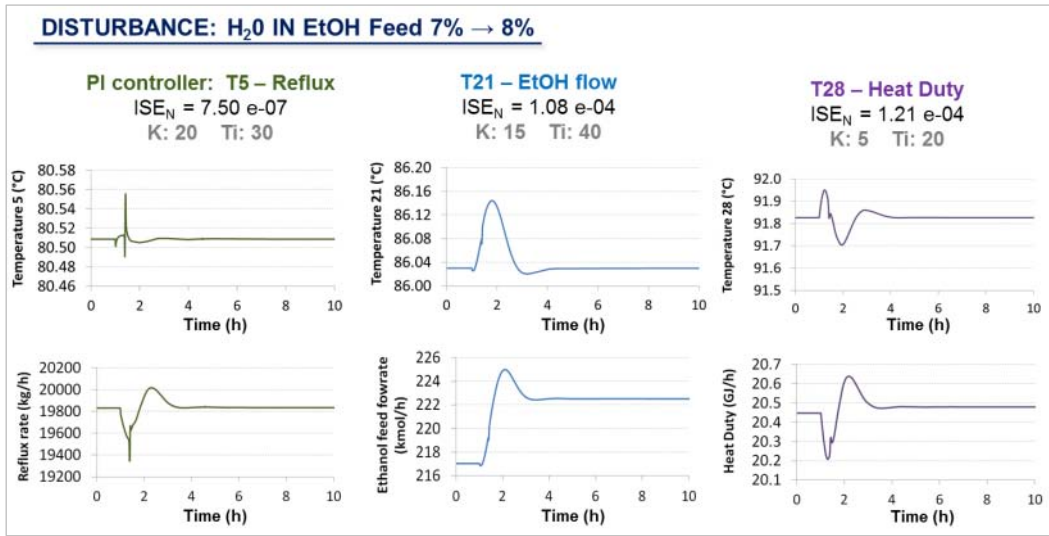


Figure AV.17. Inferential control variables after an increase of water in ethanol feed, column Design30c

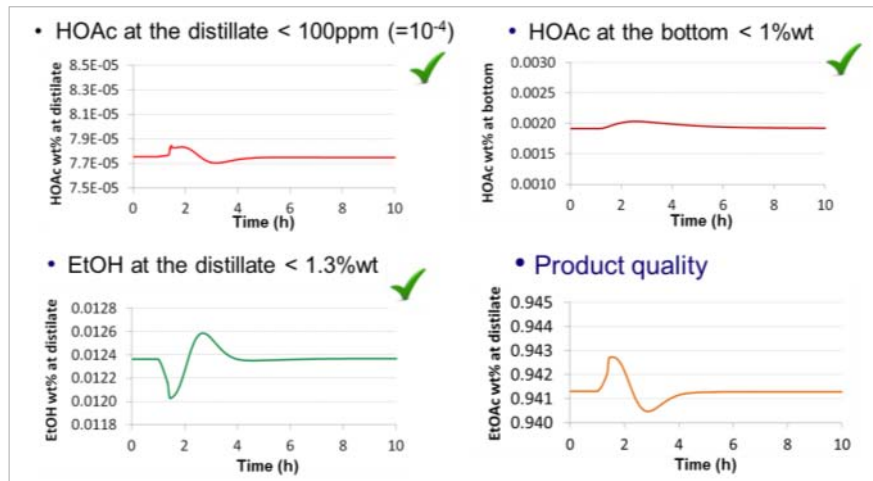


Figure AV.18. Inferential control specifications after an increase of water in ethanol feed, column Design30c

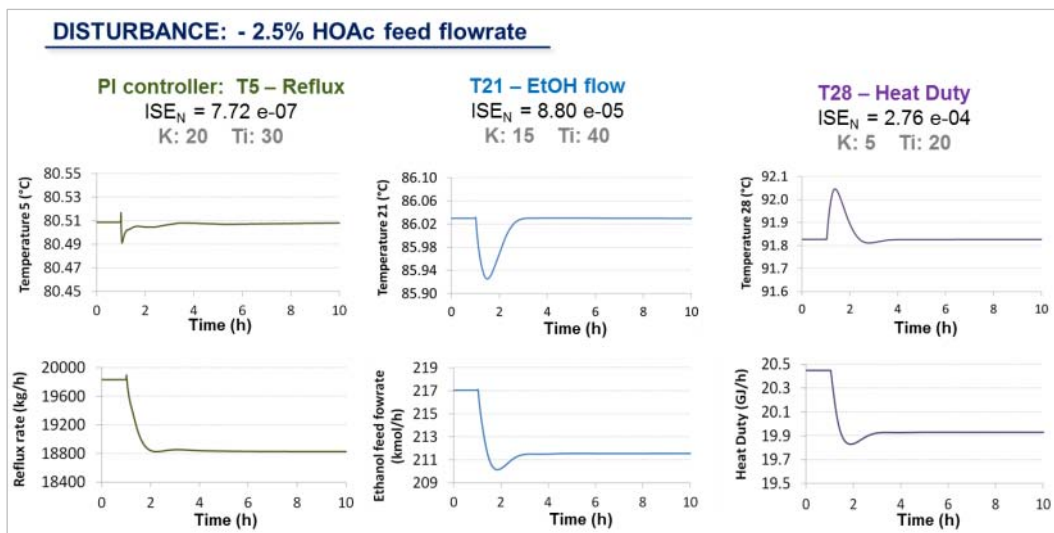


Figure AV.19. Inferential control variables after a decrease of acid feed flow rate, column Design30c

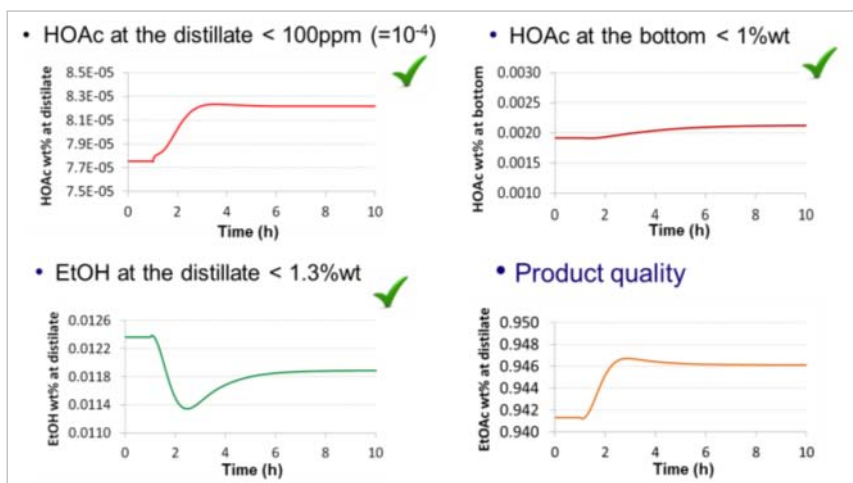


Figure AV.20. Inferential control specifications after a decrease of acid feed flow rate, column Design30c

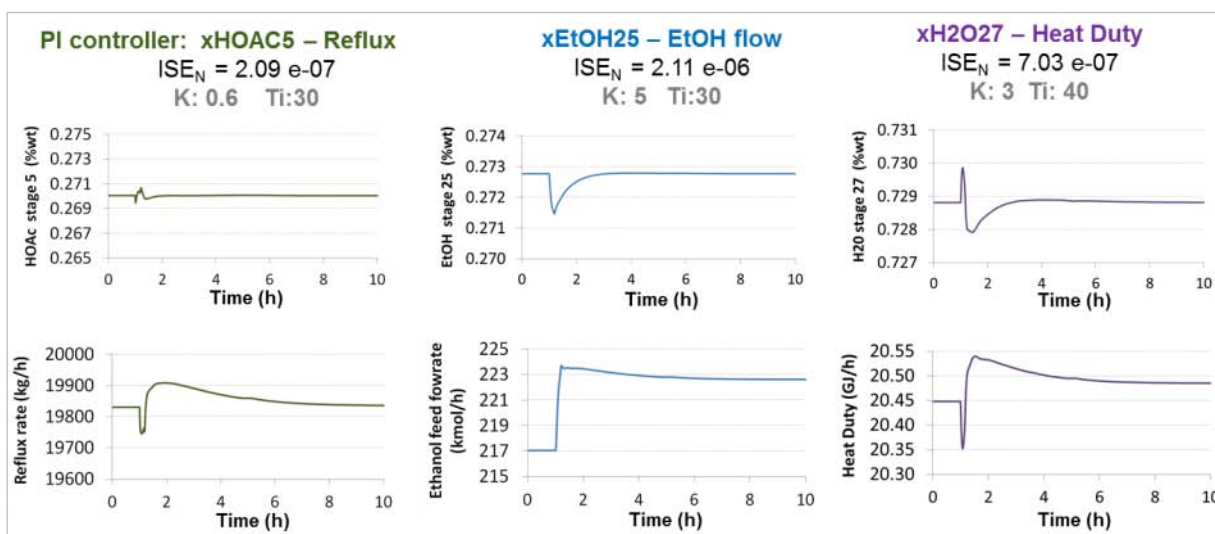


Figure AV.21. Composition control variables after an increase of water in ethanol feed, column Design30c

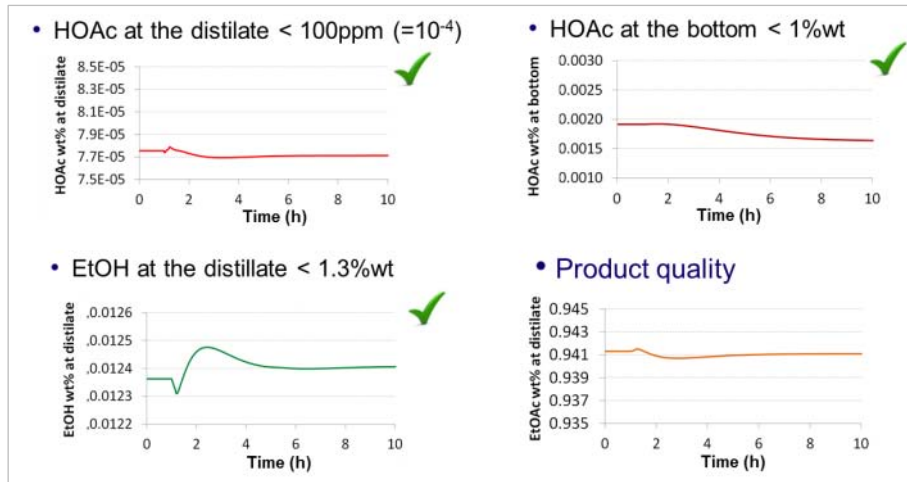


Figure AV.22. Composition control specifications after an increase of water in ethanol feed, column Design30c

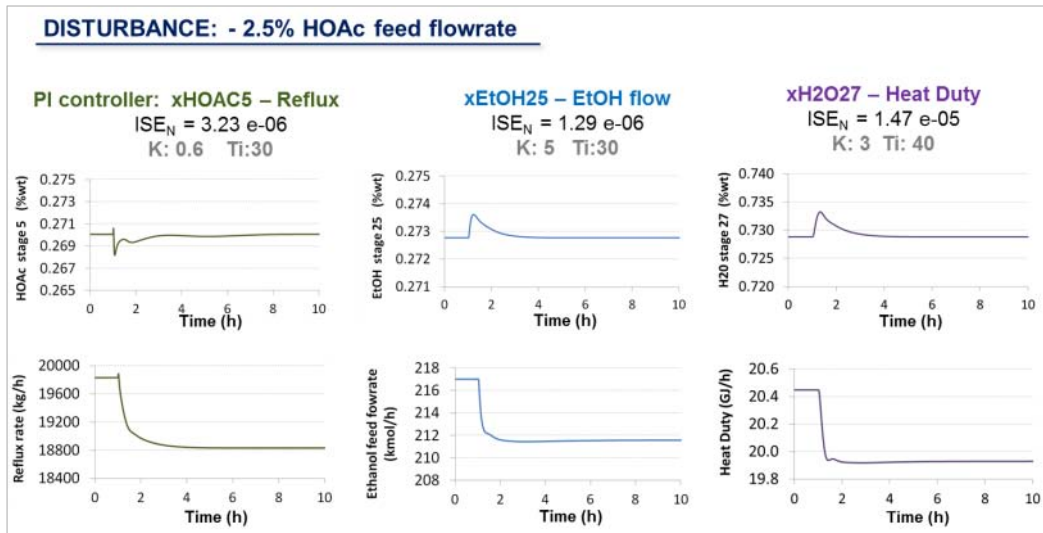


Figure AV.23. Composition control variables after a decrease of acid feed flow rate, column Design30c

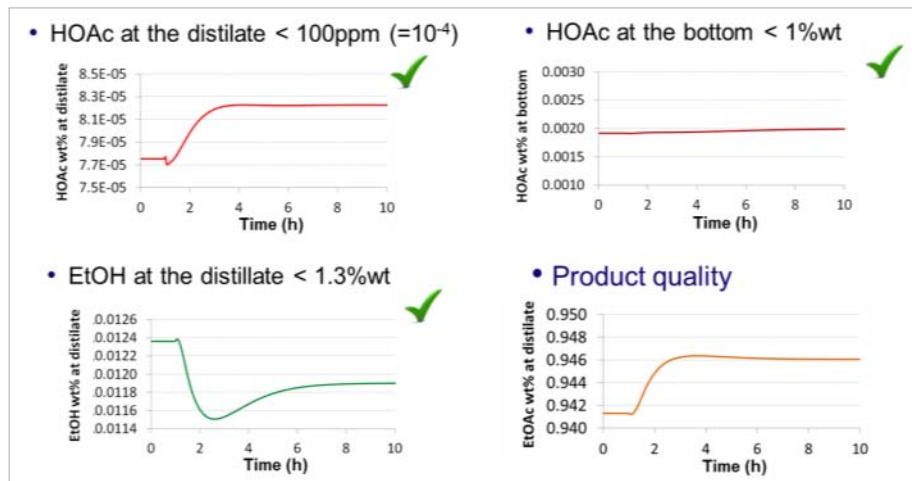


Figure AV.24. Composition control specifications after a decrease of acid feed flow rate, column Design30c

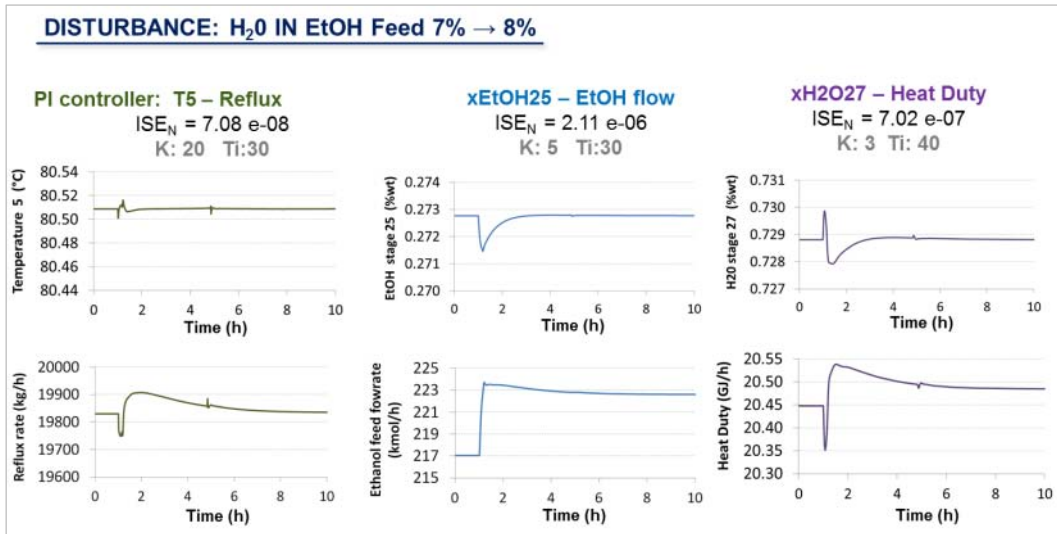


Figure AV.25. Temperature and composition control variables after an increase of water in ethanol feed, column Design30c

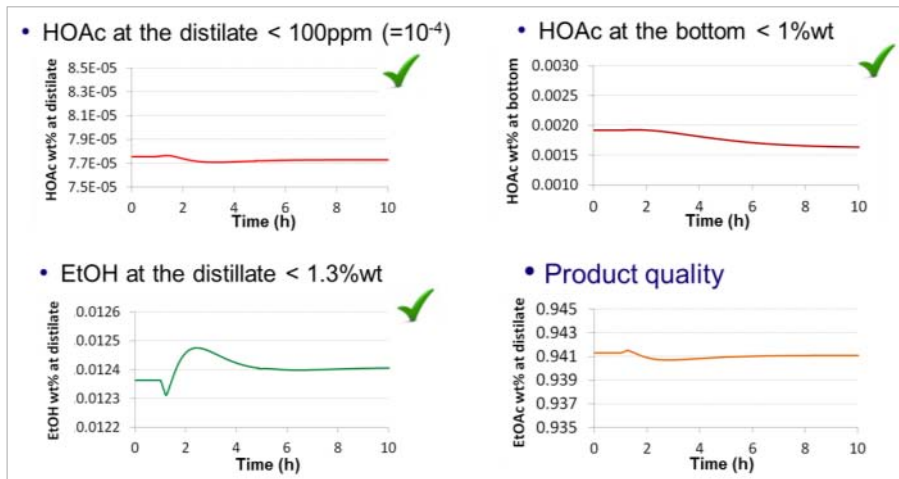


Figure AV.26. Temperature and composition control specifications an increase of water in ethanol feed, column Design30c

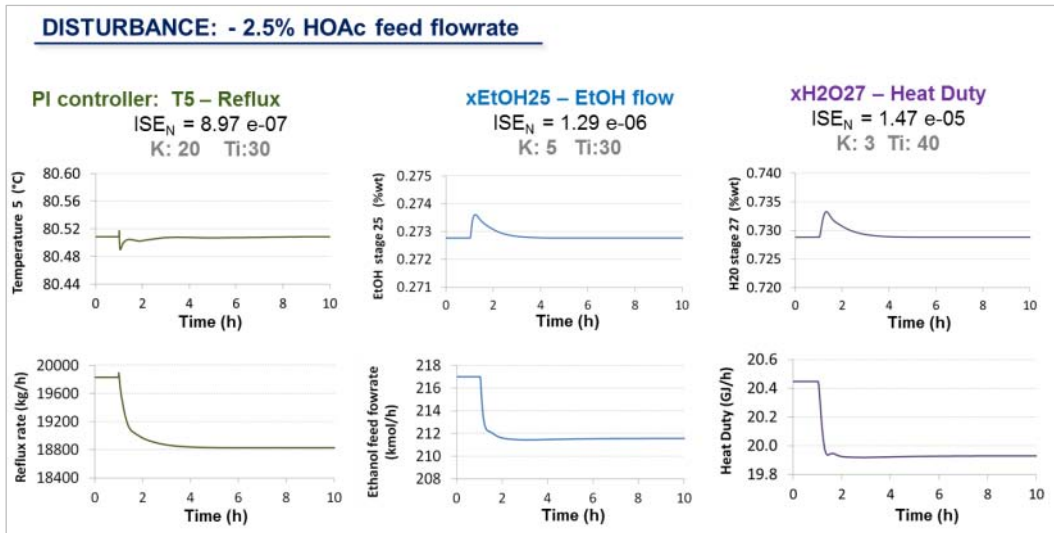


Figure AV.27. Temperature and composition control variables after a decrease of acid feed flow rate, column Design30c

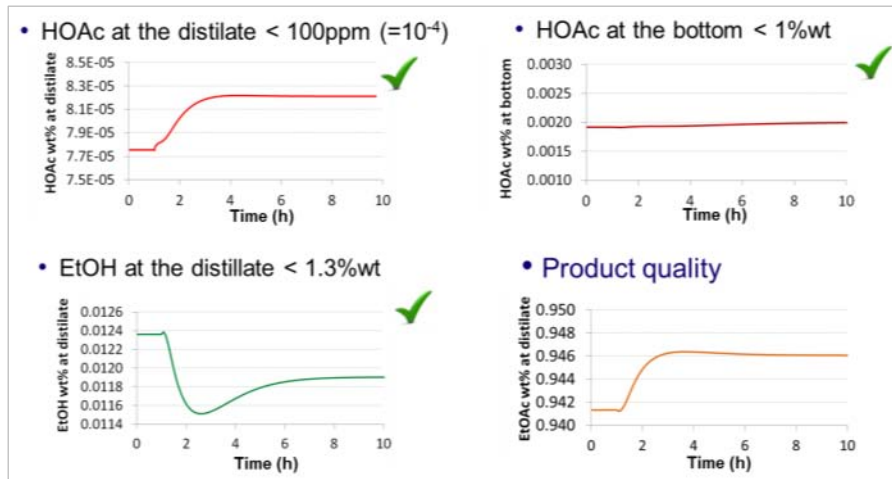


Figure AV.28. Temperature and composition control specifications after a decrease of acid feed flow rate, column Design30c

Etude de l'intégration de la contrôlabilité et de la diagnosticabilité des colonnes de distillation réactive dès la phase de conception. Application à la production d'acétate d'éthyle.

La distillation réactive est un exemple emblématique de l'intensification de procédés. Cependant, le couplage réaction/séparation génère des complexités importantes en termes de dynamique, de contrôle et de supervision qui constituent une barrière pour leur mise en œuvre industrielle. Ces aspects doivent être considérés dès la phase de conception sous peine de concevoir une colonne difficilement contrôlable. Une méthodologie existante est étendue afin d'y intégrer les aspects de contrôlabilité et de diagnosticabilité. L'étape de conception étudie les courbes de résidu et extractives réactives, identifie les paramètres opérationnels et propose des configurations de colonne respectant les spécifications. La meilleure configuration est choisie sur des critères de contrôlabilité par l'analyse de différents indicateurs quantitatifs et qualitatifs identifiés à l'aide de simulations en régime permanent et dynamique. La méthodologie est appliquée à la production industrielle d'acétate d'éthyle. Deux campagnes expérimentales ont permis de fiabiliser le modèle de simulation de la colonne. La méthodologie permet d'identifier les sensibilités et montre que il est possible d'agir sur les trois degrés de liberté de la colonne double alimentation pour atteindre les spécifications industrielles ; les variables contrôlées sont sélectionnées dans des sections spécifiques, similaires pour différentes configurations de colonne. Concernant le diagnostic, l'utilisation de capteurs de composition semble la plus pertinente mais la complexité de leur utilisation industrielle (cout) peut être contournée par la sélection d'un nombre plus important de capteurs de température judicieusement positionnés. Les résultats de contrôlabilité et de diagnosticabilité sont en cohérence et bien intégrés dans la conception des colonnes réactives.

Mots clés: distillation réactive, conception, simulation dynamique, catalyse hétérogène, contrôlabilité, diagnosticabilité, acétate d'éthyle

Study on the integration of controllability and diagnosability of reactive distillation columns as from the conceptual design step. Application to the production of ethyl acetate.

Reactive distillation involves complexities on process dynamics, control and supervision. This work proposes a methodology integrating controllability and diagnosability as from conceptual design. The choice of the most appropriate feasible configuration is conducted through an indices-based method, regarding steady-state and dynamic simulations, for the ethyl acetate production. Experimental campaigns were performed to acquire reliable models. The methodology highlights the process sensitivities and shows that three degrees of freedom of the double-feed column can be manipulated to ensure the industrial specifications; the controlled variables are selected at similar specific locations for all column configurations. Concerning diagnosis, the use of composition sensors seems to be the most appropriate solution, but the same performances can be reached with more temperature sensors judiciously placed.

Key words: reactive distillation, process design, dynamic modeling, heterogeneous catalyst, controllability, diagnosability, ethyl acetate

- Solvay – Research and Innovation Center, 85 avenue des Frères Perret - BP 62 – F-69192 St Fons, France
- Université de Toulouse; INPT, UPS; Laboratoire de Génie Chimique; 4 Allée Emile Monso, F-31030 Toulouse, France
- CNRS, Laboratoire d'Analyse et d'Architecture des Systèmes; 7 avenue du Colonel Roche, F-31077 Toulouse, France
- Departamento de Engenharia Química, Escola Politécnica da Universidade de São Paulo, Av. Professor Lineu Prestes, 05088-900 São Paulo, Brasil